Universidad Autónoma de Madrid

Escuela politécnica superior

Proyecto fin de carrera

"Design of ultra-wideband filters for a wireless broadband communications system."

Ingeniería de Telecomunicación

Antonio Castillo León

Noviembre 2009

"Design of ultra-wideband filters for a wireless broadband communications system."

AUTOR: Antonio Castillo León

TUTOR: Liam Barry

PONENTE: José Luis Masa Campos

Grupo de Radiocomunicaciones y Comunicaciones Ópticas

Escuela Politécnica Superior

Universidad Autónoma de Madrid

Noviembre 2009

Abstract

In this project, several **Ultra Wideband (UWB) filters** are developed for its integration in an **UWB Radio Over Fiber (ROF) communications system**. ROF is a technology where light is modulated by a radio signal and transmitted over an optical fiber link to one or multiple transceivers, where after a simple optoelectric conversion, signal is then radiated to the air by an antenna to facilitate wireless access.

Two main objectives are covered in the project.

First, developing a complete design cycle of **several bandpass filters** in the UWB working spectrum, from 3.1 to 10.6 Ghz, starting with the analysis and ending with the construction and measurements of the obtained filters. Microwave engineering techniques, that can also be applied to develop other microwave elements such as transformers or couplers, were used to accomplish it.

Band-pass coupled-line filters fabricated using microstrip technology have been chosen to carry out the designs, given that the final filters obtained with this technology are compact, with a low fabrication cost and easily integrable with active devices such as diodes or transistors.

To summarize, two filters have been designed and built. The first one going from **3.1 to 4.7 Ghz,** lower part of the working spectrum, and a second one going from **6.3 to 7.9 Ghz**, for the upper-band. A third filter for the whole UWB band, **3.1 to 10.6 Ghz,** was sketched and it is still in development, but finally was not included in this work given its complexity.

Final devices obtained have been measured with a network analyzer to evaluate its response and obtain conclusions of its selectivity, group delay, quality factor and other parameters of microwave filters.

The second main objective addressed in the project has been the integration of these filters in an **optical transmission system**, that sends digital data using an optical carrier modulated by an **UWB radio signal** that complies with **ECMA-368 [1] standard**. The components of the system were, in one of the ends, a transmitter which generates a **Multiband Orthogonal Frequency-Division Multiplexing (MB-OFDM)** signal that drives a laser, sending the signal through optical fiber and reaching a photo-detector in the other end. This photo-detector does the optoelectric conversion, obtaining the UWB signal that is then transmited through the

antenna and radiated to the air. Finally the signal reaches a receiver that is able to decode and check its parameters such as quality, error rate, etc.

With these tests, filters are used in a real system and its performance is evaluated. Measurements of the whole system are also taken to obtain conclusions on its behavior when changing important parameters, testing it with and without the filters to measure the real UWB ROF system performance. This way, a technology in constant expansion these days has been tested.

This work has even produced a publication in an international conference before the conclusion of this report, and will be continued in the near future with hopefully more published work as an outcome. The paper was published in **CIICT 09 (China-Ireland International Conference on Information and Communication Technologies)** and it is included in the **Appendix**.

With the name of **"Investigation of dispersive fading in UWB over fiber systems."**, it is a detailed study of dispersive fading in the system where the filters were introduced and where several tests were conducted. Most of them are included in this report and additional ones are explained in this published paper.

Key words

UWB, Ultra WideBand, ROF, radio over fiber, coupled-line filter, microstrip lines, microwave filter synthesis, Chebyshev response, bandpass, S parameters, ABCD parameters, insertion loss method, optical fiber, wireless, PER, Packet error rate, laser, photo-detector.

Resumen

En este proyecto se desarrolla el diseño de unos **filtros UWB** para su integración en un **sistema de comunicaciones UWB ROF**. En la tecnología ROF, una señal luminosa es modulada por una señal de radio y transmitida a través de un enlace de fibra óptica hasta el/los receptores, donde tras una simple conversión opto-eléctrica, la señal es emitida al ambiente por una antena y puede ser recogida por receptores inalámbricos.

En el proyecto se cubren dos objetivos principales.

Por un lado el llevar a cabo el ciclo completo de diseño de **varios filtros paso banda** en el espectro de trabajo UWB, de 3.1 a 10.6 GHz, empezando por el análisis y hasta llegar a la construcción y medida. Para ello se han usado técnicas que se engloban dentro de la ingeniería de microondas-milimétricas, y que pueden ser además aplicadas a la implementación de otro tipo de dispositivos de microondas como transformadores o acopladores.

Se ha optado por el diseño de **filtros paso banda de líneas acopladas en tecnología microstrip** para llevar a cabo su construcción ya que éstas son compactas, suelen tener un bajo coste de fabricación, y se pueden integrar fácilmente con dispositivos activos como diodos y transistores.

En concreto se han diseñado y construido dos filtros, uno de **3.1 a 4.7 GHz** para la banda inferior de trabajo. Un segundo filtro desde **6.3 a 7.9 GHz**, para la banda superior de trabajo. Y finalmente un tercer filtro para la banda UWB completa, de **3.1 a 10.6 GHz**, fue comenzado y está aún siendo desarrollado, pero no se incluyó en este trabajo por su complejidad.

Finalmente se han realizado medidas de los dispositivos mediante analizador de redes, para evaluar su funcionamiento y extraer conclusiones de sus características de selectividad, retardo de grupo, factor de calidad y otros parámetros típicos de filtros de microondas.

Por otro lado se han integrado estos filtros en un **sistema completo de transmisión óptica**, que envía datos en forma digital utilizando una portadora óptica, modulada por una señal de radiofrecuencia que cumple el **estándar UWB ECMA-368 [1]**. En un extremo tenemos un emisor que genera una señal **MB-OFDM** que excita directamente un láser, enviando la señal a través de una fibra óptica y llegando a un foto-detector. En este foto-detector se realiza una conversión opto-eléctrica, obteniendo de nuevo la señal UWB que es irradiada por la antena. Finalmente un elemento receptor capta esta señal, la decodifica y comprueban sus parámetros de calidad, tasas de error, etc.

Con estas pruebas, se han puesto en práctica los filtros en un sistema real y se ha evaluado su rendimiento. Desarrollando un estudio con medidas del sistema UWB ROF completo. Variando parámetros importantes y comparando también el rendimiento con y sin filtros. De esta forma, ha sido analizada en detalle una tecnología en constante expansión hoy en día.

Este trabajo ha producido incluso una publicación en una conferencia internacional antes de la conclusión de este proyecto, y se espera que será continuado en el medio plazo con más publicaciones como resultado. El papel fue publicado en **CIICT 09 (Conferencia Internacional**

China-Irlanda sobre Tecnologías de la Información y Comunicaciones) y está incluida en el **Apéndice**.

Con el nombre de **"Investigation of dispersive fading in UWB over fiber systems."**, es un estudio detallado de los efectos de dispersión que ocurren en la fibra del sistema donde los filtros han sido introducidos y donde varios tests fueron llevados a cabo. La mayoría de ellos están incluidos en este trabajo y algunos adicionales son explicados en esta publicación.

Palabras Clave

Radio sobre fibra, filtro de líneas acopladas, línea microstrip, síntesis de filtros de microondas, paso banda, parámetros S, parámetros ABCD, método de pérdidas de inserción, fibra óptica, inalámbrico, tasa de error de paquete, láser, fotodetector.

Acknowledgments

I would like to thank professor Liam Barry, from Dublin City University, for giving me this opportunity and helping me in everything he could during my stay. I will always be very thankful for his effort and big contribution.

Agradecer a Jose Luis Masa por su colaboración, tanto en la universidad como en este proyecto, ya que su ayuda y consejo han sido inestimables en ambos casos.

A mi novia por haberme acompañado en la aventura que ha supuesto mi carrera, y como colofón este proyecto en el extranjero.

Y finalmente agradecer profundamente las posibilidades brindadas para hacer este proyecto y mi carrera, a las únicas personas que siempre han creído en mi firmemente, apoyándome en todo cuanto era necesario. Un porcentaje muy importante del mérito es de ellos.

A mis padres.

Antonio Castillo León

Junio de 2009.

This Project has been developed in the Radio and Optical Communications Laboratory in the School of Electronic Engineering jointly with RINCE Research Institute, at Dublin City University, Ireland, from October 2008 to June 2009.

Contents

List of Figures

List of Tables

1

Introduction.

1.1 Motivation and focus

In this project, **two main objectives are addressed**. On one side, focus is put in **designing a single component** in detail, the already mentioned filters, and its integration in a system. On the other side, a **whole system implementation** and tests are done to measure the performance of the overall optical transmission system with the filters included in it.

Starting from the design of the filters for different parts of the system, and going up to the level of system integration and tests, this project covers the main stages of system development.

1.1.1 Filter design

Filter design has been a key element in electronics since its beginnings. Selectively choosing a defined frequency range of the spectrum is needed from any point of view to define our working space, and also to treat the information differently, as separated channels, depending on the frequency our signal is received and processed. Filter design is a **major element in communications systems** and has increased in complexity as working frequencies have risen.

A key aspect for better directivity in signal transmission, smaller antenna sizes and higher bandwidth is the rise of our working signal's frequency. In preceding decades, a continued improvement has been achieved and so the systems can now be smaller and have better characteristics, but at the expense of more complicated system design techniques and more demanding component designs.

Since theoretical studies done by the researcher **James Clerk Maxwell** in years from 1885 to 1887, in which he predicted the existence of Electromagnetic (EM) waves, up to our days, the improvement on current designs and the ability to work at higher frequencies has been a constant which has boosted the capacity of the systems, speeds, transmission techniques and everything associated.

Frequency (Hz)

3×10^5 3×10^6 3×10^7 3×10^8 3×10^9 3×10^{10} 3×10^{11} 3×10^{12} 3×10^{13} 3×10^{14}

| Long wave radio | AM broadcast radio | Shortwave radio | VHF TV | FM broadcast radio | Microwaves | Far Infrared | Infrared | Visible light |

10^3 10^2 10 1 10^{-1} 10^{-2} 10^{-3} 10^{-4} 10^{-5} 10^{-6}

Wavelength (m)

Typical Frequencies

AM broadcast band	535–1605 kHz
Short wave radio band	3–30 MHz
FM broadcast band	88–108 MHz
VHF TV (2–4)	54–72 MHz
VHF TV (5–6)	76–88 MHz
UHF TV (7–13)	174–216 MHz
UHF TV (14–83)	470–890 MHz
US cellular telephone	824–849 MHz
	869–894 MHz
European GSM cellular	880–915 MHz
	925–960 MHz
GPS	1575.42 MHz
	1227.60 MHz
Microwave ovens	2.45 GHz
US DBS	11.7–12.5 GHz
US ISM bands	902–928 MHz
	2.400–2.484 GHz
	5.725–5.850 GHz
US UWB radio	3.1–10.6 GHz

Approximate Band Designations

Medium frequency	300 kHz to 3 MHz
High frequency (HF)	3 MHz to 30 MHz
Very high frequency (VHF)	30 MHz to 300 MHz
Ultra high frequency (UHF)	300 MHz to 3 GHz
L band	1–2 GHz
S band	2–4 GHz
C band	4–8 GHz
X band	8–12 GHz
Ku band	12–18 GHz
K band	18–26 GHz
Ka band	26–40 GHz
U band	40–60 GHz
V band	50-75 GHz
E band	60-90 GHz
W band	75-110 GHz
F band	90-140 GHz

Table 1.1: Electromagnetic spectrum allocation, from [2], Chapter 1.

Those are the reasons why in the microwave field development, filters are a main part. Microwave term refers to signals with frequency between **300Mhz and 300 Ghz**, with a corresponding wavelength $\lambda = c/f$, **from 1m to 1nm**, as it is shown in **Table 1.1**. They represent a field in which designing is very hard, because whereas in lower frequencies general circuit theory is applicable and it gives very accurate results, as frequency rises new phenomena must be taken into account, complicating the designs and the estimation of its behavior in real life once they are built.

Bandpass filters are essential devices in many radio-frequency/microwave engineering areas. Communication systems in this band have experienced a big development in late years, to give support to different applications such as: **satellite TV, mobile communications, military and civilian radar systems, medical systems**, and so on. The rise of these systems has evolved in more demanding specifications and designs for the hardware devices that form part of them, being filters one of the key elements. [10]

With this background already stated, the objective of this part of the project is the com-
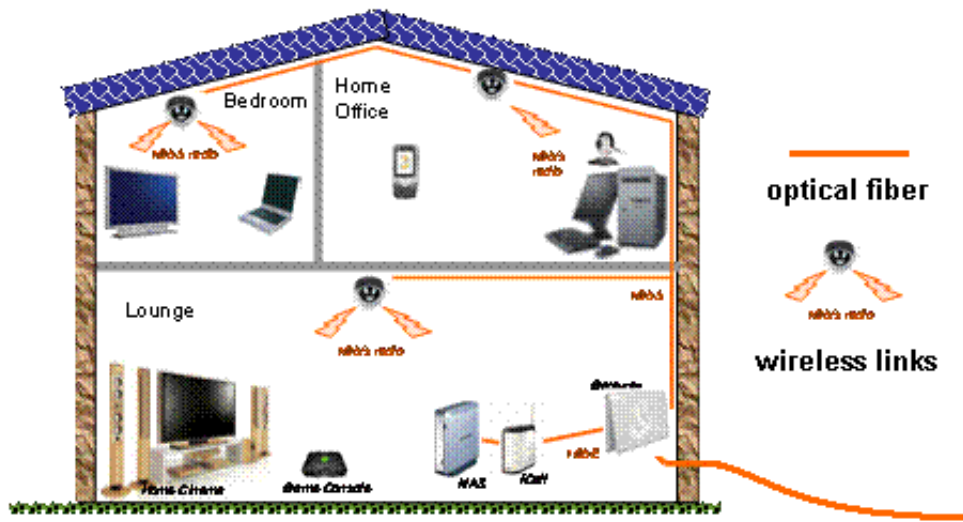
Figure 1.1: UWB-ROF system scheme.

pletion of the design cycle of some **UWB filters** using parallel coupled-lines and microstrip technology, obtaining comparable results as to commercially designed ones. In the second part, the development of an **UWB ROF system**, and the realization of different performance tests to characterize it will complete the work.

1.1.2   UWB and ROF technologies

UWB is a new technology in big expansion these days. It is considered as the new wireless, high-bandwidth, technology standard. It allows transmission at high data-rates, up to 480Mbps using a very high bandwidth, but with low power emissions and low signal to noise ratio needed. It also has a low detection probability and high performance in multipath channels, given its high resistance to multipath fading.

For all these advantages it is a very interesting technology, but with some problems, one of them being that those high bit-rates are only achievable at low distances, such as 10m. This is the point were ROF technology supports UWB.

ROF technology allows to send radio signals directly through optical fiber, doing just an electro-optical conversion of the UWB signal at the RF signal generation point, driving a laser and sending this beam through the necessary length of fiber. Then an opto-electrical conversion is done in the other ends, by means of photo-detectors. Once the RF signal is again obtained, it is necessary to amplify and then radiate it through the antennas that would be located at the ends.

The combination of these two technologies has big advantages and represents a new focus on signal transmission over optical fiber. That is why we have concentrated in developing these filters, that we can then integrate in this kind of system, exploring an emerging technology, **transmission of UWB signals using ROF**.

The final filters have been introduced in this system and we have measured important parameters, obtaining an in-detail characterization of both the system and the filters and checking

how they affect the final specifications, measuring the improvement obtained.

In the tests we have been able to directly transmit radio signals over the fiber, allowing to increase the range of these signals, that for a typical UWB system are limited to about 10 meters, to any distance required up to several kilometers, as we have confirmed in the laboratory, given the low losses optical fiber has.

With this work we hope to cover a wide spectrum of ideas, starting from the specific design of some system components, the microstrip coupled-lines band pass filters, and going all the way up to the final integration and test of the whole system, with measurements on its behavior and final thoughts in the real profits these combined technologies can give to real systems.

1.2   Report structure

The report has two main parts. In chapters 2 to 6, it talks about filter design techniques, starting from transmission lines and explaining in detail the process followed to design microwave filters. And a second part, in chapters 7 and 8, speaks about the core technologies and different components the final system uses. It then also explains the system developed and shows the performance results obtained.

The first part of the report talks about the next topics.

Chapter 2 on page 11 starts speaking about transmission lines, the main theory behind them and how to represent and obtain a suitable model, both of transmission and microstrip lines, with details on microstrip coupled-lines. It is very useful for our analysis to describe the behavior at high frequencies correctly, given that they are going to be used in a wide working range.

Chapter 3 on page 25 concentrates in microwave networks, the next big basic idea behind filter design. This allows us to consider different elements as blocks and combine them, representing our final system and giving us the required response we want. In this chapter the main ideas explained are network matrices and ABCD and S parameters.

Once the two main basic ideas behind filter design are covered: transmission lines characterization and microwave networks analysis, we can move on in **Chapter 4 on page 35** and describe the process involved in designing microwave filters. Starting from the two main methods used: **image parameter** and **insertion loss,** and showing in detail the second one, given it is the one used to design the type of filters we need. Then we speak about different practical filter responses and about Chebyshev response in detail, which is the one we are going to use for the designed filters.

In **Chapter 5 on page 47** we show how to design a coupled-line bandpass filter. The steps involved in the design of a practical coupled-line bandpass filter, equations and concepts needed are treated in detail. Finally, conversions needed to be done for a required specific response are explained.

In **Chapter 6 on page 57** we finally present the designed filters and give details about the main characteristics and problems found. Measured data, diagrams, response, reflections, etc are shown. They are analyzed in detail and also images of the design process are shown. Computer-aided Design (CAD) program design is explained, describing every parameter and step of the process in detail. We will talk about the construction technology used and do an in-detail characterization of the built filters.

By contrast, in the second part of the report we center our focus in the system we have developed and its performance.

We start in **Chapter 7 on page 107** explaining the main ideas behind the technologies we put into practice in the system under test, with an in-detail characterization and explanation on how they are implemented.

In **Chapter 8 on page 121** we present the graphs and results obtained from the system, with and without the filters, and analyzing how they impact performance. We will make an in detail analysis of the components and show every important idea obtained from the work developed.

In **Chapter 9 on page 145** we explain in detail the conclusions obtained from the project developed, and speak about possible future work and interesting paths to follow in case work done in this project would be continued.

To finish, a comprehensive list of terms used through the report is given in the **Definitions part on page i**, with its corresponding explanations to expand the information given on certain important related topics.

In the **Appendix on page v**, some graphs and tables are all shown with the idea of having important data to complete a filter design all together in the back of the project. Code used to produce some of the results is also showed in the end and the publications obtained from this work are also presented.

1.3 Motivación y objetivos.

En este proyecto, **dos objetivos principales son cubiertos**. Por un lado, **se diseña un componente en detalle**, los ya mencionados filtros, y se integran dentro de un sistema mayor. Por otro lado, **se diseña e implementa completamente un sistema de transmisión óptico**, con pruebas llevadas a cabo para medir el rendimiento, una vez se integran en él los filtros diseñados.

Comenzando por el diseño de los filtros para varios puntos del sistema, y llegando hasta el nivel superior de integración de todos los componentes y realización de pruebas, este proyecto cubre las principales etapas del desarrollo de un sistema completo.

1.3.1 Diseño de filtros

El diseño de filtros ha sido un elemento clave en la electrónica desde sus comienzos. Seleccionar un rango definido del espectro es necesario desde cualquier punto de vista para definir nuestro espacio de trabajo, y también para tratar la información recibida de forma diferente, como canales separados, dependiendo de la frecuencia a la que nuestra señal sea recibida y procesada. El diseño de filtros **es un elemento muy importante en los sistemas de comunicaciones** y ha aumentado mucho en complejidad cuando las frecuencias de trabajo han ido creciendo.

Un aspecto clave para obtener mejor directividad en la transmisión de nuestras señales, tamaños de antena más pequeños y un ancho de banda mayor, es el aumento de nuestra frecuencia de trabajo. En las decádas pasadas, se ha conseguido una mejora contínua y ahora los sistemas pueden ser más pequeños y tener mejores prestaciones, pero a costa de unas técnicas de diseño de los sistemas y de componentes más complejas.

Desde los estudios teóricos llevados a cabo por el científico **James Clerk Maxwell** en los años de 1885 a 1887, en los que predijo la existencia de ondas electromagnéticas, hasta nuestros días, la mejora en los diseños actuales y la habilidad de trabajar a frecuencias más altas ha sido una constante que ha multiplicado la capacidad de los sistemas, velocidades, técnicas de transmisión y todos los parámetros asociados.

Esas son las razones por las que en el campo del diseño de microondas, los filtros son una parte principal. El término microondas se refiere a señales con frecuencia entre **300Mhz and 300 Ghz**, con una longitud de onda correspondiente $\lambda = {}^{c}\!/_{f}$, **de 1m a 1nm**, como se muestra en la **Tabla 1.1**. Representan un rango en el que el diseño es complicado, porque aunque para frecuencias bajas la teoría general de circuitos es aplicable y da buenos resultados, cuando la frecuencia aumenta, efectos adicionales han de ser tenidos en cuenta, complicando los diseños y la estimación de su comportamiento en la vida real una vez que éstos sean construidos.

Los filtros paso banda son elementos esenciales en muchas áreas de la ingeniería de microondas. Los sistemas de comunicaciones en esta banda han experimentado un gran desarrollo en estos últimos años, para dar soporte a diferentes aplicaciones como: **televisión por satélite, comunicaciones móviles, sistemas de radar militares y civiles, sistemas médicos, y**

otros. La mayor demanda de estos sistemas ha significado especificaciones más exigentes de los equipos y de los componentes que forman parte de ellos, siendo los filtros un componente clave. [10]

Una vez explicados los objetivos generales, la parte inicial y principal del proyecto completará el ciclo de diseño de unos **filtros UWB** usando lineas acopladas paralelas y tecnología microstrip, con el objetivo de obtener resultados comparables a filtros disponibles de forma comercial. La segunda parte comprenderá el desarrollo de un **sistema de comunicaciones UWB de radio sobre fibra,** así como la realización de pruebas de rendimiento para caracterizarlo, lo que completará el trabajo.

1.3.2   Tecnologías UWB y ROF

UWB es una nueva tecnología en expansión hoy en día. Es considerada como el nuevo estándar inalámbrico de gran velocidad. Permite la transmisión de datos hasta a 480Mbps usando un gran ancho de banda, pero con una baja emisión de potencia y una baja relación señal/ruido. También tiene una baja probabilidad de detección y un buen rendimiento en canales con propagación multicamino, dado que es resistente al desvanecimiento ocasionado por éstos.

Por todas estas ventajas es una tecnología muy interesante, pero con algunos problemas, uno de ellos el que esas altas velocidades sólo se pueden conseguir a distancias cortas, de menos de 10m. Éste es el punto donde la tecnología ROF complementa a UWB.

La tecnología de **radio sobre fibra (ROF)** permite enviar señales de radio directamente a través de fibra óptica, realizando sólo una conversión electro-óptica de la señal de radio UWB en el punto de generación de ésta, excitando después un láser y mandando la señal óptica a través de la longitud necesaria de fibra. Después una conversión opto-eléctrica se realiza en el otro extremo, a través de un fotodetector. Una vez que se obtiene de nuevo la señal de radio, es necesario amplificarla y luego radiarla a través de las antenas localizadas en los extremos.

La combinación de las dos tecnologías tiene grandes ventajas y representa un nuevo enfoque en la transmisión de señales a través de fibra óptica. Es por ello que se ha centrado el trabajo en diseñar estos filtros, que se pueden integrar en este tipo de sistemas, explorando una tecnología emergente, la **transmisión de señales UWB usando ROF.**

Los filtros construidos han sido introducidos en el sistema y se han medido sus parámetros más importantes, obteniendo una caraterización en detalle tanto del sistema general como de los filtros y comprobando cómo éstos afectan las especificaciones de la señal, midiendo la mejora obtenida.

En las pruebas hemos sido capaces de transmitir directamente señales de radio a través de la fibra, permitiendo incrementar el rango de éstas, que para un sistema típico serían de alrededor de 10m, hasta una distancia de varios kilómetros, como hemos confirmado en el laboratorio, dadas las bajas pérdidas que tiene la fibra óptica.

Con este trabajo esperamos cubrir un amplio espectro de ideas, comenzando por el diseño

específico de algunos componentes del sistema, los filtros de líneas acopladas paralelas en tecnología microstrip, y llegando hasta la integración de los componentes necesarios en un sistema completo que fue luego caracterizado en su totalidad. Con medidas de su rendimiento y conclusiones sobre su funcionamiento y aplicación real de la combinación de las tecnologías analizadas, así como sus beneficios.

1.4 Estructura

El proyecto tiene dos partes principales. En los Capítulos del 2 al 6, habla sobre técnicas de diseño de filtros, comenzando a hablar de línes de transmisión y explicando en detalle el proceso seguido para diseñar filtros de microondas. Y una segunda parte, en los Capítulos 7 y 8, que habla sobre las tecnologías principales y diferentes componentes que usa el sistema final. Luego también habla sobre el sistema desarrollado y muestra los resultados de rendimiento obtenidos.

La primera parte del trabajo habla de los siguientes temas.

El **Capítulo 2 en la página 11** comienza hablando de líneas de transmisión, la teoría detrás de ellas y cómo representar y obtener un modelo adecuado, tanto de transmisión como de las líneas microstrip, profundizando en las líneas microstrip paralelas acopladas.

El **Capítulo 3 en la página 25** habla de redes de microondas, la siguiente idea básica detrás del diseño de filtros. Ésto permite considerar los diferentes elementos como bloques y combinarlos, representando nuestro sistema final y dando la respuesta requerida. En este capítulo las ideas principales son las matrices de redes y los parámetros ABCD y S.

Una vez que las ideas básicas tras el diseño de filtros han sido cubiertas: caracterización de líneas de transmisión y análisis de redes de microondas, en el **Capítulo 4 en la página 35** continuamos con la descripción del proceso de diseño de filtros de microondas. Comenzando por los dos métodos principalmente usados: el de **parámetros imagen** y el de **pérdidas de inserción**, y mostrando en detalle el segundo, dado que es el más usado y el necesario para los filtros que vamos a construir. Después hablamos de las diferentes respuestas prácticas de filtros y sobre Chebyshev en particular, que es la respuesta que vamos a usar para el diseño de nuestros filtros.

En el **Capítulo 5 en la página 47** mostramos cómo diseñar un filtro paso banda de líneas paralelas acopladas. Los pasos necesarios en el diseño práctico de los filtros, ecuaciones y conceptos necesarios son tratados en detalle. Finalmente se explican las conversiones necesarias para obtener un respuesta específica.

En el **Capítulo 6 en la página 57** finalmente presentamos los filtros diseñados y damos detalles sobre las características principales y los problemas encontrados. Los datos medidos, diagramas, respuestas, reflexiones, etc son también mostrados. Después éstos son analizados en detalle y se muestran imágenes del proceso de diseño.

El proceso seguido usando programas de diseño asistido por ordenador también es explicado, describiendo los parámetros usados y los diferentes pasos en detalle. Además, hablaremos

sobre la tecnología de construcción usada y haremos una caracterización en detalle de los filtros construidos.

De forma diferente, la segunda parte del trabajo está centrada en el sistema desarrollado y su rendimiento.

Comenzamos en el **Capítulo 7 en la página 107** explicando las ideas básicas detrás de las tecnologías puestas en práctica en el sistema bajo análisis, con una caracterización en detalle y explicación de cómo son implementados.

En el **Capítulo 8 en la página 121** presentamos los gráficos y resultados obtenidos de las pruebas del sistema, con y sin los filtros, y analizamos como afectan al rendimiento. Haremos un análisis en detalle de los componentes y explicaré las ideas y conclusiones más importantes obtenidas del trabajo realizado.

En el **Capítulo 9 en la página 145** explicamos en detalle las conclusiones obtenidas del proyecto desarrollado, y hablamos del posible trabajo futuro y los posibles caminos a seguir en caso de que el trabajo hecho en este proyecto fuese continuado.

Para finalizar, se da una lista detallada de términos usados en el trabajo en las **Definiciones en la página i,** con las explicaciones correspondientes para ampliar la información dada sobre ciertos términos importantes relacionados.

En el **Apéndice en la página v**, se muestran algunos gráficos y tablas con la idea de recopilar al final del proyecto todo lo necesario para acometer el diseño de filtros de líneas acopladas en microstrip. Además, el código usado para obtener algunos de los resultados también aparece aquí. Finalmente también se presenta una publicación que este trabajo ha producido.

2

Transmission lines.

2.1 Introduction

In this chapter, an introduction on transmission lines is going to be conducted. The main ideas behind electromagnetic waves transmission over transmission lines will be explained, and its characterization from the analytical point of view will be obtained. We will present the **lumped-element circuit model** for transmission lines and wave propagation equations. We will also give details about the properties of different physical transmission technologies. An in-detail view for the case of **microstrip lines**, which are the ones going to be used on our filters' design, will be also shown. And finally equations for the **coupled-line directional couplers** in microstrip will be explained.

Transmission line theory bridges the gap between field analysis and basic circuit theory, and so it is of significant importance in microwave network analysis. Wave propagation on transmission lines can be approached from an extension of circuit theory or from a specialization of Maxwell's equations. When both points of view are shown, it is easy to see that equations that describe wave propagation are very similar to those for plane wave propagation.
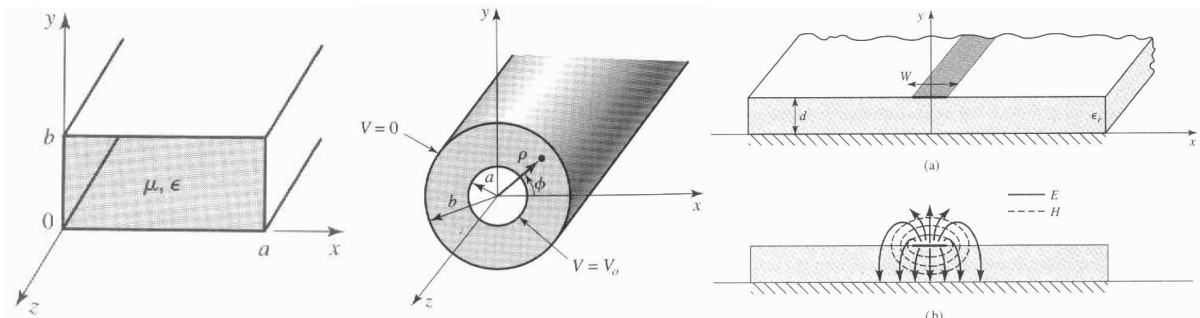
Figure 2.1: Waveguide, coaxial cable and microstrip line schematics, from [2], Chapter 3.

Characteristic	Coaxial	Waveguide	Strip-line	Microstrip
Preferred mode	TEM	TE_{10}	TEM	Quasi-TEM
Dispersion	None	Medium	None	Low
Bandwidth	High	Low	High	High
Loss	Medium	Low	High	High
Power capacity	Medium	High	Low	Low
Physical size	Large	Large	Medium	Small
Ease of fabrication	Medium	Medium	Easy	Easy
Ease of integration	Hard	Hard	Fair	Easy

Table 2.1: Comparison of common transmission lines and waveguides, from [2], Chapter 3.

2.2 Types of transmission lines

Main types of transmission lines and its characteristics are going to be shown now. The election of one or another is mainly due to the application given to it and for the most part, on the working frequency and the related insertion losses that the line will have at that frequency.

Waveguides.

Can be rectangular or circular and are used today for many different applications ranging in frequency from **1Ghz to 220Ghz**. Today, a lot of microwave circuitry is fabricated using planar transmission lines, such as microstrip and strip-line. This is done to be able to miniaturize the circuits, given than waveguides are big, expensive and complex to fabricate. However waveguides are still used in high-power systems, millimeter wave systems and in some precision test applications.

The waveguide can propagate Transverse Magnetic (TM) and Transverse Electric (TE) modes, but not Transverse Electro-Magnetic (TEM), since only one conductor is present. Also TM and TE modes have cutoff frequencies below which propagation is not possible.

Coaxial line.

Coaxial cable has a wire conductor in the center, a circumferential outer conductor and an insulating dielectric medium separating these two conductors. The outer conductor is usually sheathed in a protective PVC outer jacket.

The dimension and material of the conductors and insulation determine the cables characteristic impedance and attenuation at various frequencies. General working frequency is in the lower part of the spectrum, from **1Ghz to 10 Ghz**. It has a good bandwidth, it can manage medium power transmission and has low attenuation losses in the working band.

Planar transmission line.

There are several kinds like strip-line, microstrip, coplanar... They are made out of some conductors and its working band is in the low part of the spectrum, from **1Ghz to 10Ghz**. These

lines are compact, have a low cost and can be fabricated by lithographic processes, to be easily integrated with other passive or active devices.

They manage low power transmission and have high losses.

2.3   Lumped-element circuit model for a transmission line

Circuit analysis assumes that the physical dimensions of a network are much smaller than the electrical wavelength, while transmission lines may be a considerable fraction of a wavelength, or many wavelengths, in size. Thus **a transmission line is a distributed-parameter network**, where voltages and currents can vary in magnitude and phase over its length.

To model this behaviour, a transmission line is schematically represented as a two-wire line, since transmission lines (for TEM wave propagation) always have at least two conductors.

A line of infinitesimal length Δz can be modeled as a lumped-element circuit where R, L, G, C are per unit length quantities defined as:

R: series resistance per unit length, for both conductors, in Ω/m.

L: series inductance per unit length, for both conductors, in H/m.

G: shunt conductance per unit length, in S/m.

C: shunt capacitance per unit length, in F/m.

The series inductance **L** represents the total self-inductance and the shunt capacitance **C** is due to the close proximity of the two conductors.
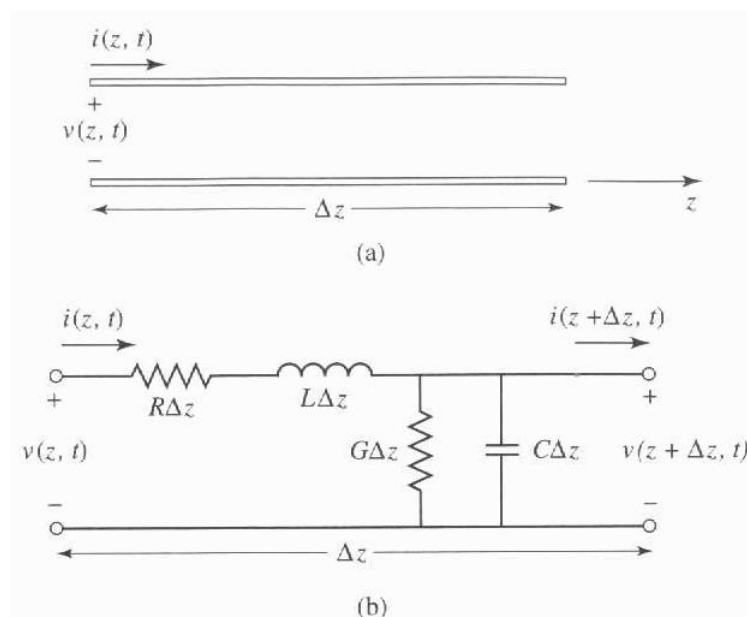
Figure 2.2: a) Definitions of voltage and current and b) equivalent circuit, for an incremental length of transmission line, from [2], Chapter 2.

Also, the series resistance **R** represents the resistance due to the finite conductivity of the conductors, and the shunt conductance **G** is due to dielectric loss in the material between conductors. Therefore both R and G represent loss.

With these ideas in mind, a finite length of transmission line can be viewed as a cascade of sections as shown in **Figure 2.2**. Where Kirchhoff's voltage and current law can be applied to give:

$$v(z,t) - R\Delta z\, i(z,t) - L\Delta z \frac{\partial i(z,t)}{\partial t} - v(z + \Delta z, t) = 0$$
$$i(z,t) - G\Delta z\, v(z + \Delta z, t) - C\Delta z \frac{\partial v(z + \Delta z, t)}{\partial t} - i(z + \Delta z, t) = 0$$

$$(2.1)$$

Dividing by Δz and taking the limit as $\Delta z \to 0$ gives the following differential equations:

$$\frac{\partial v(z,t)}{\partial z} = -R\, i(z,t) - L \frac{\partial i(z,t)}{\partial t}$$
$$\frac{\partial i(z,t)}{\partial z} = -G\, v(z,t) - C \frac{\partial v(z,t)}{\partial t}$$

$$(2.2)$$

For the sinusoidal steady-state condition, with cosine-based phasors, they can be simplified:

$$\frac{\partial V(z)}{\partial z} = -(R + jwL)\, I(z)$$
$$\frac{\partial I(z)}{\partial z} = -(G + jwC)\, V(z,t)$$

$$(2.3)$$

Obtaining equations that are very similar to Maxwell's curl equations.

2.3.1 Wave propagation on a transmission line

The two equations shown in the previous section can be solved simultaneously to give wave equations for $V(z)$ and $I(z)$ in our transmission line:

$$\frac{\partial^2 V(z)}{\partial z^2} - \gamma^2 V(z) = 0$$
$$\frac{\partial^2 I(z)}{\partial z^2} - \gamma^2 I(z) = 0$$

$$(2.4)$$

where γ is the complex propagation constant, which is a function of frequency.

$$\gamma = \alpha + j\beta = \sqrt{(R + jwL)(G + jwC)}$$

$$(2.5)$$

The result for the traveling wave solutions can be found as:

$$V(z) = V_0^+ e^{-\gamma z} + V_0^- e^{\gamma z}$$
$$I(z) = I_0^+ e^{-\gamma z} + I_0^- e^{\gamma z}$$

$$(2.6)$$

where $e^{-\gamma z}$ term represents wave propagation in the +z direction and the $e^{\gamma z}$ term represents wave propagation in the -z direction. From these equations you can obtain current, voltage and

characteristic impedance (Z_0) in the line. That can be defined as:

$$Z_0 = \frac{R + jwL}{\gamma} = \sqrt{\frac{R + jwL}{G + jwC}} \tag{2.7}$$

And converting back to the time domain, the voltage waveform can be expressed as:

$$v(z,t) = \left|V_0^+\right| cos(wt - \beta z + \phi^+)e^{-\alpha z} + \left|V_0^-\right| cos(wt + \beta z + \phi^-)e^{\alpha z} \tag{2.8}$$

where $\phi^{\pm}$ is the phase angle of the complex voltage $V_o^{\pm}$. And we find that the wavelength on the line and the phase velocity are:

$$\lambda = \frac{2\pi}{\beta} \qquad v_p = \frac{\omega}{\beta} = \lambda f \tag{2.9}$$

At this stage we have the characterization of the propagation of a wave inside a transmission line.

2.3.2 The lossless line

The above solution was for a general transmission line, including loss effects. In many practical cases, however, the loss of the line is very small and so can be neglected, resulting in a simplification of the above results. If we make $R = G = 0$, the propagation constant would be:

$$\gamma = \alpha + j\beta = 0 + jw\sqrt{LC} \tag{2.10}$$

So attenuation (α) would be zero and the characteristic impedance reduces to:

$$Z_0 = \sqrt{\frac{L}{C}} \tag{2.11}$$

Which is a real number, and the general solutions for voltage and current on a lossless transmission line can then be written simplified as:

$$V(z) = V_0^+ e^{-j\beta z} + V_0^- e^{j\beta z}$$
$$I(z) = \frac{V_0^+}{Z_0} e^{-j\beta z} + \frac{V_0^-}{Z_0} e^{j\beta z} \tag{2.12}$$

And the wavelength and phase velocity would be:

$$\lambda = \frac{2\pi}{\beta} = \frac{2\pi}{w\sqrt{LC}} \qquad v_p = \frac{\omega}{\beta} = \frac{1}{\sqrt{LC}} \tag{2.13}$$

Which is a simpler characterization of the line that can be used in case the loss is very small.

2.4   Microstrip transmission lines

Microstrip lines are one of the most popular types of planar transmission lines, primarily because they can be fabricated by photo-lithographic processes and are easily integrated with other passive and active microwave devices, elements such as diodes and transistors. This is why they are going to be the physical lines used in our system, and as such, they are going to be analytically characterized in detail in this section.

The structure of a microstrip line is presented in **Figure 2.3**. As seen in it, the presence of the dielectric, and the fact that it doesn't fill the air region above the strip, complicates the behavior and analysis of a microstrip line. It has some (usually most) of its field lines in the dielectric region, concentrated between the strip conductor and the ground plane, and some fraction of them in the air region above the substrate. For this reason the **microstrip line cannot support a pure TEM wave**, since the phase velocity of TEM fields in the air region is different from the one at the fields in the dielectric region. Thus, a phase match at the dielectric-air interface would be impossible to attain for a TEM wave.

The exact fields of a microstrip line constitute a **hybrid TM-TE wave**, and require advanced analysis techniques for its characterization. However, in most practical applications the dielectric substrate is electrically very thin ($d \ll \lambda$), and so the fields are **quasi-TEM**. With this simplification, fields are essentially the same as those of the static case. Thus, good approximations for the phase velocity, propagation constant and characteristic impedance can be obtained, simplifying the calculations.

In this structure, the phase velocity and propagation constant can be expressed as:

$$v_p = \frac{c}{\sqrt{\epsilon_e}} \qquad \beta = k_0\sqrt{\epsilon_e} \tag{2.14}$$

where ϵ_e is the effective dielectric constant of the microstrip line that satisfies the relation: $1 < \epsilon_e < \epsilon_r$, since some of the lines are in the dielectric region and some are in air. It is dependent on substrate thickness (d) and conductor width (W).
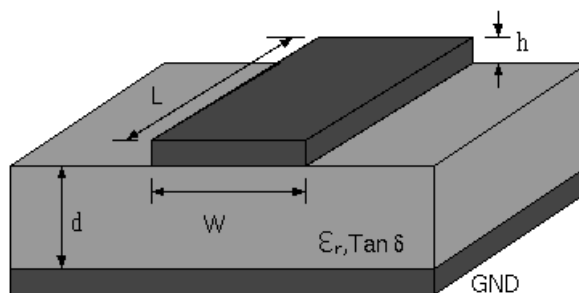
Figure 2.3: Microstrip dimensions scheme.

Effective dielectric constant, characteristic impedance and attenuation

The design formulas for the effective dielectric constant, characteristic impedance and attenuation of a microstrip line are going to be presented here. These equations are obtained from the application of a numerical method to obtain the solution of the capacitance per unit length of a microstrip line. And can be done solving the propagating wave equations in the structure, but it is out of the scope for this project and won't be presented here. Only the equations will be showed.

First, the effective dielectric constant of a microstrip line is given by:

$$\epsilon_e = \frac{\epsilon_r + 1}{2} + \frac{\epsilon_r - 1}{2} \frac{1}{\sqrt{1 + 12d/W}} \tag{2.15}$$

Which can be interpreted as the dielectric constant of a homogeneous medium that replaces the air and dielectric regions of the microstrip. The characteristic impedance can then be calculated as:

$$Z_0 = \begin{cases} \frac{60}{\sqrt{\epsilon_e}} ln(\frac{8d}{W} + \frac{W}{4d}) & for\, W/d \leq 1 \\[2em] \frac{120\pi}{\sqrt{\epsilon_e}[W/d + 1.393 + 0.667 ln(W/d + 1.444)]} & for\, W/d \geq 1 \end{cases} \tag{2.16}$$

And also, for a given characteristic impedance Z_0, dielectric constant ϵ_r, and h, the W/d ratio can be found as:

$$W/d = \begin{cases} \frac{8e^A}{e^{2A} - 2} & for\, W/d < 2 \\[1em] \frac{2}{\pi} \left[B - 1 - ln(2B - 1) + \frac{\epsilon_r - 1}{2\epsilon_r} \left\{ ln(B - 1) + 0.39 - \frac{0.61}{\epsilon_r} \right\} \right] & for\, W/d > 2 \end{cases} \tag{2.17}$$

where:

$$A = \frac{Z_0}{60} \sqrt{\frac{\epsilon_r + 1}{2}} + \frac{\epsilon_r - 1}{\epsilon_r + 1} \left(0.23 + \frac{0.11}{\epsilon_r} \right)$$

$$B = \frac{377\pi}{2Z_0\sqrt{\epsilon_r}}$$

And considering microstrip as a quasi-TEM line, the attenuation due to dielectric loss can be determined as:

$$\alpha_d = \frac{k_0\epsilon_r(\epsilon_e - 1)\, tan\delta}{2\sqrt{\epsilon_e}(\epsilon_r - 1)} \, (Np/m) \tag{2.18}$$

And the attenuation due to conductor loss is given approximately by:

$$\alpha_c = \frac{R_s}{Z_0 W} \, (Np/m) \tag{2.19}$$
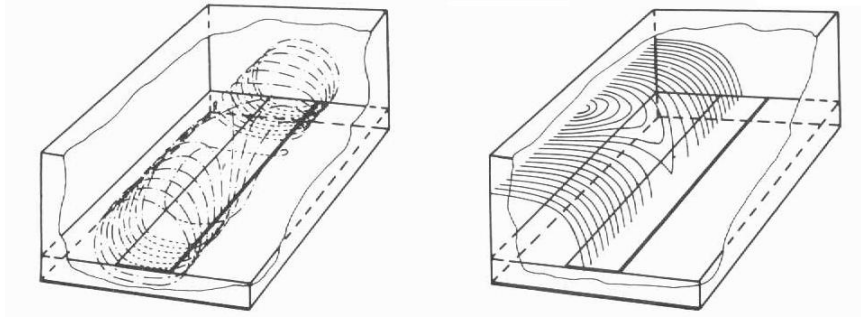
Figure 2.4: Microstrip magnetic (left) and electric (right) fields, from [3], Chapter 3.

where $R_s = \sqrt{\omega\mu_0/2\sigma}$ is the surface resistivity of the conductor. For most microstrip substrates, conductor loss is much more significant than dielectric loss, although there are some exceptions.

With these equations, the most important relations that characterize microstrip lines have been presented. With them, we can obtain the measurements they should have in case we want a certain value of impedance or vice versa. We will also be able to know the attenuation they will cause due to dielectric and conductor losses given by its $tan\delta$ and resistivity values respectively.

They are the first useful equations to design structures using microstrip technology that have been shown at the moment.

2.5   Coupled-line directional couplers

After microstrip lines, the basic component for microstrip coupled-lines band-pass filters, the **coupled-line directional coupler,** is going to be detailed in this section. It is the key part for the design of these filters, that can give a band-pass response, and be adjusted depending on the amount of them used (order of the filter) and its measurements. Which will give a different response and set different transmission zeros/poles in the band according to its physical arrangement.

When two unshielded transmission lines are close together, power can be coupled between the lines due to the interaction of the electromagnetic field of each line. Such lines are referred to as **coupled transmission lines**, and usually consist of three conductors in close proximity, although more conductors can be used.

Coupled transmission lines are usually assumed to operate in the TEM mode, which is rigorously valid for strip-line structures and approximately valid for microstrip structures. In general, a three-wire line can support two distinct propagating modes, what can be used to implement directional couplers, hybrids and filters.

Theory will be introduced first, then design data will be shown and the operation of a single-section of coupled-lines will be analyzed. These results will be then extended to cover filter design in **Chapter 5**.
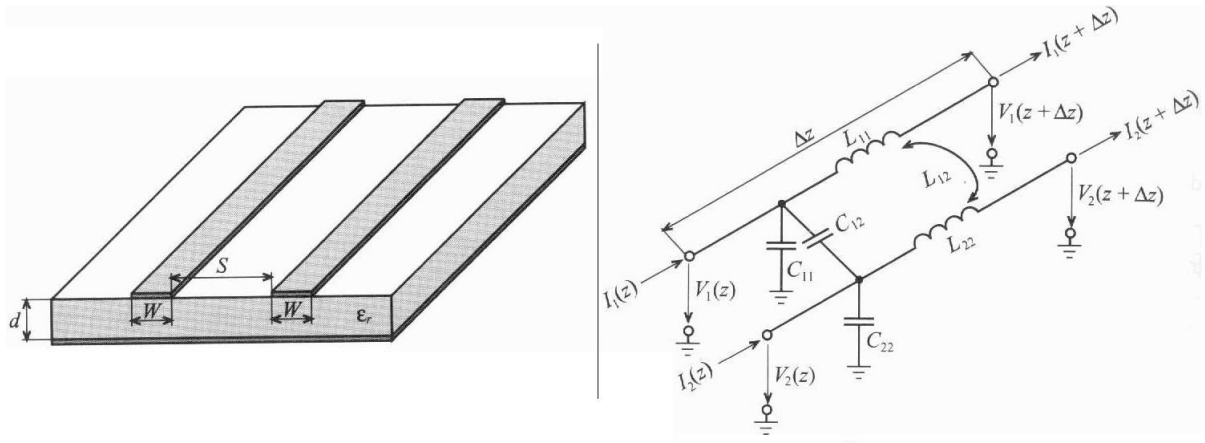
Figure 2.5: Coupled lossless microstrip transmission lines and equivalent circuit diagram with appropriate voltage and current definitions, from [4], Chapter 5.

2.5.1 Coupled line theory.

Coupled lines or any other three-wire line can be represented by the structure shown in **Figure 2.5**. If we assume TEM propagation, then the electrical characteristics of the coupled lines can be completely determined from the effective capacitances between the lines and the velocity of propagation on them.

A **modeling approach** of coupled microstrip line interaction is established when the geometry depicted in **Figure 2.6** is considered. With capacitive and inductive coupling phenomena between the lines and ground also presented.

In this structure, two lines of width W and negligible thickness, are separated over a distance S and attached to a dielectric medium of thickness d and dielectric constant ε_r. Here, it is possible to define an even and odd mode, dividing the problem in two different stages and defining voltage and currents such that:

$$V_e = \tfrac{1}{2}(V_1 + V_2) \qquad I_e = \tfrac{1}{2}(I_1 + I_2)$$
$$V_{od} = \tfrac{1}{2}(V_1 - V_2) \qquad I_{od} = \tfrac{1}{2}(I_1 - I_2)$$

(2.20)

When establishing the fundamental equations for two lines with even and odd modes of operation, we get a set of first-order, ordinary coupled differential equations as:

$$\begin{cases} -\frac{dV_e}{dz} = j\omega(L_{11} + L_{12})I_e \\\\ -\frac{dI_e}{dz} = j\omega(C_{11} + C_{12})V_e \end{cases}$$

$$\begin{cases} -\frac{dV_{od}}{dz} = j\omega(L_{11} - L_{12})I_{od} \\\\ -\frac{dI_{od}}{dz} = j\omega(C_{11} - C_{12})V_{od} \end{cases}$$

(2.21)

Even and odd modes are a key concept in our analysis at this stage. They allow to decouple the governing equations of coupled lines, dividing the problem and obtaining the characteristic
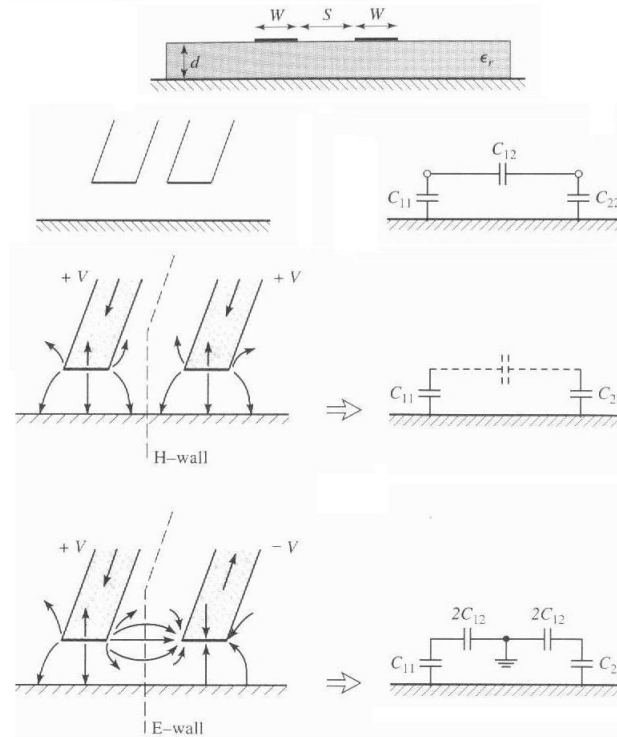
Figure 2.6: Three-wire coupled transmission line with even and odd mode excitations, and its equivalent capacitive networks, from [2], Chapter 7.

line impedances in terms of even and odd mode capacitances and respective phase velocities separately. They are very useful to obtain a good response characterization in an intuitive way, based in an equivalent structure that of the coupled-line section.

As depicted in **Figure 2.5**, C_{12} would represent the capacitance between the two strip conductors, while C_{11} and C_{22} represent the capacitance between one conductor and ground. If the strip conductors are identical in size and location relative to the ground conductor, then $C_{11} = C_{22}$.

For these coupled lines, there are two special types of excitations:

- **Even mode**, where the currents in the strip conductors are equal in amplitude and in the same direction.

- **Odd mode**, where the currents in the strip conductors are equal in amplitude and in opposite directions.

Both are also shown in **Figure 2.6**.

For the **even mode**, the electric field has even symmetry about the center line, and no current flows between the two strip conductors. This leads to the equivalent circuit shown, where C_{12} is open-circuited. The resulting capacitance of either line to ground for this mode is:

$$C_e = C_{11} = C_{22} \tag{2.22}$$

And assuming that the two strips conductors are identical in size and location, the characteristic impedance for the even mode is:

$$Z_{0e} = \sqrt{\frac{L}{C_e}} = \frac{\sqrt{LC_e}}{C_e} = \frac{1}{\nu_{pe}C_e} = \frac{\omega}{\beta_e C_e} \tag{2.23}$$

where ν_p is the phase velocity of propagation on the line.

For the **odd mode**, the electric field lines have an odd symmetry about the center line, and a null voltage exists between the two strip conductors. We can imagine this as a ground plane through the middle of C_{12}, which leads to the equivalent circuit shown. In this case, the effective capacitance between either strip conductor and ground is:

$$C_o = C_{11} + 2C_{12} = C_{22} + 2C_{12} \tag{2.24}$$

and the characteristic impedance for the odd mode is:

$$Z_{0o} = \sqrt{\frac{L}{C_o}} = \frac{\sqrt{LC_o}}{C_o} = \frac{1}{\nu_{po}C_o} = \frac{w}{\beta_o C_o} \tag{2.25}$$

Where ν_p and β are the phase velocity and phase constant, respectively, of the even and odd mode of the coupled line. Z_{0e} or Z_{0o} are the characteristic impedances of one of the strip conductors relative to ground when the coupled line is operated in the even or odd mode. An arbitrary excitation of a coupled line can always be treated as a superposition of appropriate amplitudes of even and odd modes.

If the lines are placed in a homogeneous medium of dielectric constant ϵ_r, the even and odd mode phase velocities are equal and given by:

$$\nu_{po} = \nu_{pe} = \frac{c}{\sqrt{\epsilon_r}}$$

However, if the lines are in an inhomogeneous dielectric medium (such as coupled microstrip lines), the even and odd mode phase velocities are, in general, different and given by:

$$\nu_{pe} = \frac{c}{\sqrt{\epsilon_{ree}}}$$

$$\nu_{po} = \frac{c}{\sqrt{\epsilon_{reo}}}$$

where ϵ_{ree} and ϵ_{reo} are defined as the even and odd mode effective dielectric constants respectively, and can be determined using:

$$\epsilon_{ree} = \frac{C_e}{C_{0e}}$$

$$\epsilon_{reo} = \frac{C_o}{C_{0o}}$$

where C_{0e} and C_{0o} denote the even and odd mode capacitance of either line obtained by replacing the relative permittivity of the surrounding dilectric material by unity. C_e and C_o denote the corresponding capacitances in the presence of the inhomogeneous dielectric medium.

Using the previous equations, the characteristic impedances reduce to:

$$Z_{0e} = \frac{1}{c\sqrt{C_e C_{0e}}}$$
$$Z_{0o} = \frac{1}{c\sqrt{C_o C_{0o}}}$$

(2.26)

For **quasi-TEM lines**, such as microstrip, results of capacitances per unit can be obtained numerically or by approximate quasi-static techniques.

For symmetric coupled microstrip lines, a design graph like the one shown in the **Appendix, Table 9.7**, can be used to determine the necessary strip widths and spacing for a given set of characteristic impedances, Z_{0e} and Z_{0o}. But these results do not scale with dielectric constant, so design graphs must be made for a specific value of this parameter.

Another difficulty with microstrip coupled lines is that the **phase velocity is usually different for the two modes of propagation**, since the two modes operate with different field configurations near the air-dielectric interface. This will occur because the even mode has less fringing field in the air region than the odd mode. Thus its effective dielectric constant should be higher, indicating a smaller phase velocity for the even mode. This effect will have a degrading effect on coupler directivity.

Therefore, the main parameters describing the properties of the quasi-TEM mode of coupled microstrip lines are the effective dielectric constants of the odd and even modes. These constants determine both propagation constants and characteristic impedances of the even and odd modes, Z_{0e} and Z_{0o}, which in the end dictate the response of these kind of sections.

2.6   Conclusions

In this chapter, the basic transmission lines have been presented. The **lumped-elements circuit model for transmission lines** has been explained, putting the emphasis in the microstrip line, which is the one being used in our filters design.

With the equations presented for microstrip lines, it is possible to calculate the dimensions of a required microstrip section, knowing the substrate's characteristics, to obtain a certain impedance at a certain frequency. This way we have the **basic tools to design and build basic microstrip sections** with a specific behavior, which is the first step towards the design of microstrip circuits.

Then with the **coupled-lines theory** and the characterization of a directional coupler shown, the equations to obtain the behaviour for a coupled-line section were also explained. They were based in quasi-TEM modes and the even and odd modes ocurring in the structure, that model its behaviour.

But equations describing **quasi-TEM modes** are only valid in the 2 to 4Ghz frequency range for a 1mm thick substrate, and up to 8Ghz for a 0.5mm thick substrate. When these limits are exceeded, it is necessary to take into account the frequency dispersion of the effective dielectric constant and the shift in value of the characteristic impedance with frequency. Working at higher frequencies adds complexity and limitations to the microstrip line design. [11]

This type of coupling is best suited for weak couplings, as tight coupling requires lines that are too close together to be practical, or a combination of even and odd mode characteristic impedances than is non-realizable.

But taking into account the limitations for microstrip design, it is possible to develop **high frequency microstrip filters** with the important tools and equations that will be shown in the next chapters, taking the steps towards the completion of microstrip filters design.

3

Microwave network analysis.

3.1   Introduction

Circuits operating at low frequencies, which have small dimensions relative to the wavelength of the signals we are working with, can be treated as an interconnection of lumped passive or active components with unique voltages and currents defined at any point in the circuit. In this situation the circuit dimensions are small enough so that there is negligible phase change from one point in the circuit to another. Fields can be then considered as TEM supported by two or more conductors. This leads to quasi-static type of solution to **Maxwell's equations**, and to the well-known Kirchhoff voltage and current laws and impedance concepts of circuit theory.

This powerful and useful set of techniques for analyzing low-frequency circuits is, however, not directly applicable to microwave circuits, although circuit and network concepts can be extended to handle many microwave analysis and design problems of practical interest. The reason to do this is to take the much easier way of applying simple and intuitive ideas of circuit analysis instead of solving Maxwell's equations for the same microwave problem.

Usually the **solution to Maxwell's equation is too complex**, giving us electric and magnetic fields at all points in space. But we usually are interested only in voltage or current at a set of terminals, the power flow through a device, or some other type of global quantity, as opposed to a detailed description of the response at all points in space.

This is the reason why in this chapter we are going to concentrate on detailing the basic procedure for microwave network analysis, which is the application of the concepts of **circuit theory to high frequency systems design**, and that will be a key idea in the design and characterization of microwave filters.

To be able to obtain a network matrix of a defined system, first a set of basic and standard electromagnetic problems are analyzed rigorously, using field analysis and Maxwell's equations. Doing so, it is possible to obtain quantities directly related to a circuit or transmission line

25

parameter. This allows the **element to be treated as a distributed component** characterized by its length, propagation constant and characteristic impedance. At that point it is possible to interconnect various components and use network and/or **transmission line theory to analyze the behavior of the entire system** of components, without needing in detail characterization of each one.

So, lets start speaking about network matrices, a main idea behind microwave filter characterization.

3.2   Network matrix

In practice, many microwave networks consist of a cascade connection of two or more two-port networks. In this case it is convenient to define a 2x2 transmission, or ABCD matrix, for each two-port network. We will then see that the **ABCD matrix** of the cascade connection of two or more two-port networks can be easily found by multiplying the ABCD matrices of the individual two-ports. These are the main needed tools to characterize a microwave filter, giving us an idea on how the system works by knowing the relationship between the input introduced and the output we are going to obtain of a set of boxes, network matrices.
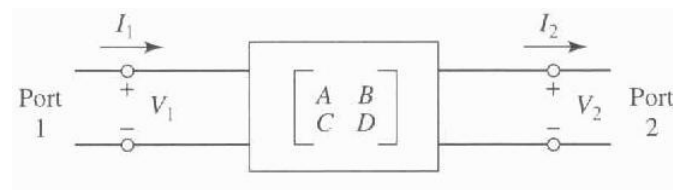
Figure 3.1: A two-port network, from [2], Chapter 4.

The ABCD matrix is defined for the two-port network shown in **Figure 3.1** in terms of the total voltage and current as shown:

$$\begin{cases} V_1 = AV_2 + BI_2 \\ I_1 = CV_2 + DI_2 \end{cases} \tag{3.1}$$

or in matrix form as:

$$\begin{bmatrix} V_1 \\ I_1 \end{bmatrix} = \begin{bmatrix} A & B \\ C & D \end{bmatrix} \begin{bmatrix} V_2 \\ I_2 \end{bmatrix} \tag{3.2}$$

We have to mention that this equation is for a two-port network where I_2 is defined as a flow going out of port 2, for it to be coincident with the next current that flows into the adjacent network if we are dealing with a cascade network. In case we only want to analyze a single isolated network, I_2 will be a flow entering port 2, which would make it have a negative sign in both equations, $-I_2$.
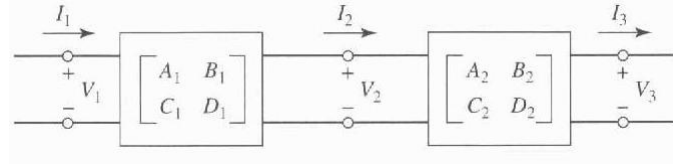
Figure 3.2: A cascade connection of two two-ports networks, from [2], Chapter 4.

If we need to analyze this cascade connection of two two-port network as shown in **Figure 3.2**, we have that:

$$\begin{bmatrix} V_1 \\ I_1 \end{bmatrix} = \begin{bmatrix} A_1 & B_1 \\ C_1 & D_1 \end{bmatrix} \begin{bmatrix} V_2 \\ I_2 \end{bmatrix}$$

$$\begin{bmatrix} V_2 \\ I_2 \end{bmatrix} = \begin{bmatrix} A_2 & B_2 \\ C_2 & D_2 \end{bmatrix} \begin{bmatrix} V_3 \\ I_3 \end{bmatrix}$$

To obtain the matrix of the cascade connection, we substitute one in the other, which equals the product of the ABCD matrices of the individual two-port networks

$$\begin{bmatrix} V_1 \\ I_1 \end{bmatrix} = \begin{bmatrix} A_1 & B_1 \\ C_1 & D_1 \end{bmatrix} \begin{bmatrix} A_2 & B_2 \\ C_2 & D_2 \end{bmatrix} \begin{bmatrix} V_3 \\ I_3 \end{bmatrix}$$

Note that the order of multiplication of the matrix must be the same as the order in which the networks are arranged, since matrix multiplication is not commutative in general.

3.3 Relation to Impedance Matrix

In a similar way as with ABCD matrices, it is also possible to describe a system network by means of and **admittance or impedance matrix**, giving a relationship between voltage and current in the circuit by means of impedance (Z) or admittance (Y).

Where for the different ports, as shown in **Figure 3.3**, the relationship would be:

$$\left\{ \begin{array}{c} v_1 \\ v_2 \\ \vdots \\ v_N \end{array} \right\} = \{Z\} \left\{ \begin{array}{c} i_1 \\ i_2 \\ \vdots \\ i_N \end{array} \right\} \qquad \left\{ \begin{array}{c} i_1 \\ i_2 \\ \vdots \\ i_N \end{array} \right\} = \{Y\} \left\{ \begin{array}{c} v_1 \\ v_2 \\ \vdots \\ v_N \end{array} \right\}$$

Being Z and Y matrices of the form:

$$Z = \left\{ \begin{array}{cccc} Z_{11} & Z_{12} & \cdots & Z_{1N} \\ Z_{21} & Z_{22} & \cdots & Z_{2N} \\ \vdots & \vdots & \ddots & \vdots \\ Z_{N1} & Z_{N2} & \cdots & Z_{NN} \end{array} \right\} \qquad Y = \left\{ \begin{array}{cccc} Y_{11} & Y_{12} & \cdots & Y_{1N} \\ Y_{21} & Y_{22} & \cdots & Y_{2N} \\ \vdots & \vdots & \ddots & \vdots \\ Y_{N1} & Y_{N2} & \cdots & Y_{NN} \end{array} \right\}$$

$$where: \quad Z_{nm} = \frac{v_n}{i_m}\Big|_{i_k=0} \qquad\qquad where: \quad Y_{nm} = \frac{i_n}{v_m}\Big|_{v_k=0}$$
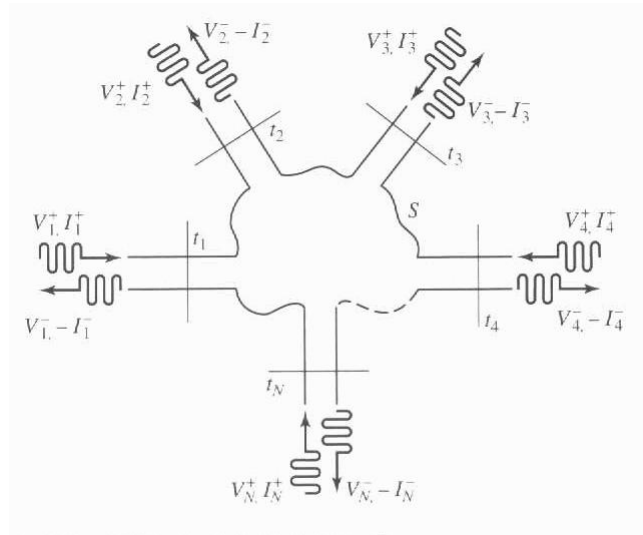
Figure 3.3: Arbitrary N port microwave network, from [2], chapter 4 .

Knowing the Z parameters of a network, it is possible to determine the ABCD parameters. Thus, from the definition of the ABCD parameters in 3.2 on page 26 and from the defining relations of the Z parameters, for the case of a two-port network we have:

$$\begin{cases} V_1 = I_1 Z_{11} - I_2 Z_{12} \\ V_2 = I_1 Z_{21} - I_2 Z_{22} \end{cases} \tag{3.3}$$

And we have that the relation would be:

$$A = \left.\frac{V_1}{V_2}\right|_{I_2=0} = \frac{Z_{11}}{Z_{21}} \qquad B = \left.\frac{V_1}{I_2}\right|_{V_2=0} = \frac{Z_{11}Z_{22}-Z_{12}Z_{21}}{Z_{21}}$$

$$C = \left.\frac{I_1}{V_2}\right|_{I_2=0} = \frac{1}{Z_{21}} \qquad D = \left.\frac{I_1}{I_2}\right|_{V_2=0} = \frac{Z_{22}}{Z_{21}}$$

Two port microwave networks are so frequent in practice that the use of equivalent circuits to represent them is widely used. Useful conversions between different two port networks parameters are included in the **Appendix on page v**.

By using terminal planes and characterization by direct measurement, the properties of the different two port "black boxes" can be represented in terms of **network parameters Z, Y, S and ABCD**. It is also useful to replace the black box by an equivalent circuit containing a few idealized components that give a similar response to that of the system being studied. Obtaining models that can be combined easily inside complex systems.

Some important properties of network matrices are:

- If the network is reciprocal[1] then $Z_{12} = Z_{21}$, and these equations can be used to show the relation between AD and BC which is: $AD - BC = 1$.

---

[1]A reciprocal network is one in which the power losses are the same between any two ports regardless of direction of propagation (scattering parameter S21=S12, S13=S31, etc.)

- If the network is symmetrical then $A = D$.

- And if the network has no losses, then A and D will be pure real and B and C will be pure imaginary.

3.4 Scattering parameters

In all technical literature regarding Radio Frequency (RF) systems, the scattering or **S-parameters representation** plays a central role. These are of big importance because practical system characterizations can no longer be accomplished through simple open- or short-circuit measurements, as it is normally done in low-frequency applications.

When we reach higher working frequencies even a wire itself will present an inductance that can be of substantial magnitude and affect the whole circuit response. Even with an open circuit, we will also have capacitive loading at the terminal, and so open/short-circuit conditions needed to determine **ABCD parameters** can no longer be guaranteed. Moreover, when dealing with wave propagation phenomena, it is not desirable to introduce a reflection coefficient with magnitude near or equal unity. Because this discontinuity will cause undesirable voltage and/or current wave reflections, leading to oscillations which will affect our network response.

With the **S-parameters**, RF engineers have a very useful tool to characterize the two-port network description of practically all RF devices without requiring unachievable terminal conditions.

3.4.1 Definition

S-parameters are power wave descriptors that allow us to define the input-output relations of a network in terms of incident and reflected power waves at desired point in the circuit as shown in **Figure 3.4**.

We define an incident normalized power wave a_n and a reflected normalized power wave b_n as:

$$\begin{cases} a_n = \frac{1}{2\sqrt{Z_0}}(V_n + Z_0 I_n) \\ \\ b_n = \frac{1}{2\sqrt{Z_0}}(V_n - Z_0 I_n) \end{cases} \tag{3.4}$$

where the n index refers to port 1 or 2 and Z_0 is the characteristic impedance of the connecting lines on the input and output sides of the network. We will assume for simplicity that both impedance have the same value.

With the above formulas we can obtain the following voltage, current and power expressions:

$$\begin{cases} V_n = \sqrt{Z_0}(a_n + b_n) \\ \\ I_n = \frac{1}{\sqrt{Z_0}}(a_n - b_n) \end{cases} \tag{3.5}$$
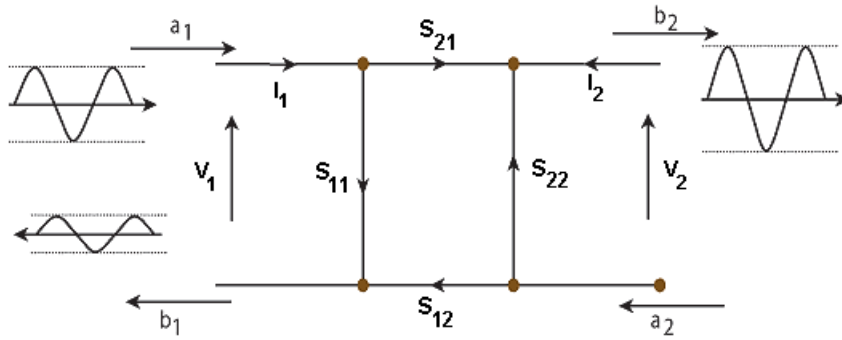
Figure 3.4: Convention used to define S-parameters for a two port network.

$$P_n = \frac{1}{2}Re\left\{V_n I_n^*\right\} = \frac{1}{2}Re\left\{|a_n|^2 - |b_n|^2 + (b_n a_n^* - b_n^* a_n)\right\} = \frac{1}{2}\left(|a_n|^2 - |b_n|^2\right) \tag{3.6}$$

Where $(b_n a_n^* - b_n^* a_n)$ is purely imaginary, and physically we can obtain that the average power delivered through port n is equal to the power in the incident wave minus the power in the reflected wave.

So, the definition of a generalized scattering matrix (S-parameters matrix) would be:

$$\left\{\begin{array}{c} b_1 \\ b_2 \\ \vdots \\ b_M \end{array}\right\} = \left[\begin{array}{cccc} S_{11} & S_{12} & \cdots & S_{1M} \\ S_{21} & S_{22} & \cdots & S_{2M} \\ \vdots & \vdots & \ddots & \vdots \\ S_{M1} & S_{M2} & \cdots & S_{MM} \end{array}\right] \left\{\begin{array}{c} a_1 \\ a_2 \\ \vdots \\ a_M \end{array}\right\} \tag{3.7}$$

$$where: \quad S_{ij} = \left.\frac{b_i}{a_j}\right|_{ak=0}$$

And for a two-port network:

$$\left\{\begin{array}{c} b_1 \\ b_2 \end{array}\right\} = \left[\begin{array}{cc} S_{11} & S_{12} \\ S_{21} & S_{22} \end{array}\right] \left\{\begin{array}{c} a_1 \\ a_2 \end{array}\right\} \tag{3.8}$$

This matrix is known as dispersion or S-parameters matrix where term definitions are:

$$S_{11} = \left.\frac{b_1}{a_1}\right|_{a_2=0} = \frac{reflected\,power\,wave\,at\,port\,1}{incident\,power\,wave\,at\,port\,1}$$

$$S_{21} = \left.\frac{b_2}{a_1}\right|_{a_2=0} = \frac{transmited\,power\,wave\,at\,port\,2}{incident\,power\,wave\,at\,port\,1}$$

$$S_{22} = \left.\frac{b_2}{a_2}\right|_{a_1=0} = \frac{reflected\,power\,wave\,at\,port\,2}{incident\,power\,wave\,at\,port\,2} \tag{3.9}$$

$$S_{12} = \left.\frac{b_1}{a_2}\right|_{a_1=0} = \frac{transmited\,power\,wave\,at\,port\,1}{incident\,power\,wave\,at\,port\,2}$$

The conditions $a_2 = 0$ and $a_1 = 0$ imply that no power waves are returned to the network

at either port 2 or port 1. This can only be ensured when the connecting transmission lines are terminated into their characteristic impedance.

As with the ABCD parameters, in case the network analyzed has some special characteristics, the parameters will meet certain properties:

- If the network is reciprocal, then $S_{12} = S_{21}$.

- If the network is symmetrical then additionally $S_{11} = S_{22}$,.

- For a passive network with no losses, transmitted and reflected powers must equal incident power, meeting the following equations:

$$|S_{21}|^2 + |S_{11}|^2 = 1$$
$$|S_{12}|^2 + |S_{22}|^2 = 1$$

(3.10)

And if we generalize these properties for multi-port networks, we obtain:

- If the network is passive then every matrix element has a module smaller than unity: $|S_{jk}| < 1$

- If the network is reciprocal then: $|S| = |S^t| \Leftrightarrow S_{ij} = S_{ji}$

We can also express the normalized input and output waves in terms of time averaged power, using the voltage, current and power expressions in conjunction with S parameters, as they are closely related to power relations:

$$P_1 = \frac{1}{2} \frac{|V_1^+|^2}{Z_0} \left(1 - |\Gamma_{in}|^2 \right) = \frac{1}{2} \frac{|V_1^+|^2}{Z_0} \left(1 - |S_{11}|^2 \right)$$

(3.11)

where the reflection coefficient at the input side is expressed in terms of S_{11}under matched output according to:

$$\Gamma_{in} = \frac{V_1^-}{V_1^+} = \left. \frac{b_1}{a_1} \right|_{a_2=0} = S_{11}$$

(3.12)

And we can also define the Voltage Standing Wave Ratio (VSWR) at port 1 in terms of S_{11} as:

$$VSWR = \frac{1 + |S_{11}|}{1 - |S_{11}|}$$

(3.13)

VSWR gives us a measure of how well a load is impedance-matched to a source.

Furthermore, we can identify the incident and reflected power, obtaining the total power at port 1(under matched output conditions):

$$P_1 = P_{inc} + P_{ref} = \frac{1}{2} \left(|a_1|^2 - |b_1|^2 \right) = \frac{|a_1|^2}{2} \left(1 - |\Gamma_{in}|^2 \right)$$

(3.14)
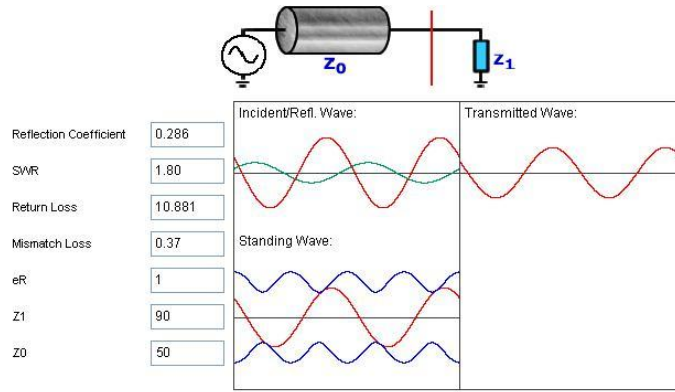
Figure 3.5: Voltage standing wave ratio representation.

And the same idea applies in case of $S_{11} = 0$, where all available power from the source is delivered to port 1 of the network.

$$P_2 = \frac{1}{2}\left(|a_2|^2 - |b_2|^2\right) = \frac{|a_2|^2}{2}\left(1 - |\Gamma_{out}|^2\right) \tag{3.15}$$

3.4.2 Meaning of S-parameters

As already mentioned in previous section, S-parameters can only be determined under conditions of perfect matching on the input or output side. In order to record S_{11} and S_{21} we have to ensure that on the output side the line impedance Z_0 is matched, to be $a_2 = 0$.

As shown in **Figure 3.6**, this configuration allows to compute S_{11} by finding the **input reflection coefficient**:

$$S_{11} = \Gamma_{in} = \frac{Z_{in} - Z_0}{Z_{in} + Z_0} \tag{3.16}$$

And with port 2 properly terminated we have:

$$S_{21} = \left.\frac{b_2}{a_1}\right|_{a_2=0} = \left.\frac{\frac{V_2^-}{\sqrt{Z_0}}}{\frac{(V_1 + Z_0 I_1)}{2\sqrt{Z_0}}}\right|_{I_2^+ = V_2^+ = 0} \tag{3.17}$$

Replacing V_1 by the generator voltage V_{G1} minus the voltage drop over the source impedance Z_0, then the expression $V_{G1} - Z_0 I_1$ gives:
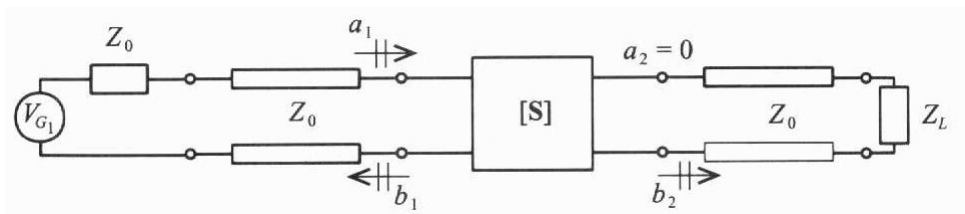
Figure 3.6: Measurement of S_{11} and S_{21} by matching Z_0 to Z_L at port 2, from [4] Chapter 4.

$$S_{21} = \frac{2V_2^-}{V_{G1}} = \frac{2V_2}{V_{G1}} \tag{3.18}$$

The voltage at port 2 is related to the generator voltage, and thus specifies the **forward voltage gain** of the network, and if we square it, we would obtain **forward power gain**:

$$G_0 = |S_{21}|^2 = \left| \frac{2V_2}{V_{G1}} \right|^2 \tag{3.19}$$

If we reverse the measurement procedure and attach a generator voltage V_{G2} to port 2 and properly terminate port 1, as shown in **Figure 3.7,** we can then determine S_{22} and S_{12}:

To compute S_{22} we need to find the output reflection coefficient Γ_{out} in a similar way as already done with S_{11}:

$$S_{22} = \Gamma_{out} = \frac{Z_{out} - Z_0}{Z_{out} + Z_0} \tag{3.20}$$

And for :

$$S_{12} = \left. \frac{b_1}{a_2} \right|_{a_1=0} = \left. \frac{\frac{V_1^-}{\sqrt{Z_0}}}{\frac{(V_2+Z_0 I_2)}{2\sqrt{Z_0}}} \right|_{I_1^+=V_1^+=0} \tag{3.21}$$

The term S_{12} can be simplified by substituting V_2 by $V_{G2} - Z_0 I_2$ giving:

$$S_{12} = \frac{2V_1^-}{V_{G2}} = \frac{2V_1}{V_{G2}} \tag{3.22}$$

known as the **reverse voltage gain** of the network, obtaining **reverse power gain** if we square it:

$$G_r = |S_{12}|^2 = \left| \frac{2V_1}{V_{G2}} \right|^2 \tag{3.23}$$

These parameters are the ones we are able to measure when we work at microwave frequencies and are highly useful to describe system behavior.
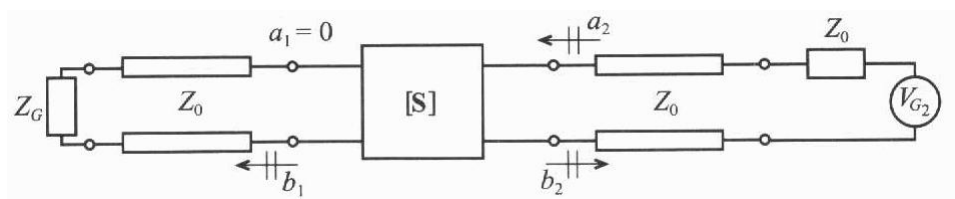
Figure 3.7: Measurement of S_{22} and S_{12} by matching Z_0 to Z_G at port 1, from [4] Chapter 4.

3.5   Conclusions

The main basic ideas and useful parameters behind **microwave networks** have been covered in this chapter, showing an useful way to characterize microwave components and combine them in more complex circuits, having a way to calculate its final behavior using network matrices.

The theoretical basics behind **transmission lines characterization** that allows to obtain a detailed EM description of the components was also covered in the previous chapter, so with both of these important tools, we can now go on and concentrate in **applying them to the microwave filter design field**, which we will start covering in the next chapter.

We will make use of these important concepts to develop and define the process of microwave filter design. We will explain what are the main techniques for microwave filter design, how to apply them, and finally obtain a theoretical prototype that will then be converted to a physical structure.

4

Microwave filters design.

4.1   Introduction

A **microwave filter** is a two-port network used to control the frequency response at a certain point in a microwave system. It provides transmission at frequencies within the pass-band of the filter and attenuation in the rest of the band, the stop-band. Typical frequency responses include low-pass, high-pass, bandpass and band-reject characteristics.

Microwave filter theory and practice began in the years preceding World War II. The image parameter method of filter design was developed in the late 1930s and was useful for low-frequency filters in radio and telephony. In the early 1950s a group at Stanford Research Institute, consisting of G. Matthaei, L. Young, S. Cohn and others, became very active in microwave filter and coupler development. Many good publications where the result of these investigations and some of them are still valuable references in the field.

Today, most **microwave filter design** is done with sophisticated computer-aided design (CAD) packages, but based on the insertion loss method, developed during these years. Microwave filter design is still these days a very active research area due to the advancements in network synthesis with distributed elements, low temperature semiconductors and the use of active devices in filtering circuits. Much research is done nowadays to enhance and simplify filter design methods and its results, improving them for higher frequencies, low cost materials and new applications.

The perfect filter would have infinite attenuation in the stop-band, and zero insertion loss with a linear phase response (to avoid signal distortion) in the pass-band. Of course, such filters do not exist in practice, so compromises must be made, and that is the main part of filter design.

Two main methods were developed to achieve best results and are, still today, being used. The **image parameter design method** is the simpler method for filter design and it was also the first developed. It was developed from the knowledge acquired from periodic structures
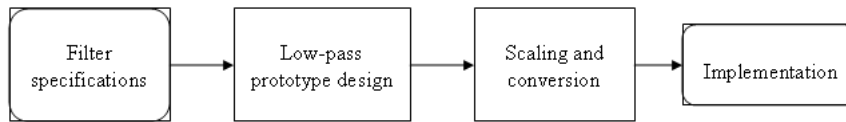
Figure 4.1: Filter design flow chart.

consisting of a cascade of two port networks, given they exhibit basic passband and stopband responses that are easily analyzed and can be reproduced specifying a desired passband and stopband characteristics. Using this cascade of simpler two-port filter sections it is possible to obtain the desired cutoff frequencies and attenuation characteristics, but it is not possible to specify a frequency response over the complete operating range.

Although relatively simple, it has the disadvantage that an arbitrary frequency response cannot be incorporated into the design. Also the design procedure must often be iterated many times to achieve the desired results. Anyway the method is still very useful for simple filters and provides a link between basic infinite periodic structures and practical filter design. It also finds application nowadays in solid-state traveling-wave amplifiers and slow wave components design.

On the other side, we have the **insertion loss design method**, a more modern design procedure that uses network synthesis techniques to design filters with a completely specified frequency response. The design is simplified by beginning with low-pass filter prototypes that are normalized in terms of impedance and frequency. Then, transformations are applied to convert the prototype design to the desired frequency range and impedance level.

This method improved the main problems of image parameter, where once we had the final design configuration, there was no clear way to improve it to fit our needs in that particular design. On the contrary, insertion loss method allows a high degree of control over the passband and stopband amplitude and phase characteristics, with a systematic way to synthesize a desired response. In all cases the insertion loss method allows filter performance to be improved in a straightforward way, using a higher order filter (more reactive elements in the design) at the expense of a more complex final configuration.

The necessary tradeoffs can be evaluated to best meet the application requirements. A Chebyshev response is able to satisfy the sharpest cutoff response needed, or a better phase response can be obtained by using a linear phase design. It all depends on the goals we need to meet.

To finish this introduction, it is important to say that both methods provide in the end lumped elements filters. And for microwave applications, such designs must usually be modified to use distributed elements consisting of transmission lines we can fabricate, as we mentioned on the introduction of this project. To this end, Richard's transformation and Kuroda identities provide the tools to take this step.

4.2   Filter parameters

In analyzing the various trade-offs when dealing with filters, the following parameters play key roles, giving information of its main characteristics:

- **Insertion loss:** ideally, a perfect filter would introduce no power loss in the passband. It would have zero insertion loss. But in reality we have to expect a certain amount of power loss associated with the filter. The insertion loss quantifies how much below the 0dB line the power amplitude response drops.

$$IL = 10 \log P_{LR} = 10 \log \frac{P_{in}}{P_L} = -10 \log(1 - |\Gamma_{in}|^2) \tag{4.1}$$

Being P_{in} the input power from the source, P_L the power delivered to the load and Γ_{in} the reflection coefficient looking into the filter.

- **Ripple:** the flatness of the signal in the passband can be quantified by specifying the ripple or difference between maximum and minimum amplitude response in dB. Chebyshev filter response allows us to control the magnitude of the ripple.

- **Bandwith:** for a bandpass filter, it is the difference between upper and lower frequencies typically recorded at the 3dB attenuation points above the passband.

$$BW^{3dB} = f_u^{3dB} - f_L^{3dB} \tag{4.2}$$

- **Shape factor:** this factor describes the sharpness of the filter response by taking the ratio between the 60dB and the 3dB bandwidths:

$$SF = \frac{BW^{60dB}}{BW^{3dB}} = \frac{f_u^{60dB} - f_L^{60dB}}{f_u^{3dB} - f_L^{3dB}} \tag{4.3}$$

- **Rejection:** for an ideal filter we would obtain infinite attenuation level for the undesirable signal frequencies. However, in reality we expect an upper bound due to the deployment of a finite number of filter components. Practical designs often specify 60dB as the rejection rate since it can readily be combined with the shape factor.

In **Figure 4.2** the filter parameters are best illustrated by way of a generic bandpass attenuation profile. The magnitude of the filter's attenuation behavior is plotted with respect to the normalized frequency Ω, being center frequency f_c normalized to $\Omega = 1$ and 3dB lower and upper cut-off frequencies symmetric with respect to this center frequency.
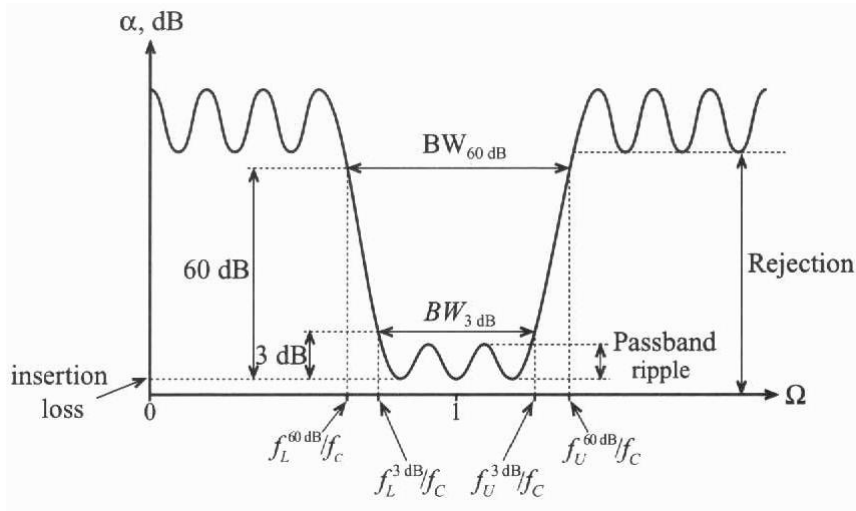
Figure 4.2: Generic attenuation profile for a bandpass filter, from [4], Chapter 5.

Quality factor

One additional parameter describing the selectivity of the filter is **quality factor Q**, which generally defines the ratio of the average stored energy to the energy loss per cycle at the resonant frequency:

$$
\begin{aligned}
Q &= w \left. \frac{average\,stored\,energy}{energy\,loss\,per\,duty\,cycle} \right|_{w=w_c} = \\
&= w \left. \frac{average\,stored\,energy}{power\,loss} \right|_{w=w_c} = w \left. \frac{W_{stored}}{P_{loss}} \right|_{w=w_c}
\end{aligned}
\tag{4.4}
$$

This can be best seen by viewing the filter as a two-port network connected to a source at the input side and a load at the output.

It is then possible to consider the power loss as the loss associated with the external load and the filter itself. The resulting quality factor is named **loaded Q**, or Q_{LD}. Interestingly, if we take the inverse of the loaded Q, we see that:

$$
\frac{1}{Q_{LD}} = \frac{1}{w} \left(\frac{power\,loss\,in\,filter}{average\,stored\,energy} \right)\Bigg|_{w=w_r} + \frac{1}{w} \left(\frac{power\,loss\,in\,load}{average\,stored\,energy} \right)\Bigg|_{w=w_r}
\tag{4.5}
$$

Since the total power loss is comprised of the power losses due to the presence of the filter and the load. This can be written as:

$$
\frac{1}{Q_{LD}} = \frac{1}{Q_F} + \frac{1}{Q_E} \qquad or \qquad Q_{LD} = \frac{f_c}{f_U^{3dB} - f_L^{3dB}} \equiv \frac{f_c}{BW^{3dB}}
\tag{4.6}
$$

where Q_F and Q_E are the **filter Q** and the **external Q**. And f_c is the resonance frequency of the filter.
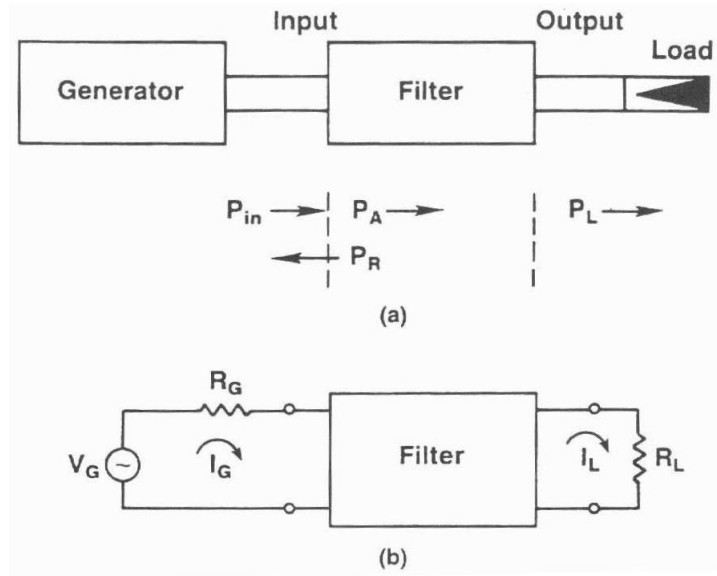
Figure 4.3: General filter network configuration and equivalent circuit for power-transfer calculations, from [5], Chapter 9.

4.3   Filter design by the insertion loss method

Insertion loss is the most used method to design filters and it is going to be explained in detail in this section. This will be the first step in the design of the filter. [12]

To model the desired filter response, a **polynomial transfer function** such as Butterworth, Chebyshev or Bessel is used following the insertion loss method. This will give a response with the emphasis in certain characteristics that will be detailed in the next section, **practical filter responses**.

The choose of one or another response will result in a combination of inductors and capacitors of values g_1, g_2, g_3, ... g_n that will render in a **low-pass filter** that can be normalized to 1Ω and a 1 rad cutoff frequency. After that, it is simply a matter of **scaling the g values** of the elements to obtain the desired frequency response and insertion loss of the filter. These will depend on the needs of our particular design.

To obtain other filter types such as high-pass, bandpass and band-stop, a **frequency transformation** is needed in addition to the scaling to obtain the desired characteristics.

To complete the design of a filter by the insertion loss method, the filter response has to be first defined by its insertion loss, or power loss ratio, P_{LR}.

$$P_{LR} = \frac{Power\,available\,from\,source}{Power\,delivered\,to\,load} = \frac{1}{1 - |\Gamma(w)|^2} \tag{4.7}$$

This quantity is the reciprocal of $|S_{12}|^2$ if both load and source are matched. And given that a filter is a passive (no active elements inside the filter) and reciprocal network, then $|S_{12}| = |S_{21}|$.

The insertion loss (IL) in dB is:

$$IL = 10 \log P_{LR} \tag{4.8}$$

The reflection coefficient magnitude $|\Gamma(\omega)|^2$ is an even function of ω ($|\Gamma(\omega)|^2 = |\Gamma(-\omega)|^2$). Therefore it can be expressed as a polynomial in ω^2:

$$\left|\Gamma(w)\right|^2 = \frac{M(w^2)}{M(w^2) + N(w^2)} \tag{4.9}$$

Where M and N are real polynomials in ω^2. Substituting this form in equation 4.7 gives the following:

$$P_{LR} = 1 + \frac{M(w^2)}{N(w^2)} \tag{4.10}$$

For a filter to be physically realizable its power loss ratio must be of the form shown above in equation 4.10, but any kind of $\Gamma(w)$ function is not valid, because specifying the power loss ratio, simultaneously constrains the reflection coefficient, $\Gamma(w)$.

With some details to take into account, this is the final aspect of the transfer function that the filter must have for it to satisfy our specifications and be realizable. Next step is to fulfill those polynomials with the required type of response according to our needs. [13]

4.4   Practical filter responses

Depending on which factor we want to put the emphasis on, we will decide to use one or another **filter response** for our design. Depending on the amount of insertion loss we can deal with, the maximum ripple amplitude, the bandwidth necessary for the passband, the shape factor (sharpness of the filter response) and rejection coefficient (amount of the rejection rate on the stopband) we will choose one or another.

Maximally flat or Butterworth

It is an optimum response in the sense that it provides the flattest possible passband response for a given filter order. It is obtained by derivation of the normalized element values, L and C. The response would be specified by:

$$P_{LR} = 1 + k^2 (\frac{\omega}{\omega_c})^{2N} \tag{4.11}$$

where N is the order of the filter, and ω_c is the cutoff frequency. The passband extends from $\omega = 0$ to $\omega = \omega_c$. With $\omega > \omega_c$, the attenuation increases linearly with frequency, as shown in **Figure 4.4**. The insertion loss increases at the rate of of 20N dB/decade.

The Butterworth prototype values can be calculated from **equations 4.12** but are also tabulated in **Table 9.4**, in the **Appendix**.
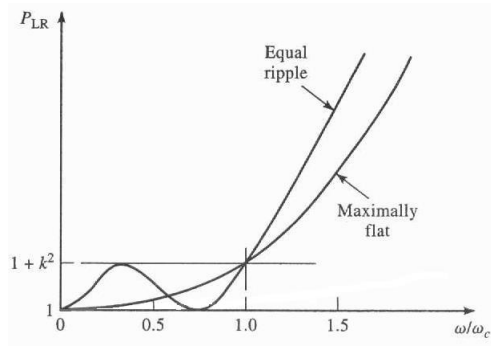
Figure 4.4: Maximally flat and equal-ripple low-pass filter responses comparison for N=3, from [2], Chapter 8.

$$g_0 = 1$$

$$g_l = 2sin(\frac{(2l-1)\pi}{2n}) \qquad l = 1, 2, ... n$$
$$\vdots$$
$$g_{n+1} = 1 \qquad for\,all\,n \tag{4.12}$$

And then these values can be easily scaled to obtain a maximally flat low pass filter, with the desired filter input termination resistance R and cutoff frequency $\omega_1 = 2\pi f_1$ as:

$$L = gR/\omega_1$$

$$C = g/(\omega_1 R)$$

However, if another type of response is needed, as it is our case where we want to obtain a band-pass one, then a frequency scaling would be needed in addition. This is going to be explained in detail in the next section.

Equal ripple or Chebyshev

For this response, a Chebyshev polynomial is used to specify the insertion loss of an N-order low-pass filter as:

$$P_{LR} = 1 + k^2 T_N^2(\frac{\omega}{\omega_c}) \tag{4.13}$$

This response will give a sharper cutoff than a maximally flat one, although the passband response will have ripples of amplitude $1 + k^2$, since $T_N(x)$ oscillates between ± 1.

For large x, $T_N(x) = \frac{1}{2}(2x)^N$, so for $\omega \gg \omega_c$ the insertion loss becomes:

$$P_{LR} = \frac{k^2}{4}(\frac{2\omega}{\omega_c})^{2N} \tag{4.14}$$

which also increases at the rate of 20N dB/decade. But the insertion loss for the Chebyshev case is $(2^{2N})/4$ greater than the binomial response at any given frequency $\omega \gg \omega_c$.

The Chebyshev prototype values can be calculated from equations below but are also tabulated, as shown in **Table 9.3** in the **Appendix**. With the cutoff frequency defined as the ripple value, the low-pass prototype g values are:

$$g_0 = 1$$

$$g_1 = \frac{2a_1}{\gamma}$$

$$\vdots$$

$$g_k = \frac{4a_{k-1}a_k}{b_{k-1}g_{k-1}} \qquad k = 2, 3, \dots n \qquad (4.15)$$

$$\vdots$$

$$g_{n+1} = 1 \qquad for\, n\, odd$$

$$g_{n+1} = coth^2(\beta/4) \qquad for\, n\, even$$

where:

$$a_k = sin\left[\frac{(2k-1)\pi}{2n}\right] \qquad k = 1, 2, \dots n$$

$$b_k = \gamma^2 + sin^2\left(\frac{k\pi}{n}\right) \qquad k = 1, 2, \dots n$$

$$\beta = ln\left(coth\frac{A_c}{17.37}\right) \qquad (4.16)$$

$$\gamma = sinh\left(\frac{\beta}{2n}\right)$$

In general, a ripple value level A_c in the 0.01 to 0.2dB range is used.

Other responses.

There are other frequency responses that can be used for the design of filters, like for example the **elliptic function** and **linear phase.** But these filter responses are not going to be detailed here because they weren't considered for our designs.

As the specifications for our filters were not very tight, without a strict cutoff rate nor linear phase response required, only the ones explained here, Butterworth and Chebyshev responses, were considered as suitable for our designs. That's why we only analyze and show those two. For other responses details see [4, 9, 2].

Once the values for the coefficients are calculated, we have defined the **lumped elements of the low pass filter ladder prototype**. From this prototype, conversions will be done to obtain the response at the necessary frequency and with realizable values for the components, as will be shown in the next section.

Different conversions will then be needed depending on what technology is used to actually build the filter. In our case, where we use coupled-lines sections in microstrip, the required process will be covered in the next chapter.
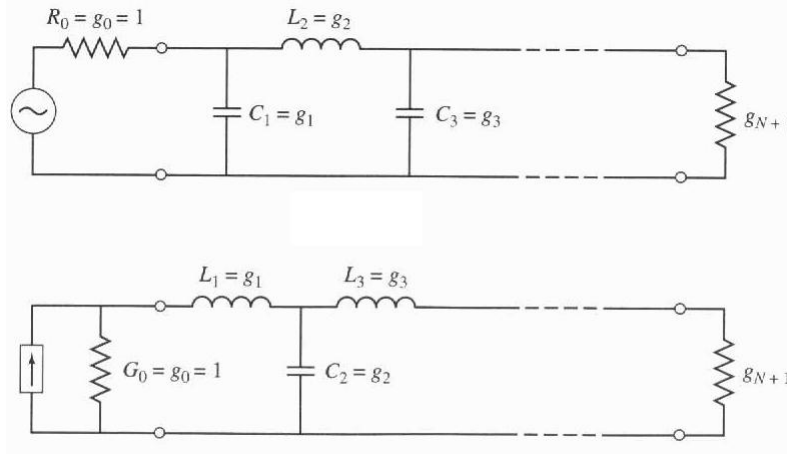
Figure 4.5: Ladder circuits for low-pass filter prototypes and their element definitions, from [2], chapter 8.

4.5 Filter prototype

The defined **low pass filter ladder prototype** with lumped elements values obtained, will look like the one in **Figure 4.5**. These are numbered, with the filter having N reactive elements, that alternate between series and shunt connections being defined as:

$$
\begin{aligned}
g_0 &=
\begin{cases}
generator\ resistance\ (first\ network) \\
generator\ conductance\ (second\ network)
\end{cases} \\[2em]
\begin{matrix} g_k \\ (k = 1\,to\,N) \end{matrix} &=
\begin{cases}
inductance\ for\ series\ inductors \\
capacitance\ for\ shunt\ capacitors
\end{cases} \\[2em]
g_{N+1} &=
\begin{cases}
load\ resistance\ if\ g_N\ is\ a\ shunt\ capacitor \\
load\ conductance\ if\ g_N\ is\ a\ series\ inductor
\end{cases}
\end{aligned}
\tag{4.17}
$$

Both circuits can be considered as the dual of each other, and both will give the same response. The use of one or another will mostly depend on the easier conversions that could be done to obtain the simpler and realizable filter structure with the required response.

In addition, it will be necessary to **determine the size, or order, of the filter**. This is usually dictated by the insertion loss at some frequency in the stopband of the filter. It can be obtained looking at tables that show the attenuation characteristics in dB for various orders (N) versus normalized frequency $\left(\left| \frac{\omega}{\omega_c} \right| - 1 \right)$. This tables, for both Butterworth and Chebyshev responses can be seen in the **Appendix**, **tables 9.6 and 9.5**.

The next step, after we know the order we need for the filter and the values of the coefficients, would be to make the necessary conversions, first to scale the response in frequency, and second to obtain realizable values for elements in terms of resistance, inductance and capacitance.

4.6   Filter transformation

With the low pass filter prototypes already calculated, the problem is that they correspond to a normalized design having a source impedance of $R_s = 1\Omega$ and a cutoff frequency of $\omega_c = 1$. In this section it is going to be explained how to scale these designs in terms of impedance and frequency. This way we will have the response converted to give a bandpass characteristic at the required characteristic impedance, which is what we are going to need for our filters.

Impedance scaling

In the prototype design, the source and load resistances are unity (except for equal-ripple filters with even N, which have non unity load resistance). A source resistance of R_0 can be obtained by multiplying the impedances of the prototype design by R_0. Then, if we let primes denote impedances scaled quantities, we have the new filter component values given by:

$$
\begin{aligned}
L' &= R_0 L \\
C' &= \frac{C}{R_0} \\
R'_s &= R_0 \\
R'_L &= R_0 R_L
\end{aligned}
\tag{4.18}
$$

Where L, C, and R_L are the component values for the original prototype, and the obtained component values L', C', and R'_L will be the values for the final elements of the filter being built.

Frequency scaling

To obtain the required pass-band response from our low pass filter prototype the following calculations will have to be done, replacing the elements for the low pass prototype with the ones obtained from the conversion. With ω_1 and ω_2 denoting the edges of the required passband, then a bandpass response can be obtained using the following frequency substitution:

$$
\frac{1}{\Delta}\left(\frac{\omega}{\omega_0} - \frac{\omega_0}{\omega}\right) \rightarrow \omega
\tag{4.19}
$$

where:

$$
\Delta = \frac{\omega_2 - \omega_1}{\omega_0}
$$

is the fractional bandwidth of the passband. The center frequency is ω_0, and can be chosen as the geometric mean of ω_1 and ω_2 as $\omega_0 = \sqrt{\omega_1 \omega_2}$.

Then the transformation maps the low-pass filter prototype response for $\omega_c = 1$ to the bandpass response as shown in **Figure 4.6** as follows:
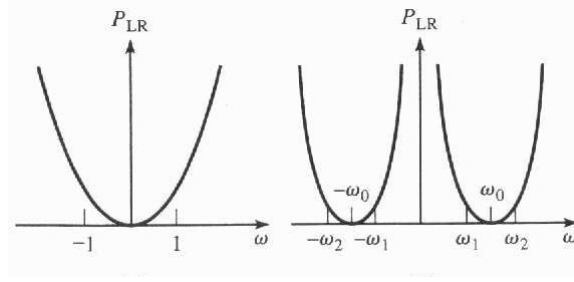
Figure 4.6: Bandpass frequency transformation, from [2], Chapter 8.

When $\omega = \omega_0$, $\frac{1}{\Delta}\left(\frac{\omega}{\omega_0} - \frac{\omega_0}{\omega}\right) = 0$

When $\omega = \omega_1$, $\frac{1}{\Delta}\left(\frac{\omega}{\omega_0} - \frac{\omega_0}{\omega}\right) = \frac{1}{\Delta}\left(\frac{\omega_1^2 - \omega_0^2}{\omega_0\omega_1}\right) = -1$

When $\omega = \omega_2$, $\frac{1}{\Delta}\left(\frac{\omega}{\omega_0} - \frac{\omega_0}{\omega}\right) = \frac{1}{\Delta}\left(\frac{\omega_2^2 - \omega_0^2}{\omega_0\omega_2}\right) = 1$

And the new filter elements are determined by using (4.19) in the expressions for the series reactance and shunt susceptances.

$$jX_k = \frac{j}{\Delta}\left(\frac{\omega}{\omega_0} - \frac{\omega_0}{\omega}\right)L_k = j\frac{\omega L_k}{\Delta\omega_0} - j\frac{\omega_0 L_k}{\Delta\omega} = j\omega L'_k - j\frac{1}{\omega C'_k}$$

which shows that a series inductor, L_k, is transformed to a series LC circuit with element values:

$$L'_k = \frac{L_k}{\Delta\omega_0}$$
$$C'_k = \frac{\Delta}{L_k\omega_0}$$

(4.20)

And similarly.

$$jB_k = \frac{j}{\Delta}\left(\frac{\omega}{\omega_0} - \frac{\omega_0}{\omega}\right)C_k = j\frac{\omega C_k}{\Delta\omega_0} - j\frac{\omega_0 C_k}{\Delta\omega} = j\omega C'_k - j\frac{1}{\omega L'_k}$$

which shows that a shunt capacitor, C_k, is transformed to a shunt LC circuit with element values:

$$L'_k = \frac{\Delta}{C_k\omega_0}$$
$$C'_k = \frac{C_k}{\Delta\omega_0}$$

(4.21)

These equivalent circuits are shown in **Table 4.1**. The low pass filter elements are converted to series resonant circuits (low impedance at resonance) in the series arms, and to parallel resonant circuits (high impedance at resonance) in the shunt arms. Both will have a resonant frequency of ω_0.
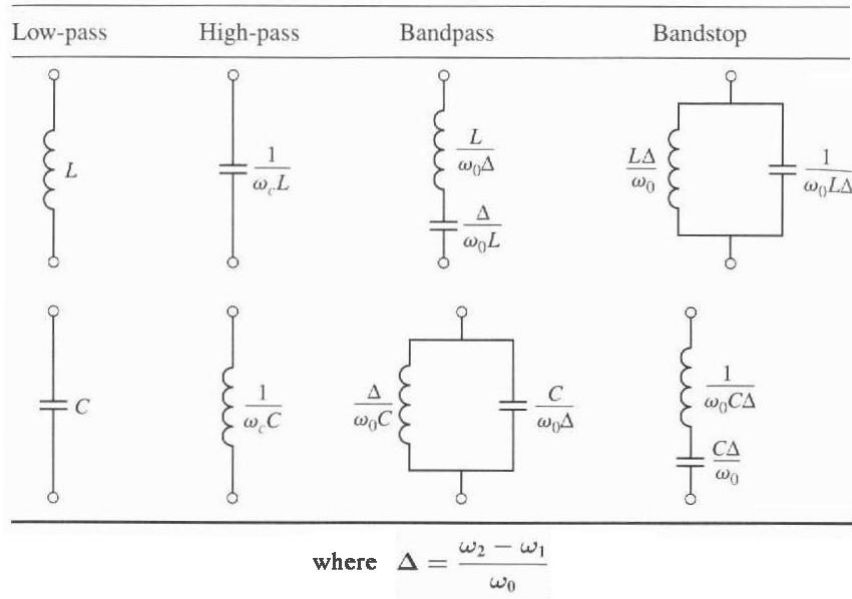
Table 4.1: Prototype filter transformations, from [2], Chapter 8.

4.7 Conclusions

In this chapter, the main theoretical concepts of filter design have been explained. This way, the base in which the calculations to design our filters rely on were given. The theoretical method behind it was shown, **insertion loss**, and then the corresponding transformation to obtain a **prototype with the required characteristics** that we need. With the required frequency and impedance conversions, that dictate the pass and rejection bands of the filter, and other parameters like shape and steepness.

Once the prototype is obtained, the next step is its physical design, obtaining the **physical dimensions of the filter**. But the method to convert this prototype into a physically buildable design depends on the technology being used, because a microwave filter can be built using many different materials, types of transmission lines and configurations, and depending on them, the necessary equations and calculations will be different.

In our case, as we are going to rely in coupled-line sections, the next chapter will give details on how these sections work, and what calculations are necessary to obtain a **coupled-line sections bandpass filter** prototype that matches the calculated requirements obtained using the equations described in this chapter.

Finally, after all the theoretical design is accomplished, and the physical measurements are obtained, it is necessary to **simulate it, using a CAD program** that will confirm the results, and make sure that the final behavior of the filter will be as expected. If this doesn't happen, modifications can be done with these programs to obtain the required results. These final steps will be explained in **Chapter 6**, where details are given in the simulation and final construction process of the filter.

5

Coupled-line bandpass filters.

5.1   Introduction

Parallel-coupled transmission lines can be used to construct many types of filters. They are the main piece for the construction of our band-pass filters and allow to obtain a certain frequency response, setting transmission poles at the desired frequency points. It also allows for a gradual improvement of the response as complexity is increased, by using a higher level filter with an increasing number of sections, that will more accurately model our desired response with steeper rejection rates.

By contrast, previously used direct-coupled resonator filters tended to have excessive lengths and can be reduced significantly in size by the use of parallel-coupled lines. Since this results in much tighter coupling, greater bandwidths are possible. But for these designs, it must be taken into account that the first spurious response occurs at two to three times the center frequency, depending upon the media. This may not be important for the system where the filters will be integrated, but in the opposite case, it will be a main problem that will have to be addressed.

Fabrication of **multi-section bandpass** or band-stop **coupled-line filters** is particularly easy in microstrip or strip-line form for bandwidths less than 20%. Wider bandwidth filters generally require very tightly coupled-lines, which are difficult to fabricate, but it all depends on the fabrication technology being used. With separations for microstrip technology that can be fabricated as small as of 0.05 mm.

In this chapter, it will first be shown the filter characteristics of a **single quarter-wave coupled-line section**, which is the basic block used to build our filters. Then it will be shown how these sections can be used to design bandpass filters with all related equations and procedures explained. [12]
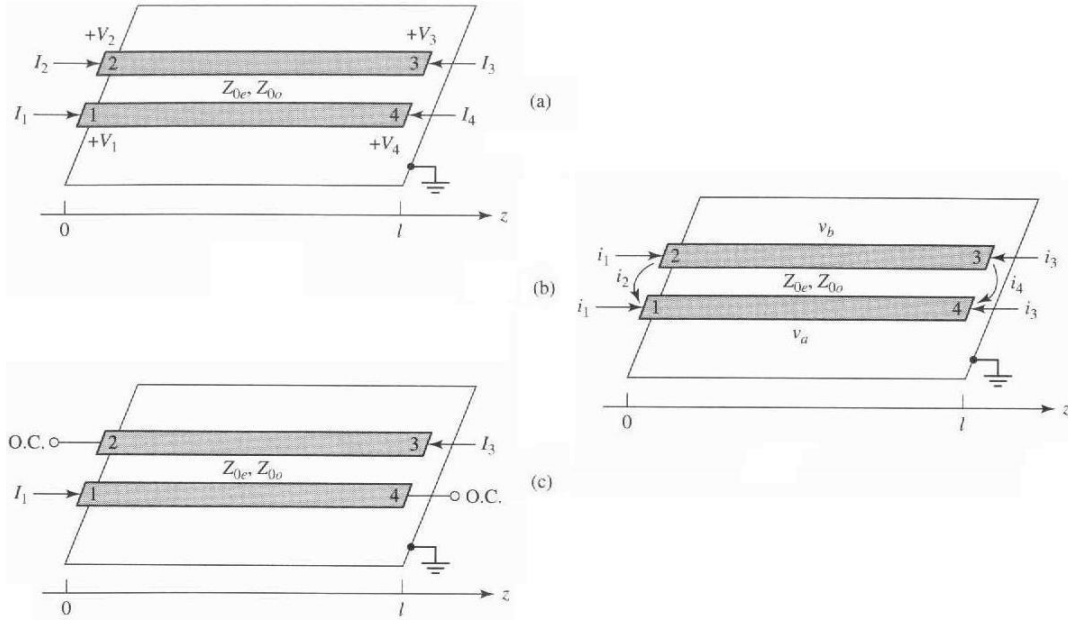
Figure 5.1: Parameters definition for a coupled-line section. a) Voltage and current, b) Even and odd mode current sources and c) section with a bandpass response. From [2], Chapter 8.

5.2 Filter properties of coupled-line sections

We will start showing the properties of a single coupled-line section, with port voltage and current definitions. The open-circuit impedance matrix for this four-port network will be obtained by considering the superposition of even and odd mode excitations, which are shown in **Figure 5.1.**

Th current sources i_1 and i_3 drive the line in the even mode, while i_2 and i_4 drive the line in the odd mode. By superposition, it is seen that the total port currents, I_i, can be expressed in terms of the even and odd mode currents as:

$$\begin{aligned}
I_1 &= i_1 + i_2 \\
I_2 &= i_1 - i_2 \\
I_3 &= i_3 - i_4 \\
I_4 &= i_3 + i_4
\end{aligned} \tag{5.1}$$

First consider the **line as being driven in the even mode by the i_1 current sources**. If the other ports are open-circuited, the impedance seen at port 1 or 2 is:

$$Z_{in}^e = -jZ_{0e}cot\beta l \tag{5.2}$$

The voltage on either conductor can be expressed as:

$$v_a^1(z) = v_b^1(z) = V_e^+[e^{-j\beta(z-l)} + e^{j\beta(z-l)}] = 2V_e^+cos\beta(l-z) \tag{5.3}$$

so the voltage at port 1 or 2 is:

$$v_a^1(0) = v_b^1(0) = 2V_e^+ cos\beta l = i_1 Z_{in}^e \tag{5.4}$$

This result and equation 5.2 can be used to rewrite equation 5.3 in terms of i_1 as:

$$v_a^1(z) = v_b^1(z) = -jZ_{0e}\frac{cos\beta(l-z)}{sin\beta l}i_1 \tag{5.5}$$

And the voltages due to current sources i_3 driving the line in the even mode are:

$$v_a^3(z) = v_b^3(z) = -jZ_{0e}\frac{cos\beta z}{sin\beta l}i_3 \tag{5.6}$$

Now consider the **line as being driven in the odd mode by current** i_2. If the other ports are open-circuited, the impedance seen at port 1 or 2 is:

$$Z_{in}^o = -jZ_{0o}cot\beta l \tag{5.7}$$

The voltage on either conductor can be expressed as:

$$v_a^2(z) = -v_b^2(z) = V_0^+[e^{-j\beta(z-l)} + e^{j\beta(z-l)}] = 2V_0^+cos\beta(l-z) \tag{5.8}$$

Then the voltage at port 1 or port 2 is:

$$v_a^2(0) = -v_b^2(0) = 2V_0^+cos\beta l = i_2 Z_{in}^o \tag{5.9}$$

This result and equation 5.7 can be used to rewrite equation 5.9 in terms of i_2 as:

$$v_a^2(z) = -v_b^2(z) = -jZ_{0o}\frac{cos\beta(l-z)}{sin\beta l}i_2 \tag{5.10}$$

Similarly, the voltages due to current i_4 driving the line in the odd mode are:

$$v_a^4(z) = -v_b^4(z) = -jZ_{0o}\frac{cos\beta z}{sin\beta l}i_4 \tag{5.11}$$

And the total voltage at port 1 is:

$$V_1 = v_a^1(0) + v_a^2(0) + v_a^3(0) + v_a^4(0) = -j(Z_{0e}i_1 + Z_{0o}i_2)cot\theta - j(Z_{0e}i_3 + Z_{0o}i_4)csc\theta \tag{5.12}$$

where the results of equations 5.5, 5.6, 5.10 and 5.11 were used, and $\theta = \beta l$.

As the next step, equations 5.1 can be solved for the different i_j in terms of the Is:

Circuit	Image Impedance	Response
	$Z_{i1} = \dfrac{2Z_{0e}Z_{0o}\cos\theta}{\sqrt{(Z_{0e}+Z_{0o})^2\cos^2\theta - (Z_{0e}-Z_{0o})^2}}$ $Z_{i2} = \dfrac{Z_{0e}Z_{0o}}{Z_{i1}}$	Low pass
	$Z_{i1} = \dfrac{2Z_{0e}Z_{0o}\sin\theta}{\sqrt{(Z_{0e}-Z_{0o})^2 - (Z_{0e}+Z_{0o})^2\cos^2\theta}}$	Bandpass
	$Z_{i1} = \dfrac{\sqrt{(Z_{0e}-Z_{0o})^2 - (Z_{0e}+Z_{0o})^2\cos^2\theta}}{2\sin\theta}$	Bandpass
	$Z_{i1} = \dfrac{\sqrt{Z_{0e}Z_{0o}}\,\sqrt{(Z_{0e}-Z_{0o})^2 - (Z_{0e}+Z_{0o})^2\cos^2\theta}}{(Z_{0e}+Z_{0o})\sin\theta}$ $Z_{i2} = \dfrac{Z_{0e}Z_{0o}}{Z_{i1}}$	Bandpass

Table 5.1: Different coupled-line circuit configurations and responses, from [2], Chapter 8.

$$i_1 = \tfrac{1}{2}(I_1 + I_2)$$

$$i_2 = \tfrac{1}{2}(I_1 - I_2)$$

$$i_3 = \tfrac{1}{2}(I_3 + I_4) \tag{5.13}$$

$$i_4 = \tfrac{1}{2}(I_4 - I_3)$$

and use these results in equation 5.12:

$$V_1 = \frac{-j}{2}(Z_{0e}I_1 + Z_{0e}I_2 + Z_{0o}I_1 - Z_{0o}I_2)cot\theta - \frac{j}{2}(Z_{0e}I_3 + Z_{0e}I_4 + Z_{0o}I_4 - Z_{0o}I_3)csc\theta \tag{5.14}$$

This result gives the top row of the open-circuit impedance matrix [Z] that describes the coupled-line section. From symmetry, all other matrix elements can be found once the first row is known. And they are:

$$Z_{11} = Z_{22} = Z_{33} = Z_{44} = \tfrac{-j}{2}(Z_{0e} + Z_{0o})cot\theta$$

$$Z_{12} = Z_{21} = Z_{34} = Z_{43} = \tfrac{-j}{2}(Z_{0e} - Z_{0o})cot\theta$$

$$Z_{13} = Z_{31} = Z_{24} = Z_{42} = \tfrac{-j}{2}(Z_{0e} - Z_{0o})csc\theta \tag{5.15}$$

$$Z_{14} = Z_{41} = Z_{23} = Z_{32} = \tfrac{-j}{2}(Z_{0e} + Z_{0o})csc\theta$$

A two-port network can be formed from coupled-line sections by terminating two of the four ports in either open or short circuits. There are ten possible combinations, with different
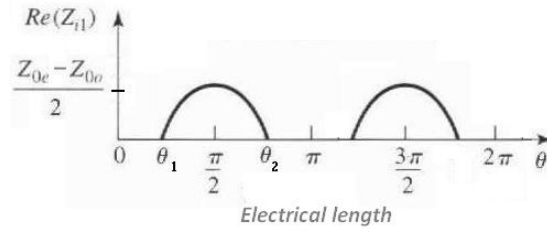
Figure 5.2: Real part of the image impedance of the bandpass open-circuited coupled-line network, from [2], Chapter 8.

frequency responses, including low-pass, band-pass, all pass and all stop. But for band-pass filters we are only interested in three of them, which are shown in **Table 5.1**, discarding all-pass and all-stop configurations. From these bandpass configurations, we are most interested in the case of open circuits terminations, as they are easier to fabricate than short circuits.

For the case of open circuits, $I_2 = I_4 = 0$, so the four-port impedance matrix equations reduce to:

$$V_1 = Z_{11}I_1 + Z_{13}I_3$$
$$V_3 = Z_{31}I_1 + Z_{33}I_3$$
(5.16)

where Z_{ij} is given in equation 5.15.

We can analyze the filter characteristics of this circuit by calculating the image impedance (which is the same at ports 1 and 3), and the propagation constant.

Generically, the image impedance in terms of the Z-parameter is:

$$Z_i = \sqrt{Z_{11}^2 - \frac{Z_{11}Z_{13}^2}{Z_{33}}} = \frac{1}{2}\sqrt{(Z_{0e} - Z_{0o})^2 csc^2\theta - (Z_{0e} + Z_{0o})^2 cot^2\theta} \qquad (5.17)$$

And when the coupled-line section is $\lambda/4$ long ($\theta = \pi/2$), the image impedance can be reduced to:

$$Z_i = \frac{1}{2}(Z_{0e} - Z_{0o}) \qquad (5.18)$$

which is real and positive, since $Z_{0e} > Z_{0o}$. But when $\theta \to 0$ or π, then $Z_i \to \pm j\infty$, indicating a stopband.

The real part of the image impedance is shown in **Figure 5.2**, where the cutoff frequencies can be found as:

$$cos\theta_1 = -cos\theta_2 = \frac{Z_{0e} - Z_{0o}}{Z_{0e} + Z_{0o}} \qquad (5.19)$$

And the propagation constant can be calculated as:

$$cos\beta = \sqrt{\frac{Z_{11}Z_{33}}{Z_{13}^2}} = \frac{Z_{11}}{Z_{13}} = \frac{Z_{0e} + Z_{0o}}{Z_{0e} - Z_{0o}}cos\theta \qquad (5.20)$$

which shows β is real for $\theta_1 < \theta < \theta_2$, where $\theta_2 = \pi - \theta_1$ and $\cos\theta_1 = (Z_{0e} - Z_{0o})/(Z_{0e} + Z_{0o})$.

At this points we have the characterization of a coupled-line section, its amplitude response and cutoff frequencies and also its propagation constant. We also showed that they are real, so they can be calculated and used to describe the response in a real filter.

5.3   Design equations for coupled-lines bandpass filters.

The design of parallel-coupled line filters was formulated by Cohn [14] and has been refined over the years for different types of designs. For a typical **n section parallel-coupled filter**, the values of the low pass prototype g_0, g_1, g_2, $g_3 ... g_{n+1}$ for either maximally flat or equal-ripple response have to be computed using equations 4.12 or 4.15. Then, as shown in **Figure 5.3**, the filter is assembled from **n+1 sections of equal length ($\lambda/4$) at the center frequency**, giving a structure of n resonators. The electrical design is specified by the even and odd mode characteristics impedances Z_{0o} and Z_{0e} on the parallel conductors. Using these impedances, the transmission line dimensions of each section can be determined.

Bandpass filters can be made with cascaded coupled line sections of the form showed in **Figure 5.3**. In this section we are going to obtain the design equations for the filters of this type, starting from the equations of a single coupled line section, that can be approximately modeled by the equivalent circuit shown in **Figure 5.4**. [14, 15]

We will calculate the image impedance and propagation constant of the equivalent circuit and show that they are approximately equal to a coupled line section for $\theta = \frac{\pi}{2}$, which will correspond to the center frequency of the bandpass response.

The ABCD parameters of the equivalent circuit can be computed using basic ABCD matrices for transmission lines showed in the **Appendix**, **Table 9.1**.

$$
\begin{bmatrix} A & B \\ C & D \end{bmatrix} = \begin{bmatrix} \cos\theta & jZ_0\sin\theta \\ \frac{j\sin\theta}{Z_0} & \cos\theta \end{bmatrix} \begin{bmatrix} 0 & \frac{-j}{J} \\ -jJ & 0 \end{bmatrix} \begin{bmatrix} \cos\theta & jZ_0\sin\theta \\ \frac{j\sin\theta}{Z_0} & \cos\theta \end{bmatrix} =
$$
$$
= \begin{bmatrix} (JZ_0 + \frac{1}{JZ_0})\sin\theta\cos\theta & j(JZ_0^2\sin^2\theta - \frac{\cos^2\theta}{J}) \\ j(\frac{1}{JZ_0^2}\sin^2\theta - J\cos^2\theta) & (JZ_0 + \frac{1}{JZ_0})\sin\theta\cos\theta \end{bmatrix}
$$
(5.21)

And the ABCD parameters for the admittance inverter can be obtained by considering it as a quarter-wave length of transmission of characteristic impedance $\frac{1}{J}$. The image impedance of the equivalent circuit is:

$$
Z_i = \sqrt{\frac{B}{C}} = \sqrt{\frac{JZ_0^2\sin^2\theta - (1/J)\cos^2\theta}{(1/JZ_0^2)\sin^2\theta - J\cos^2\theta}}
$$
(5.22)

which, at center frequency $\theta = \frac{\pi}{2}$, equals to:

$$
Z_i = JZ_0^2
$$
(5.23)
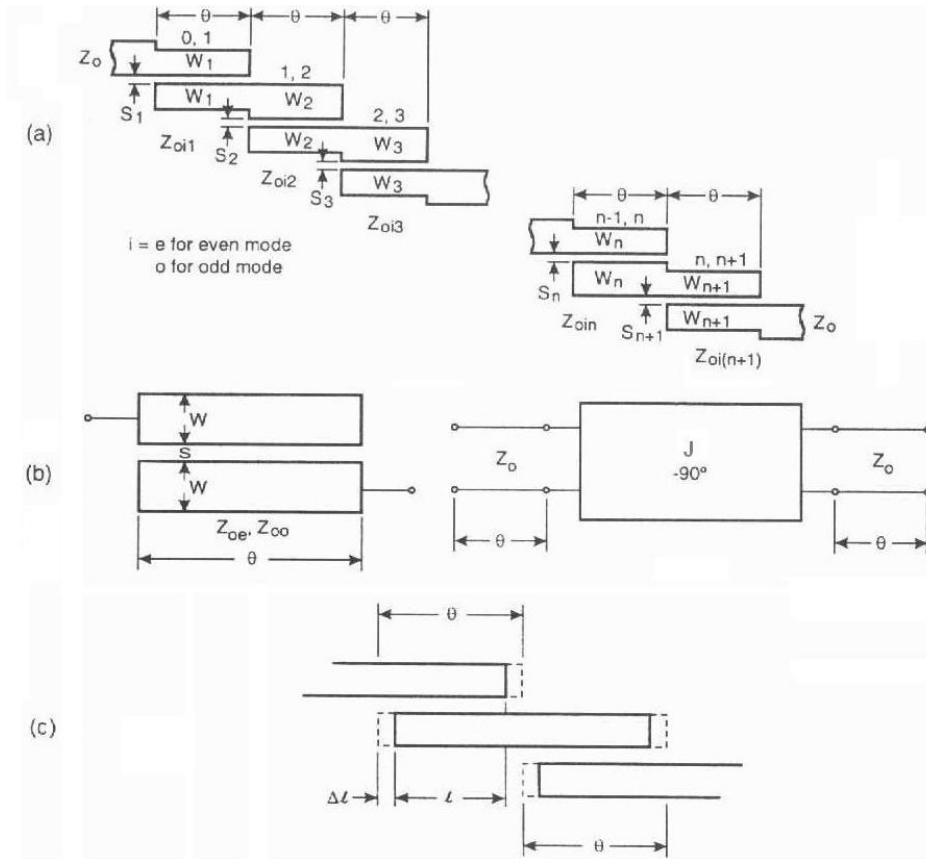
Figure 5.3: Parallel coupled transmission line resonator filter, a) scheme b) section and its equivalent and c) end effects , from [5], Chapter 9.
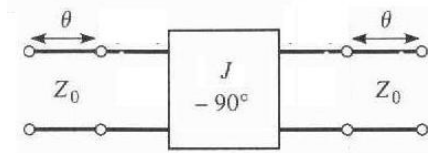
Figure 5.4: Equivalent circuit of a coupled-line section, from [2], Chapter 8.

And the propagation constant is:

$$cos\beta = A = \left(JZ_0 + \frac{1}{JZ_0}\right) \sin\theta \, \cos\theta \tag{5.24}$$

Equating the image impedances in equations 5.18 and 5.23, and the propagation constants of equations 5.20 and 5.24, gives the following:

$$\frac{1}{2}(Z_{0e} - Z_{0o}) = JZ_0^2$$

$$\frac{Z_{0e}+Z_{0o}}{Z_{0e}-Z_{0o}} = \left(JZ_0 + \frac{1}{JZ_0}\right) \tag{5.25}$$

where $\sin\theta \approx 1$ for θ near $\frac{\pi}{2}$ is assumed. The equations can be solved for even and odd mode line impedances to give:

$$Z_{0e} = Z_0[1 + JZ_0 + (JZ_0)^2]$$
$$Z_{0o} = Z_0[1 - JZ_0 + (JZ_0)^2]$$

(5.26)

And the J inverters for the various sections are defined in terms of the g_0, g_1, g_2, $g_3 \dots g_{n+1}$ elements as follows:

$$Z_0 J_1 = \sqrt{\frac{\pi \Delta}{2g_1}}$$

$$Z_0 J_n = \frac{\pi \Delta}{2\sqrt{g_{n-1}g_n}} \qquad for\ n = 2,\ 3,\ \dots N,$$

(5.27)

$$Z_0 J_{N+1} = \sqrt{\frac{\pi \Delta}{2g_N g_{N+1}}}$$

where $\triangle = (\omega_2 - \omega_1)/\omega_0$ is the fractional bandwidth of the filter. [16]

After calculating $Z_0 Jn$ for the N sections, the **even and odd mode impedances** of the coupled lines are calculated from relations 5.26, finally obtaining them to characterize each coupled-line section of the filter.

The **physical dimensions of the filter sections** are then calculated for the obtained Z_{0e} and Z_{0o}. This process can be done using equations and procedures as described in [17, 18] or tables like the one showed in the **Appendix, table 9.7**. From them, we will obtain values for the widths and separations of the different coupled-line sections once the dielectric material and the thickness of the PCB board are given. [19]

Lengths of the different sections

In our design, the value of the length for the different sections is calculated to be $\lambda/4$ at the center frequency of the filter. An approximate value for the physical length can be obtained from the average value of the even and odd velocities, equating it to 90° or $\frac{\pi}{2}$, that is:

$$\theta = \frac{2\pi}{\lambda}l = \frac{2\pi}{\lambda_0}\frac{\sqrt{\epsilon_{ree}} + \sqrt{\epsilon_{reo}}}{2}l = \frac{\pi}{2}$$

(5.28)

A more accurate value for the length of the resonator is obtained by taking into account the open-end discontinuity capacitance, which gives rise to an additional line length $\triangle l$ as shown in **Figure 5.3** c). In this case, the line length calculated from equation 5.28 is shortened at each end by $\triangle l$:

$$\triangle l = \frac{0.6 C_0 Z_{01}}{(\sqrt{\epsilon_{ree}} + \sqrt{\epsilon_{reo}})}$$

(5.29)

where $\triangle l$ is in millimeters, the open-end capacitance C_0 in picofarads, and $Z_{01} = \sqrt{Z_{0e}Z_{0o}}$.

In parallel-coupled microstrip filters, the **physical lengths of the coupled sections** are the same for both the even and odd modes, and we obtain an asymmetrical passband response with deterioration of the upper stopband from differences in phase velocities in these two modes.

To improve the stopband performance, the phase velocities of the two modes should be equalized. Various techniques can be used to do this, including over-coupling the resonators, suspending the substrate, using capacitors at the end of the coupled sections... but they were not applied for our designs.

5.4   Losses in microstrip

When electromagnetic fields travel through material media they are affected by its properties. These properties of the physical medium are described mainly by the already mentioned **permittivity** and also **conductivity and loss tangent**.

The **complex permittivity** of the medium is defined as:

$$\varepsilon = \varepsilon' - j\varepsilon'' \tag{5.30}$$

And applying Maxwell's equation it can also be obtained a quantity of interest, **loss tangent**, which is defined as:

$$\tan \delta = \frac{\omega\epsilon'' + \sigma}{\omega\epsilon'} \tag{5.31}$$

where $\omega\epsilon''$ is the loss due to dielectric damping and σ is the conductivity loss, so the numerator can be considered as the total effective **conductivity** in the medium.

Therefore for our microstrip lines, which can be considered as a lossy medium, a complex propagation constant can be defined as:

$$\gamma = \alpha + j\beta = j\omega\sqrt{\mu\varepsilon}\sqrt{1 - j\frac{\sigma}{\omega\varepsilon}} \tag{5.32}$$

where α is the attenuation constant that represents the losses in the physical medium and β is the phase constant. Then at the frequency being considered ω, the permitivitty is $\varepsilon = \varepsilon_0\varepsilon_r$ being $\varepsilon_0 = 8.854 \times 10^{-12}$ F/m, and ε_r is dependent on the substrate of the boards being used. The permeability is $\mu = \mu_0$ where $\mu_0 = 4\pi \times 10^{-7}$ H/m with conductivity σ also depending on the conductor material of the boards.

Also depending on the type of medium being considered, these propagation parameters can be simplyfied as shown in **Table 5.2** in the next page for lossless, lossy or good conductor mediums.

It is also interesting to note that to obtain the quality factor of the loss tangent for our resonators, the following relation can be used:

$$Q = \frac{\beta}{2\alpha} = \frac{2\pi}{2\lambda\alpha} = \frac{\pi f_0\sqrt{\varepsilon_r}}{c\alpha} \tag{5.33}$$

	Type of Medium		
Quantity	Lossless $(\epsilon'' = \sigma = 0)$	General Lossy	Good Conductor $\epsilon'' \gg \epsilon'$ or $\sigma \gg \omega\epsilon'$
Complex propagation constant	$\gamma = j\omega\sqrt{\mu\epsilon}$	$\gamma = j\omega\sqrt{\mu\epsilon}$ $= j\omega\sqrt{\mu\epsilon'}\sqrt{1 - j\dfrac{\sigma}{\omega\epsilon'}}$	$\gamma = (1+j)\sqrt{\omega\mu\sigma/2}$
Phase constant (wavenumber)	$\beta = k = \omega\sqrt{\mu\epsilon}$	$\beta = \mathrm{Im}(\gamma)$	$\beta = \mathrm{Im}(\gamma) = \sqrt{\omega\mu\sigma/2}$
Attenuation constant	$\alpha = 0$	$\alpha = \mathrm{Re}(\gamma)$	$\alpha = \mathrm{Re}(\gamma) = \sqrt{\omega\mu\sigma/2}$
Impedance	$\eta = \sqrt{\mu/\epsilon} = \omega\mu/k$	$\eta = j\omega\mu/\gamma$	$\eta = (1+j)\sqrt{\omega\mu/2\sigma}$
Skin depth	$\delta_s = \infty$	$\delta_s = 1/\alpha$	$\delta_s = \sqrt{2/\omega\mu\sigma}$
Wavelength	$\lambda = 2\pi/\beta$	$\lambda = 2\pi/\beta$	$\lambda = 2\pi/\beta$
Phase velocity	$v_p = \omega/\beta$	$v_p = \omega/\beta$	$v_p = \omega/\beta$

Table 5.2: Propagation parameters for different media, from [2], Chapter 1.

which will give quite a low value for a microstrip resonator, giving also a bad result for insertion losses. Although it must be noticed that to obtain a better Q, a bigger area (to obtain a lower conductivity resistance) will be needed, and this is not possible using microstrip structures, which tend to be quite small.

5.5 Conclusions

With the equations and procedures described in this chapter, starting from the **analytical description of the filtering properties of a coupled-line section**, and up to the **design equations for a coupled line band-pass filter** made of several coupled lines sections, we have covered the most important theoretical tools to design this type of filters.

As we have explained, knowing the basic theory behind them that we showed in previous chapters, and applying the described methods, will allow us to obtain a **set of coefficients** that represent the values of the different components of the circuit model. Then, by solving some equations, we will obtain the **even and odd mode impedances** that describe each section. Finally, after doing a conversion, we will obtain the **physical measurements of every section** that form the filter.

It will then be necessary to set all these parameters of the final sections of the structure, including loss, attenuation, conductivity and other characteristics of the substrate, in the simulation software. This way we will obtain a **realistic model to simulate and obtain the final response** expected once the filter is built.

Following this method, we have designed the two filters built for the UWB ROF system. In the next chapter we are going to show the details of the adjustments done to the filters and the simulation of the filter models. Then, after some iterations and once we obtained the required frequency response and characteristics, they were finally built and measured.

6

Designs conducted and results.

6.1 Introduction

The practical part of the project has involved the design of three filters and the construction of two of them, with the process being done up to three times for one of the filters because the results were not accurate enough. With the first two filters the idea was to cover a part of the UWB spectrum, the first one going from **3.1 to 4.7 Ghz (Band Group 1)** and the second one going from **6.3 to 7.9 Ghz (Band Group 3)**. With the third filter the idea was to cover the frequency band going from **3.1 to 10.6 Ghz (whole UWB band),** but it wasn't finally included in this report given its complexity. The first two filters have been designed as fifth order Chebyshev band pass filters with at least 15dB adaptation specification for the pass-band.

All this was done with the idea in mind of designing the necessary filters for a whole UWB system which transmits and receives through different bands. Using for example BG1 to transmit and BG3 to receive, with a third filter covering the whole band and eliminating noise and interference. These filters have a final application, and a role, in a complete UWB transceiver system, as it has already been explained, and will be detailed in the final chapters of this project.

By doing this, we have covered in the project the objectives of designing different filters using procedures for the microwave band and also the use of specific software, as it is the **AWR Design Environment (Microwave Office)** and its **Electromagnetic design tool (EM Sight Simulator).** This last one being used for the in detail electromagnetic simulation of the final structures being built.

The first filter is designed to cover the band from **3.1 to 4.7Ghz** (fractional 40%) with a parallel coupled-lines with open-ended configuration as described in chapter 5.2.

The second filter covers the band from **6.3 to 7.9Ghz** (fractional 20%) with the same configuration, adapting the previous filter for the new required pass-band, using all the previous work. That way, it wasn't necessary to start the design process from scratch all over again.

Figure 6.1: Plain PCB board.

For the third filter, as the pass-band was so wide, **3.1 to 10.6 Ghz** (fractional 110%), the focus of the work had to be changed, and it was necessary to start all over again from a lumped elements design. Then the elements were converted to microstrip elements using equivalents and simulated to keep the desired response of the filter at each stage. This was a complex work still being done and finally wasn't included in this report. [15]

6.2   Boards used

The boards used were double-sided plain copper prototype boards with epoxy glass **Flame Retardant 4 (FR-4) as substrate**. These boards are the most used ones for low-complexity microwave designs given that they have a good price/quality relationship. They have good mechanical resistance and good isolation still being quite cheap.

The main disadvantage is that the behavior worsens as working frequency is risen, being not so good at our lower frequency, 3.1 Ghz, and quite bad at the higher one in the UWB band, 10.6 Ghz. That is why we had to take some precautions in the designs and build some filters more than twice to obtain the desired frequency, as we will explain later on. [20, 21]

The specifications of the used board are:

- Dimensions: 457x305 mm

- Copper thickness (T): 0.0356mm

- Dielectric constant (ε_r): 4.1

- Depth (H): 1.6 mm

- Loss tangent $\approx$ 0.02

With the substrate specifications and the main filter characteristics decided, the steps taken to design and build them are going to be explained in detail for each one.
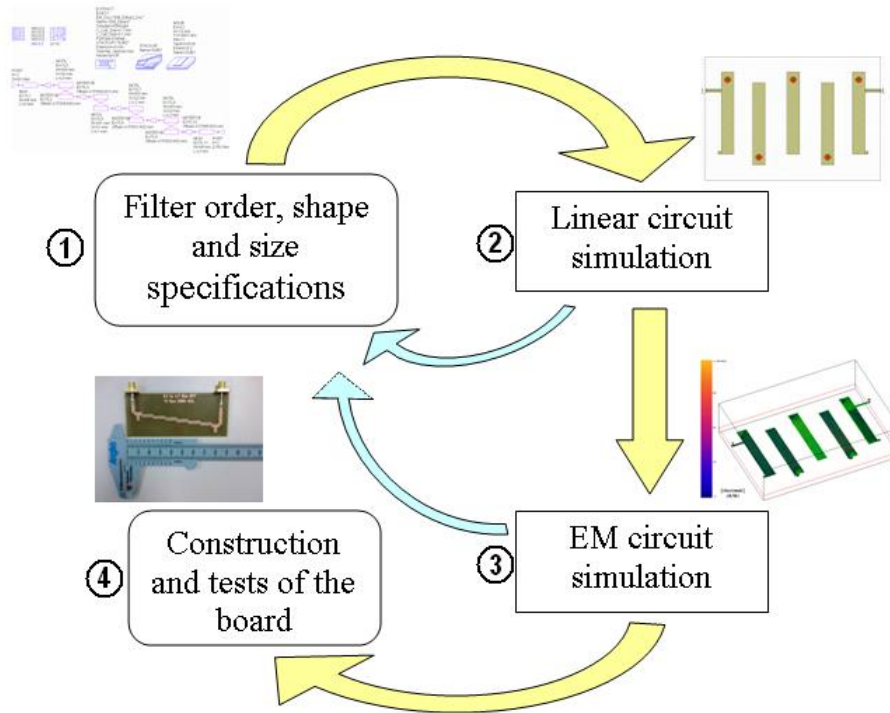
Figure 6.2: Filter design and construction flow chart.

6.3   Software used

To design and simulate the filters, a microwave simulation program from AWR company has been used, the **AWR Microwave Office** design software suite. It is a PC platform software for microwave elements design and has all the necessary modules to perform high-frequency design in a PC environment.

- Linear circuit simulators.

- Non-linear circuit simulators.

- Electromagnetic (EM) analysis tools.

- Integrated schematic and layout.

- Statistical design capabilities.

- Parametric cell libraries with built-in design-rule check (DRC).

The modules we used for the design of the filters were mainly three: **the schematic and layout tool, the linear circuit simulator and the EM analysis tool.**

The first one was used to **define the structure measurements and characteristics**, defining the exact size of each track of the filter and the coupled-line parts, and also giving details on the substrate characteristics like: ε_r (relative permittivity), H (substrate thickness), T (copper thickness), $\tan\delta$ (loss tangent) and some more. The linear circuit simulator was used
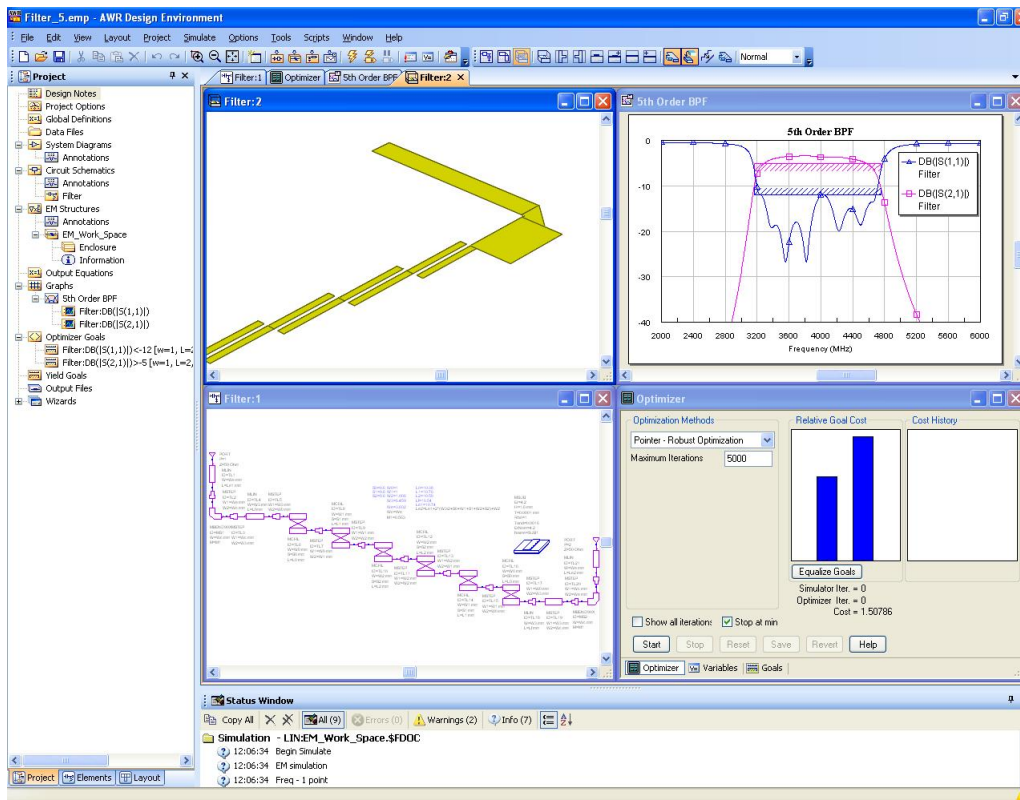
Figure 6.3: AWR Microwave Office software work environment.

to perform a **simulation of the behavior of the filters** with these defined parameters, and obtain an approximation of the response of the filter.

Finally, and once the filter was completely defined and the response very near to the desired one, the EM analysis was performed to check final details and **behavior of the filter taking into account every electromagnetic effect** happening in it.

Normally some iterations of the process were needed to obtain the required results. From the specifications calculated, changes were made to improve the linear simulation response. With feedback from the linear simulation or the EM simulation, process was iterated several times, as shown in the graph. If all the steps were taken with positive results, then the filter was ready for its construction, connectors soldering and laboratory testing.

The flow of the designing process explained above and followed is shown in **Figure 6.2,** and the software work environment can be seen in **Figure 6.3**, where different modules are showed all together in the same window.
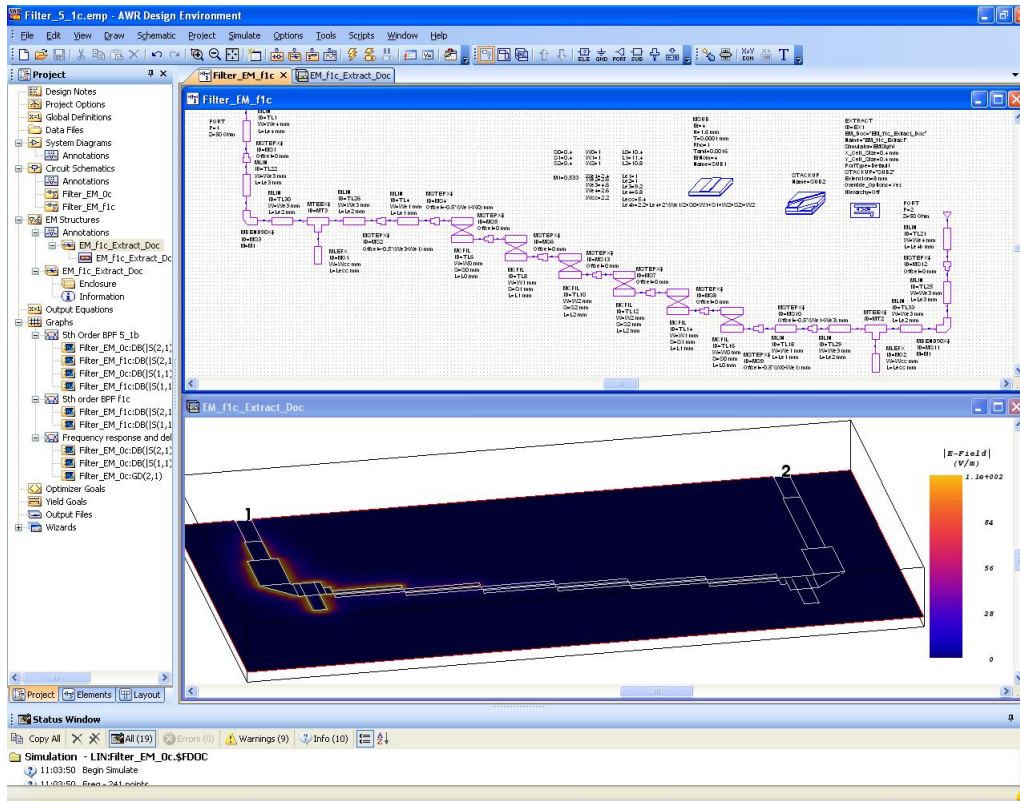
Figure 6.4: AWR Microwave Office software linear and EM simulators.

6.4   Linear and electromagnetic simulations

Once we have a circuit model with the parameters of the filter set in the **computer CAD software**, it is time to simulate its response and begin its optimization process.

First step then is to simulate this model, by using a **linear simulation**, that using mathematical representations for each section of the circuit and according to the parameters introduced, depicts the behavior that the whole structure should have once it is built. This simulation has the advantage of being quite accurate and fast to calculate, that way it can give a good idea of the filter response, and let us see the impact that changes in our design cause to the final behavior, being a very useful tool to optimize it.

For this kind of simulations, only the **definition of a substrate** was necessary. This gave the program details on the permittivity, thickness, conductivity and other parameters of the substrate that the filter was going to be built in. They needed to be specified because the mathematical models describing the different sections depend on them.

But given that the different parts are represented by mathematical models, this method does not tell exactly what would happen physically in the real filter. It doesn't calculate propagation in the real structure and joints between sections, that are important to represent small details that can affect our filter, like spurious resonances, transverse modes, etc.

To get a more accurate characterization once the optimization is in an advanced stage and we have a fairly final model, a second type of simulation is needed. This is an **EM simulation** which is more complex and will take more time to calculate, but will actually calculate the

electromagnetic field traveling in the structure, giving an in detail characterization of it, and describing much more accurately how the frequency behavior of the filter will be.

This simulation takes into account more parameters, and will definitely represent in a very accurate manner its final behavior. That is why it needs to define, additionally to the previously defined substrate, a **stackup and extraction module definitions**. The first one describes the housing where the filter will be working and additional details on the substrate. And the second one dictates how the structure will be described in the EM simulator mesh, allowing to set certain parameters for the accuracy and time that it will take for the necessary calculations.

Both simulator modules are shown in **Figure 6.4**. The linear simulator is on the top with the parameters defining the different section models of the schematic. The electromagnetic simulator is shown on the bottom, where the defined structure being simulated can be seen.

6.5   Optimization of the designs

To obtain the required response from the filter simulations, a **first basic model** is designed and simulated, to make sure it meets the design requirements. This model is then modified to obtain the necessary shape and physical characteristics for our particular design, while keeping a fairly adequate response. Once the design process is taking place, it is necessary to **optimize the design**, by changing different parameters of the filter: lengths, widths, spacings... to obtain also the necessary frequency response that matches the specifications.

It is important to meet, both the **necessary physical and frequency characteristics**, with a design that needs to have measurements above a minimum (the minimum size that can be fabricated with the technology available, 0.2mm in our case) and with the simplest possible shape. This way we won't have big problems to simulate accurately its behavior and then fabricate it.

It is also very important to obtain the best frequency response, the higher above requirements as possible, because once the filter is built, multiple small variations on the construction will occur. Also the real material will introduce small defects that will affect the response, worsening it a bit (or too much if the calculations were not accurate enough).

These modifications can be done **by hand**, if we know in advance what parameter we want to modify, using the **tune tool** in the program. This way we can set a variable for any of the parameters of the filter, that we can tune, seeing in real time how it affects the estimated response. It is very useful to change some parameters slightly and improve some minor glitches happening in the system.

The other option available to tune our design is the **optimizer**. This module of the program allows to set certain restrictions (**optimizer goals**) to the design: a maximum attenuation, a minimum reflection rate or any other parameter for a frequency range, giving certain limits to their shape. The program is also given the list of possible parameters it can tune, and the value range for each one. This way a cost function with a certain amount of variables is calculated,
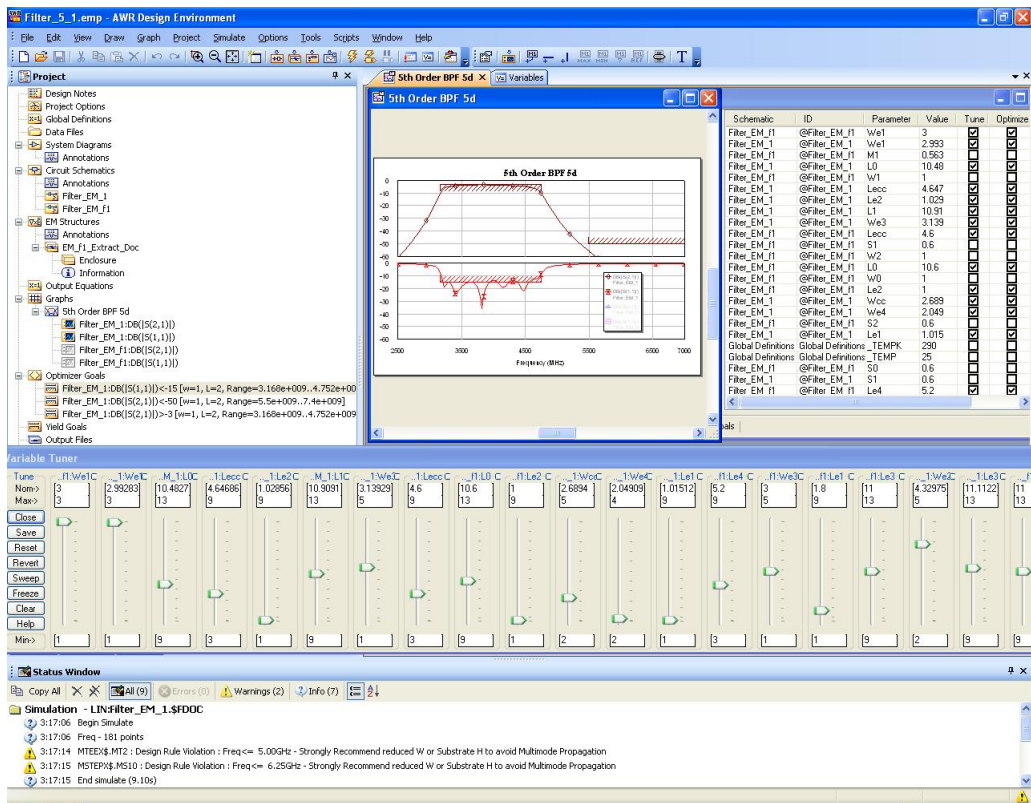
Figure 6.5: AWR Microwave Office software optimization and manual tuning tools.

and it can be optimized by the program using multiple methods like pointer, random, gradient optimization, simplex optimizer, simulated Annealing....

Both modules of the program, manual tuning and optimizer, can be seen in **Figure 6.5**.

It is quite a **fast way to optimize our design automatically**, depending on the complexity of the goals introduced and the number of variables allowed to modify. But if used properly and together with the knowledge of the designer, it can obtain very good results in short time periods. Of course, the more complex the structure and the more parameters we let the program tune, the more time it will need to reach minimum (optimal points) for our design.

This was the method used to **obtain a good response** once the design had major changes introduced, tuning distances and measures of certain sections of the filters. But the process had to be iterated several times, and depending on the direction followed by the optimizer, it was necessary to stop and change the filter shape, to maybe introduce stubs or other sections that could have the same effect the program was trying to obtain. This way the filter was improved, and the required filter sections added.

In the end, this was then followed by **manual tuning**, once the general response and filter shape were good enough, to improve minor details of the shape and response of the designed filters, polishing final details before its construction.
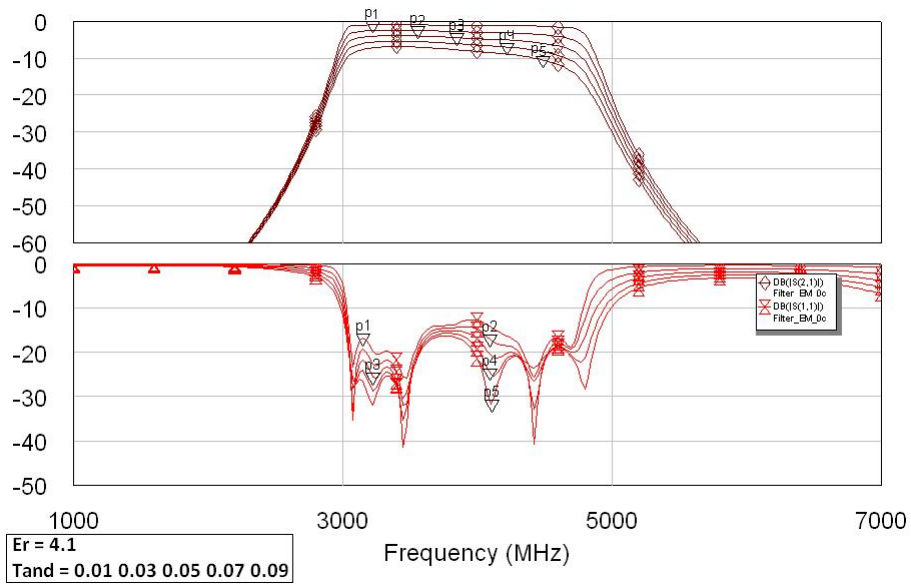
Figure 6.6: Responses of a filter for different values of $\tan\delta$.
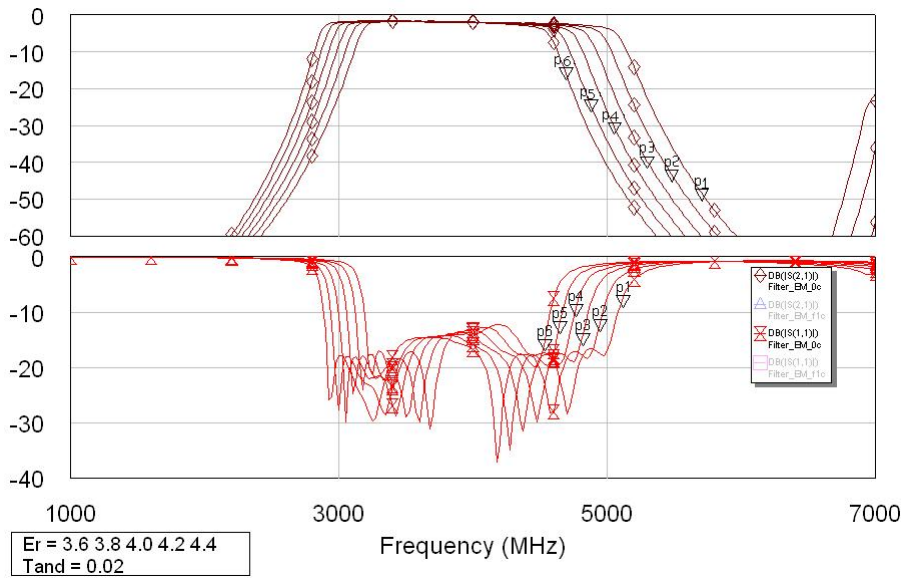
Figure 6.7: Responses of a filter for different values of ε_r.

6.6 Built filters response and its simulation.

The parameters defined in the microwave simulation program will dictate the final response that our built filter will have. So it is important to set them as accurately as possible to obtain best results. The measurements of the different coupled sections are the main parameters that will define the pass-band of our filter, but their accuracy will finally depend on the method being used to build our filters.

Apart from the structure measurements, other important parameters that will clearly affect the accuracy of the filters' model are the $\tan\delta$ (loss tangent) and the ε_r (relative permittivity). Both describe the losses behaviour of the material related to the frequency of the travelling signal. These parameters respectively change the position of the pass-band in frequency and its

Figure 6.8: ProtoMat H100 circuit board plotter.

width. But they are not variable, and depend on the material of the board used. So it is very important to build previous test filters to compare the values stated by the board maker and the real estimated ones upon construction. By doing this, we will be able to have a good model of the boards, and the simulations done will be as accurate as possible.

Having done this for our boards, we finally decided to use the values of $\tan \delta = 0.02$ and $\varepsilon_r = 4.1$. This way, although we still got band shift in frequency due to the change in value of other parameters, the simulation was quite accurate in describing the behaviour of the filter finally built.

6.7   Construction

Once the response of the filter in the simulations, linear and electromagnetic, was good enough and complied with the required characteristics, it was time to build the filter and measure its response. [22]

From the AWR Microwave Office program, a **layout description file** was obtained, that was then edited in a separated program to give final details to the copper layers. The filter passband specifications, date and version were written for them to appear milled in the layer for identification purposes. Once editing was finished, a final **Gerber file** was obtained from this program and was sent out for construction.

The construction of the filter was done in the same labs, with a **circuit board plotter from LPKF** company, the **ProtoMat H100 shown in Figure 6.8.** It is a printed circuit board prototyping system that mechanically produces prototype PCBs by milling the copper layered boards. It does so by following the circuit geometry specified by a layer description file, and it can take from 20 minutes to an hour for the kind of filters we designed, depending on its complexity.

It is software driven, with automatic spindle speed regulation, between 10.000 and 60.000 rpm, and positioning. It allowed for the fabrication of our designs with a high degree of accuracy and following an uncomplicated process, with no need of chemicals or other treatments to be applied to the boards.
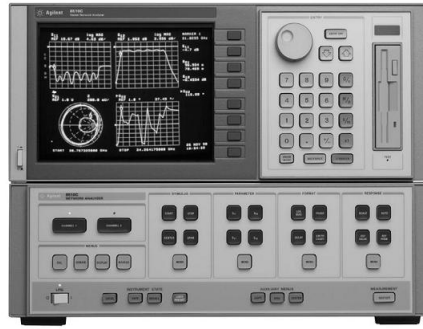
Figure 6.9: HP 8510C Vector Network Analyzer picture.

The **results obtained were very accurate**, with only about **0.1mm deviation** in certain points, so the filter response was affected very little by the difference in measures from the model to the built prototype. The responses obtained had no variations because of the fabrication process, given that it was quite accurate for our designs needs. The problems came mostly because of the behavior of the FR4 substrate of the board at the frequencies we were working.

6.8   Measurements

The measurements of the filters were done using a VNA from the company HP, nowadays Agilent. It was a **8510 series**, shown in **Figure 6.9**, and capable of measuring two port networks from 50Mhz to 50Ghz in frequency. So it was able to measure the kind of filters we designed with no problems.

It was very important to do a calibration of the system by a **TOSL (thru, open, short, load) full two-port calibration**, using the calibration kit that comes with the analyzer, to obtain the most accurate measurements out of our filter. By doing the calibration, the system compensates the possible mismatches occurring in the cables and connections.

It calculates a **twelve terms mathematical error model** that is used to correct all systematic errors. That way, it compensates the measurements obtained from the network being measured, allowing for a more accurate characterization. [23]

By using the analyzer, we managed to obtain **transmission, reflection and group delay measurements** of our filters, characterizing its behavior for the working band, making sure it had low losses and low reflection. But also characterizing a wide bandwidth around it, making sure the filters were rejecting signals out of our band of interest, and that possible spurious pass bands appearing were not a problem.
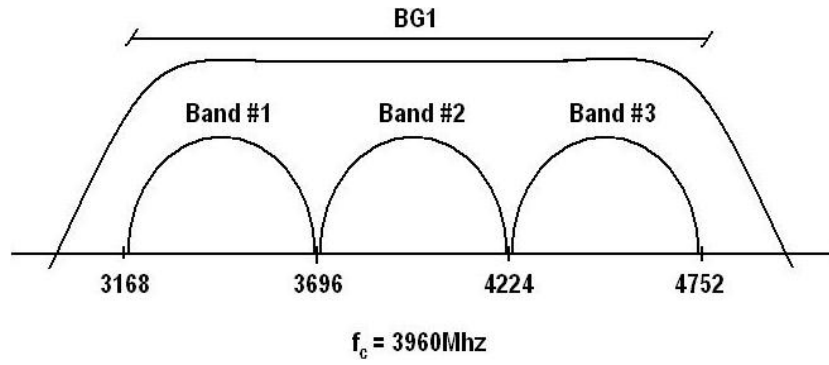
Figure 6.10: BG1 band-pass filter specifications.

6.9   First design: 3.1 to 4.7 Ghz BPF

The first design has the next characteristics:

- Type of filter: band-pass

- Type of response: Chebyshev

- Center frequency: 3.9 Ghz

- Filter order: 5

- Relative bandwidth: 40%

- Return loss: 15dB

- Impedance: 50Ω

6.9.1   Design procedure

To start designing this filter, first step was to set up the specifications for it. Center frequency and width of the passband, attenuation requirements and the kind and order of the response going to be used.

$$\omega_l = 3168Mhz$$

$$\omega_c = 3960Mhz \qquad (6.1)$$

$$\omega_u = 4752Mhz$$

With those frequencies, the order needed for the filter that was calculated to be N=5, and the impedances at the input and output of 50Ω. At this stage we have every specification needed to start designing the filter.

The element values for a fifth order Chebyshev with 3dB ripples are:

$$G = \begin{bmatrix} 1 & 3.4817 & 0.7618 & 4.5381 & 0.7618 & 3.4817 & 1 \end{bmatrix} \qquad (6.2)$$

n	g_n	$Z_0 J_n$	Z_{0e}	Z_{0o}	W/d	S/d	S	W
1	3.4817	0.4248	80.26	37.78	0.61	0.33	0.528	0.976
2	0.7618	0.3858	76.73	38.15	0.63	0.34	0.544	1.008
3	4.5381	0.3379	72.60	38.81	0.68	0.42	0.672	1.088
4	0.7618	0.3379	72.60	38.81	0.68	0.42	0.672	1.088
5	3.4817	0.3858	76.73	38.15	0.63	0.34	0.544	1.008
6	1	0.4248	80.26	37.78	0.61	0.33	0.528	0.976

Table 6.1: Values obtained for the different coupled-line sections, using a fifth order Chebyshev with 3dB ripples.

Then, equations 5.26 and 5.27, from section 5.3 were used in a Matlab script, showed in the **Appendix**, **algorithm 9.1**, to obtain the values in **Table 6.1**.

For the length of the sections, the following equation was used:

$$l = \frac{\lambda}{4} = \frac{75}{F(Ghz)\sqrt{\varepsilon_{eff}}} \ (mm) \tag{6.3}$$

which gave an approximate length of 10.5mm for the $\frac{\lambda}{4}$ coupled lines sections at the center frequency they were going to be used.

From this data, the **first circuit model** obtained is shown in **Figures 6.11 and 6.12.** From these graphs, although we could say that the response is good enough to be the first approach to the design, a lot of improvement can be obtained with some tuning and adjustements. But two main aspects can be noticed from it at first sight. [3]

First, our filter is going to be used in laboratory tests, with EM equipment near, and many other elements radiating in the band where the filter will be working. Therefore, it will be necessary for the filter to be housed within a grounded metal box, to provide the necessary RF isolation, and block external RF interference from other components.

As final measurements for the filter board were unknown at that moment, it was decided to place both ports in the same side of the board, for it to be easier to box into a metal housing. Therefore a couple of sections and a bend had to be added in both ends of the structure.

The second aspect was that the width difference between the 50Ω port sections of the filter and the actual width of the adjacent coupled-line sections was too big. This could give some problems and a different behavior from the one expected, so if the displacement of the two ports to the side didn't change things, this factor should be addressed.

The **second circuit model** obtained, with changes mentioned already applied, is shown in **Figures 6.13 and 6.14.** It has the sections to drive the ports to the sides introduced, and 50Ω impedance in the ends. From it, it can be noticed that the two microstrip lines adjacent to the final coupled lines sections were still quite wide after some tuning and optimization. This meant that some adjustments needed to be made to obtain thinner sections and a better adaptation in these parts.

This was required because sections which are too wide allow for the propagation of transverse modes, which are not so well predicted by the design software and can cause misbehavior of the filter once it is built.

This big difference in the width gap between the sections would contribute to a bad response. Therefore, the effect being introduced in the system by this wide section had to be created in a different manner, to keep the same filter response, but without these disadvantages. [24]

Finally, the solution for the **third circuit model,** shown in **Figures 6.15 and 6.16**, was the introduction of a couple of stubs in those sections, to obtain the needed capacitance in that part of the circuit, and allow for a thinner section that would keep the adequate behavior of the filter.

By adding the stubs, we were able to introduce the needed capacitance in that part of the circuit without having a very wide section, but instead having a thin stub connected to a narrower section. This way our requirement is achieved with a slim section that won't allow the propagation of transverse modes, but will still give the required capacitance.

The **final circuit model**, shown in **Figures 6.17 and 6.19**, which was the one finally built, is just an optimization of the third circuit model. Using the optimizer module of the program to mainly tune length and width parameters of the different sections of the filter.

This was done setting desired goals for a minimum rejection and a maximum transmission loss throughout the passband of the filter, as described before. It was necessary to carefully take into account that there were no peaks or strange connections between sections that could cause problems.

Once the figure of the filter was polished enough, and the response was as required, it was sent for construction.

First circuit model.
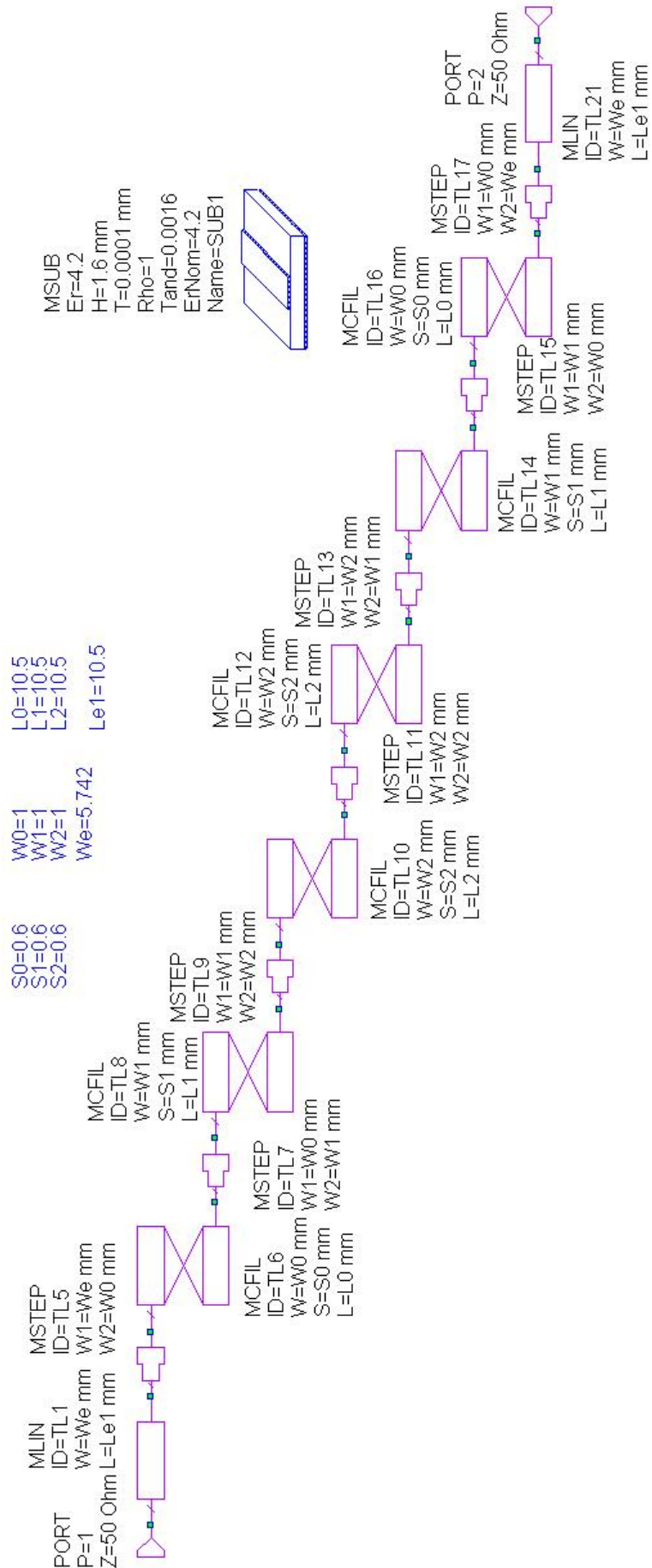
Figure 6.11: BG1 band-pass filter specifications of the first circuit model.
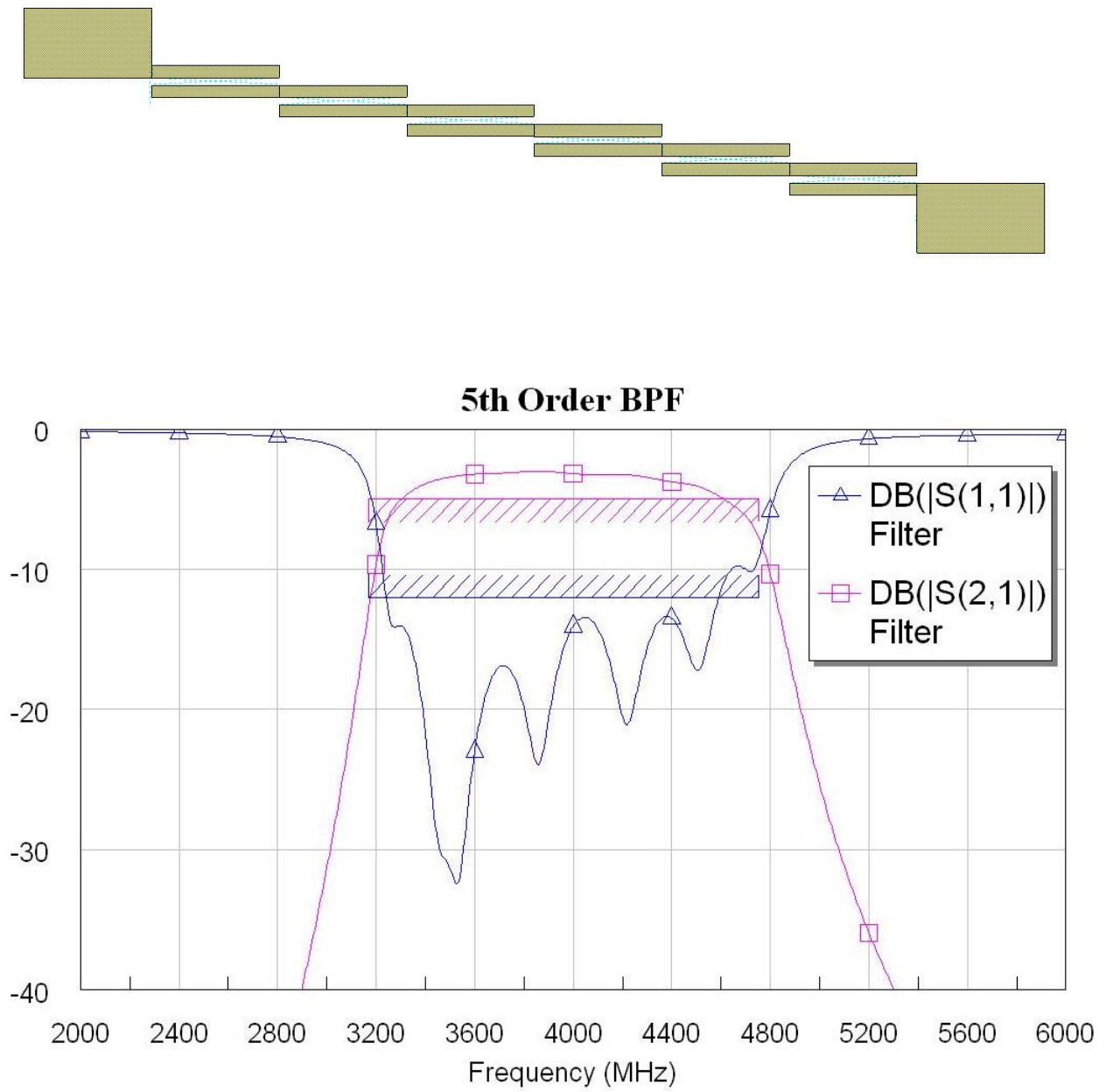
Figure 6.12: BG1 band-pass filter measurements and response of the first circuit model.

Second circuit model.
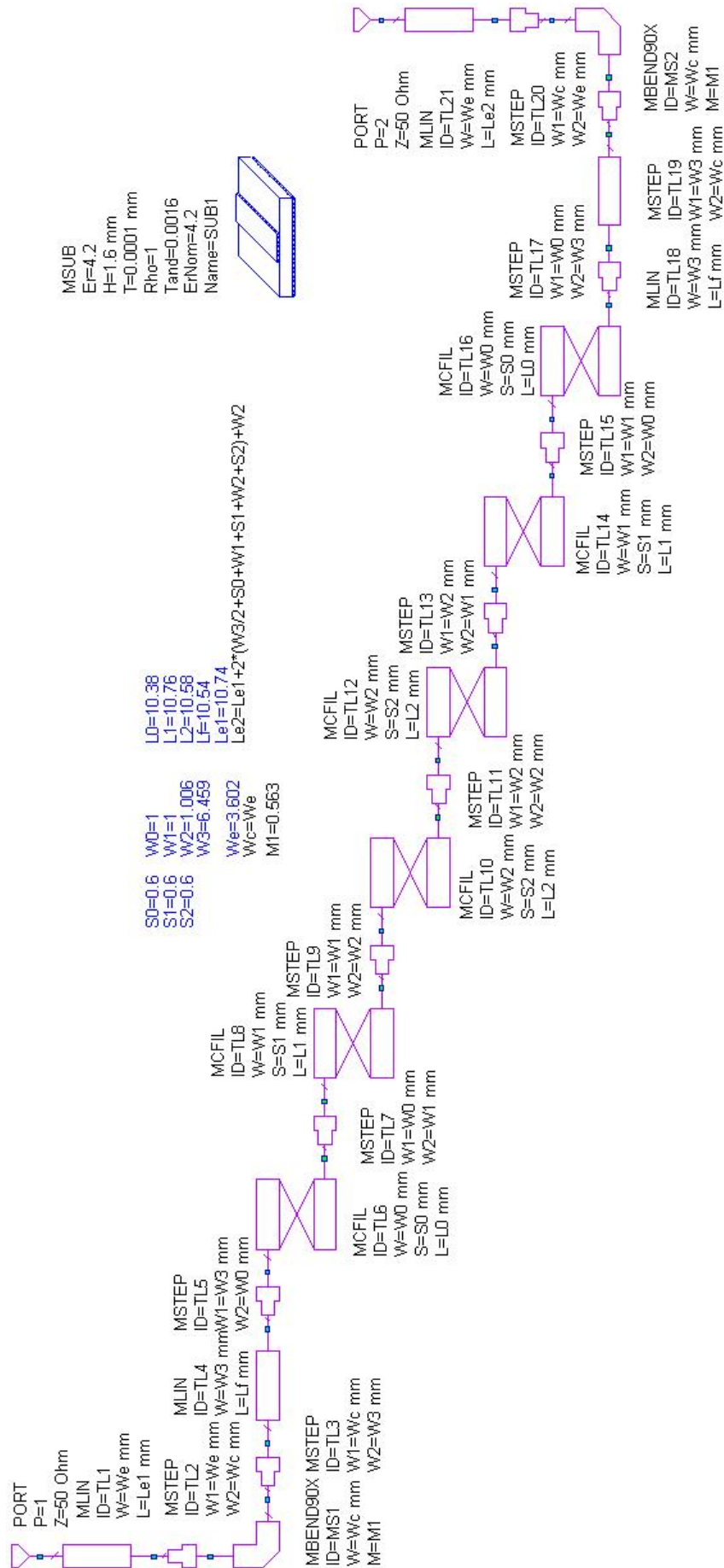
Figure 6.13: BG1 band-pass filter specifications of the second circuit model.
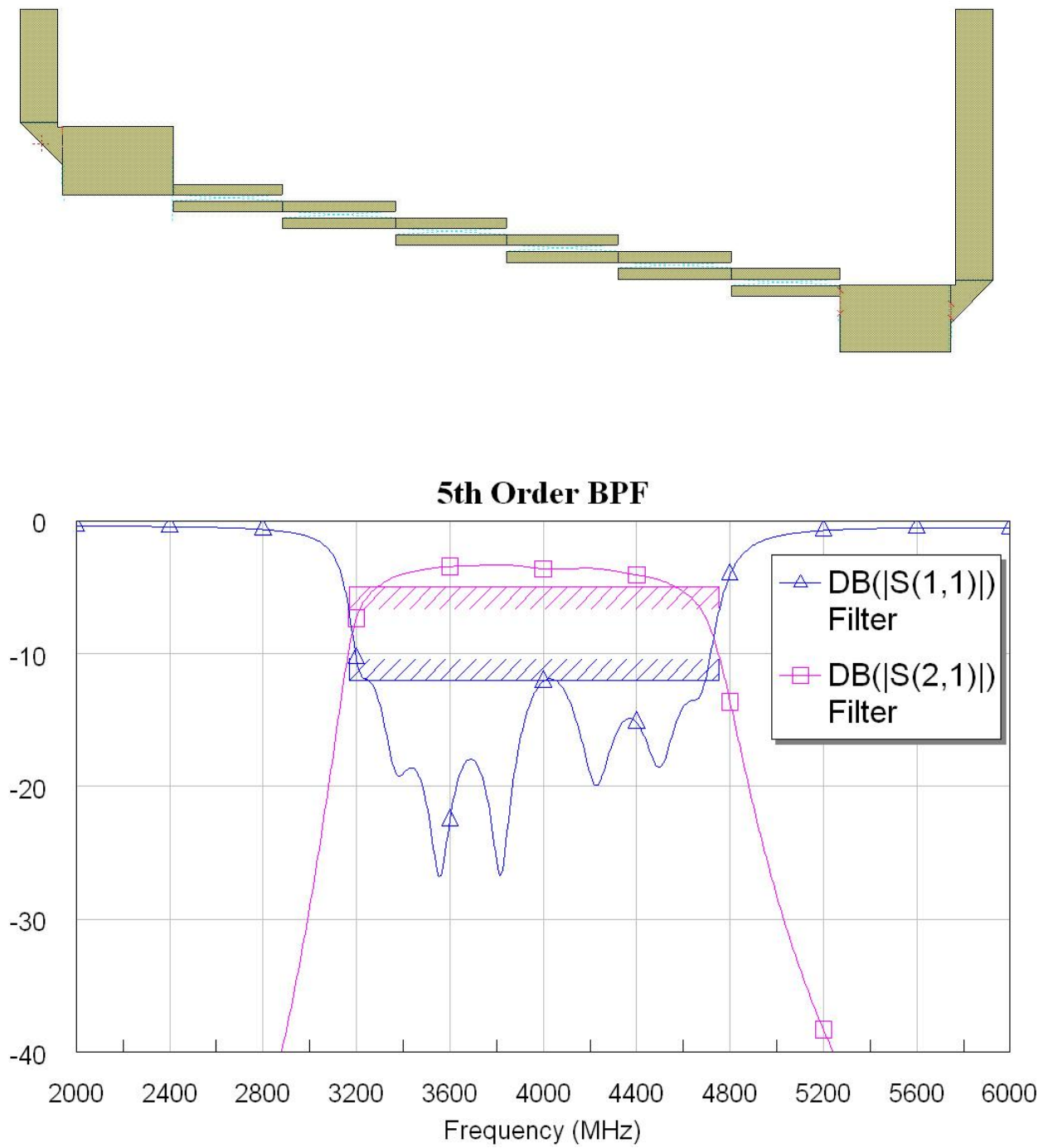
Figure 6.14: BG1 band-pass filter measurements and response of the second circuit model.

Third circuit model.

Figure 6.15: BG1 band-pass filter specifications of the third circuit model.
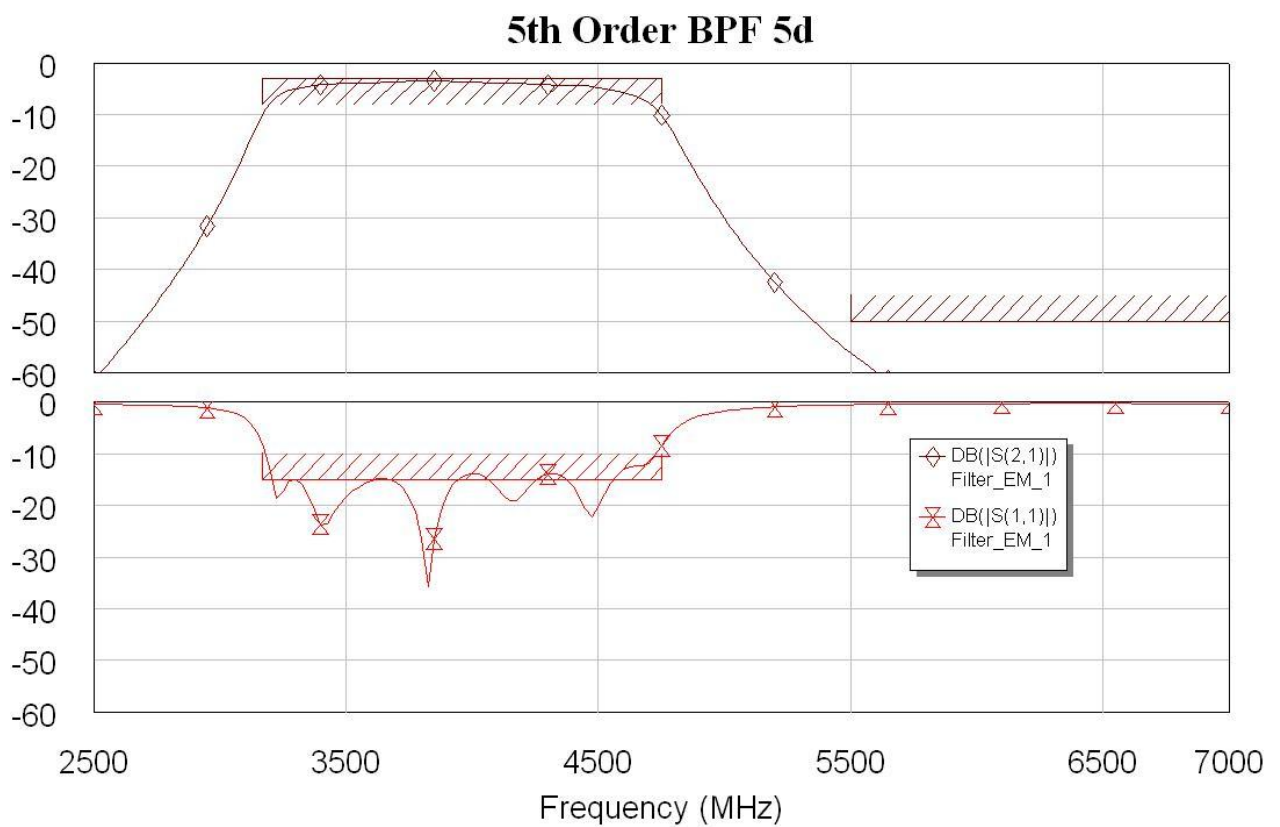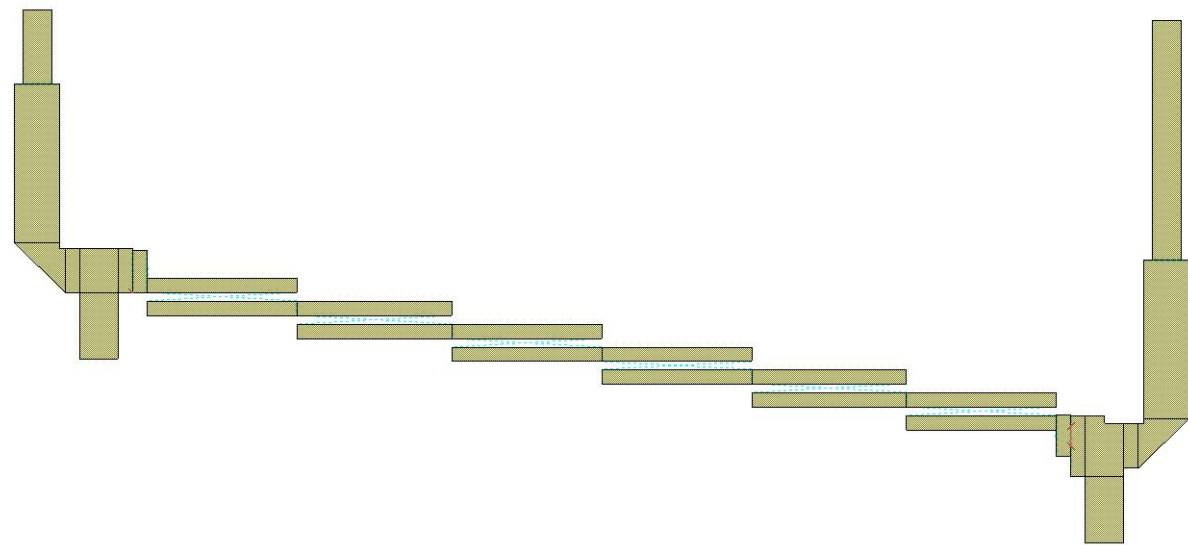
Figure 6.16: BG1 band-pass filter measurements and response of the third circuit model.

Final circuit model built.

Figure 6.17: BG1 band-pass filter specifications of the final circuit model.
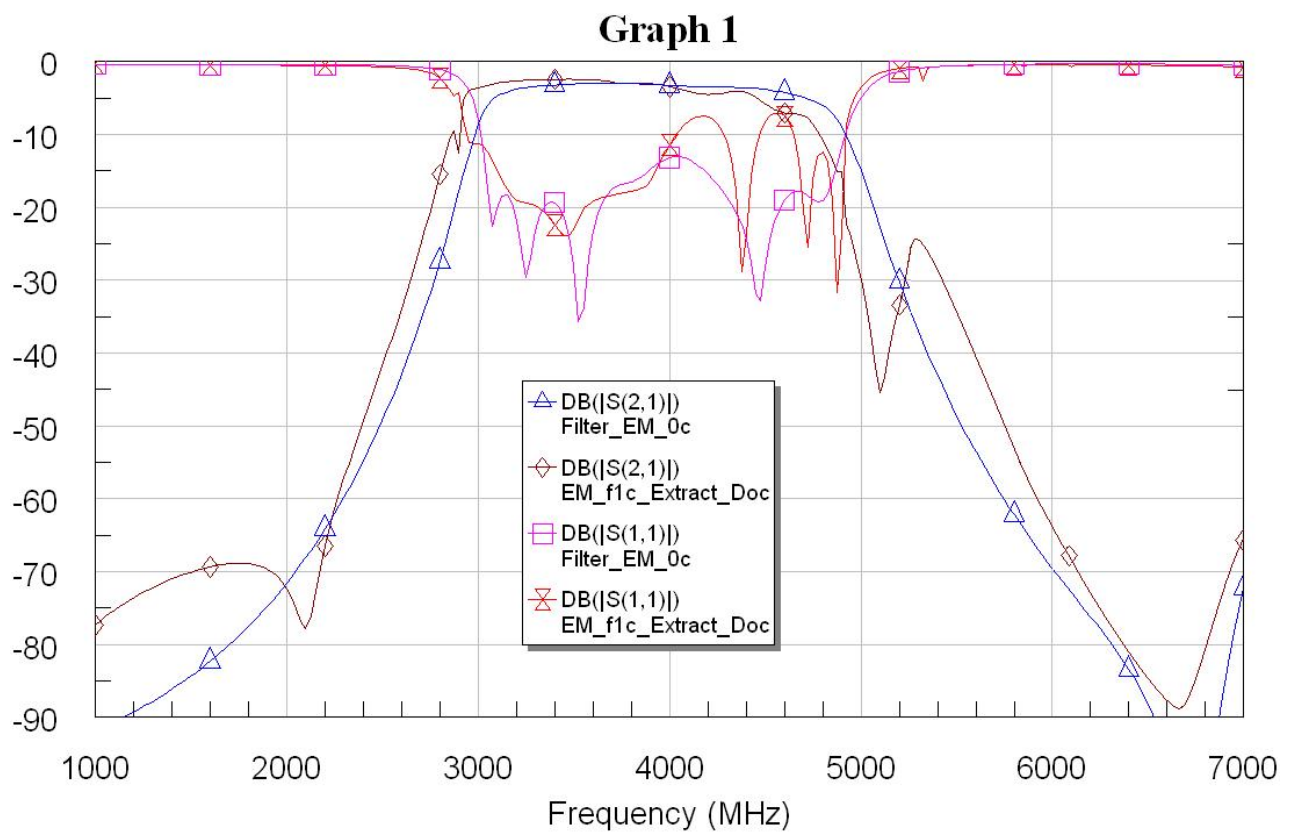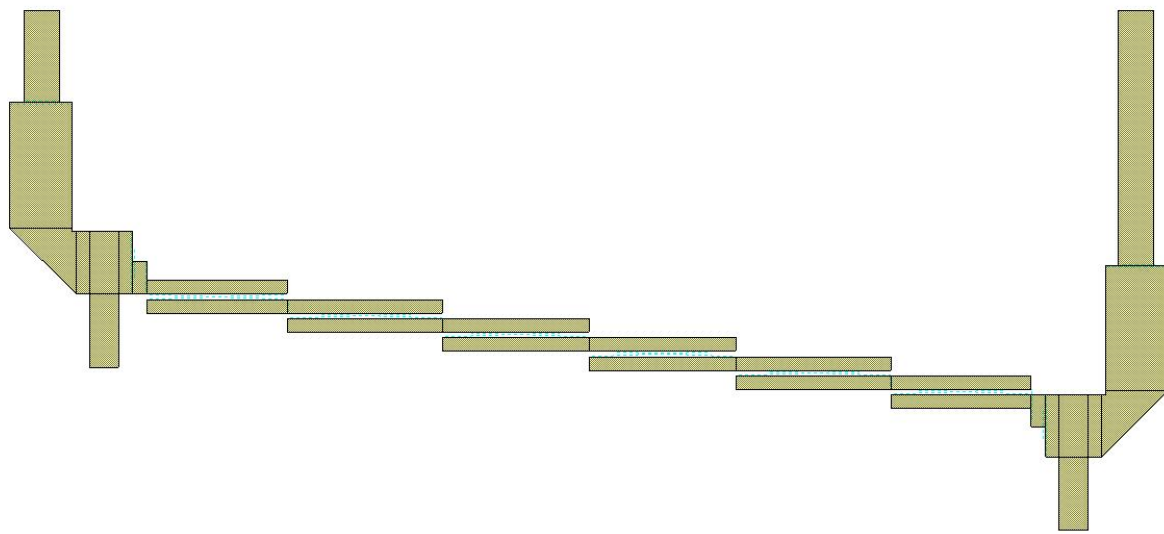
Figure 6.18: BG1 band-pass filter measurements and response of the final circuit model.
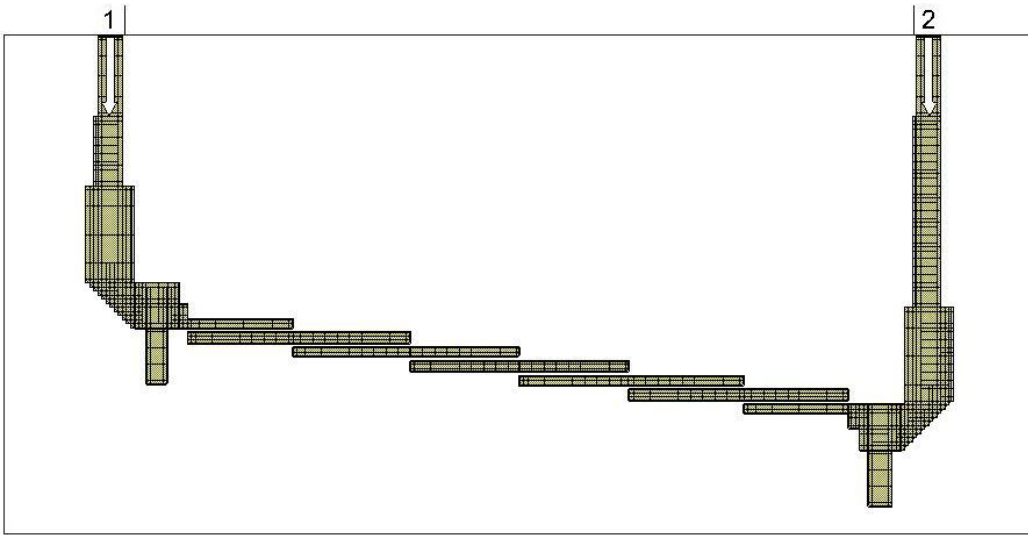
Figure 6.19: BG1 band-pass filter mesh of the final circuit model.

6.9.2 Currents and electric field distributions for the final circuit model

The **EM Sight simulator**, apart from being able to obtain the EM simulation of the filter, also allows to see a representation of the distribution of currents and electric field obtained from the simulation of the mesh defined for the circuit model. It solves a system of linear equations, using matrices for the defined mesh, that will have a bigger amount of points depending on the detail required. This way, it is possible to do it for a desired range of frequencies, being able to show an animation of the flowing current and varying electromagnetic field for a certain frequency.

Those two different kinds of graphs are shown in this section. First, in **Figure 6.20**, the representation of the currents in the filter is shown, and then the electric field in **Figure 6.21**.

Being the filter passband of 1.6 Ghz between 3.1 and 4.7 Ghz, it is seen in the center graph of both figures that at **3.9Ghz the current and Electric field flow with no problems** through the filter. This tell us that the filter doesn't oppose to the transmission of the EM wave at this frequency.

But as we represent the distributions in a frequency out of the passband, it is clearly seen that the **filter prevents the EM wave from propagating**, making currents appear with a higher intensity (as shown by the red and yellow color in the first section of the filter) and not allowing the electric field to go past the coupled lines when the frequency is below the lower or over the upper cutoff frequencies.

The current and electric fields are shown stronger **for 2.1Ghz** (only 1Ghz apart from the lower passband frequency) than **at 6.65Ghz** (1.95Ghz apart from the higher passband frequency), as shown in the first graph by the section before the coupled lines almost completely colored in red and yellow.
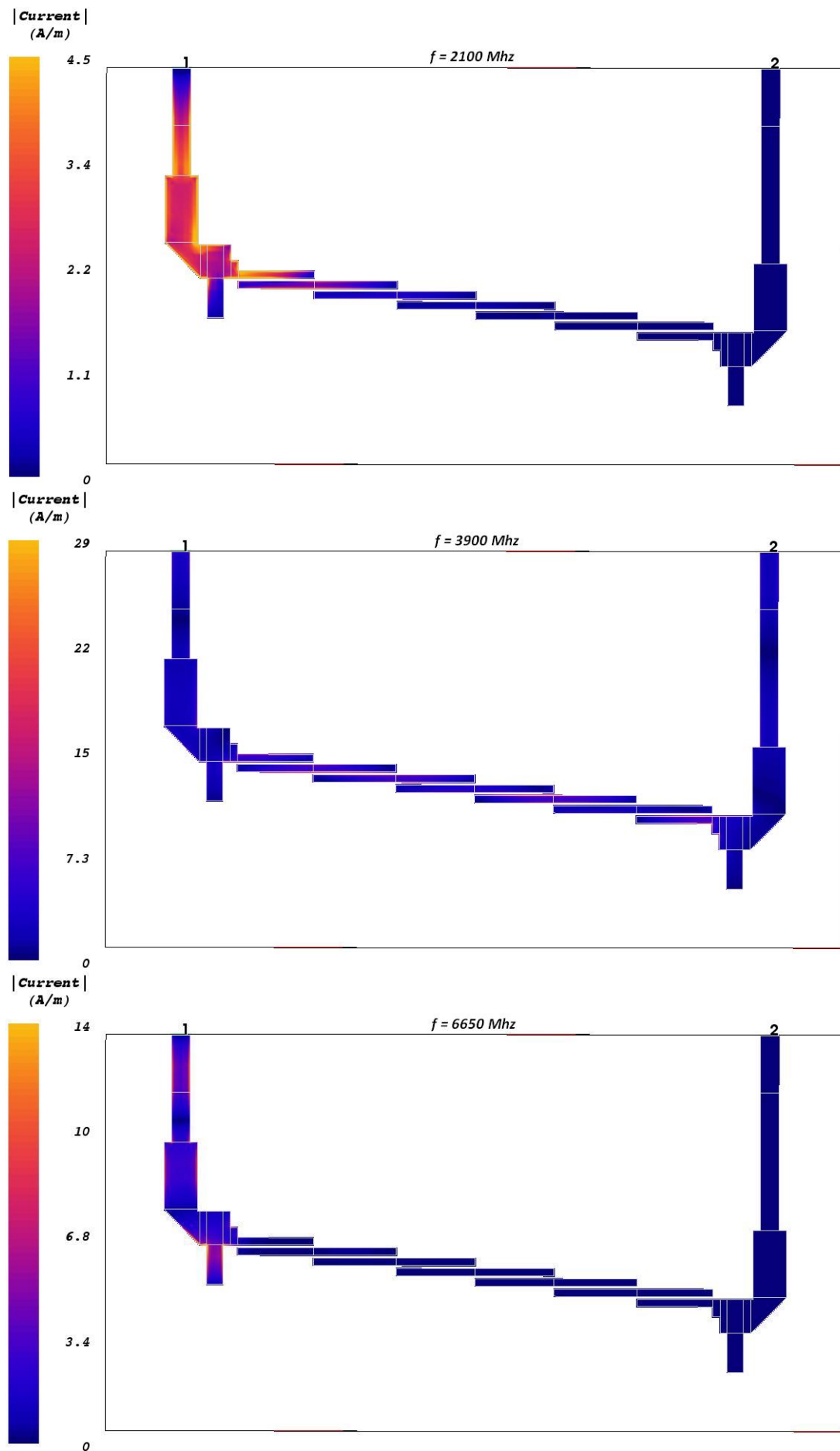
Figure 6.20: Currents distribution of the final circuit model at 2100, 3900 and 6650Mhz.
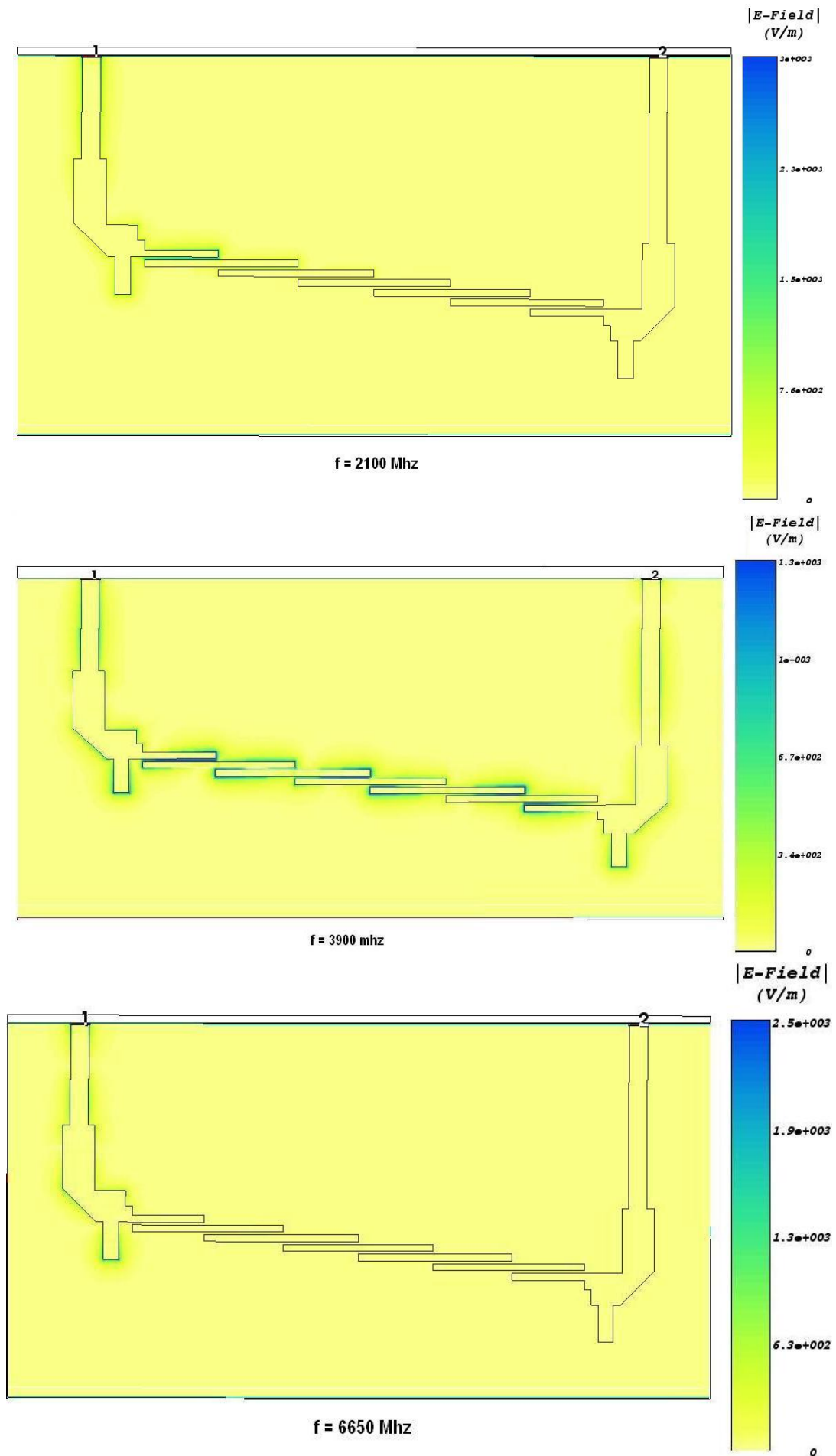
Figure 6.21: Electric field distribution of the final circuit model at 2100, 3900 and 6650Mhz..

6.9.3   Final response and characteristics obtained

Narrow response

Once the final circuit model was built, the response obtained was the one showed in **Figure 6.22**, where the response is depicted measured from both ports of the filter. It is quite a good response, with an average transmission coefficient of -5dB and a -18dB reflection coefficient, which is not a bad value, and enough for the requirements of our system.

Figures 6.23 and 6.24 then show a comparison between the obtained response and the one simulated. As can be seen, the responses are quite similar but with some minor differences.

There are two effects happening in the real filter that modify the response when compared to the simulated one: **bandpass narrows and shifts to higher frequencies**. The narrowing of the passband is caused by the losses in the real board, that also round it, and this depends on the loss tangent. The shift in frequency is caused by the permittivity value of the substrate, that cause passband central frequency to shift. If it is higher, the passband will shift down in frequency, and the opposite if it is lower.

Because both effects were taken into account in the design process, this didn't affect the final result too much, with a **final filter that meets the required bandwidth**.

Group delay

In the next plot, **Figure 6.25**, graphs of the filter group delay response are shown. First plot is an in detail view of the filter passband response, with the simulated group delay. The second one is a comparison between the obtained group delay response of the built filter and the simulated one.

As it can be seen, responses are similar, with a **slight difference and a general increase in group delay** for the filter built, although the difference between the higher and lower **group delay** points for the passband is of **about 1.2ns**. There is not much it can be done during the design process to improve it, because it is given by the steepness of the passband rejection rate, but finally it was a good value for our requirements.

Wide response

In **Figure 6.26**, the comparison between the simulated and the obtained response of the filter is shown for a very wide bandwidth, from 1 to 20 Ghz. From this wide frequency response it can be seen that the rejection rate of our filter is quite good, but that there is also a spurious and narrow passband appearing at about 12 Ghz, almost three times our filter center frequency.

This was not a major issue for our design, but should have been addressed by doing some modifications in the design in the opposite case.
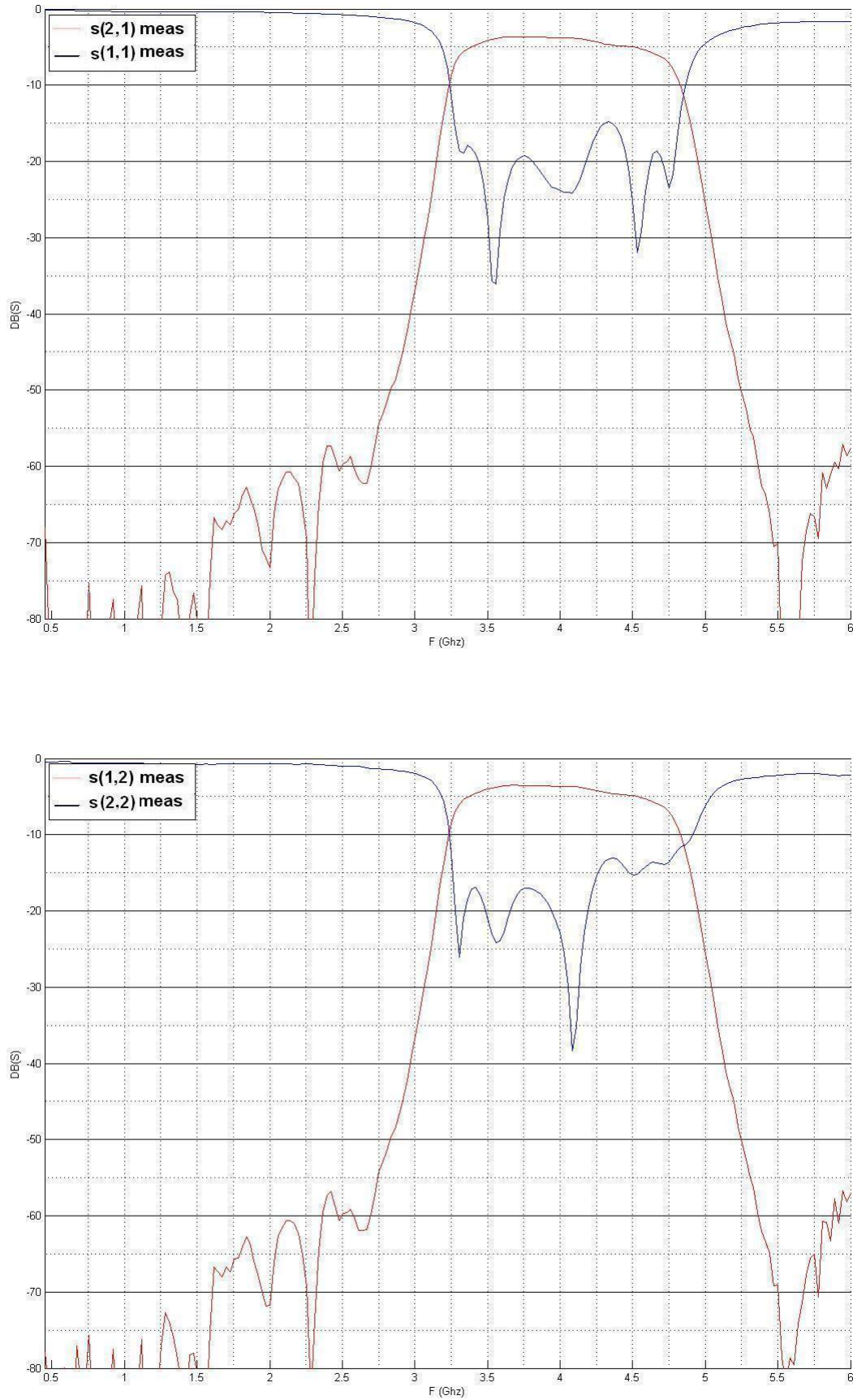
Figure 6.22: Comparison of the amplitude response and reflection coefficient measured from both ports of the filter.
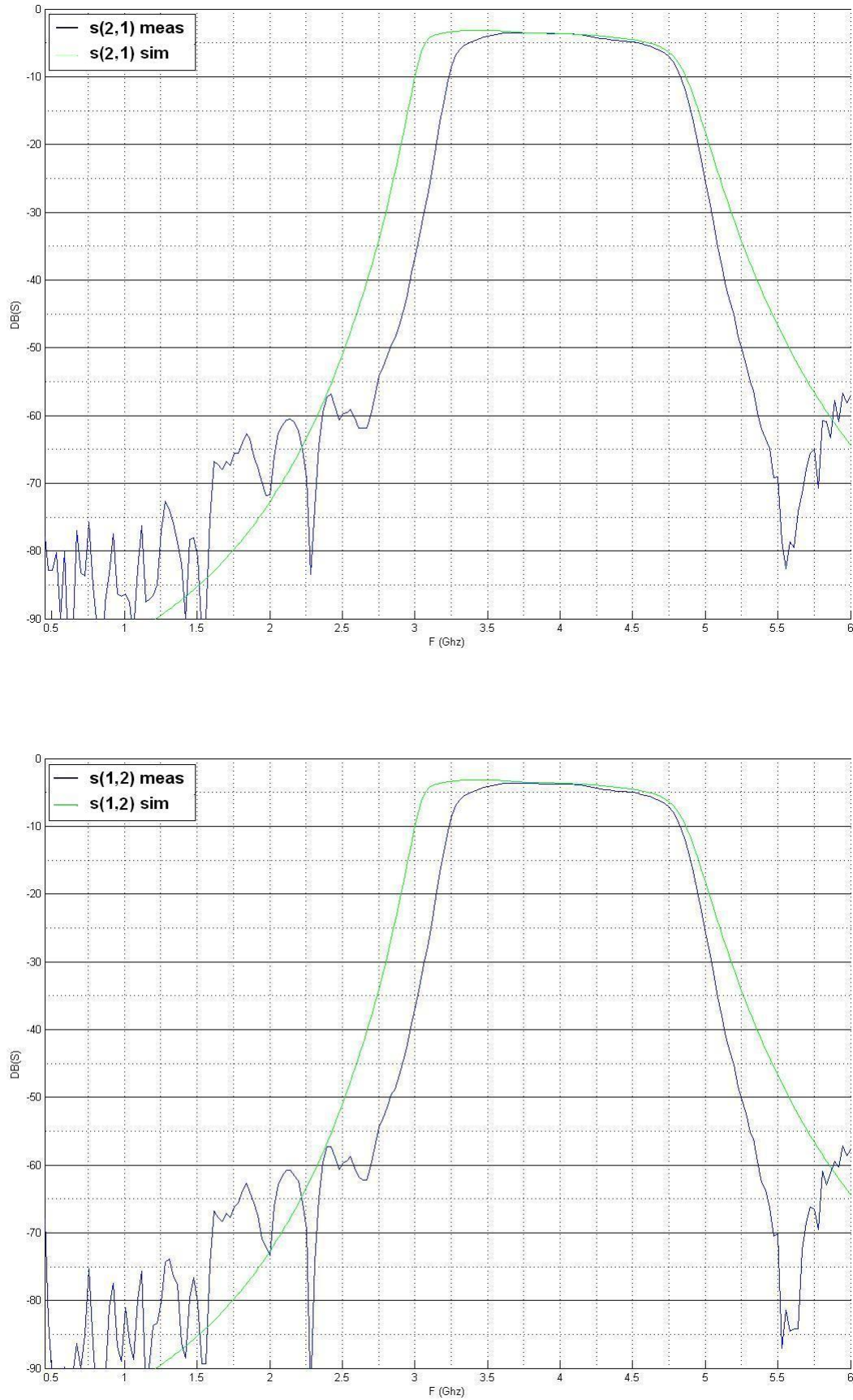
Figure 6.23: Comparison of the amplitude response of the simulated circuit model and the filter built.
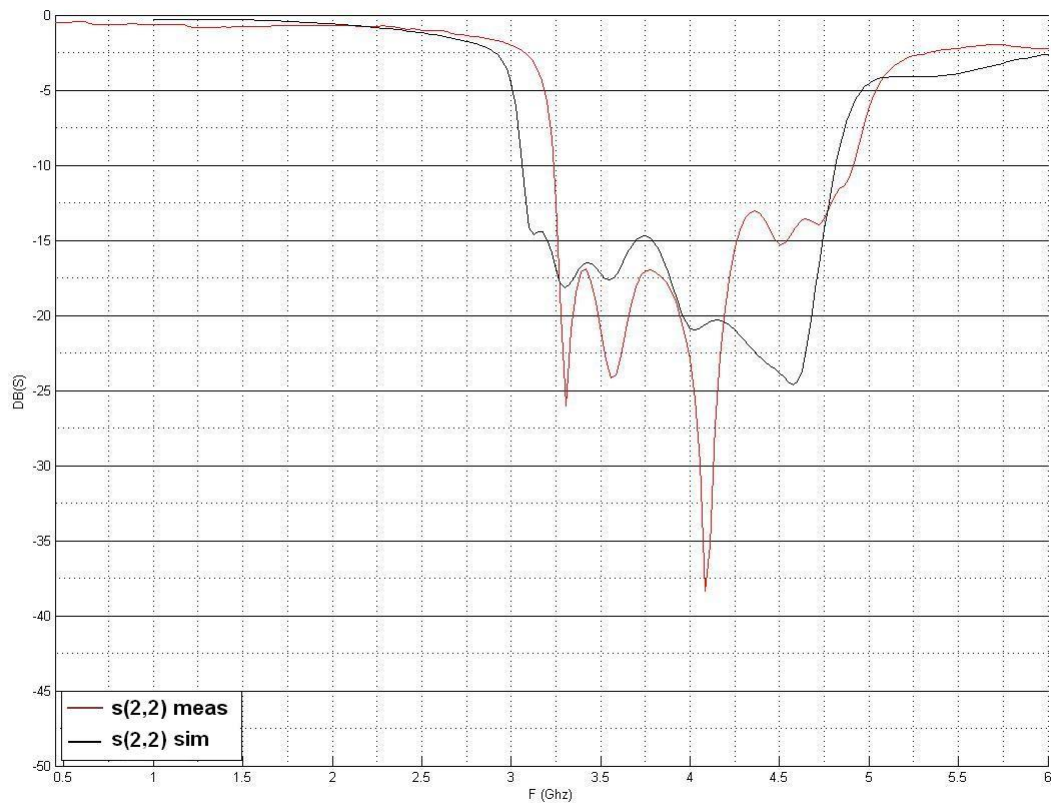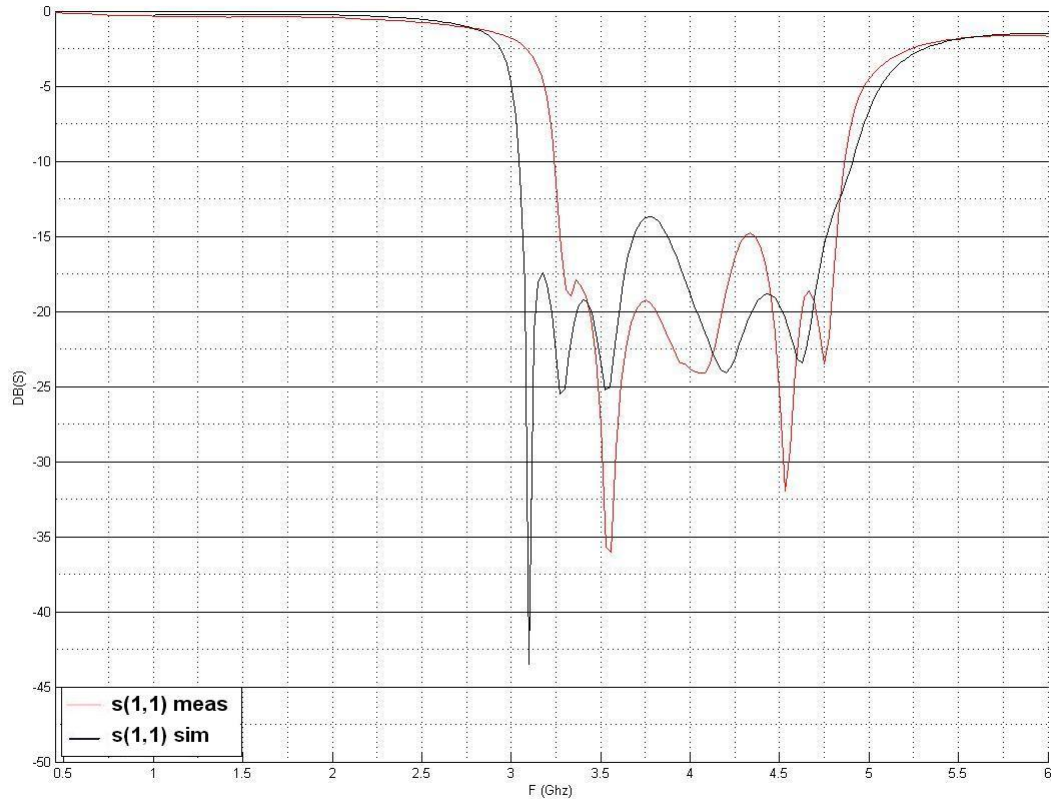
Figure 6.24: Comparison of the reflection coefficient of the simulated circuit model and the filter built.
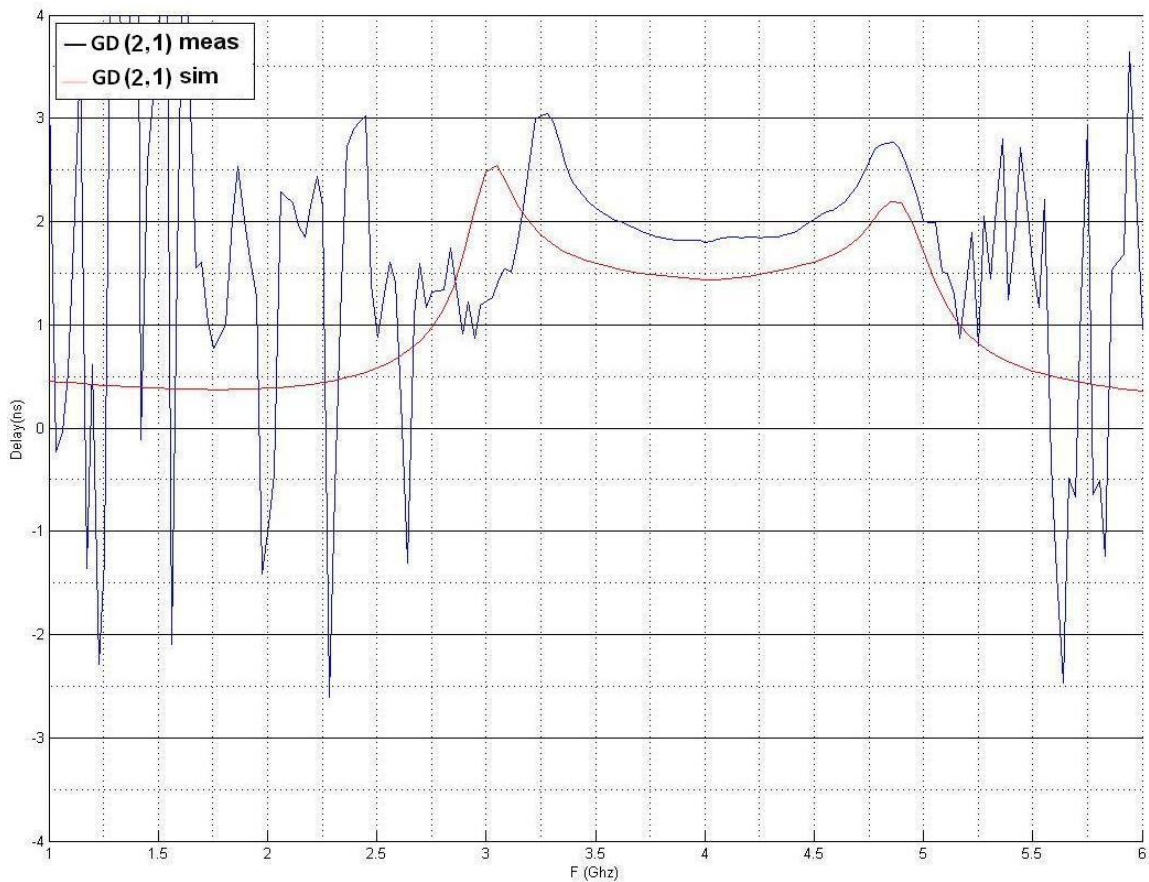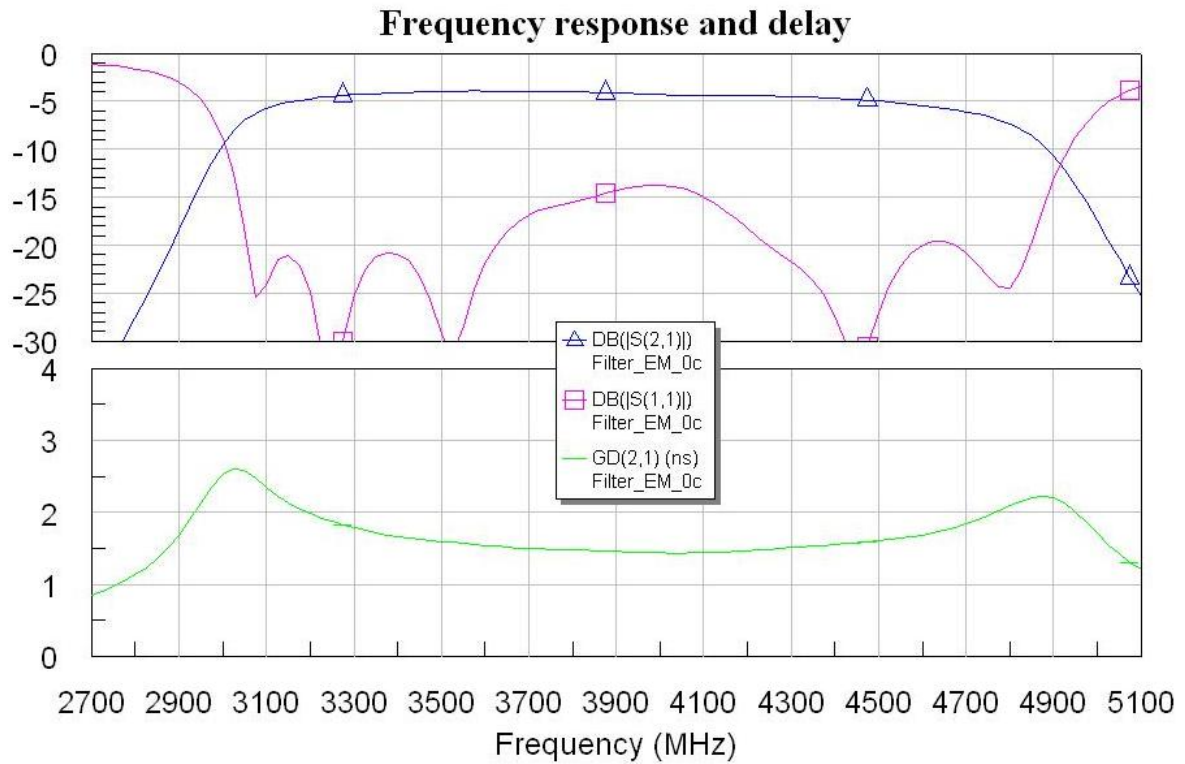
Figure 6.25: Detail of the simulated group delay response of the filter (up) and comparison between the simulated circuit model and the filter built (down).
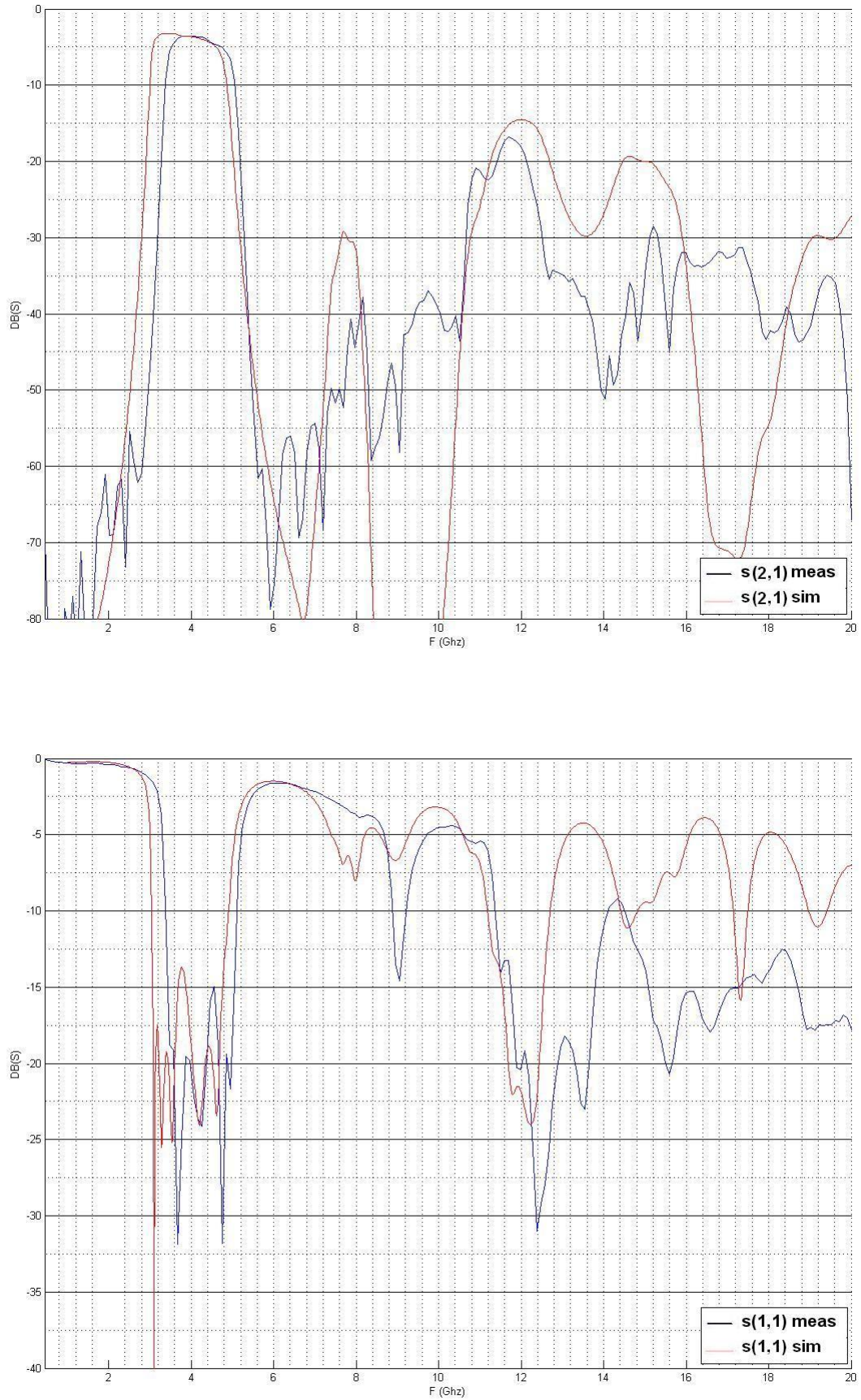
Figure 6.26: Comparison of the amplitude response and reflection coefficient of the simulated circuit model and the filter built for a wide bandwidth.

6.9.4 Filter pictures

These are pictures from the built filter measurements and while it was being characterized. The filter was measured with the VNA as shown in **Figure 6.27** after its calibration. Its connectors were 3.5mm ones.

The measurements of the coupled lines, as illustrated in detail in the filter schematic shown before in **Figure 6.17**, were around **10.5mm length, 1mm width and 0.4mm separation**. These measures were then checked in the filter built, and were quite accurate given that the limits for the fabrication process used are at 0.2mm.

The actual filter measurements were not very big, so it can be easily integrated in medium size equipment, and it is more than enough for our purposes. It was **9.5cm long and 4cm tall**, with an additional 1cm for the connectors, as shown in **Figure 6.28**.
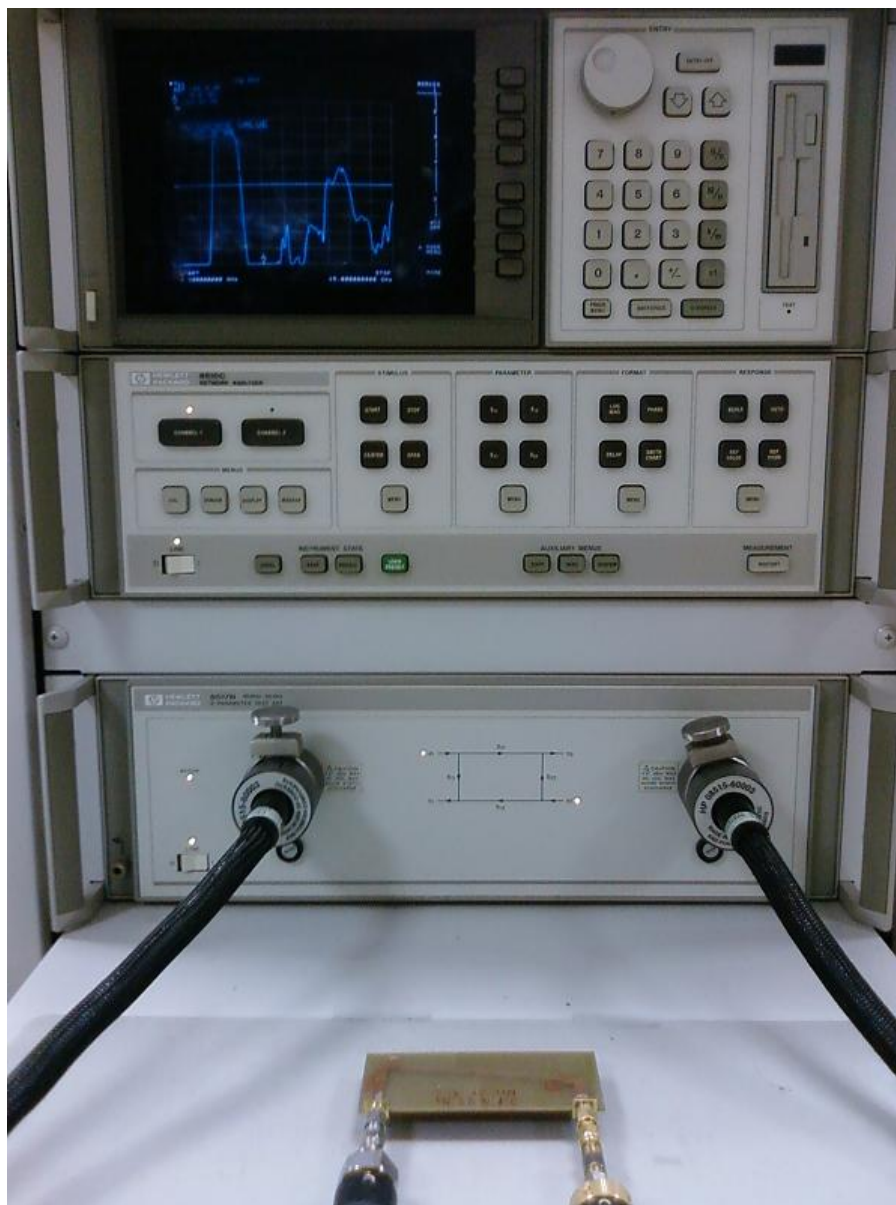
Figure 6.27: First filter built being measured in the Network Analyzer.
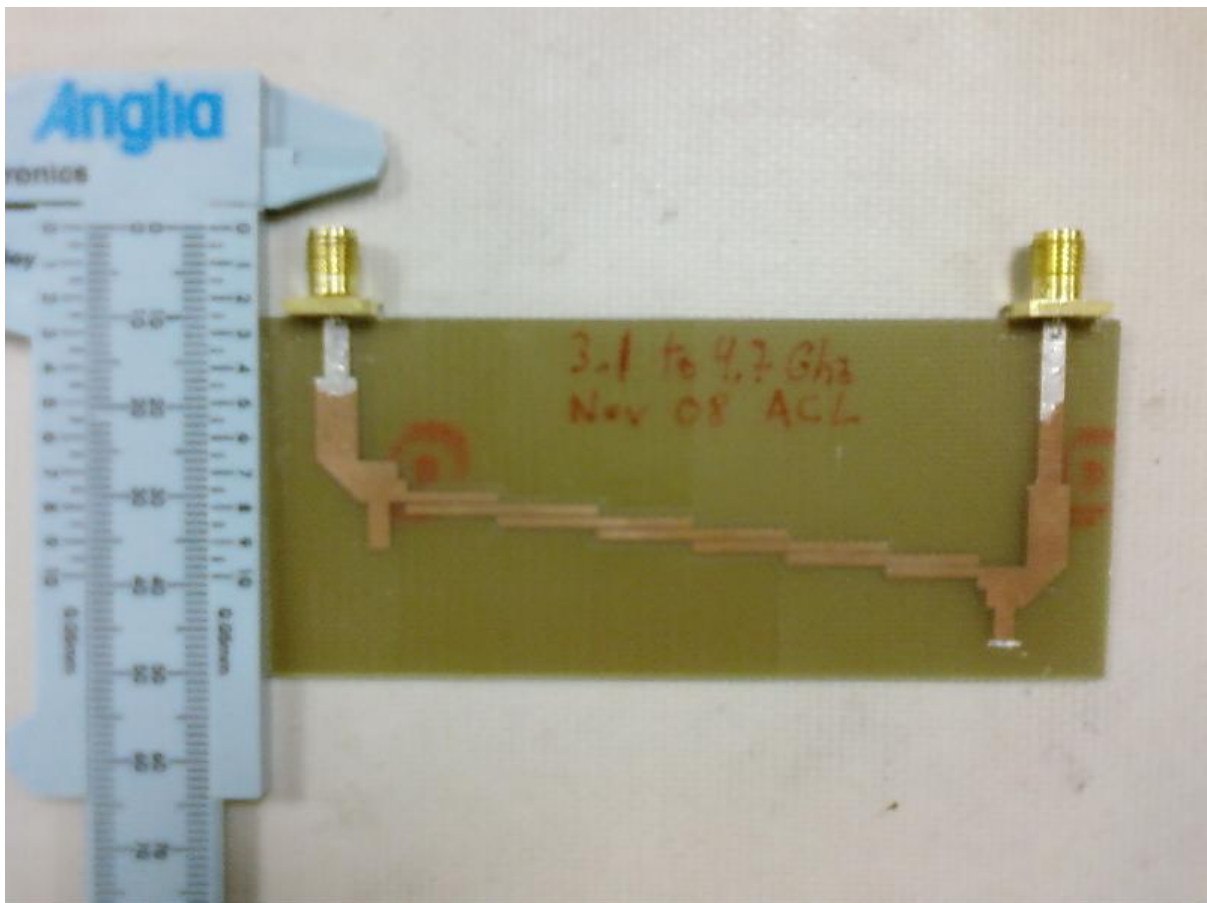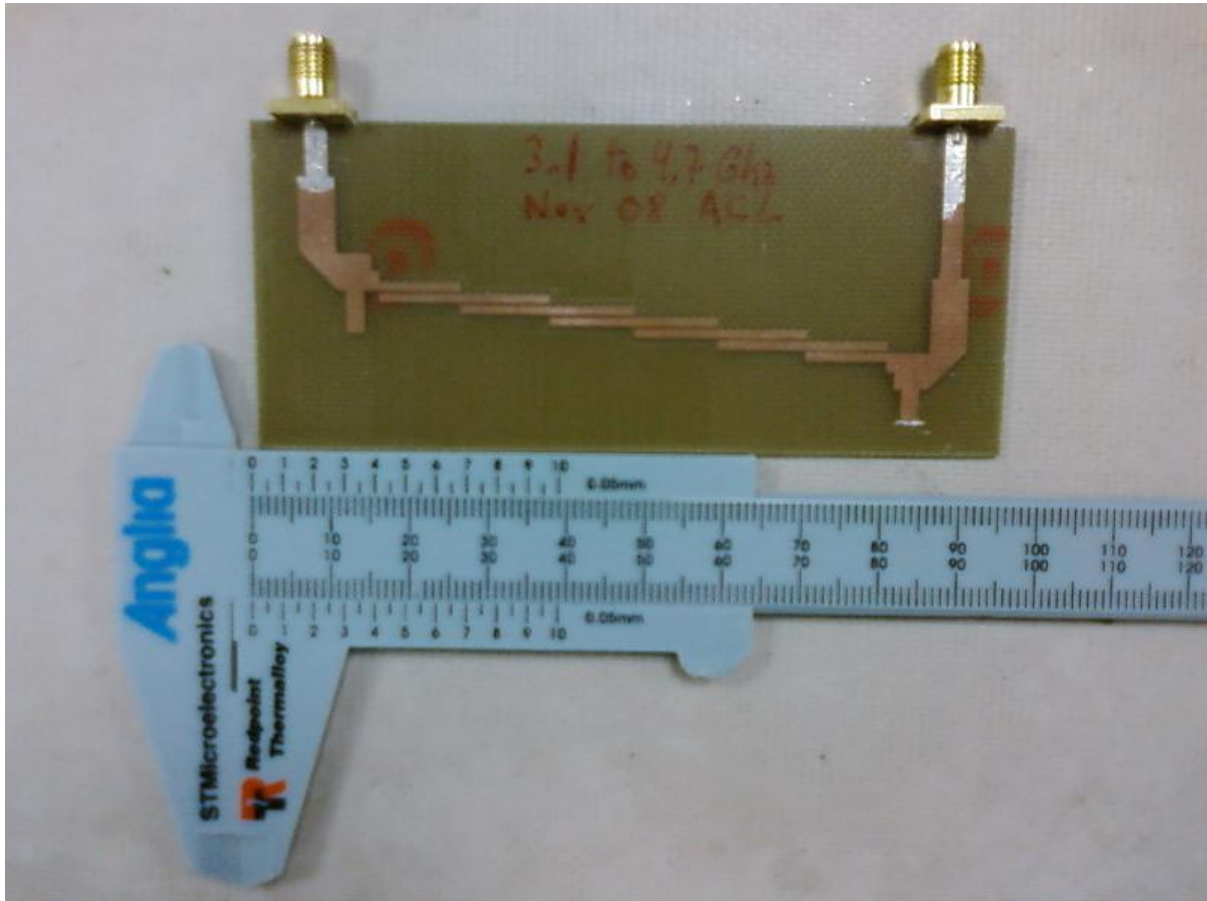
Figure 6.28: Physical measurements of the first filter built.
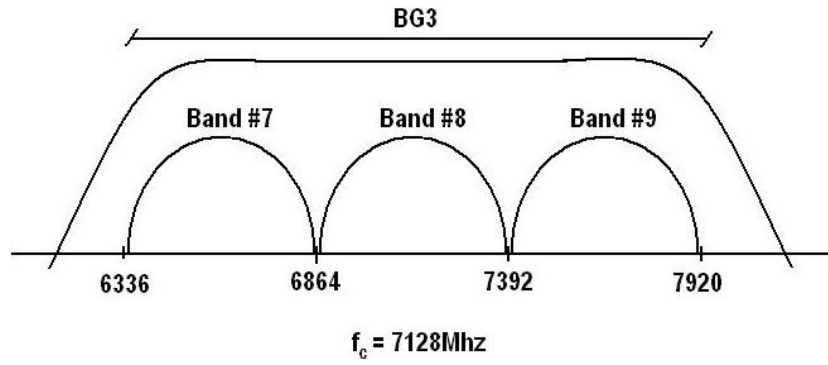
Figure 6.29: BG3 band-pass filter specifications.

6.10   Second design: 6.3 to 7.9 Ghz BPF

The second design has the next characteristics:

- Type of filter: band-pass

- Type of response: Chebyshev

- Center frequency: 7.1 Ghz

- Filter order: 5

- Relative bandwidth: 22%

- Return loss: 15dB

- Impedance: 50Ω

6.10.1   Design procedure

To start designing this filter, first step was to set up the specifications for it. Center frequency and width of the passband, attenuation requirements and the kind and order of the response going to be used.

$$\omega_l = 6336Mhz$$

$$\omega_c = 7128Mhz \qquad (6.4)$$

$$\omega_u = 7920Mhz$$

With those frequencies, the order needed for the filter that was again calculated to be N=5, and the impedances at the input and output of 50Ω. At this stage we have every specification needed to start designing the filter.

The element values for a fifth order Chebyshev with 3dB ripples used again were:

$$G = [\,1 \quad 3.4817 \quad 0.7618 \quad 4.5381 \quad 0.7618 \quad 3.4817 \quad 1\,] \qquad (6.5)$$

n	g_n	$Z_0 J_n$	Z_{0e}	Z_{0o}	W/d	S/d	S	W
1	3.4817	0.3166	70.84	39.18	0.74	0.5	0.8	1.184
2	0.7618	0.2143	63.01	41.58	0.85	0.75	1.2	1.36
3	4.5381	0.1877	61.15	42.37	0.87	0.8	1.3	1.392
4	0.7618	0.1877	61.15	42.37	0.87	0.8	1.3	1.392
5	3.4817	0.2143	63.01	41.58	0.85	0.75	1.2	1.316
6	1	0.3166	70.84	39.18	0.74	0.5	0.8	1.184

Table 6.2: Values obtained for the different coupled-line sections, using a fifth order Chebyshev with 3dB ripples.

Then, equations 5.26 and 5.27, from section 5.3 were used in a Matlab script, showed in the **Appendix**, **algorithm 9.1**, to obtain the values in **Table 6.2**.

For the length of the sections, the following equation was used:

$$l = \frac{\lambda}{4} = \frac{75}{F(Ghz)\sqrt{\varepsilon_{eff}}} \, (mm) \tag{6.6}$$

which gave an approximate length of 5.2mm for the $\frac{\lambda}{4}$ coupled lines sections at the center frequency they were going to be used.

From this data, the **first circuit model** obtained is shown in **Figures 6.30 and 6.31.** This model, as opposite to the first filter which was designed from scratch, was obtained from the modification of the second circuit model for the first filter. This way, we started with a design that already had the sections to connect both ports to the same side of the board, and other small modifications which were done previously, all integrated in the filter.

The need for a boxed filter was still necessary, and maybe more important than in the first filter, given that this one was going to work at higher frequencies, and was more prone to interference, so the same requirements for isolation into a metal housing applied.

For this first filter circuit model, width difference between the 50Ω port sections of the filter and the actual width of the adjacent coupled-line sections was too big again. As with the first filter, this could give some problems and a different behavior from the one expected. So it was taken into account while optimizing the design.

Some adjustments were again needed to obtain thinner sections, and a better adaptation in these parts. This was required because sections which are too wide allow for the propagation of transverse modes, which are not so well predicted by the design software and can cause misbehavior of the filter. The big difference in the width gap between the sections would also cause reflections and contribute to a bad response.

The **final circuit model** was obtained after some tuning of the first model. In this case, after the optimization, a stub section wasn't necessary, and the solution was to introduce more intermediate sections, that allowed for a gradually changing width. This way the big width difference between sections and the problems that could cause were fixed. The final filter obtained, with the improvements already applied, is shown in **Figures 6.32 and 6.33.**

First circuit model.
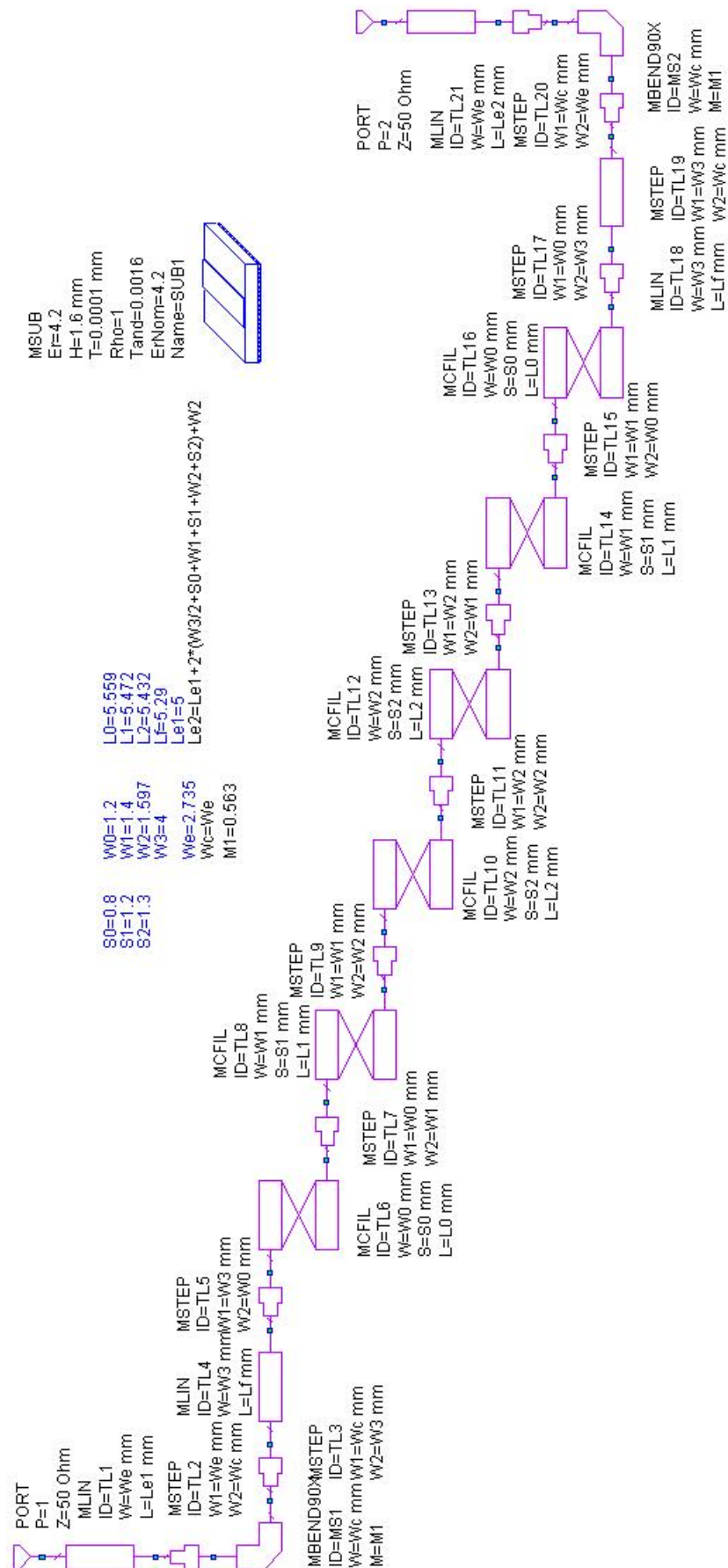
Figure 6.30: BG3 band-pass filter specifications of the first circuit model.
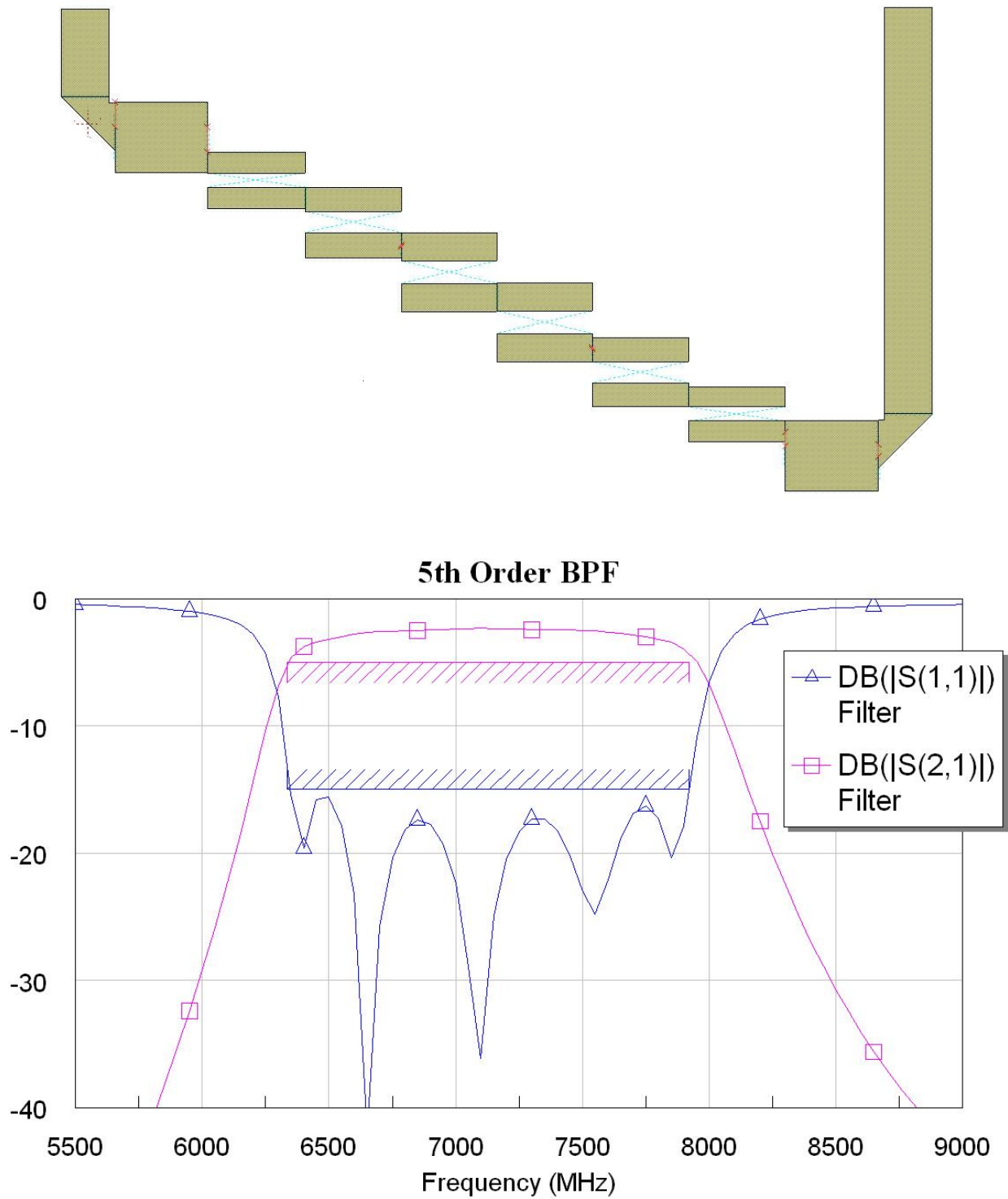
Figure 6.31: BG3 band-pass filter measurements and response of the first circuit model.

Final circuit model built.
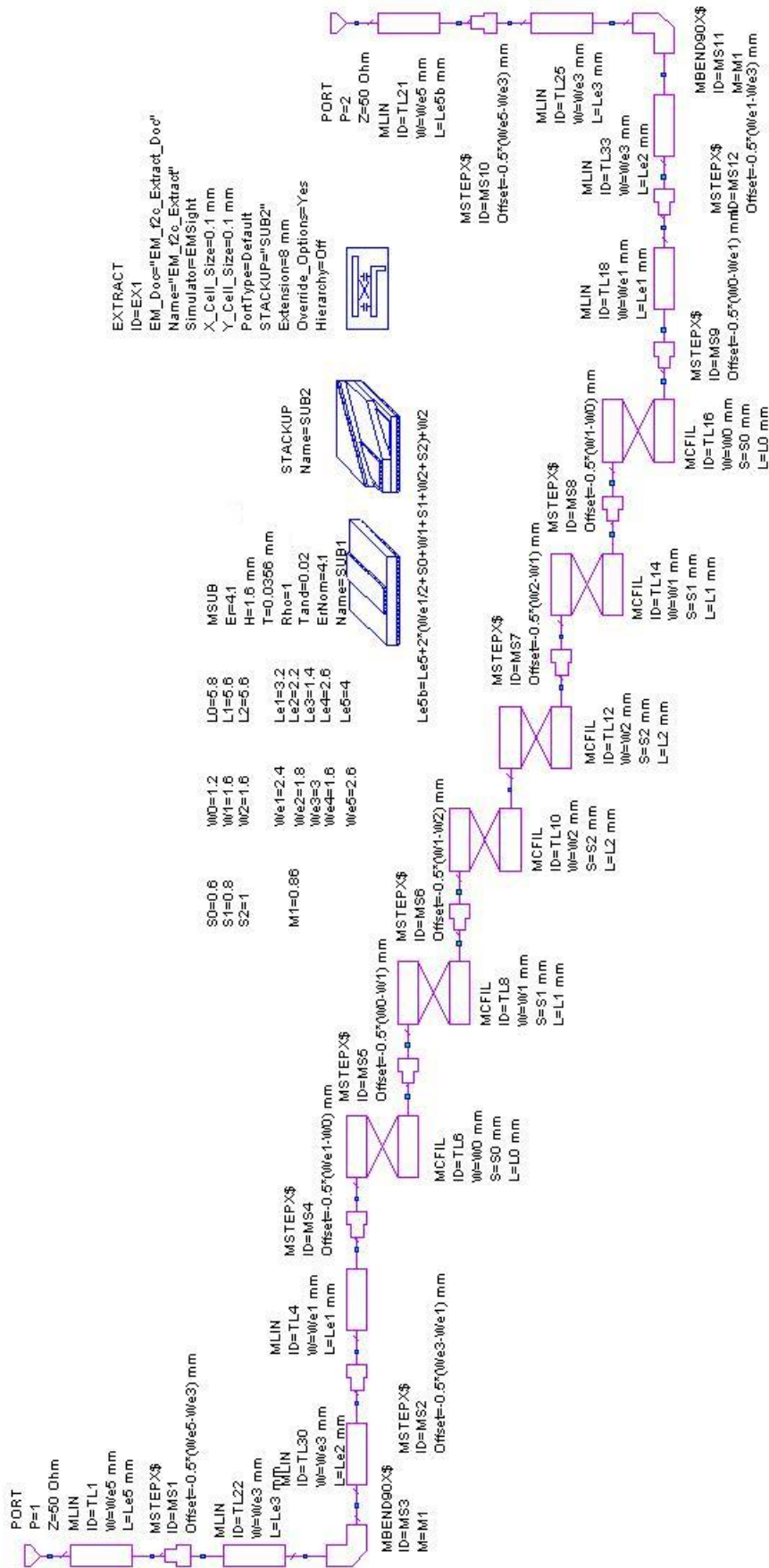
Figure 6.32: BG3 band-pass filter specifications of the final circuit model.
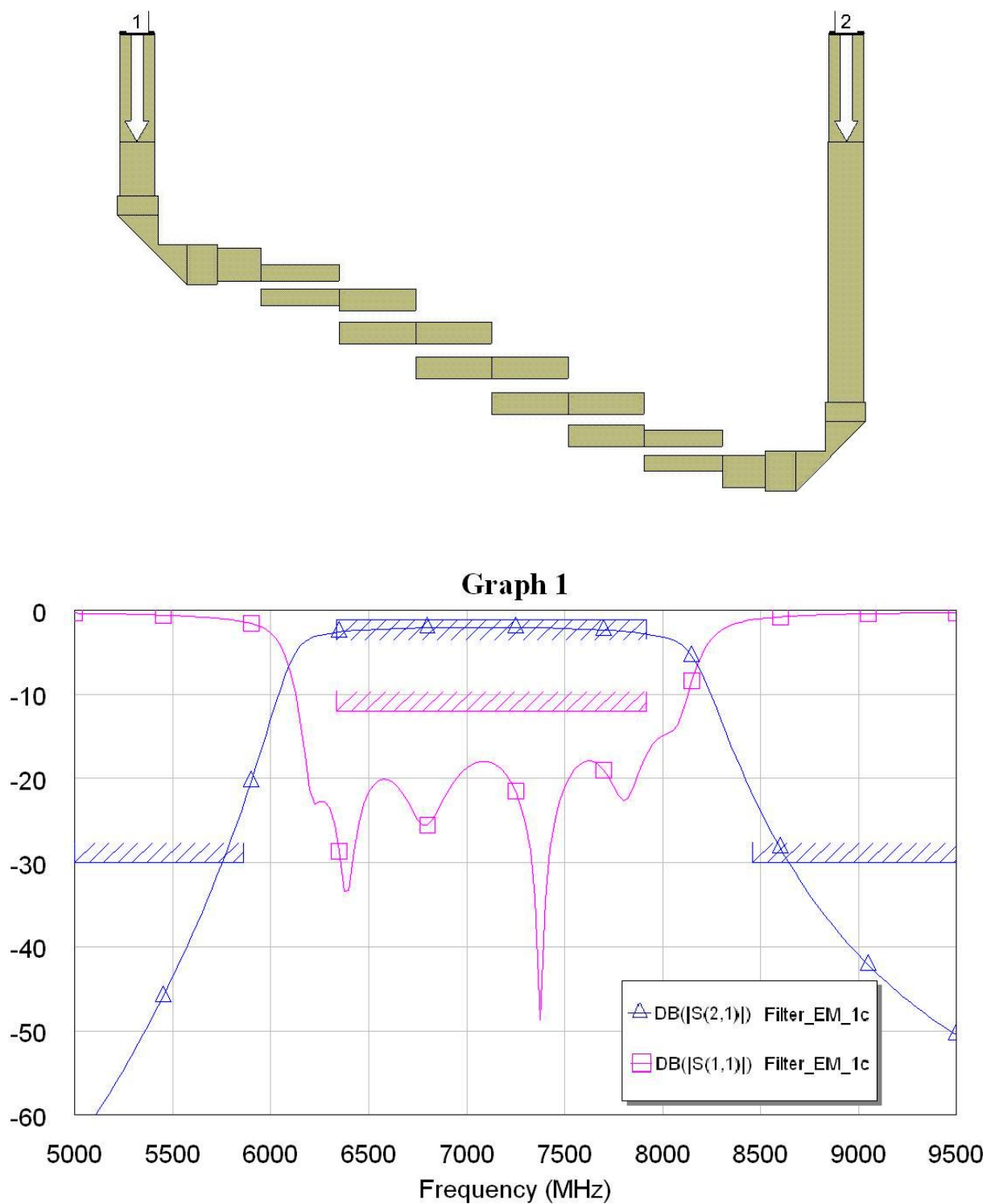
Figure 6.33: BG3 band-pass filter measurements and response of the final circuit model.
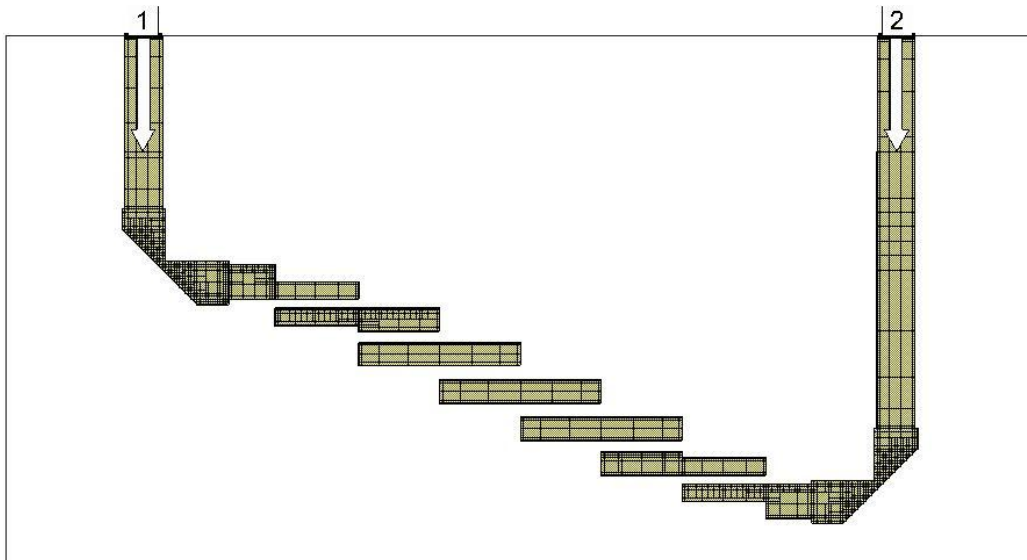
Figure 6.34: BG2 band-pass filter mesh of the final circuit model.

6.10.2 Currents and electric field distributions for the final circuit model

As done with the BG1 filter, we simulated the EM structure for this second filter, being able to show an animation of the flowing current and varying electromagnetic field for a desired range of frequencies.

These graphs are shown again for this filter. First, in **Figure 6.35**, the representation of the currents, and then, in **Figure 6.36**, the electric field.

Being the filter passband of 1.6 Ghz between 6.3 and 7.9 Ghz, it is seen in the center plot of both figures that at **7Ghz the current and Electric field flow** through the filter, making currents appear in the center of the coupled-line sections. This tell us that the filter doesn't oppose to the transmission of the EM wave at this frequency, given that it is seen how the electric field flows through the complete structure.

But as we represent the distributions in a frequency out of the passband, it is clearly seen that the **filter prevents the EM wave from propagating**, as shown by the top and bottom plots in the second figure, where it doesn't allow the electric field to go past the coupled lines when the frequency is nearer the upper and lower cutoff frequencies, making currents appear only in the section before the coupled-lines.

As we say, currents appear in the first section of the filter for both 5.5 and 8.3Ghz, but they are stronger for the first case. Also the electric fields are seen only reaching the first coupled-line section **at 5.5Ghz** (800Mhz apart from the lower passband frequency), but they get almost past the center of the structure at **8.3Ghz** (only 400Mhz apart from the higher passband frequency), as shown in the electric field plots by the coupled line sections colored in green and blue in the ends.
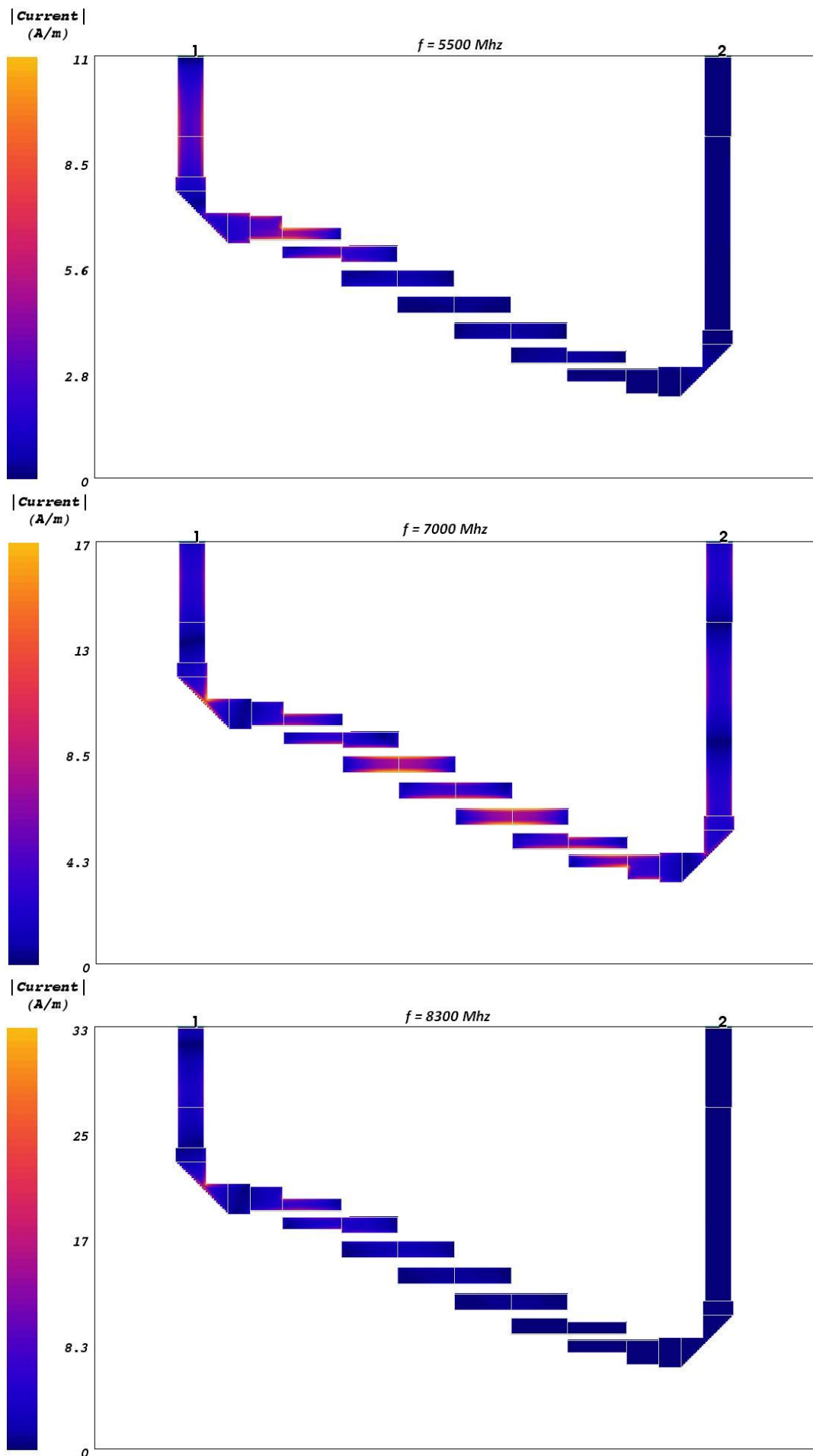
Figure 6.35: Currents distribution of the final circuit model at 5500, 7000 and 8300Mhz.
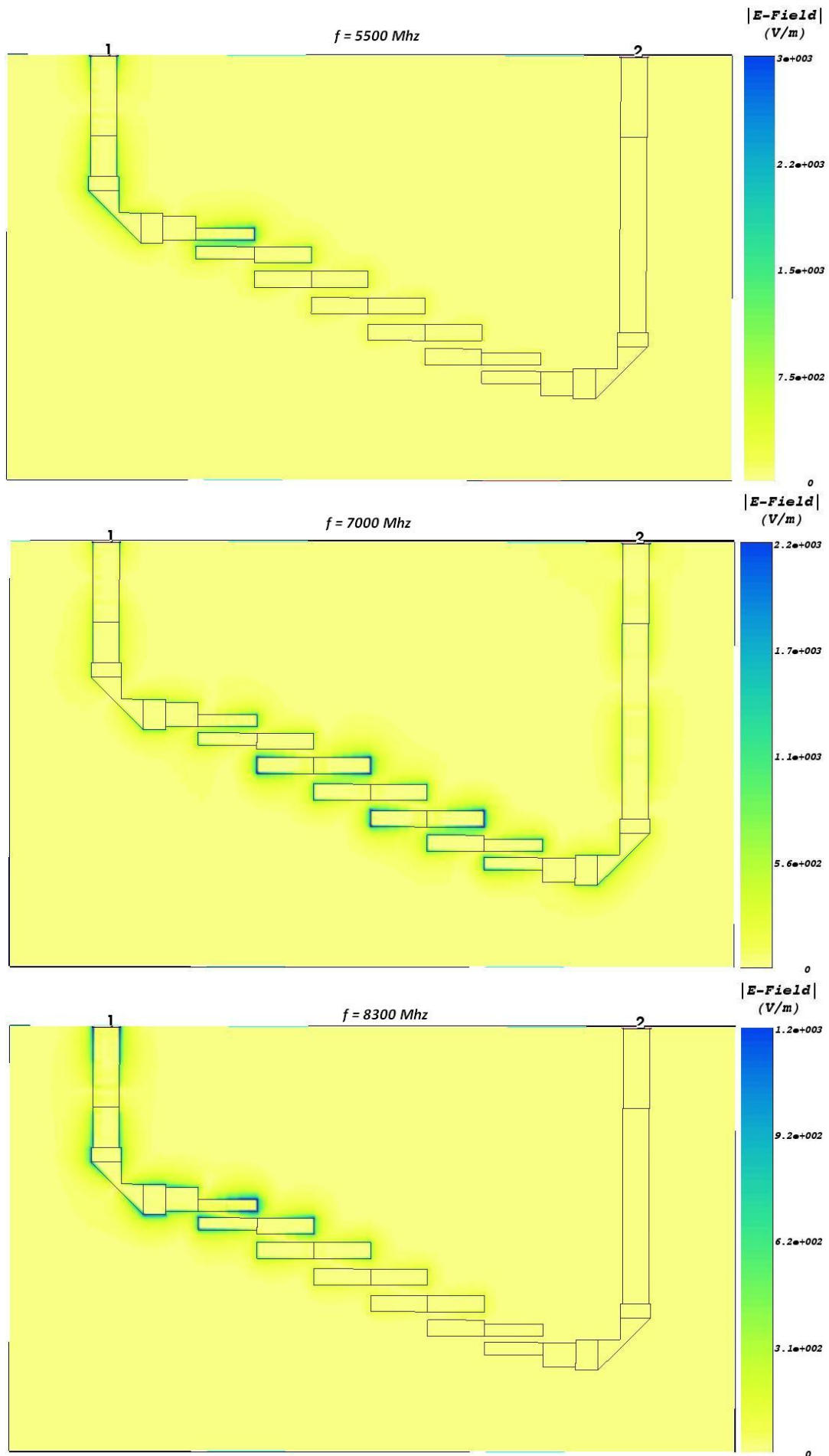
Figure 6.36: Electric field distribution of the final circuit model at at 5500, 7000 and 8300Mhz.

6.10.3   Final response and characteristics obtained

Narrow response

Once the final circuit model was built, the response obtained was the one showed in **Figure 6.37**, where the response is depicted measured from both ports of the filter. It is quite a good response, with an average transmission coefficient of -5dB and a -18dB reflection coefficient again, which is enough for the requirements of our system.

Figures 6.38 and 6.39 then show a comparison between the obtained response and the one simulated. As can be seen, the responses are similar but with differences, the main one being the roundness of it.

The same two effects happening in the first filter and modifying the response also appear here: **bandpass narrows and shifts**. But this time, the permittivity value was changed in the simulations to obtain a more accurate representation, that is why the frequency shift this time is not so evident. But the narrowing and rounding of the passband is evident, and that is because the loss tangent is not accurately set in the simulations and it is quite high at this frequency range for this substrate.

Both effects were taken into account in the design process, and although they affected the final result, the **final filter meets the required bandwidth**.

Group delay

In the next plot, **Figure 6.40**, graphs of the filter group delay response are shown. First plot is an in detail view of the filter passband response, with the simulated group delay. The second one is a comparison between the obtained group delay response of the built filter and the simulated one.

As it can be seen, responses are similar, with a **shift to lower frequencies and a difference in the lower passband part**, where the bump appearing at the lower cutoff frequency is flattened and a big peak appears at a lower frequency. But this peak is out of the passband and it is not a problem for the design. This time the difference between the higher and lower **group delay** points for the passband is of **about 0.7ns** which is a value good enough for our requirements.

Wide response

In **Figure 6.41**, the comparison between the simulated and the obtained response of the filter is shown for a very wide bandwidth, from 1 to 20 Ghz. From this wide frequency response it can be seen that the rejection rate of our filter is quite good and that there are not any spurious passbands appearing. But with a reflection coefficient that keeps worsening for the higher frequencies.
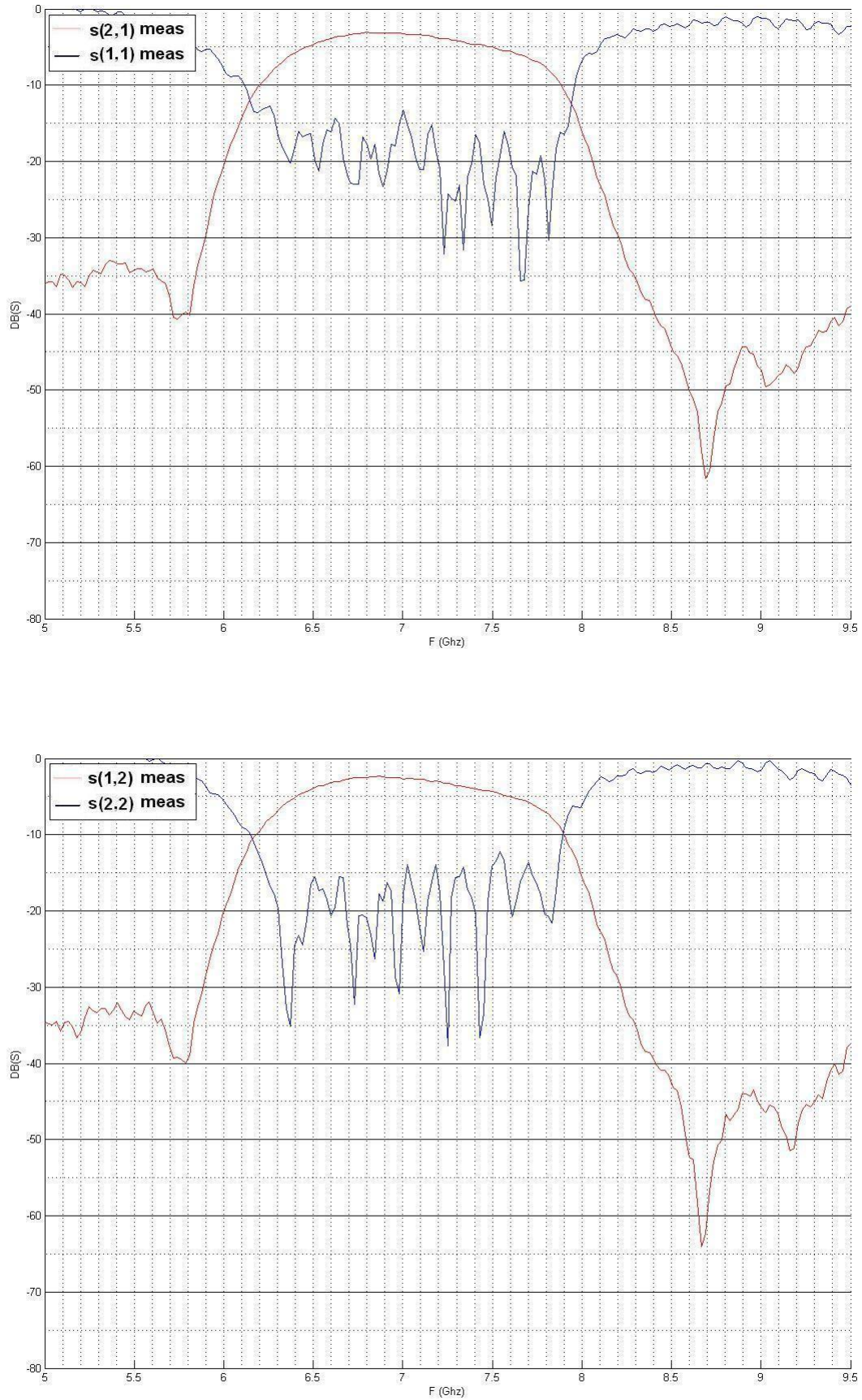
Figure 6.37: Comparison of the amplitude response and reflection coefficient measured from both ports of the filter.
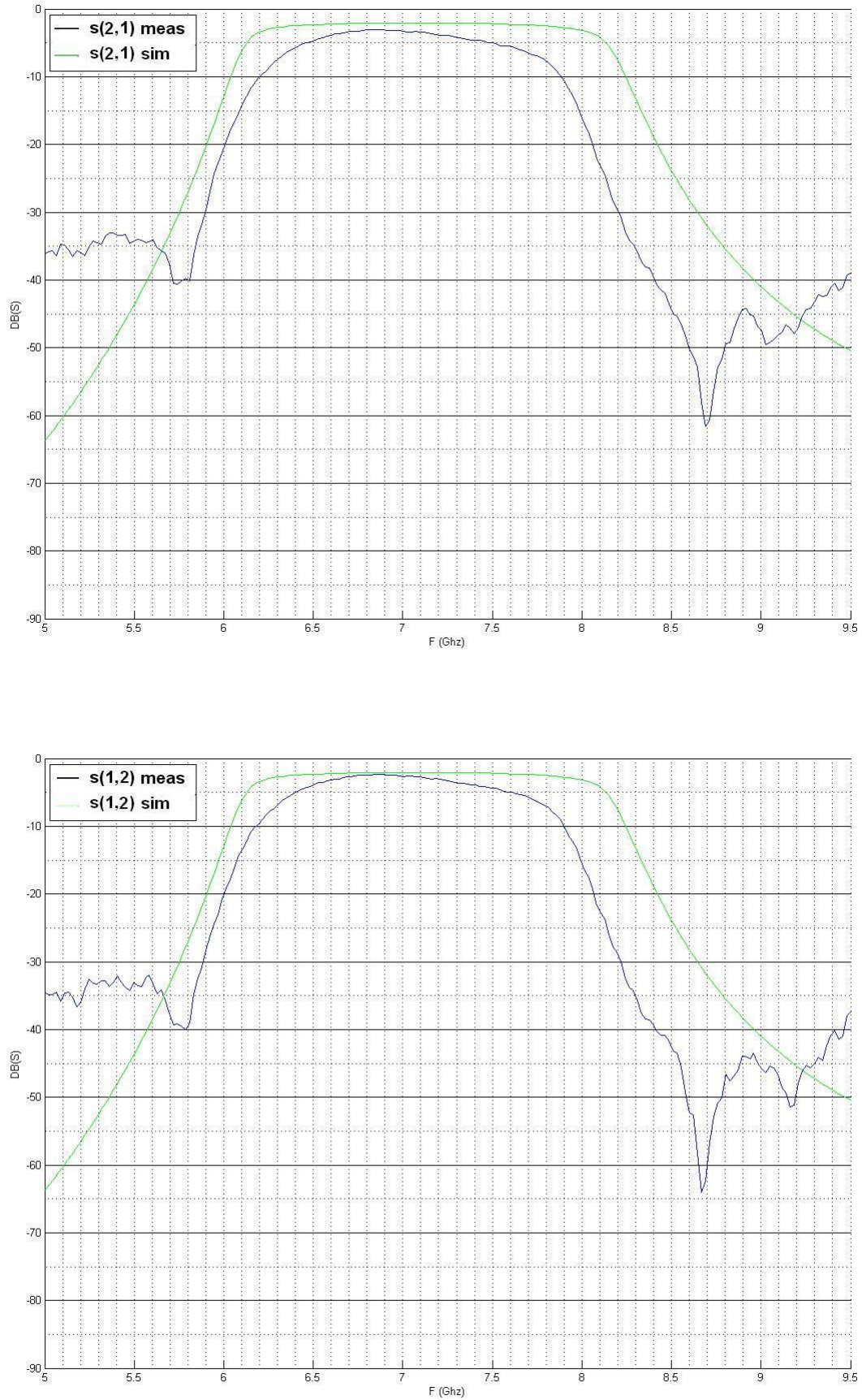
Figure 6.38: Comparison of the amplitude response of the simulated circuit model and the filter built.
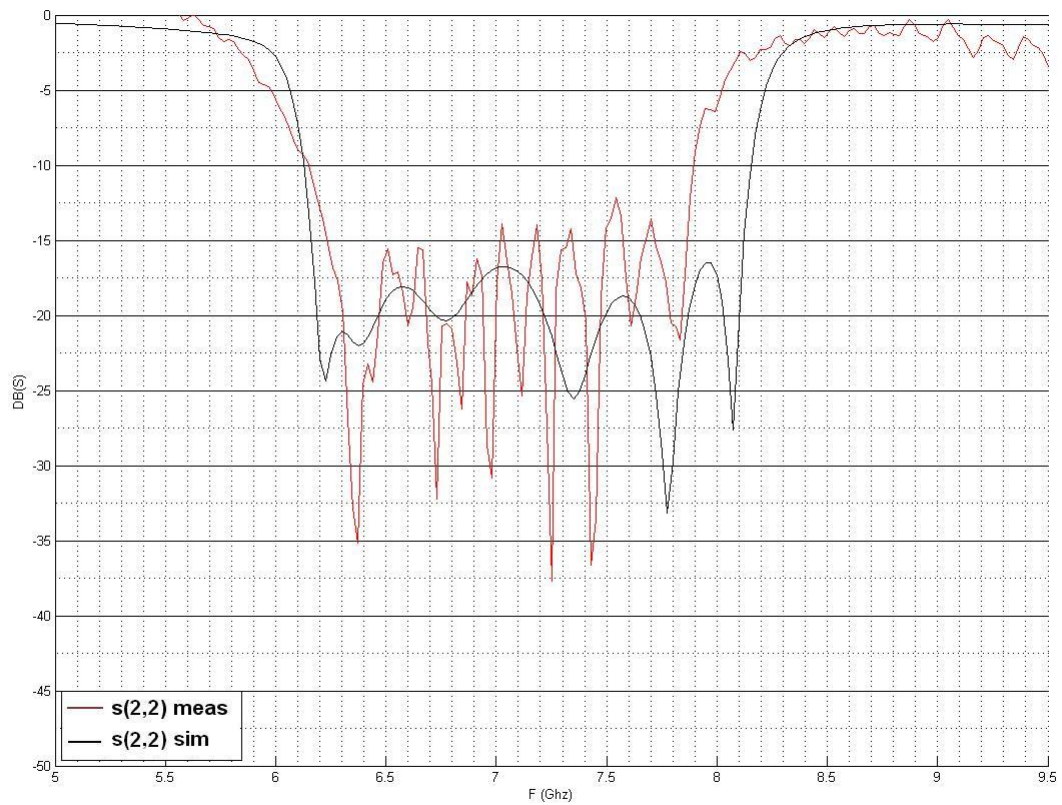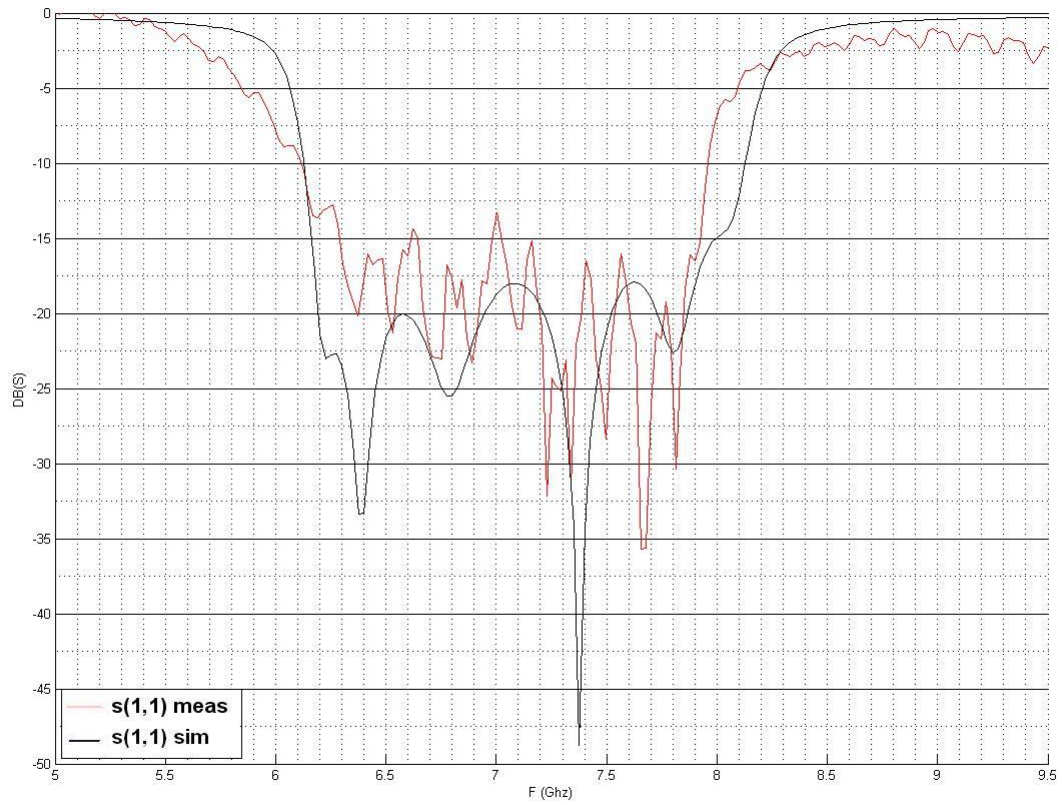
Figure 6.39: Comparison of the reflection coefficient of the simulated circuit model and the filter built.
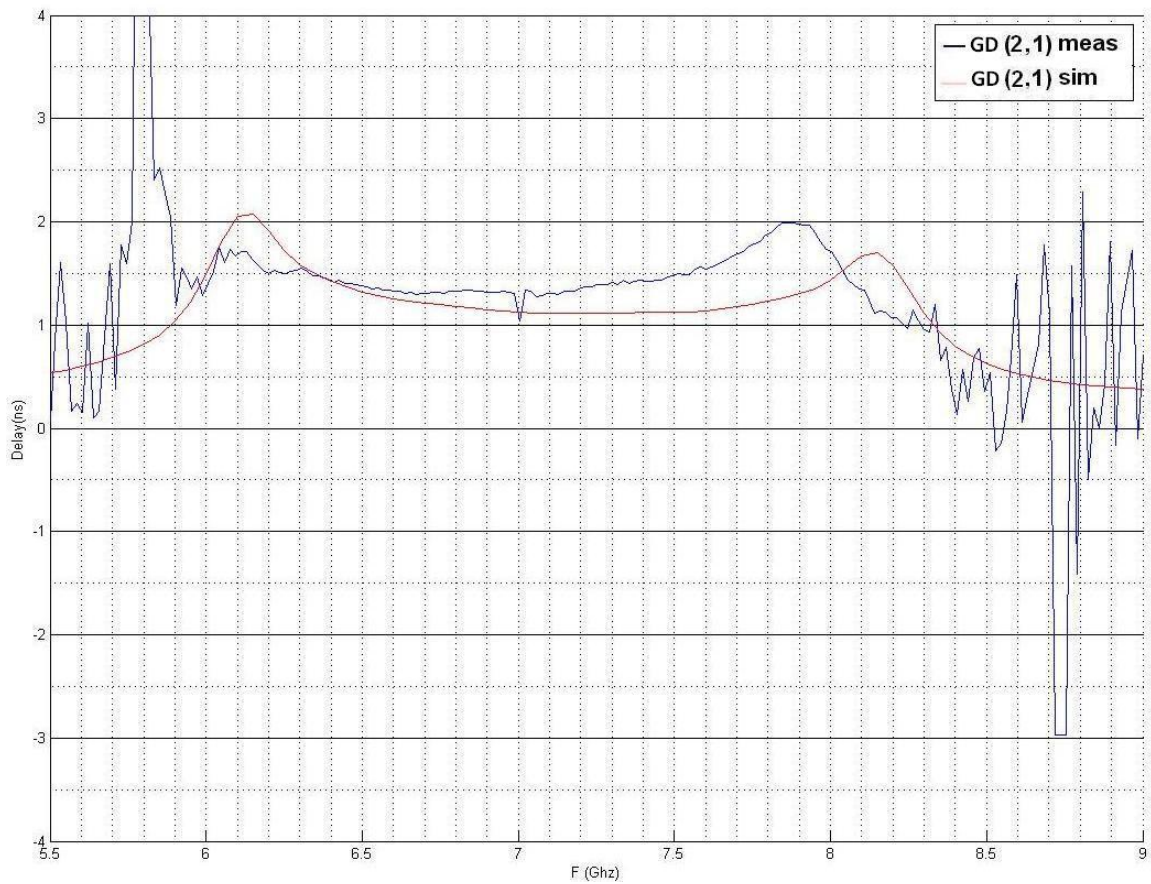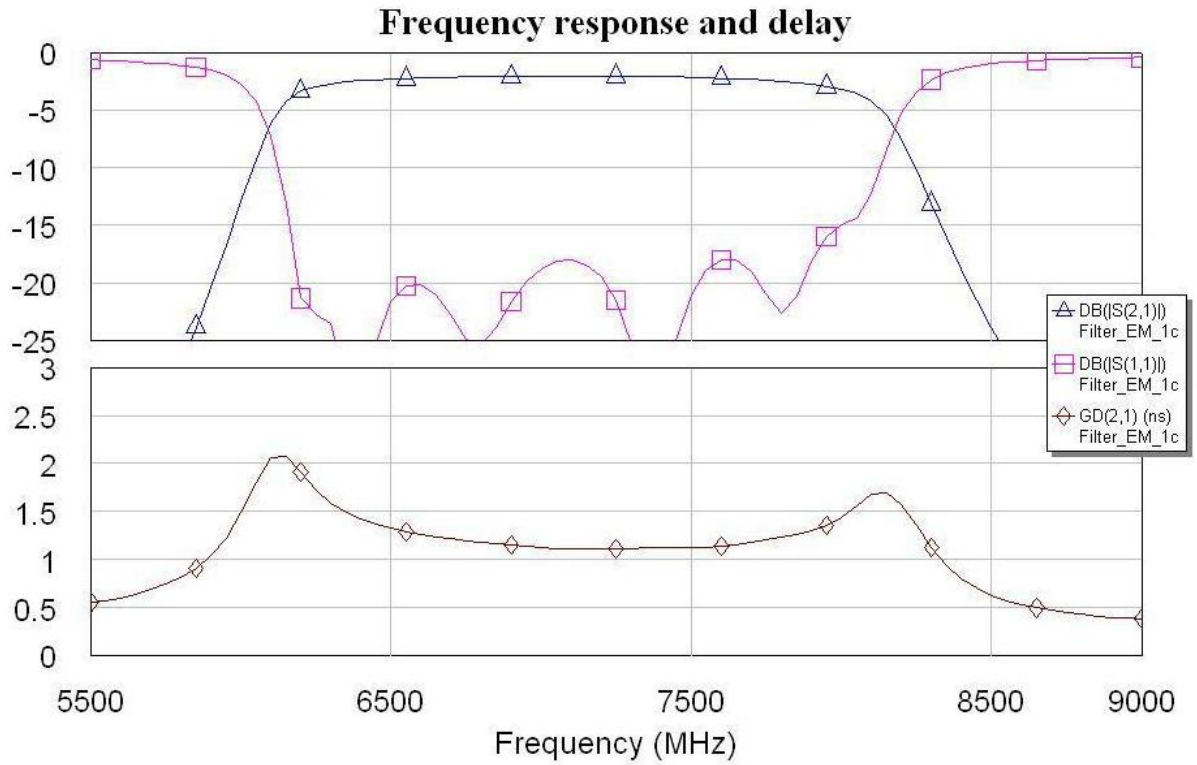
Figure 6.40: Detail of the simulated group delay response of the filter (up) and comparison between the simulated circuit model and the filter built (down).
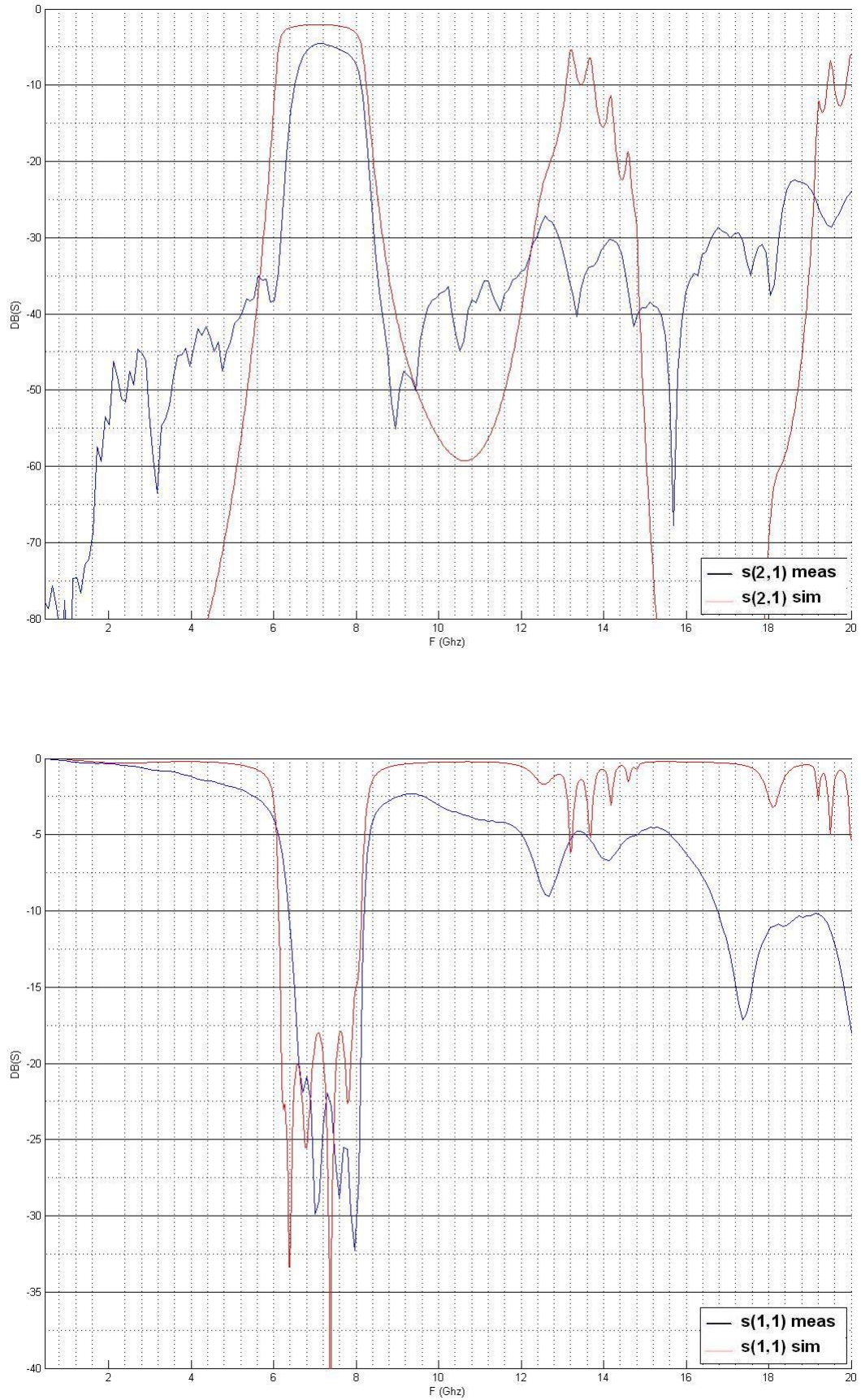
Figure 6.41: Comparison of the amplitude response and reflection coefficient of the simulated circuit model and the filter built for a wide bandwidth.

6.10.4   Filter pictures

These are pictures from the second built filter measurements and while it was being characterized. The filter was measured with the VNA as shown in **Figure 6.42** after its calibration. Its connectors were 3.5mm ones.

The measurements of the coupled lines, as illustrated in detail in the filter schematic shown before in **Figure** 6.32, were around **5.8mm length, 1.2mm minimum width (being 1.6mm the other two) and 0.8mm separation**. These measures were again tested and again quite accurately built.

The filter measurements were smaller this time. First because stubs weren't needed to obtain a good response and second because, as it was a higher frequency design, measurements are smaller: lengths, widths and separations. It was **6.3cm long and 2.8cm tall**, with an additional 1cm for the connectors, as shown in **Figure 6.43**.
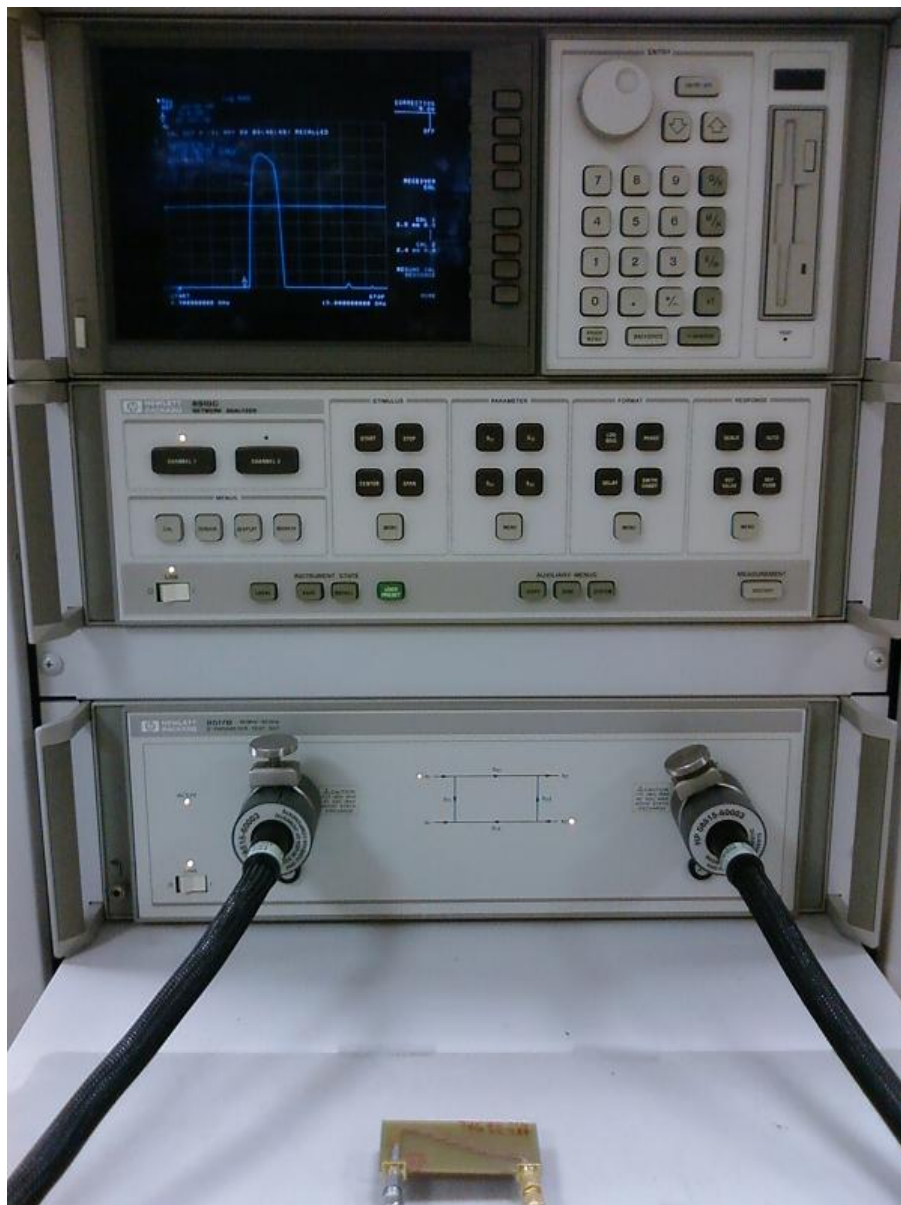
Figure 6.42: Second filter built being measured in the Network Analyzer.
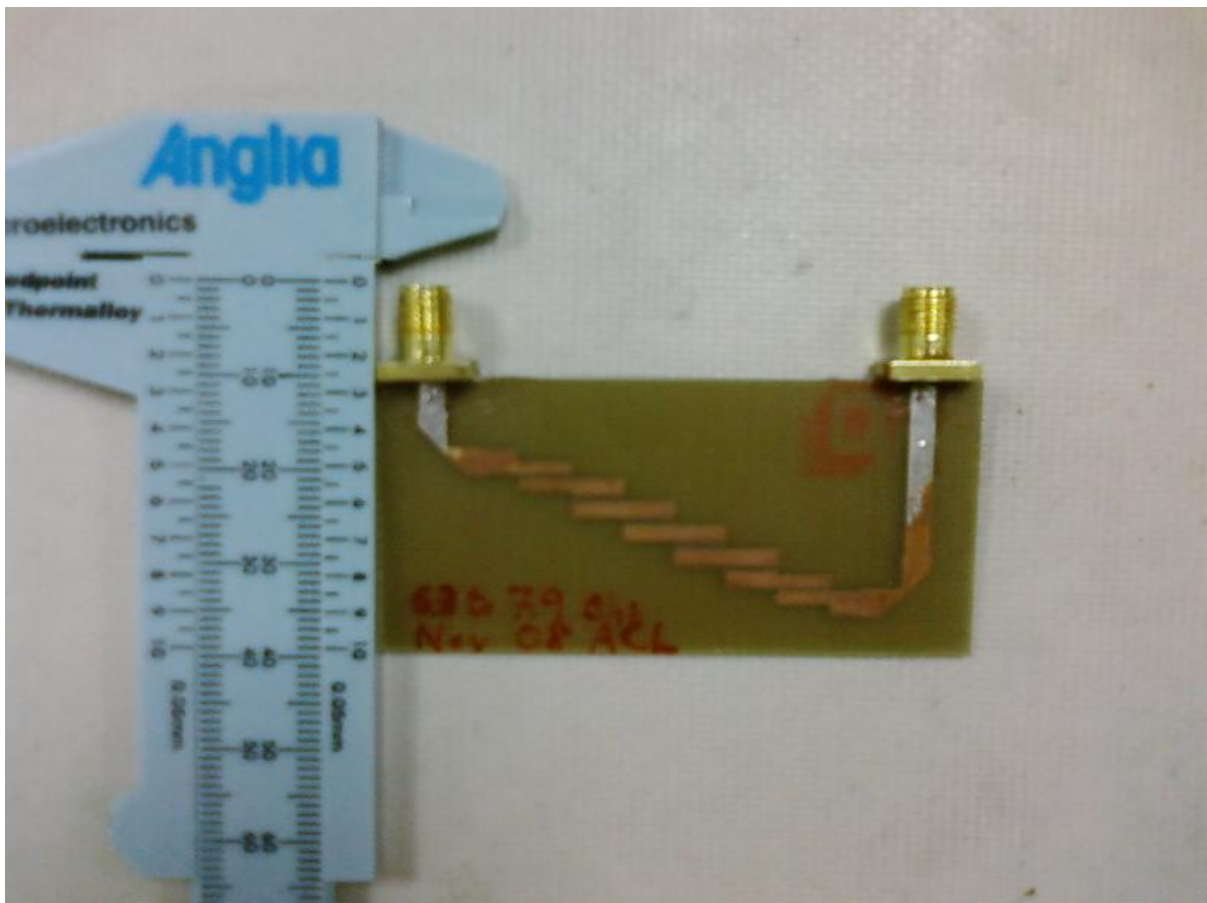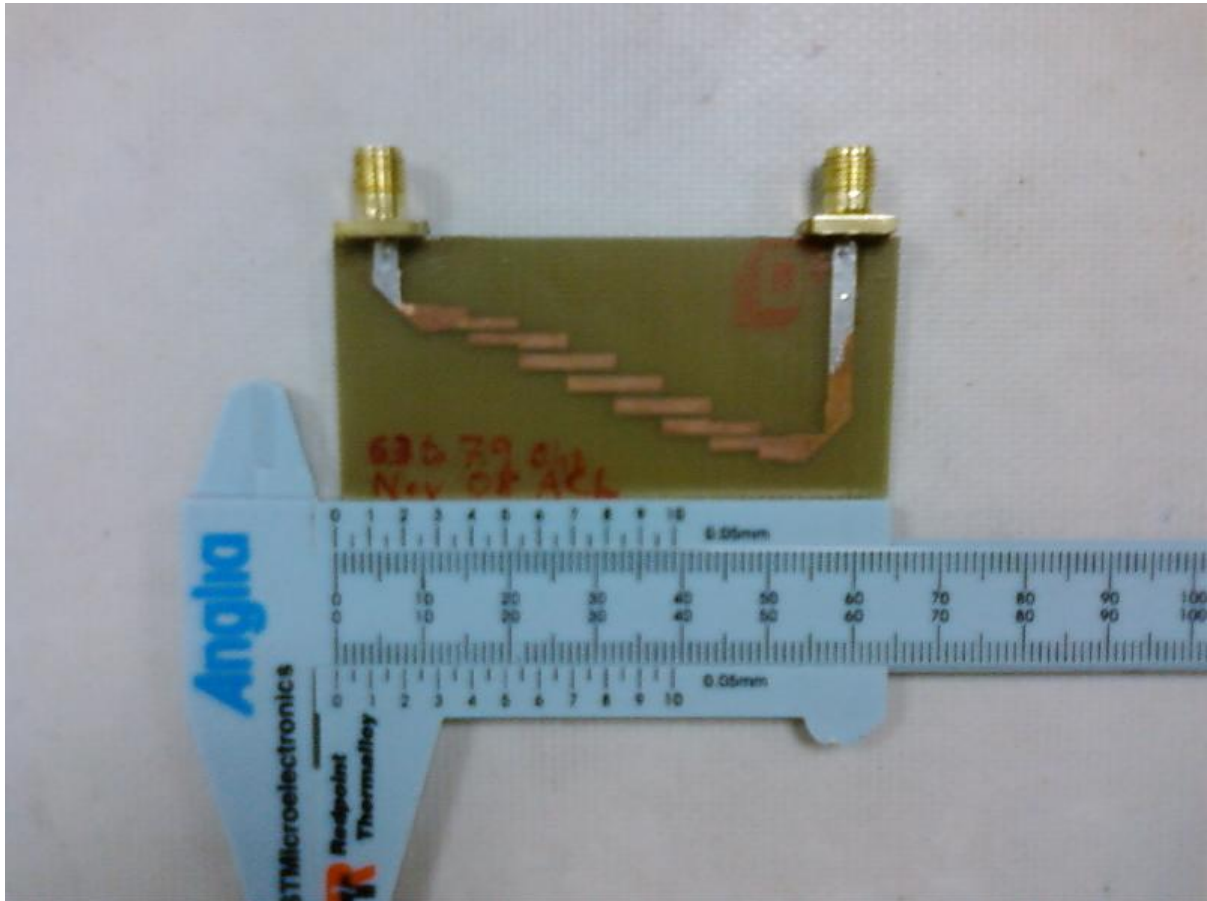
Figure 6.43: Physical measurements of the second filter built.

6.11   Conclusions

With the graphs in this chapter, we have shown the **outcome of the design process of the filters**. The measurements done of the filters characteristics: reflection coefficients, group delay and amplitude responses, even the high bandwidth ones, are good and show an adequate behavior, as the multiple tests done confirm.

In the end, we have designed quite compact filters thanks to the use of **microstrip technology**, as pictures show. They also have good characteristics, although the frequency we are using them at is on the limit to obtain good results with this technology. This affects the response, showing a deviation from the results on the simulations, with better results for the lower frequency one, but good enough in both cases.

Both filters behavior finally **meet the necessary requirements to be integrated in our complete UWBoF transmission system**, that will be explained in the next chapters. First, the key aspects about **UWB and ROF technologies**, and then the measurements and results from the tests conducted, that will be presented in the final chapter.

7

UWB and ROF technologies.

7.1 Introduction

In this chapter we describe the main two technologies applied in the developed system, UWB and ROF. By using these technologies, we managed to obtain a **high bit-rate transmission scheme which sends RF signals modulated into optical carriers.** This system could be developed as an optical distribution system for RF signals, [25] where it would be possible to use existing fiber networks already installed in buildings and many constructions to distribute RF signals, UWB signals in this case, and radiate them using antennas in every point needed. That way, with only an opto-electrical conversion in the ends of the system, we will be able to cover the designated areas wirelessly.

UWB is a commercially attractive method to implement **high speed wireless transmission** in different end-user technologies with **low power consumption**. It is a newly developed technology that uses a different focus to achieve both objectives at the same time and establishes a new way of sharing frequency spectrum.

To achieve its objectives, UWB technology transmits using a **wide bandwidth**, but with a low **power emission (-41.3 dBm/MHz)**, allowing for partial band overlapping with different systems without affecting them. One of the proposed schemes for the standard combines MB-OFDM in different sub-bands, with 128 carriers each one. Achieves maximum speeds between 320Mbps and 480Mbps, and expects to reach 1Gbps in the near future with new draft specifications. [26, 27]

ROF is a technology that offers the possibility of **transmitting RF signals, in a transparent way, over an optical fibre link distribution system**. It allows for **long distances with low latency and attenuation**, but with a frequency behavior affected by dispersive fading and nonlinear effects because of the laser and fiber responses.

In this scenario it is possible to obtain better link quality using channel compensation tech-

Unlicensed bands	Frequency of operation	Bandwidth
ISM at 2.4 Ghz	2.400-2.4835	83.5 Mhz
U-NII at 5 Ghz	5.15-5.35 Ghz	300 MHz
	5.75-5.85 Ghz	
UWB	3.1-10.6 Ghz	7.500 Mhz

Table 7.1: US spectrum allocation for unlicensed use, from [6], Chapter 1.

niques and Digital Signal Processing (DSP) as it has been done for a long time in wireless links, but there is also room for improvement by changing main parameters of the optical system as we have seen during our investigation. To base our results, we evaluate the frequency dispersion behavior of the ROF system and measure the nonlinear effects taking place, finally comparing this with the application layer level performance, measuring the Packet Error Rate (PER) obtained in the receiver end.

This way, we show the **relationship between the main parameters in the system** and the importance of adjusting them depending on the optical and RF power emitted or the length of fiber used to **obtain the best possible performance out of the system**.

7.2 Ultra Wide Band

7.2.1 Definition

UWB technology, since its regulation by Federal Communications Commission (FCC) in 2002, has been developed as a commercially attractive method to implement high speed wireless transmission in different end-user technologies with low power consumption.

It is a technology that, in one of its variants, establishes a standard for high bit-rate wireless transmission as it uses **OFDM**, a highly efficient technique adopted for many new generation systems such as **Digital video broadcasting - Terrestrial (DVB-T), Asymmetric Digital Subscriber Line (ADSL), IEEE 802.11 a/g/n, Power line communication (PLC), and Worldwide Interoperability for Microwave Access (WiMAX)**. It is highly flexible, being able to focus in performance or battery-saving and has many advantages because of the new scheme used, one of the most important being multipath fading resilience.

The FCC Report and Order (R&O), issued in February 2002, allocated 7,500 MHz of spectrum for unlicensed use of UWB devices in the 3.1 to 10.6 Ghz frequency band. This spectral allocation was the first step towards a new policy of open spectrum initiated by the FCC in the past few years and more spectral allocation for unlicensed use followed, which spreaded the use and adoption of this technology.

The FCC defines UWB as any signal that occupies more than 500 MHz bandwidth in the 3.1 to 10.6 Ghz band and that meets the spectrum mask shown in **Figure 7.1**. This is by far the largest spectrum allocation for unlicensed use the FCC has ever granted. It is even more relevant given that the operating frequency is relatively low. A comparison with the other unlicensed bands currently available and used in the United States is shown in **Table 7.1**.
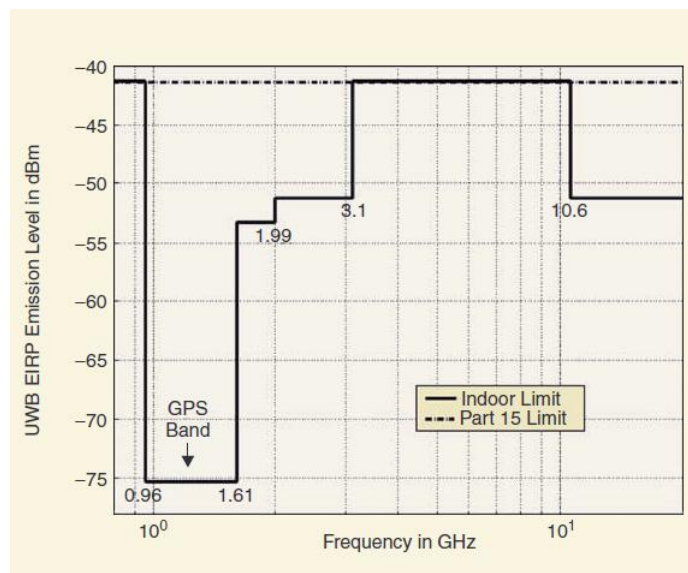
Figure 7.1: UWB spectral mask for indoor communication systems, from [6], Chapter 1.

This allocation opened up new possibilities to develop UWB technologies different from older approaches based on impulse radios. Given the spectral allocation and the new definition of UWB adopted by the FCC, UWB was not considered a technology anymore but, instead, available spectrum for unlicensed use. This means that any transmission signal that meets the FCC requirements for UWB spectrum can be used. This, of course, is not just restricted to impulse radios or high speed spread-spectrum radios pioneered by companies so far; it also applies to any technology that uses more than 500-MHz spectrum in the allowed spectral mask and with the current emission limits restrictions.

Signals that occupy different bandwidths are shown in **Figure 7.2**, where all of them have been shaped with a Gaussian envelope. Their bandwidths at the -10 dB points vary from 5 Ghz down to 5 MHz. It should be noted that all signals, with the exception of the last one, are UWB signals because they all occupy at least 500 MHz bandwidth. Their Power Spectral Density (PSD), measured in 1 MHz bandwidth, must not exceed the specified FCC limit. It is proportional to the UWB signal amplitude, bandwidth, and duty cycle, the latter defined as the ratio of the signal repetition rate and bandwidth. This means that, for a fixed PSD, the narrower the bandwidth, the smaller the allowed repetition rate for fixed amplitude. Periodic non-modulated repetition of these signals would generate a spectrum with spectral lines separated at the repetition rate, rather than the uniform spectrum envelope shown.

7.2.2   Modulation schemes

Information can be encoded in a UWB signal in a variety of methods. The most popular modulation schemes developed to date for UWB are: **Pulse Position Modulation (PPM), Pulse Amplitude Modulation (PAM), On-Off Keying (OOK), and Binary Phase Shift Keying (BPSK), also called bi-phase**.

Of course, an UWB signal is not different from any other signal, and any other modulation
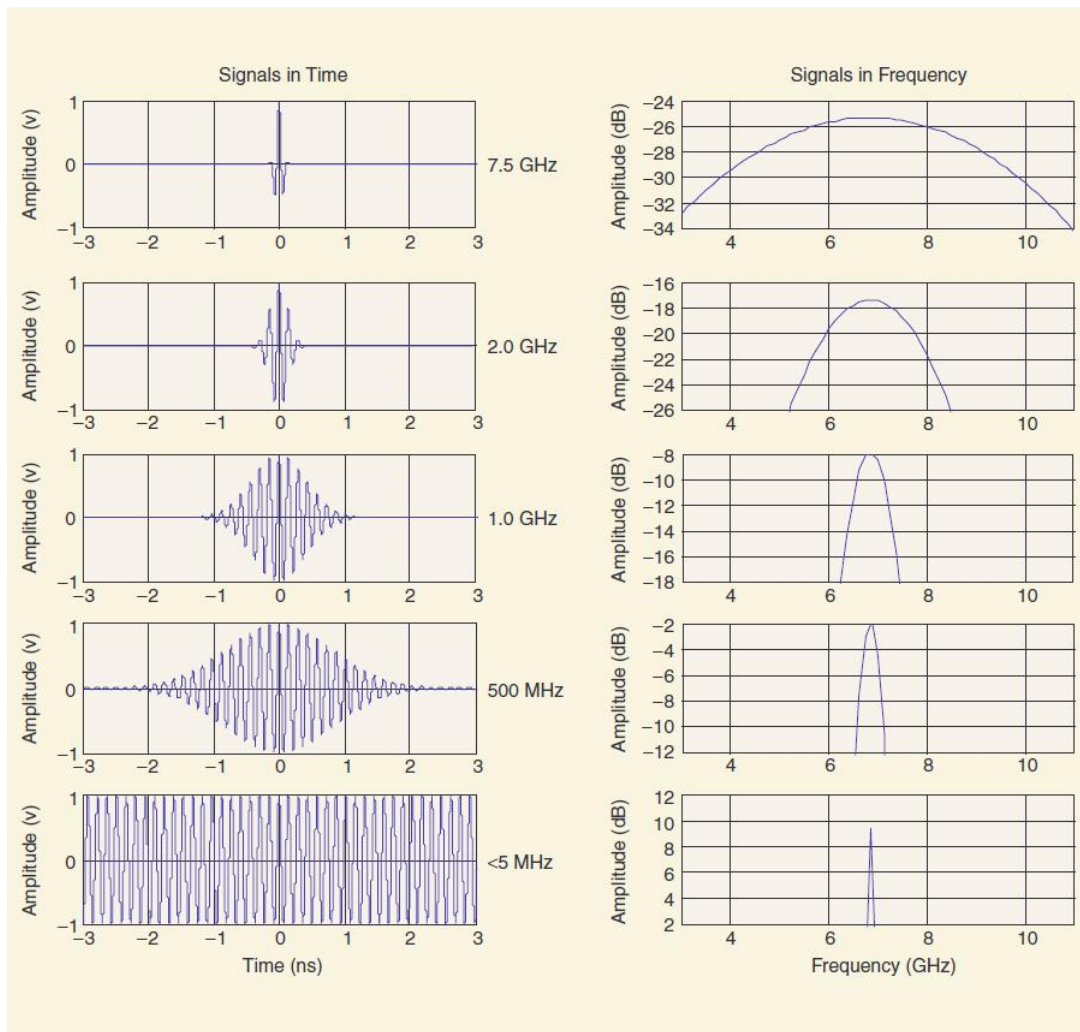
Figure 7.2: UWB signals of different bandwidth. Larger bandwidth, lower spectral density, from [6], Chapter 1.

scheme can be applied. New systems are emerging today that utilize different modulation schemes made feasible by the UWB spectrum allocation that allows narrower bandwidth signals. In the end, UWB follows the same fundamental principles of narrow-band systems.

The principles behind these modulation schemes are going to be described briefly now:

PPM

PPM is based on the principle of encoding information with two or more positions in time, referred to the nominal pulse position, as shown in **Figure 7.3**. A pulse transmitted at the nominal position represents a 0, and a pulse transmitted after the nominal position represents a 1.

The picture shows a two-position modulation, where one bit is encoded in one impulse. Additional positions can be used to provide more bits per symbol. The time delay between positions is typically a fraction of a nanosecond, while the time between nominal positions is typically much longer to avoid interference between impulses.

This scheme has been proposed to be adopted as a standard for UWB transmissions. But it
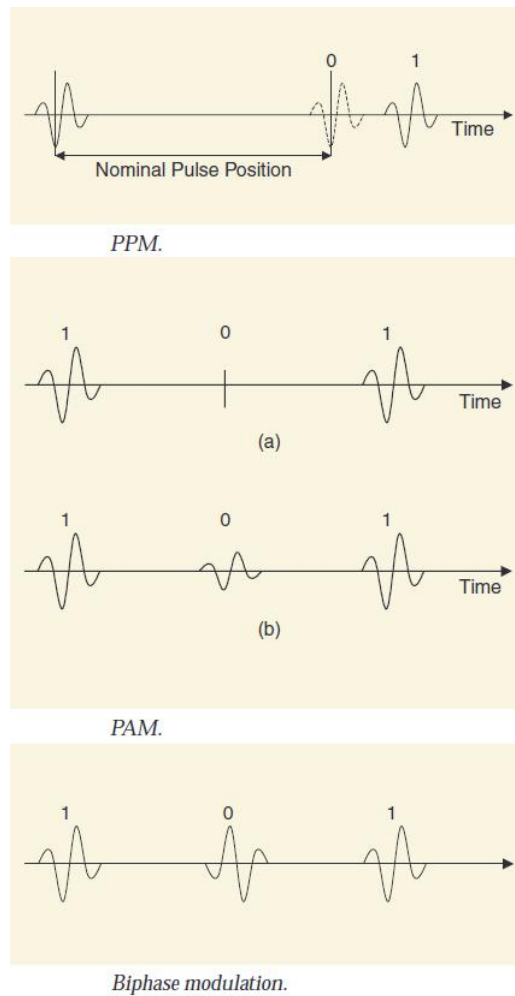
Figure 7.3: UWB modulation schemes, from [6], Chapter 1.

doesn't give the best performance and has some disadvantages over the MB-OFDM approach, so it is only being used in some systems that don't require high speed.

PAM

PAM is based on the principle of encoding information with the amplitude of the impulses, as shown in **Figure 7.3**. The picture shows a two-level modulation, respectively for zero and lower amplitude, where one bit is encoded in one impulse. As with pulse position, more amplitude levels can be used to encode more than one bit per symbol.

It is one of the simplest solutions, but giving a low performance with many disadvantages over other approaches.

BPSK (Bi-phase) Modulation

In bi-phase modulation, information is encoded with the polarity of the impulses, as shown in **Figure 7.3**. The polarity of the impulses is switched to encode a 0 or a 1.

In this case, the main disadvantage is that only one bit per impulse can be encoded because there are only two polarities available to choose from, what limits the performance.
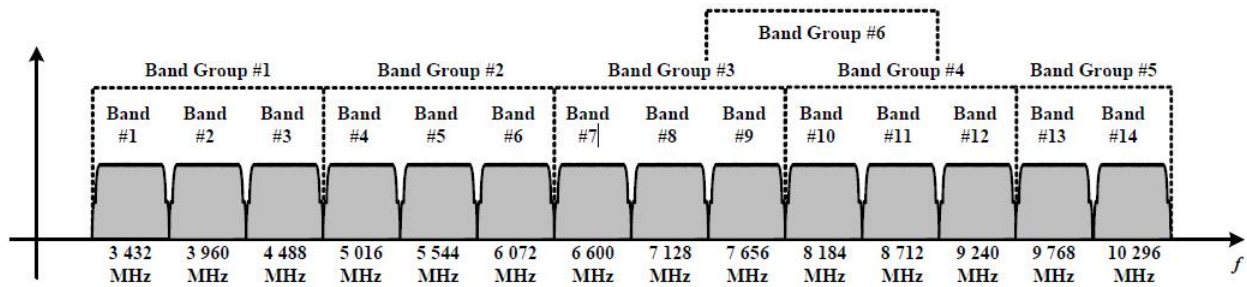
Figure 7.4: UWB systems bands distribution scheme, from [6], Chapter 1.

7.2.3   Multiple Access

The **IEEE 802.15.3a standard** requires the operation of a large number of devices and the operation of four non coordinated networks. UWB systems can utilize various methods of multiple access that are commonly used in traditional wireless systems. The first UWB systems were impulse systems that operated in a fixed single band. Therefore, they were restricted to using either a time-division multiplexing (TDM) or a code-division multiplexing (CDM) multiple-access method.

The new FCC definition of UWB, which specifies that a signal needs only to occupy 500 MHz to be compliant, has opened up the option of using frequency-division multiplexing (FDM) as a multiple-access method. This option hasn't been fully explored yet, even though it is, of course, possible with the multi-band method described in the next section.

Single-Band and Multi-band Schemes

A variety of UWB systems can be designed to use the 7,500 MHz available UWB spectrum. On the one hand, the signal can be shaped so that its envelope occupies the full spectrum. On the other hand, it can be shaped so that it occupies only 500 MHz bandwidth, allowing 14 such signals to cover the entire band, as shown in **Figure 7.4**. There are, of course, intermediate cases, e.g. five signals of 2.5 Ghz bandwidth each. Bandwidth and number of available bands generate different performance trade offs and design challenges.

In a **multi-band system**, the probability of collision from co-located, uncoordinated piconets is low because each sub-band signal is transmitted at low duty cycle. As a consequence, it reduces the errors generated by the presence of co-located piconets. Multi-band systems also permit adaptive selection of the bands to provide good interference robustness and co-existence properties, and this feature is very attractive, especially for consumer electronics devices that need to operate in uncontrolled environments.

When the system detects the presence of an 802.11a system, for example, it can avoid the use of the bands centered at those frequencies. This same feature can also be utilized to provide for different spectrum allocations in the rest of the world: the bands that share the spectrum with extremely sensitive systems can be avoided.
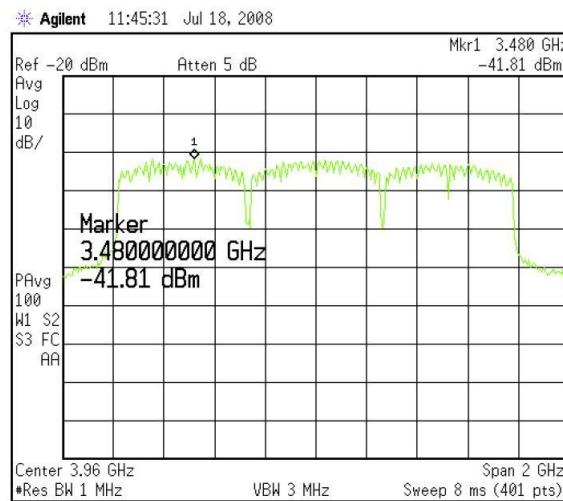
Figure 7.5: MB-OFDM WiMedia Defined UWB signal, from [7], Chapter 9.

7.2.4 WiMedia standard details

Many companies are working nowadays towards specifications that fulfill the regulations established by the FCC and other regulation boards to develop UWB wireless transmission standards. One of the most successful groups is WiMedia Alliance, an industry association that promotes UWB worldwide. They have developed a **MB-OFDM focus,** using the first **three 528Mhz bands, from 3.1 to 4.7 Ghz, 1.6Ghz total bandwidth**, reaching maximum speeds of 480Mbps. These signals would have an appearance similar to the one shown in **Figure 7.5**, with a power emission limit of -42dBm. For each band it uses a configuration of 128 carriers spaced 4.125Mhz, with the timing specifications showed in **Table 7.2**.

By applying this scheme, it is possible to transmit in many different ways, and set different carrier configurations and transmission coding rates to achieve better bit error correction or speed. This way, the standard depicted allows for a big flexibility in the systems designed.

For different speeds the device will use a different modulation and coding rate, and will be able to negotiate the speed during transmission. This way it can save battery when needed or reach full speed for the most demanding applications. The different transmission modes that can be used are shown in **Table 7.3**.

These specifications represent the most advantageous way to transmit at high speeds, using the bandwidth in the most efficient manner and transmitting the lowest possible power. This is for example the focus used in the new Wireless Universal Serial Bus (WUSB) standard, developed by the WiMedia Alliance.

For multiple access, the WiMedia Alliance approach uses two methods, the **distributed reservation protocol (DRP)** and **prioritized contention access (PCA)**. Basically both methods consist in the reservation of time slots for each device to transmit information. During a slot, a device will use frequency-hopping code division multiple access (FH-CDMA) scheme to transmit, as can be seen in **Figure 7.6**.

These are the main characteristics for a device that complies with ECMA UWB Standard

[1], that gives a general idea on the specifications of the UWB system boards that we are going to use in the project. These are also applicable to many UWB systems in development that are appearing in mass market or are going to appear soon.

Parameter	Description	Value
f_s	Sampling frequency	528 MHz
N_{FFT}	Total number of subcarriers (FFT size)	128
N_D	Number of data subcarriers	100
N_P	Number of pilot subcarriers	12
N_G	Number of guard subcarriers	10
N_T	Total number of subcarriers used	122 ($= N_D + N_P + N_G$)
D_f	Subcarrier frequency spacing	4,125 MHz ($= f_s / N_{FFT}$)
T_{FFT}	IFFT and FFT period	242,42 ns (Δ_f^{-1})
N_{ZPS}	Number of samples in zero-padded suffix	37
T_{ZPS}	Zero-padded suffix duration in time	70,08 ns ($= N_{ZPS} / f_s$)
T_{SYM}	Symbol interval	312,5 ns ($= T_{FFT} + T_{ZPS}$)
F_{SYM}	Symbol rate	3,2 MHz ($= T_{SYM}^{-1}$)
N_{SYM}	Total number of samples per symbol	165 ($= N_{FFT} + N_{ZPS}$)

Table 7.2: Timing-related parameters of the MB-OFDM UWB signals, from [1], Chapter 10.

Data Rate (Mb/s)	Modulation	Coding Rate (R)	FDS	TDS	Coded Bits / 6 OFDM Symbol (N_{CBP6S})	Info Bits / 6 OFDM Symbol (N_{IBP6S})
53,3	QPSK	1/3	YES	YES	300	100
80	QPSK	1/2	YES	YES	300	150
106,7	QPSK	1/3	NO	YES	600	200
160	QPSK	1/2	NO	YES	600	300
200	QPSK	5/8	NO	YES	600	375
320	DCM	1/2	NO	NO	1 200	600
400	DCM	5/8	NO	NO	1 200	750
480	DCM	3/4	NO	NO	1 200	900

Table 7.3: PSDU rate-dependent Parameters, from [1], Chapter 10.
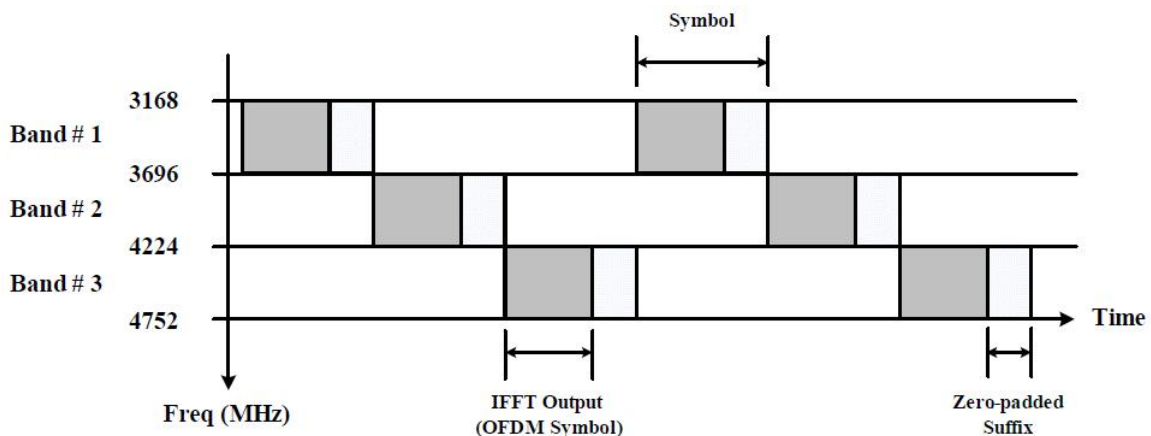
Figure 7.6: Example of transmitted signal using three bands, from [1], Chapter 10.
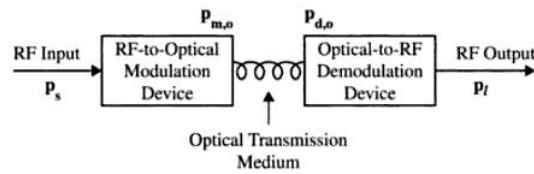
Figure 7.7: Basic components of a fiber link, from [8], Chapter 1.

7.3   Radio over fiber

Traditionally, **RF signals** are transmitted and distributed via electrical cables and waveguides. However, the attenuation of microwave RF signals in these systems increases rapidly with the frequency of the signal, ant it is specially high in the millimeter wave range. Thus limiting the range of transmission and application of these signals for certain technologies.

Optical fiber systems offer the potential for avoiding these limitations and have nowadays replaced electrical systems in many telecommunication fields. In these systems, RF signals are digitalized, and then the on/off digitally modulated optical carrier is transmitted and distributed via optical fiber. [28, 29]

However, **ROF** provides the alternative of transmitting, distributing and processing, directly without going through digital encoding process, RF signals. It will transmit and distribute these signals (including microwave and millimeter wave signals) at low cost, over long distance and with a low attenuation. For those reasons, the distance for photonic transmission and distribution of microwaves can be very long. [30]

When the modulation of an optical carrier is detected at the receiver, the RF signal is regenerated. And since the objective of a photonic link is to reproduce the RF signal at the receiver, the link can convey a wide variety of formats. In some applications the RF signal is an unmodulated carrier but in other applications the information consists of a carrier modulated with an analog or digital signal.

From the point of view of input and output ports, photonic microwave links function just as conventional microwave links. Not only RF signals can be transmitted in this manner, but microwave functions such as mixing (up- or down-conversion) of signal frequencies can also be carried out photonically.

RF photonic links contain, typically, optical carriers modulated, in an analog manner, by RF sub-carriers. After transmission and distribution, these modulated optical carriers are detected and demodulated at a receiver in order to recover the RF signals. The objective of RF photonic links is clearly to achieve the same functions as conventional microwave links. Improving them so they can achieve longer distance of transmission, reduced cost, better performance, higher operating frequency, or reduced complexity and size. Therefore the performance of a RF photonic distribution system should be evaluated in terms of the criteria for microwave links. The basic components for such links are showed in **Figure 7.7**.

7.3.1   Applications

RF photonic links are mainly attractive in three types of applications.

- In commercial communication applications, as Hybrid Fiber coax (HFC) systems, including broadcast and switched networks, provide the low cost network for **distribution of RF signals** to and from users. RF photonic technology has replaced cables in many commercial applications such as Cable Television (CATV) nowadays.

- At high frequencies, traditional microwave and millimeter wave transmission systems, using coaxial cables and metallic waveguides, have extremely large attenuation, and are complex and expensive. RF photonic systems offer an attractive alternative to these traditional electrical systems at high frequencies combining **small size and weight and immunity to electromagnetic disturbances**.

- Once the RF signal is modulated on an optical carrier, photonic techniques may be used to **process the RF signals**. A good example would be the frequency up- or down- conversion of the RF signal.

However, in photonic RF signal processing, the system performance will have additional requirements for bandwidth, efficiency and dynamic range. As such, system design considerations, choice of technologies and components, as well as a evaluation of their performance are very different for analog links than for digital optical fiber links.

For example, the on-off threshold switching voltage of the modulator is an important factor for digital communications systems while the slope efficiency is an important factor for analog modulation.

7.3.2   Main figures of merit

For microwave links, which are passive, typical performance criteria include just RF loss and frequency response. There is no nonlinear distortion or additional noise unless the signal is amplified. In photonic microwave links however, additional noise, such as the laser noise, can degrade the noise figure, and non-linearity of the modulation process can reduce the **Spurious Free Dynamic Range (SFDR) of the system**.

From the optical point of view, the magnitude of the RF intensity modulation is much less than the intensity of the unmodulated optical carrier. For this reason, one can analyze the link in the small signal approximation, and at a given DC bias operation point, the time variation of the optical intensity can be expressed as a Taylor series expansion about this DC bias point as a function of the RF signal magnitude.

There are two commonly used methods to create an RF intensity modulation of the Continuous Wave (CW) optical carrier. One is by **direct RF modulation** of the laser and the second one is by RF modulation of the CW optical carrier via an **external modulator**.

For microwave transmission and distribution using photonic links, which are more like active

RF components, the main figures of merit are:

Gain and frequency response.

Conversion efficiencies in optical systems are typically less than 10%, which leads to photonic link losses greater than 20dB. Considerable work has been done to improve the two main factors: the modulation device and the circuit that interfaces the modulation signal source to the modulation device.

The RF gain of a photonic link is frequency dependent, and it is normally a low pass frequency response with the RF bandwidth f_B defined as the frequency range from its peak value at DC to the frequency at which the gain drops by 3dB.

The three major causes of frequency dependence are:

- The **modulation device** (direct modulation or external modulation).

Direct modulation is simpler to implement but the useful bandwidth is limited to the range from DC to the laser relaxation resonance, which is typically a few tens of Ghz.

For external modulation the advantages are the wider bandwidth (about five times), lower noise figure and larger SFDR at the cost of a more complex device and higher cost.

- The **fiber**, where the interaction between it and the traveling wave can give a variable frequency behavior.

Optical signals transmission through fiber has some attenuation, typical values about 0.2dB/Km, that limit long range photonic transmission. But the main limiting effect is dispersion, which will make short optical pulses broaden, because different rays will follow different paths. This factor will limit the distance reached and will affect the frequency response for RF signal transmitted in optical carriers degrading the quality of the link.

Other nonlinear effects, many of them power-dependant, like scattering, nonlinear refractions and four-wave mixing will limit and degrade optical links performance.

- The receiver or **detector** which may have frequency dependent response.

A photo-diode generates an RF current which is proportional to the optical power at the incident frequency on it. To maximize the power transferred to the load, a matching circuit is needed, that will have a certain frequency response that could limit our system. Although for general systems this won't be the limiting factor given that the bandwidth of photo-detectors is normally higher than that of the laser, and the distortion effects are less important than the ones happening in the fiber for RF signals being transmitted.

Noise Figure (NF)

Noise plays an important role in setting the minimum magnitude signal that can be conveyed by the link and in contributing to the maximum SFDR for RF photonic links. There are three
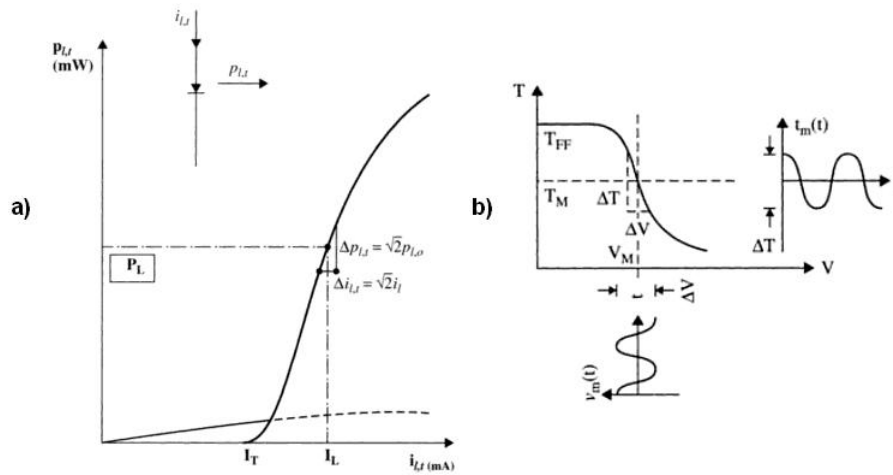
Figure 7.8: Representative plot of: a) diode laser's optical power vs the current through the laser and b) transmission T of an external modulator as a function of an input V, from [8], Chapter 1.

dominant noise sources in photonic links: **thermal, shot and relative intensity noise**. The total noise power from all these sources is simply the sum of them.

The NF of a given link will depend on the noise sources, their locations and the circuit configuration of the link. When noise is mainly caused by a dominant noise source, other noise sources can be neglected.

Spurious free dynamic range

Careful examination of the output signal in a RF photonic link will include not only the signal at the fundamental frequency but also frequencies that are harmonically related to the fundamental. There will be nonlinear distortion of the fundamental signal. For an useful optical link, it is necessary to achieve smaller harmonics than noise for a sufficient low input power.

As the input RF power at the fundamental increases, so will the output power at the harmonic frequencies. In this case SFDR will be limited by the nonlinear distortion at high input RF power.

When the fundamental is large enough to generate distortion terms that rise above the noise floor, such terms can often degrade system performance. They set a limit on the maximum level of the fundamental, which is typically less than the compression level.

The signal level which generates distortion terms equal to the noise floor is the maximum signal for which the link output is free from distortion, this is the spur-free dynamic range. The SFDR bandwidth depends on the order of the distortion, because of different signal power relations between fundamental and distortion terms. A graphical representation of these parameters can be seen in **Figure 7.9**.

Characterization of the link distortion via the SFDR is commonly applied in the design of many communication systems. In some applications the linearity is insufficient to meet the application requirements and in such cases a wide variety of linearization techniques have been developed. The principal ones in photonic links are predistortion, feedback and feed-
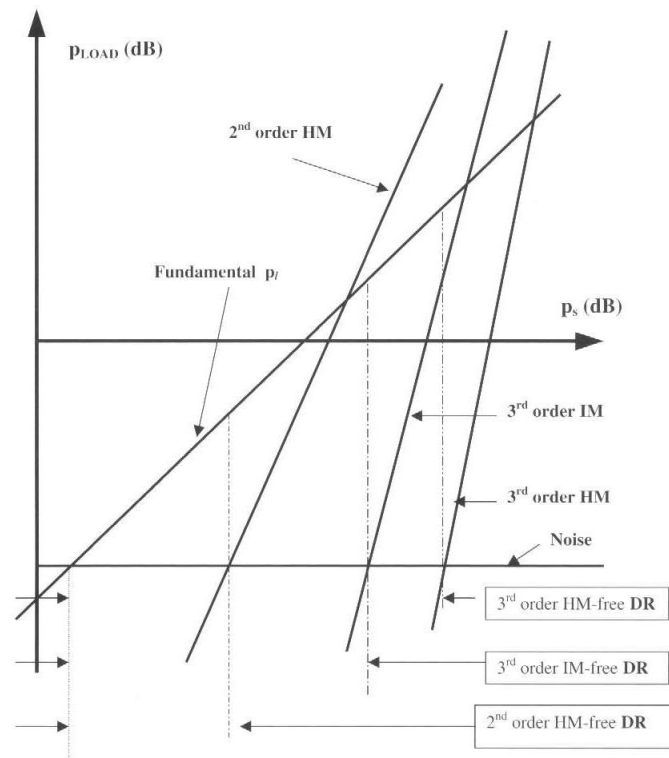
Figure 7.9: SFDR plot, from [8], Chapter 1.

forward, but these techniques will not be used for our system at this stage, so they won't be detailed here. [31, 32, 33]

7.3.3 Photonic microwave links

The basic for photonic microwave links design have been presented in this section. Although with **two different modulation methods**, direct and external, there is a **common way for the analysis and improvement** of both. [34]

Link design methodology builds on the traditional measurements such as **G, NF or SFDR** to characterize the performance of RF devices. This makes it easier to combine links with other RF components to meet system requirements.

Photonic microwave links have achieved impressive performance nowadays with bandwidth up to 150Ghz, gain of 30dB, noise figure of 4.2dB and SFDR of 130dB Hz.

This gives the option to use this kind of system links for multiple different scenarios, one of them being the distribution of other types of signals using optical carriers, as it is developed in this project. In **Figure 7.10**, a typical RF response of an optical link of a certain length, with the laser, fiber and photo-detector responses all included in the transmission is shown.

This gives an idea of the bandwidth that can be obtained without any other compensation methods, that could of course be applied if needed. This would help to minimize the adverse effects of chromatic dispersion, one of the most noticeable arising problems in these links when they are used to transmit RF signals. This effect causes the response to appear notched at certain frequency points, as can be seen in the figure. [35, 36, 37, 32]
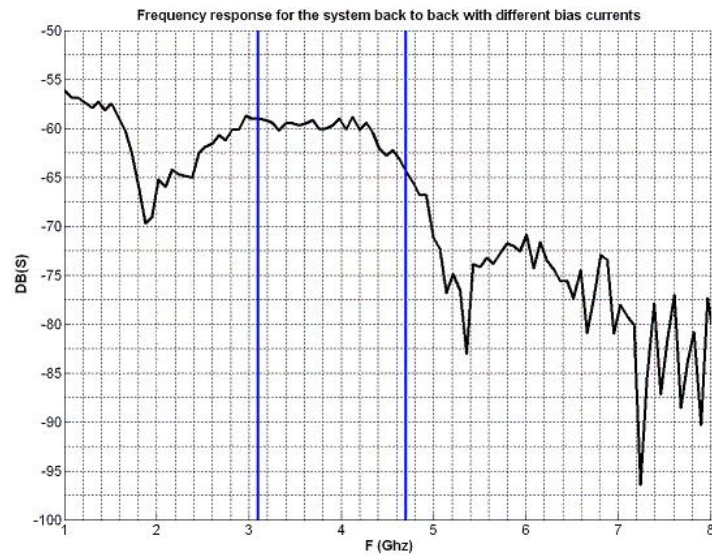
Figure 7.10: Frequency response of a low bandwidth laser.

7.4   Conclusions

In this chapter, both **UWB and ROF technologies** have been presented. With details of its fundamentals, characterization and the main advantages they have for the use we are going to give them in our project.

Both technologies have very good perspectives and are a step forward in their fields. With the combination of both and its development as a whole transmission system, many advantages are obtained, and **a new focus for a distribution method of wireless signals can be developed**, as has already been shown in theory.

Once the main characteristics of both technologies and its possibilities are shown, we will give details and explain the elements used to physically build our system in the next chapter. With the tests and performance obtained showed in the end.

8

System tests and results.

8.1 Introduction

In this chapter, a **detailed characterization of the final system built** is going to be shown.

To give a good overall view of it, we will first give the characteristics of every main component. Then we will describe in detail the setup developed with schematics and pictures, to give an overview of its structure and how it works. And finally we will give figures and explanations on the results obtained, that give a very good idea of the possibilities of this type of systems and its real applicability.

8.2 System components

In this first section we are going to describe in detail the main components used in the **UWB ROF system** developed: **boards, laser and photo-detectors, optical fiber, amplifiers and antennas**.

8.2.1 Boards used

The boards used for the system were the ones made by the Israeli company WiSair, in their **UWB Development Kit (DV9110)**. It is a commercial solution for the development of UWB applications and tests, with several high-speed data and host interfaces.

The DVK includes the 502 RF Chip, the 531 MAC/Base-band chip, WiSair's UWB antenna, and the WisMan configuration and control host utility, software that can be installed in a Windows-based PC. The boards comply with **ECMA-368 International Standard** [1] using the 3.1 to 4.7 Ghz unlicensed band, being able to transmit at different speeds and reaching a

Figure 8.1: Scheme of test boards used, from [7].

maximum one of 480Mbps. They can use different transmitting configuration being able to generate packets for transmission and testing of PER in the medium being analyzed.

Key characteristics:

- Based on the WiMedia UWB common radio platform

- Small form-factor of 1.2×2.4" (4×6cm)

- Multiple application data interfaces: Ethernet 100Mbps, RMII, MII, direct CPU, DCI, and MPEG transport stream Synchronous Parallel Interface (SPI)

- MAC-PHY standard interface (version 1.0)

- WiSair MAC (subset of WiMedia MAC)

- Parallel and serial host interface for configuration and control

- Point-to-point and point-to-multipoint network configurations

- Downloadable configuration PHY

- Standalone operation (no need for additional PC)

- Provisioning for FCC CFR47, Part 15 sub-part F for UWB transmission

Two boards were used for the tests, one as the transmitter (master board) and the other as the receiver (slave board). They were both **connected to a PC via USB connection and controlled by a software installed** on this PC that allowed to change transmission parameters and obtain performance measurements like transmission speed, data link configuration, link quality and error rate statistics.
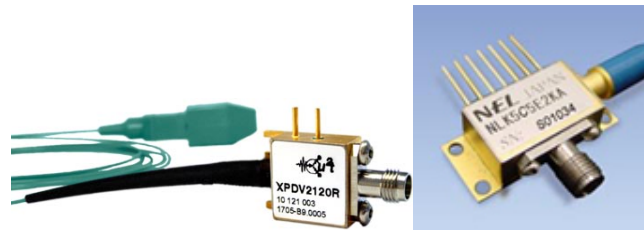
Figure 8.2: Photo-detector (left) and laser (right) used.
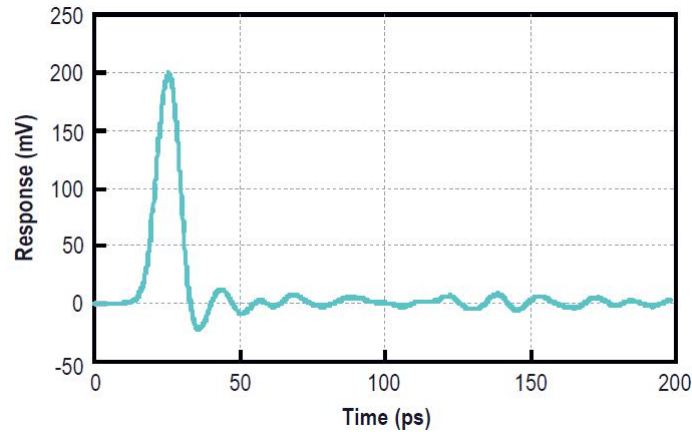
Figure 8.3: Photo-detector pulse response.

8.2.2 Laser and photo-detectors

A bidirectional setup was needed for the optical link, because the WiSair boards need to see each other and receive feedback to keep transmission. A couple of photo-detectors from the German company U2t Photonics and a couple of lasers from the Japanese company NEL were used, as shown in **Figure 8.2**.

Lasers

The lasers were the NLK5C5EBKA model from NEL company. They were **high speed 1540 and 1545nm center wavelength**, in a K-connector package with 50Ω matching resistor, with 30dB isolator and thermo-electric cooler. They had a 3mW fiber output power and a cut-off frequency of about 16Ghz, which is a very high bandwidth, much more than the one needed for our signal which has a maximum frequency of less than 5Ghz.

Photo-detectors

The photo-detectors used were the XPDV2020R and XPDV2021R models from U2t Photonics. They were **high bandwidth (50Ghz), 50Ω matched, with 40Gbps maximum speed** in a hermetically sealed package.

The photo-detector had a very sharp pulse response with very good characteristics, what allowed us to obtain the best performance for the optical link. As said before, the parameters of the photo-detector also outperformed by far the minimum requirements needed for our system.

Figure 8.4: Optical amplifier, EDFA (left) and RF amplifier (right).

This way we could obtain the optical link performance for RF signal transmission without limitations by the optical elements.

8.2.3 Optical fiber

The optical fiber used was single-mode fiber from company OFS. It had a **0.2dB/Km attenuation at 1550nm and a chromatic dispersion value of around 17 ps / nm / km**.

It is a good fiber to choose given its low price and good characteristics. Nowadays it is being installed in many new constructions and it is a good type of fiber to concentrate in, searching for the best way to transmit RF signals through it. This way the transmission methods researched can be applied in many already deployed fiber distribution networks.

8.2.4 Amplifiers

In different parts of the system, **RF and Optical amplifiers** as the ones shown in **Figure 8.4**, were used to rise the level of the transmitted and received signals. This is because after many conversion processes done in different parts of the system, the output ends up with a very low level due to low conversion rates, that must be raised again.

RF amplifiers

To amplify RF signals, **high bandwidth amplifiers of 13.5Ghz** that cover the 3.1 to 4.7 Ghz band have been used, giving a good response and **amplification level of about 20dB** with 12dBm maximum power out. They had a noise figure of about 5.8dB at 100Mhz.

Optical amplifiers

To amplify the optical signal in the 1540nm range, **Erbium Doped Fiber Amplifier (EDFA) followed by an optical filter** has been used, to limit the appearance of nonlinear frequencies outside the working band and limiting distortion. These EDFA were 1533 to 1567 nm range with a noise figure lower than 5.5dB and a saturated output power of 30 to 37dBm.
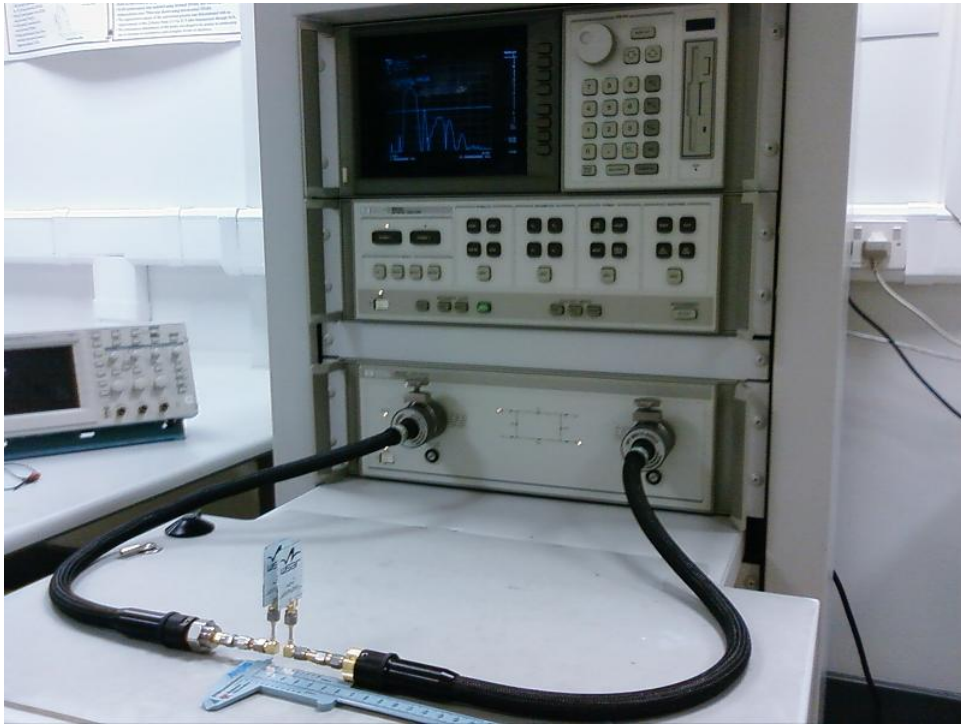
Figure 8.5: Antennas response measurements using a Network Vector Analyzer.

8.2.5   Antennas

The antennas used for the system tests were the ones included in the development kit from WiSair. They are a couple of **monopoles antennas made in microstrip technology** and designed by the Israeli company In4tel.

To measure its response, a Vector Network Analyzer (VNA) was used. Given that we had a couple of antennas, establishing a link between them, and measuring its parameters through the network analyzer would be enough to get an approximate idea of its frequency response, obtaining both S_{21} and S_{11}.

The setup to obtain these values is shown in **Figure 8.5**, where the separation between the antennas had to be equal to the **Rayleigh distance**, shown in **Figure 8.6**. This way the incident wave in the antenna will have a path difference between the axial ray and an edge ray of $\frac{\lambda}{4}$, obtaining the optimum incident power in the receiving antenna.

The Rayleigh distance is given by the next expression,

$$R_r = \frac{D^2}{2\lambda} \tag{8.1}$$

where the different parameters are:

D: antenna diameter.

λ: wavelength at the central frequency, $\lambda = \frac{c}{f}$.

For our measurements, the distance obtained was:
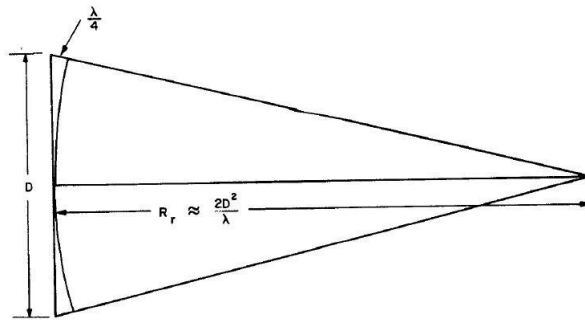
Figure 8.6: Rayleigh distance.
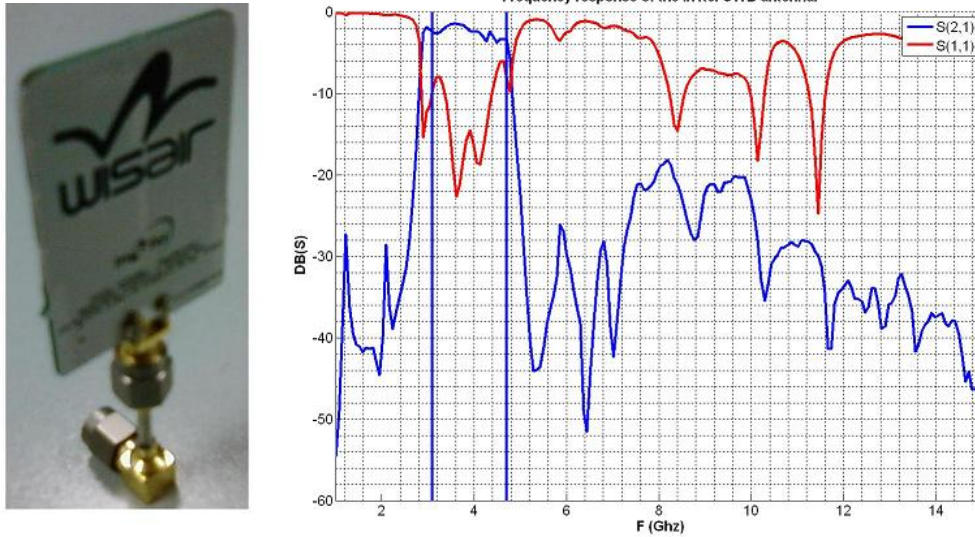
Figure 8.7: Antenna picture (left) and its frequency response graph with the working band highlighted (right).

$$R_r = \frac{0.04^2}{2 \cdot \frac{c}{f}} = \frac{0.04^2}{2 \cdot \frac{3 \cdot 10^8}{3.9 \cdot 10^9}} = 1cm \tag{8.2}$$

So the antenna measurements were obtained by separating them a distance of 1cm, and plotting the graphs obtained in the VNA, for S_{21} and S_{11} parameters. In these conditions, the radio link has the proper distance to consider the radiation pattern of the antennas equivalent to a far-field one. So we can then obtain the radio link response as a microwave circuit.

As it can be seen in the graph obtained in **Figure 8.7**, they have a good response in the pass-band, and the impairments appearing in the graph are mainly caused by the method used to measure its response. [38, 39, 40]

A main characteristic that can be seen is that the antennas work as a pass band filter for the boards, **showing a very good rejection out of the working band**, 3.1 to 4.7 Ghz. This way, a filter is not necessary for the boards once the antennas are connected, but that also tell us, that these boards don't have any filter at the input port, an important factor to have into account for measurements and system integration.

Another factor worth to mention is that the antennas used for the boards have to be the ones included, given that the two elements (**board and antenna**) are thought to be used together
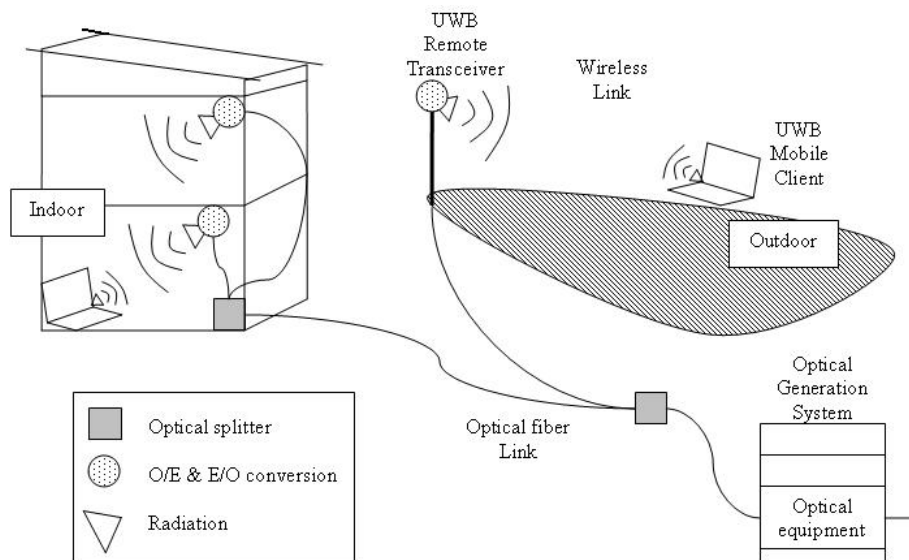
Figure 8.8: UWB ROF generic distribution system.

for them to **comply with the FCC** radiation limits for UWB systems. Although for our tests different ones were used to check power emission and limitations of the link.

8.3   System setup

The main idea behind the system setup is to **simulate an optical distribution system** where an **optical carrier is modulated by a RF signal**. In the ends of the system, this information will be converted to electrical, radiated to the air and received by mobile devices. This kind of system has loads of applications for last-mile distribution of RF signals that can be of high bit-rate, up to 1Gbps with the new UWB draft specifications. [41, 42]

This method to **generate and distribute RF signals is cheap and efficient**. It would be possible to generate the RF signal once in a central system and use already existing fiber inside buildings, campuses, business or office parks, etc to send RF-modulated optical signals, distributing them over some kilometers with low attenuation and distortion, and then reaching the transceivers that would make the opto-electrical conversion (and vice versa) and radiate the signal using small-size antennas. The opto-electrical conversion is a simple task, as opposite to a demodulation, making remote transceivers cheap and small, allowing for an easy deployment of a big number of them.

This way a required area could be covered with a big number of them at a low cost and a high reliability given that the complicated equipment would be on a main central location as shown in **Figure 8.8**.

In **Figure 8.9**, a general schematic of the system main components and the format of the signal transmitted is shown. The main modules and stages of the system are depicted for a single bidirectional path, that would be one of the many branches of an optical distribution system.

First component is the **main optical generation system**, where the information comes
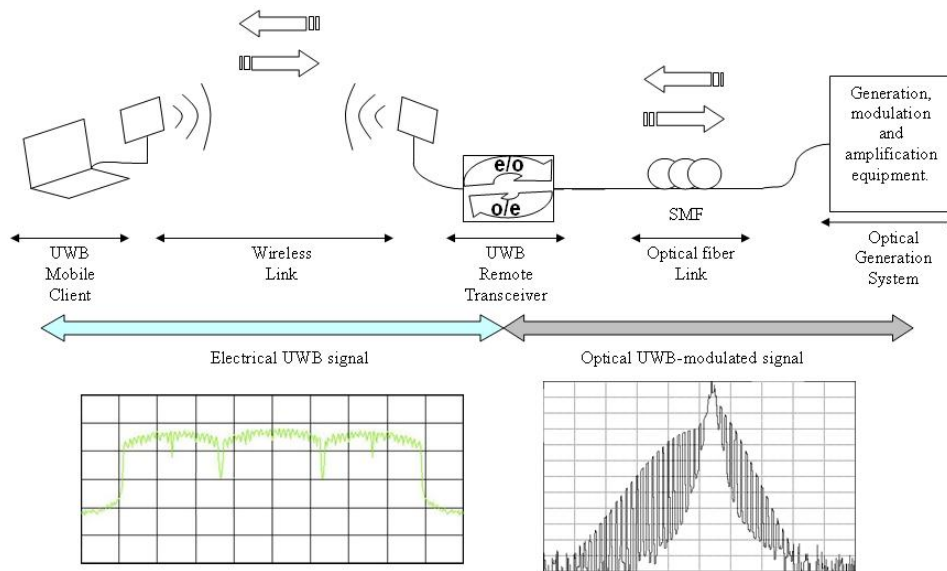
Figure 8.9: UWB ROF distribution system schematic.

from a main distribution network that can be optical or of any other kind, and would be a high speed main Metropolitan Area Network (MAN) or Wide Area Network (WAN), depending on the size of the area covered. Then this equipment will distribute the information using an optical carrier modulated by a RF UWB signal that will be generated here with the information coming from the MAN or WAN. The signal would then travel through the **optical fiber distribution system**. In the ends of the system, different **transceivers** will be installed that will radiate the signal to the air after an opto-electrical conversion. [34]

Finally this signal will be received by the **mobile users equipment**, that will normally be the final receivers. This mobile receivers will also be able to generate an UWB wireless signal to transmit over the up-link channel that will follow the opposite way. It will be wirelessly received by the transceivers, that will make an electro-optical conversion and send the signal back through the distribution network, that will in the end reach the optical receiver system, and be demodulated.

8.3.1 Detailed scheme

The idea behind the setup conducted is the characterization of the achievable main figures of this kind of systems. To do the simulation, a bidirectional path over fiber was set up, with a wireless link in the end. This way we could find maximum lengths for the optical and wireless links and maximum achievable speeds. But also other tests were conducted to measure detailed system characteristics like total attenuation and distortion occurring, that could be analyzed, giving us an idea of what were the limiting effects occurring.

In **Figure 8.10**, a detailed scheme of this UWB ROF setup with all different parts named is shown.

For this setup, the focus was put in the up-link connection because, although a bidirectional link was configured, only the up-link part has all the components, and goes through the optical
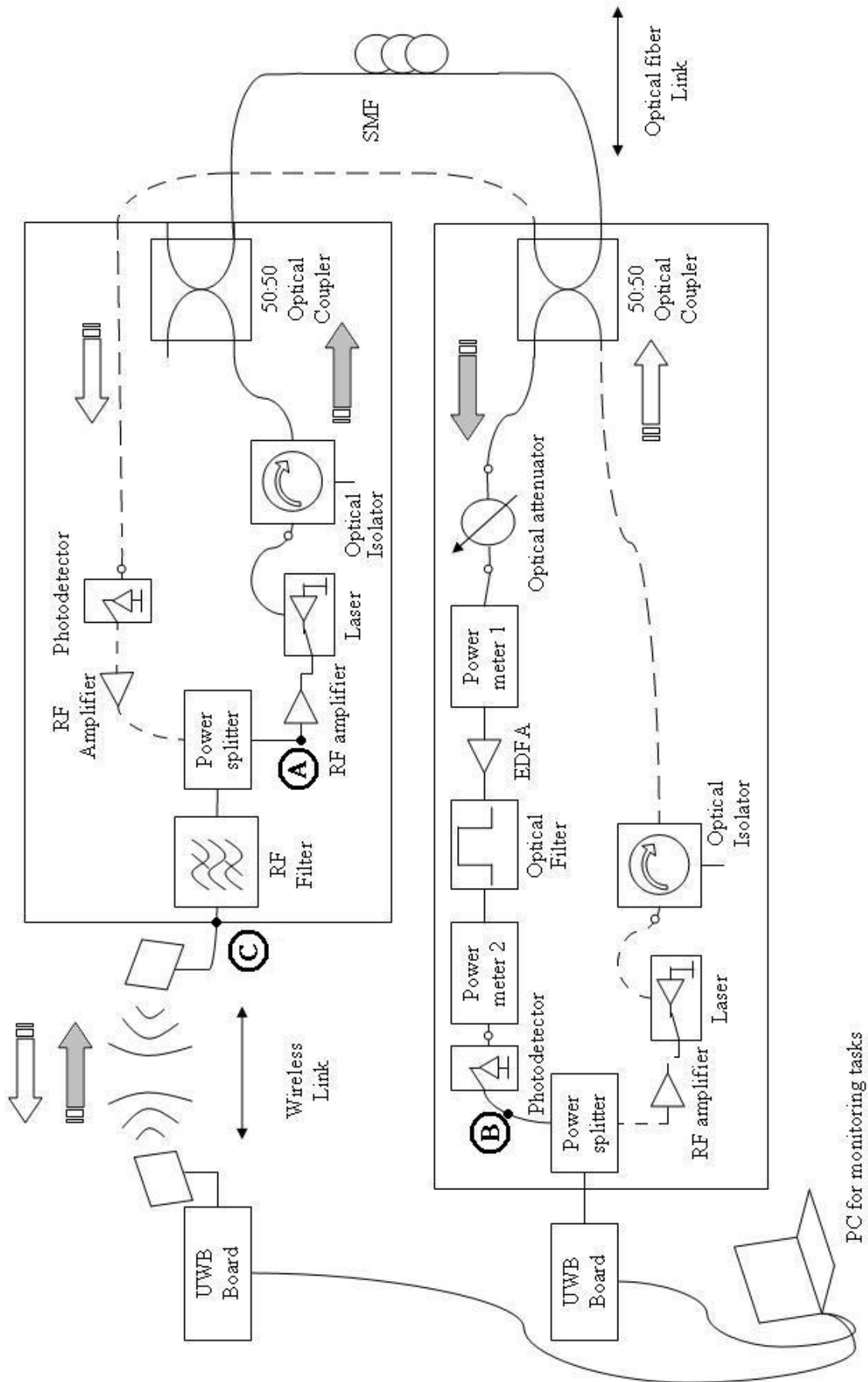
Figure 8.10: UWB ROF detailed setup scheme.

fiber reel being the main limiting part. The down-link is connected with fiber directly back to back because it is necessary for the boards to keep transmission and to isolate the up-link transmitting path, but statistics and analysis was only conducted on the up-link connection, changing fiber and wireless links length to measure performance of the system.

In the schematic, five important main parts can be noticed.

First one are the boards, the **UWB transceivers** that generate and receive the RF signal, checking its parameters and giving statistics and information about PER, quality, etc than can be viewed and saved in a computer, where boards are connected through USB.

The second part is the **wireless link**, between the transmitter board and the simulated remote transceiver side of the system. It has two antennas and amplifiers to rise the level of the received wireless signal.

The **transmitter side** is the part that receives the wireless signal, converts it to optical and sends it through the optical link.

The **optical link** is a variable reel of single mode fiber that is changed in length to test the degradation of the optical RF-modulated signal after going through it.

Then the **receiver side** which is the most complicated one. It receives the signal after being transmitted through air and a certain length of fiber. After that, the signal is amplified, filtered and converted to electrical to be sent to the receiver board which will process it and give statistics about quality, errors, etc.

8.3.2 System pictures

In this section, some pictures of the setup are shown to illustrate the elements used and the arrangement of the different components in the lab tests.

In **Figure 8.11**, the general setup is shown in the **first picture** with equipment part of it on the top shelf (EDFA, Voltage source, optical attenuator and laser controllers) and measuring systems on the right part (Optical, RF spectrum and Network analyzers). Fiber reels and the computer used to monitor the boards are also shown in the left part. In the **second picture**, an in detail view of the optical components (couplers, isolators, photo-detectors and lasers) is shown, together with the UWB filter.

In **Figure 8.12** two in detail views are shown. The **first one** shows the receiver board with its corresponding laser and RF amplifier. The **second one** shows the wireless link between the transmitter board and the optical transceiver side, with the RF and optical measuring equipment in the back.
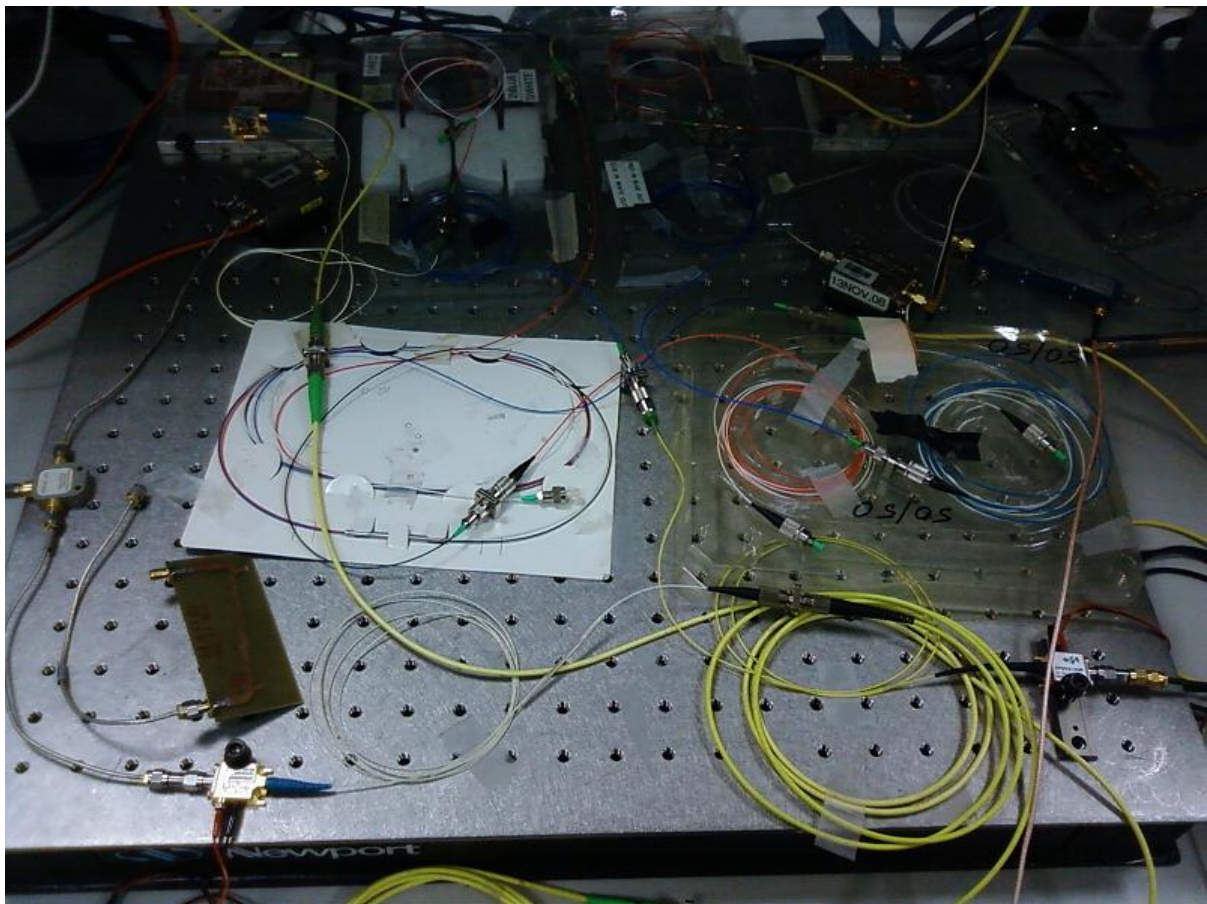
Figure 8.11: General view of the setup (up) and fiber link elements with UWB filter (down).
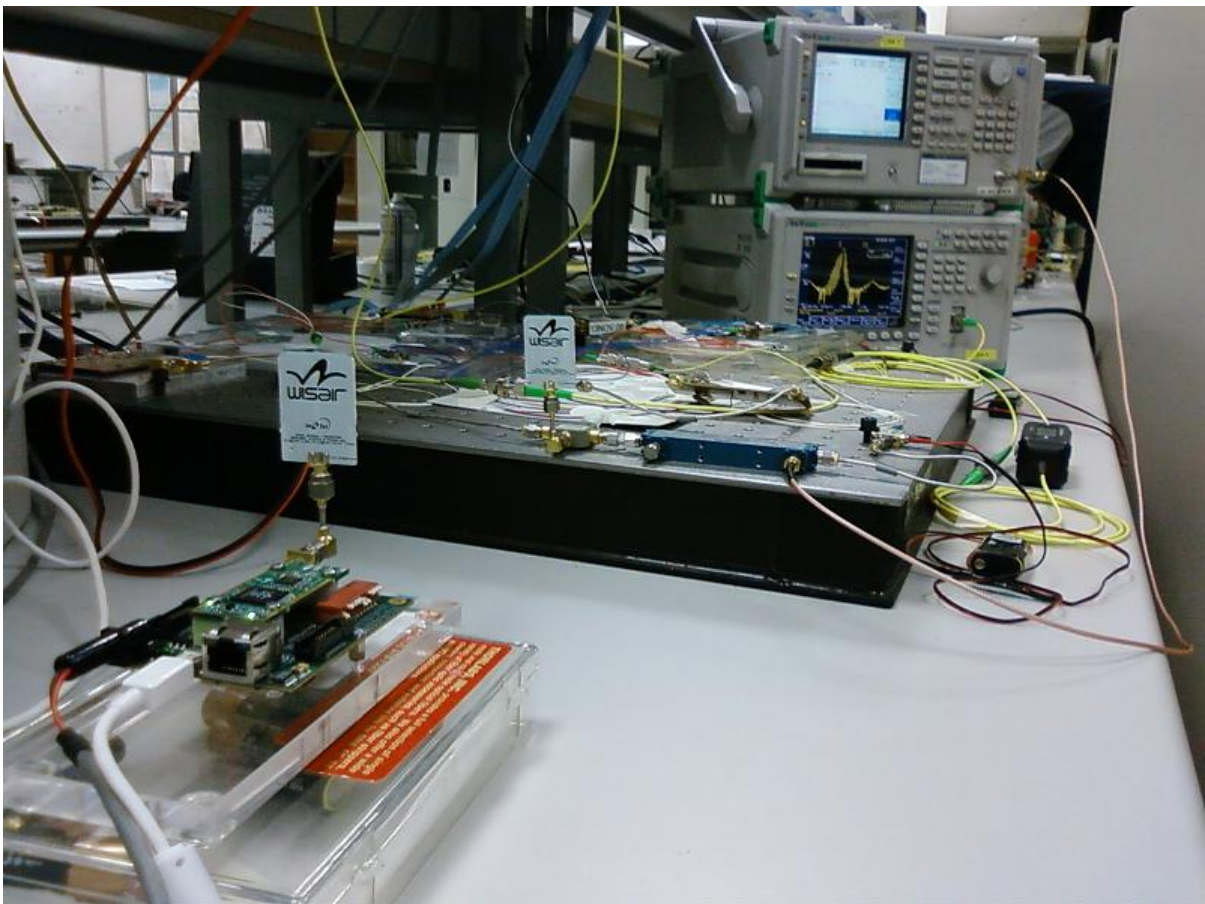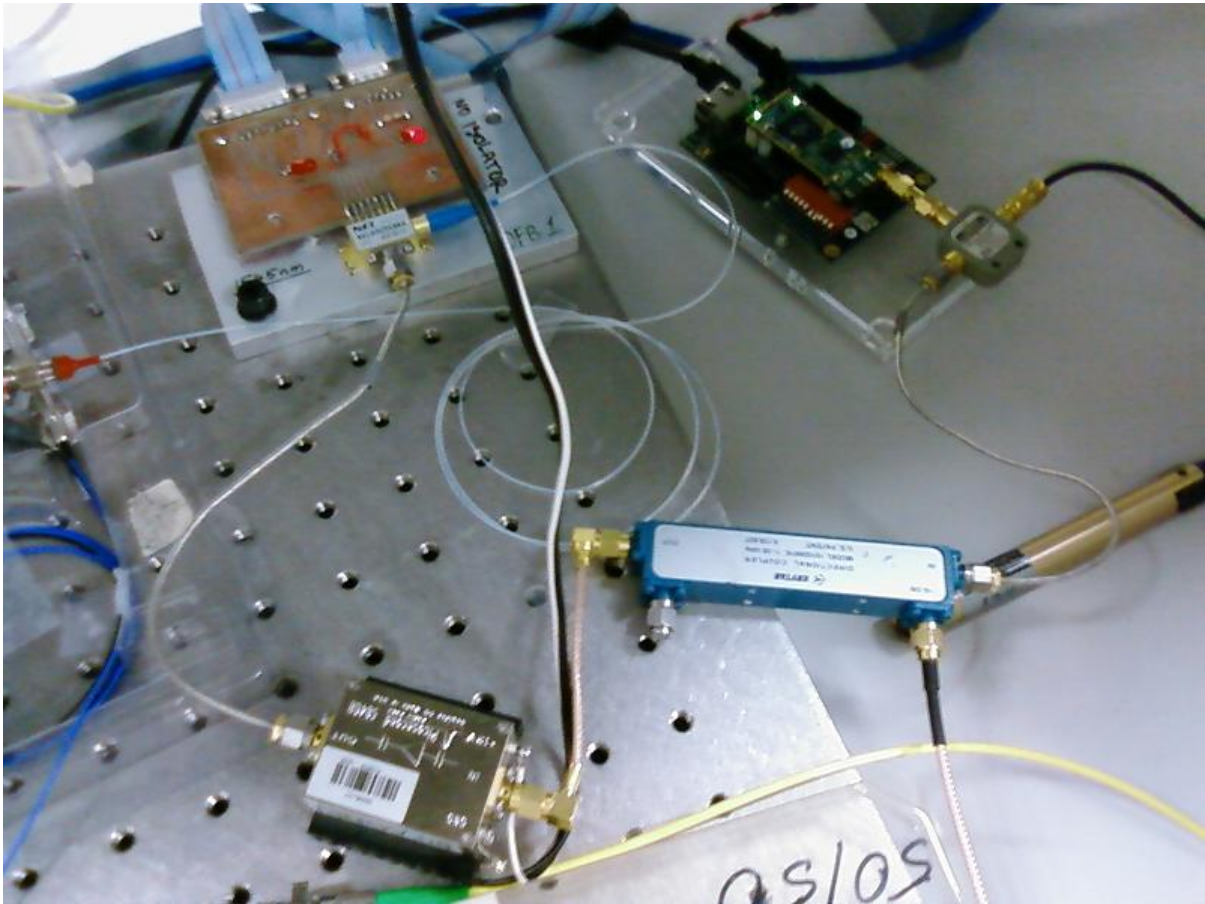
Figure 8.12: Detail of the receiver board (up) and the wireless link (down).
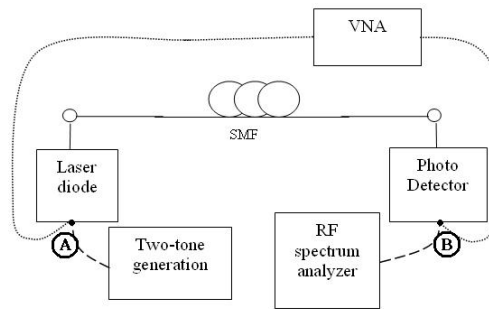
Figure 8.13: System tests schematic.

8.4 System tests

To measure the different performance figures of the system, several different kinds of tests were conducted that will be explained in this section. [43]

- **Frequency response.** The first tests conducted to get an idea of the general response of the system. They were done using a VNA to check the frequency response of our system for different lengths of fiber. This way we could obtain parameters like attenuation, group delay and reflection coefficient of the whole system, end to end. Interesting results were obtained from the graphs depending on the length of fiber used and the power injected into the fiber.

- **PER tests.** With the frequency response plots for the bandwidth between 1Ghz and 15Ghz, many details on the system behavior for different lengths of fiber were obtained. The next step would be to perform transmission tests with real packets being sent and received by the boards. This way variable performance was expected according to the quality of the frequency response, that should be matched and have a relationship, with the quality of the link.

For the **frequency response tests** of the system, the connection of the necessary equipment was done from point A to B as shown in **Figure 8.10** and summarized in **Figure 8.13**, except for some tests that were done between point C and B, to measure the whole response with the filter integrated into the system. This way the optical transmission link and the conversions done were evaluated in performance and response.

For **PER tests** the whole system was evaluated, board to board, with transmission going through the optical and electrical conversions and the optical fiber of variable length. This way, an in-depth idea of the whole transmission process quality was obtained, with detailed IP packets error rate for each different scenario, that showed how each parameter affected transmission.

After the description of the tests, the **results of the system** will be shown in the next sections.

8.5   Performance results

From the tests, different graphs were obtained detailing the response of the system in different scenarios, both for **frequency response** and **PER**.

8.5.1   Frequency response

From the **frequency response of the system** shown in the next pages, many interesting figures were obtained giving an idea of attenuation of the signal for different frequencies transmitted.

First graphs, shown in **Figure 8.14**, are taken back to back, and it can be seen how the response of the system is quite flat when bias current is risen. Although the **relaxation-oscillation curve of the laser** can be observed to appear over it, showing a small bump that moves higher in frequency when the bias current of the laser is increased.

For the next graphs, when the length of fiber is risen as shown in **Figures 8.15, 8.16 and 8.17**, it can be noticed that notches start to appear in the frequency response.

A first notch appears for **24km** at approximately 6Ghz. Then, when the system transmits through **37km**, a second one is seen at 15Ghz together with the first one that appears this time at 5Ghz. For **51Km** both notches moved to lower frequencies appearing at 4Ghz and 13Ghz. The longer the transmission path, a higher number of notches appear in the lower frequencies.

These notches appear because of the **interaction between the two optical sidebands** when they travel through the fiber, causing destructive interaction between them and lowering the power received in the end by the photo-detector, causing the notches in the frequency response. This problem could be solved by using a single sideband transmission or other compensation techniques, which at the moment are out of the scope of this investigation but have been studied by many research groups. [37, 35]

The other interesting idea is that the **bias current applied to the laser sets where the relaxation-oscillation bump appears in frequency**, interacting with the fiber response and changing it in the measured band. This way, changing bias current in the laser will also change the frequency response, so this parameter can be used to obtain a flatter frequency response in our working band, that is depicted with two lines from 3.1Ghz to 4.7 Ghz in the graphs.

For the last measurements, shown in **Figure 8.18**, the **response of the whole system with the filter** in the end and RF amplifiers to rise the level of the signal is shown. It can be noticed that the filter shows two pass-bands, as was previously explained in the filter characterization in **Chapter 6**, and that the response worsens clearly for longer distances.

Bias current has a moderate impact in the response graphs for the most of the cases, sometimes making notches appear or rising the level of the second pass-band of the filter. These would be effects to take into account in trying to obtain the best performance if the final system is going to be implemented.
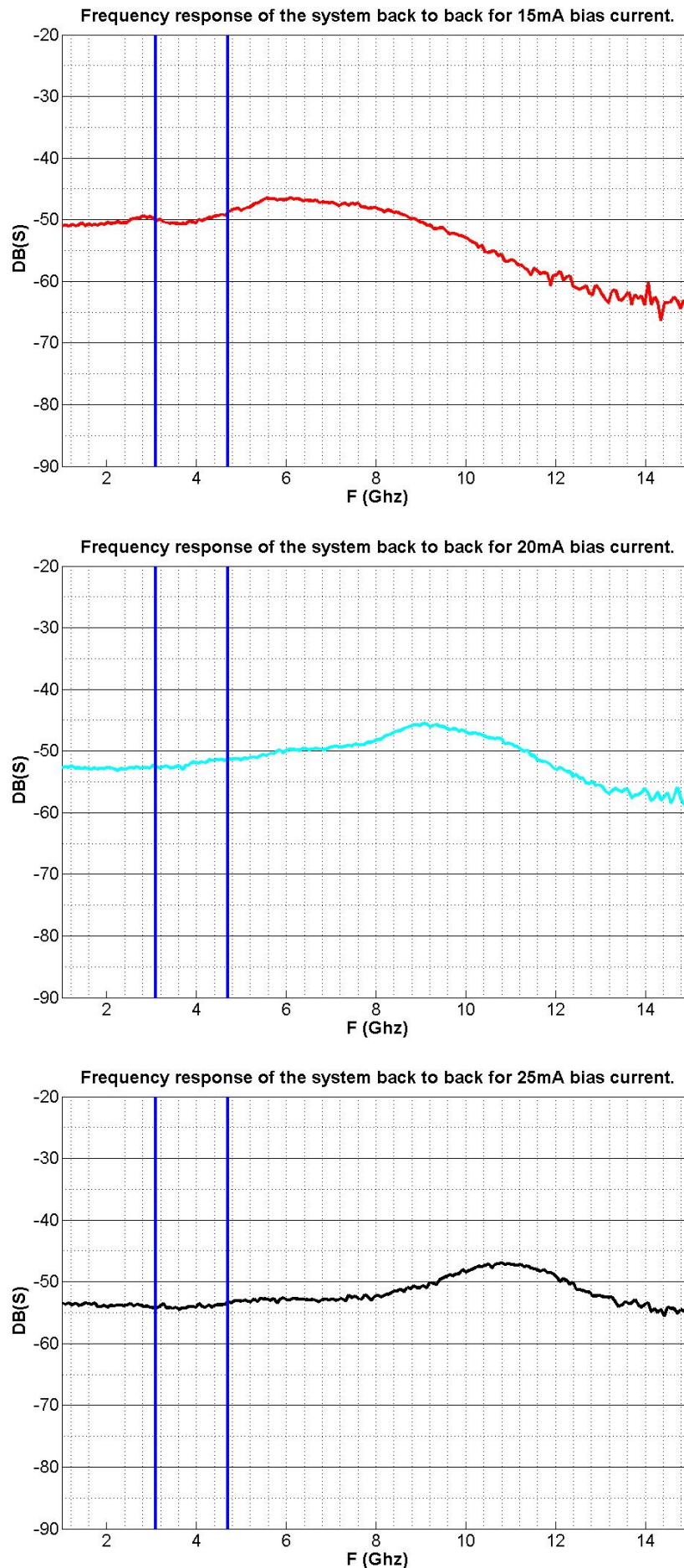
Figure 8.14: Frequency response back to back for different bias currents.

Frequency response of the system with 24km fiber length for 15mA bias current.

Frequency response of the system with 24km fiber length for 20mA bias current.

Frequency response of the system with 24km fiber length for 25mA bias current.
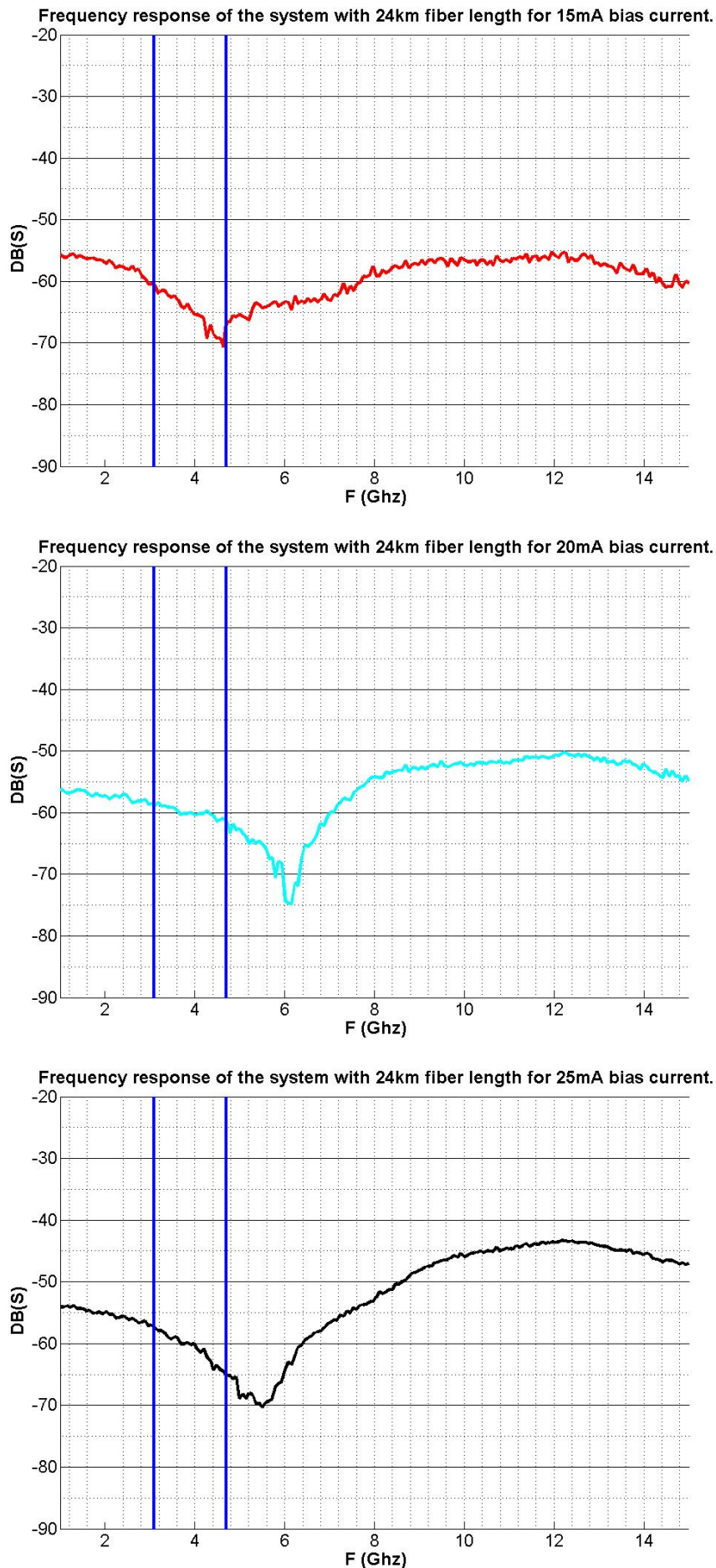
Figure 8.15: Frequency response for 24Km and different bias currents.
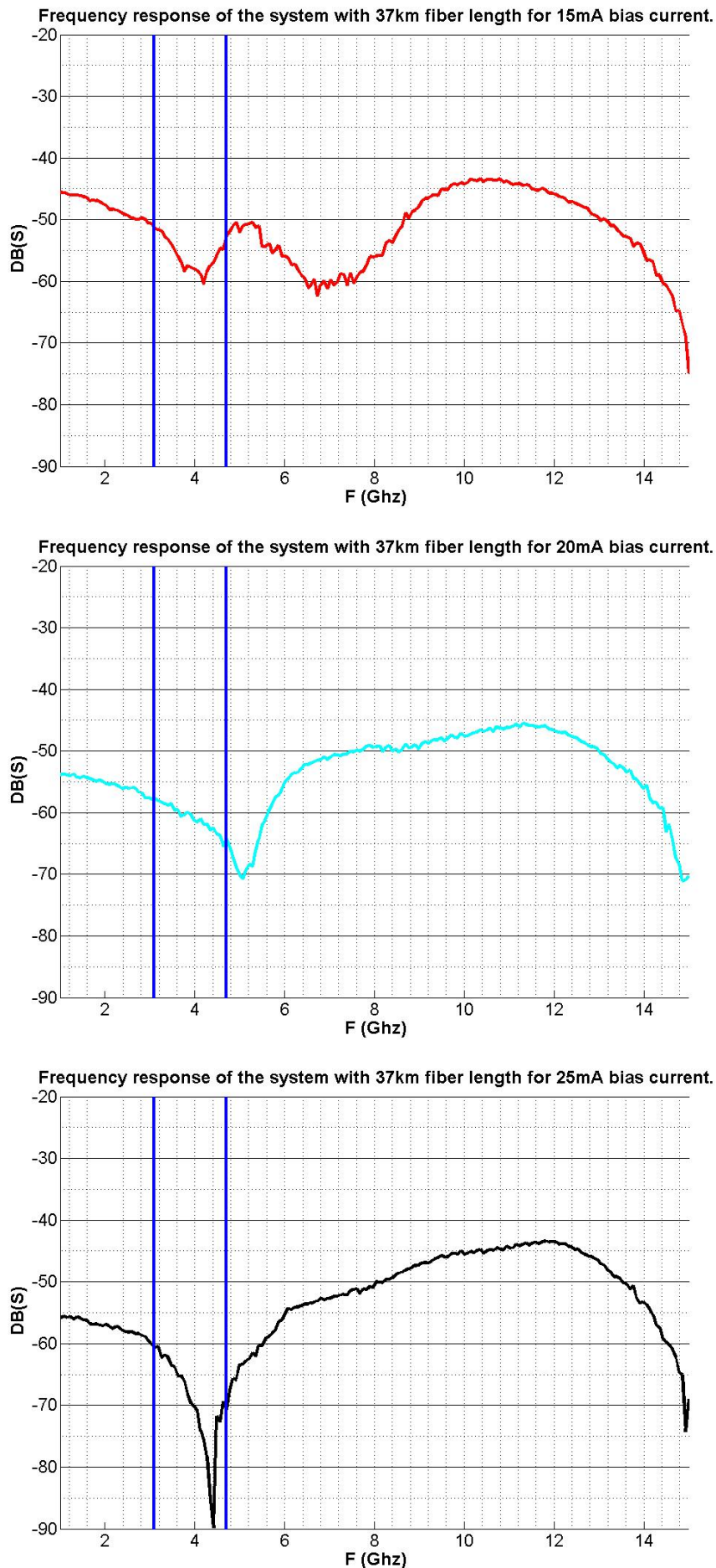
Figure 8.16: Frequency response for 37Km and different bias currents.

Frequency response of the system with 51km fiber length and 15mA bias current.

Frequency response of the system with 51km fiber length and 20mA bias current.

Frequency response of the system with 51km fiber length and 25mA bias current.
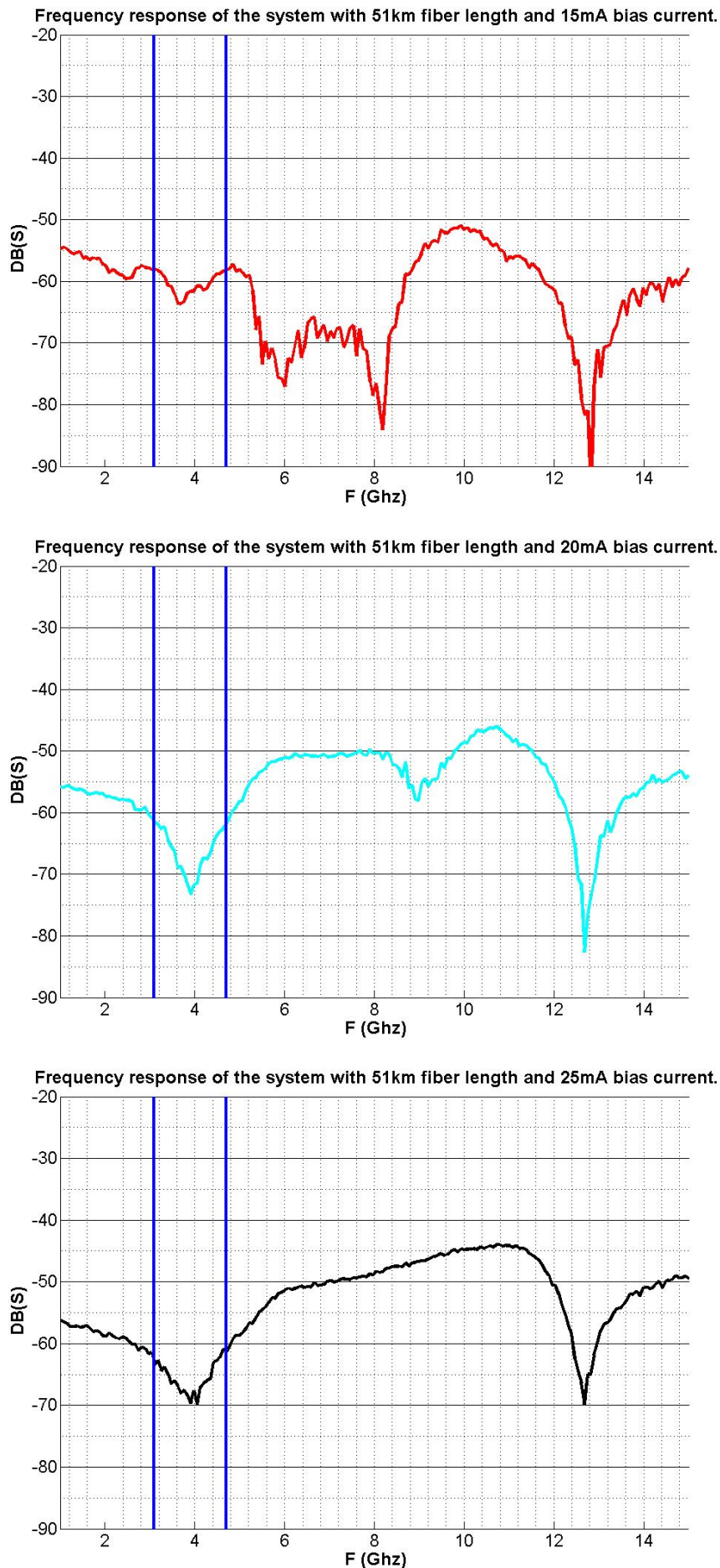
Figure 8.17: Frequency response for 51Km and different bias currents.
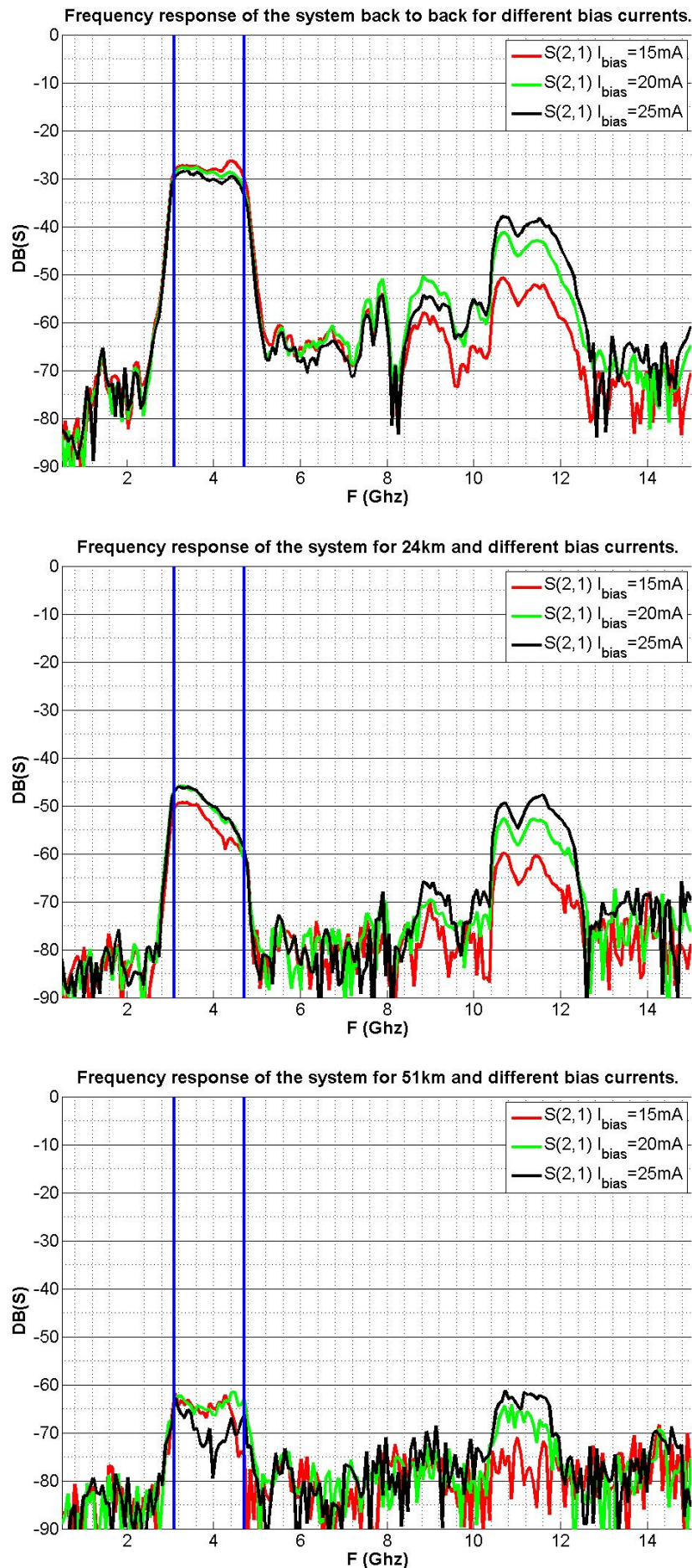
Figure 8.18: Frequency response for different lengths and bias currents.

8.5.2   PER tests

For these tests, results are shown using **3D graphs** in the next pages. These figures are used to show the performance results of the whole system link, transmitting through the optical medium, board to board. Curves depicting PER are presented, all together, for different lengths and related with optical power received.

Measurements are taken for 15, 20 and 25mA bias current applied to the laser, and shown next in **Figures 8.19, 8.20 and 8.21** respectively.

Bias current affects the frequency response of the system and obviously the PER of the IP link. The first idea that arises from the graphs is that the performance of the system doesn't worsen linearly for longer distances, but better performance peaks appear for different lengths, not related directly with the length of fiber we transmit through.

For the lower value of the bias current applied to the laser (15mA), **shown in Figure 8.19,** it is where more differences are seen, clearly showing an improvement of the PER for the 37km transmission range compared to the bad performance at the 22 to 25km range. For higher bias currents, as **shown in Figures 8.20 and 8.21,** the evolution of the performance is more predictable and the transmission needs more power with increasing length to keep the same PER, although there are still some strange behaviors in the response.

Another parameter clearly impacting performance as seen in all the three figures is the **bit-rate of the transmission**. For higher bit-rates, like **480Mbps** shown on the bottom of the three figures, the transmission cannot be established for more than 14Km, and only increasing the bias current to 25mA allows to transmit for a maximum length of 37Km.

The main ideas that can be obtained from these graphs is that the **frequency response of the system** is variable with length, but doesn't necessarily worsen, it depends on the **combination given by the fiber length response and the bias current applied to the laser**, which may give a flat response in our band of interest, improving system performance. It is also worth to mention that adverse effects occurring are more evident for lower bias current, so increasing bias current (which is approximately equal to increasing transmitted power) will improve the response and, therefore, the error rate of the transmission.

These PER curves and the good performance lengths are related with the improved frequency response we obtain for them in the previous graphs. The **flatter the frequency response, the best quality the signa**l will have, so in the cases were different parameters help to show a flat response, the **PER will also be lower** and need less optical power to reach the error free transmission point.
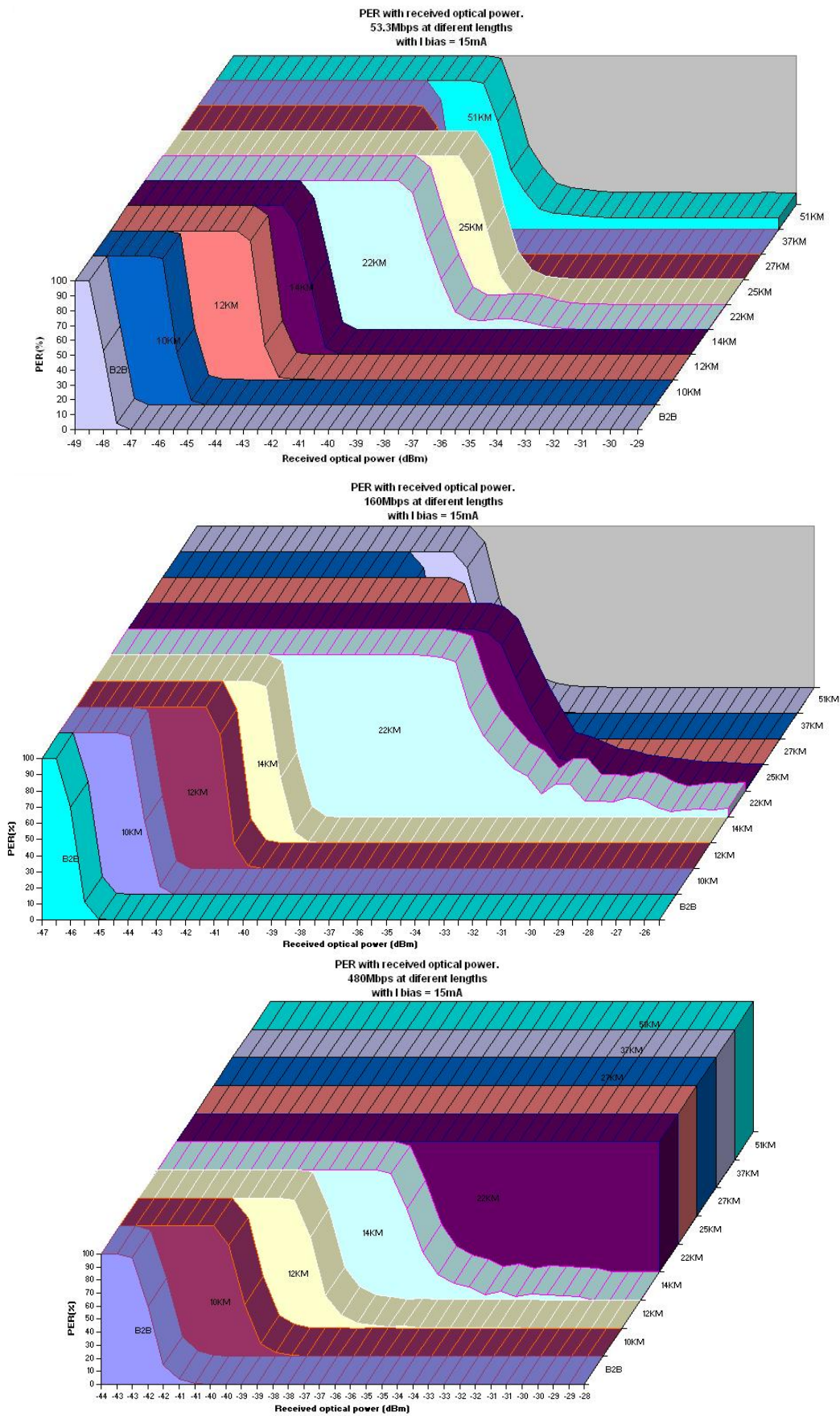
Figure 8.19: PER graphs for different bit-rates and 15mA bias current.
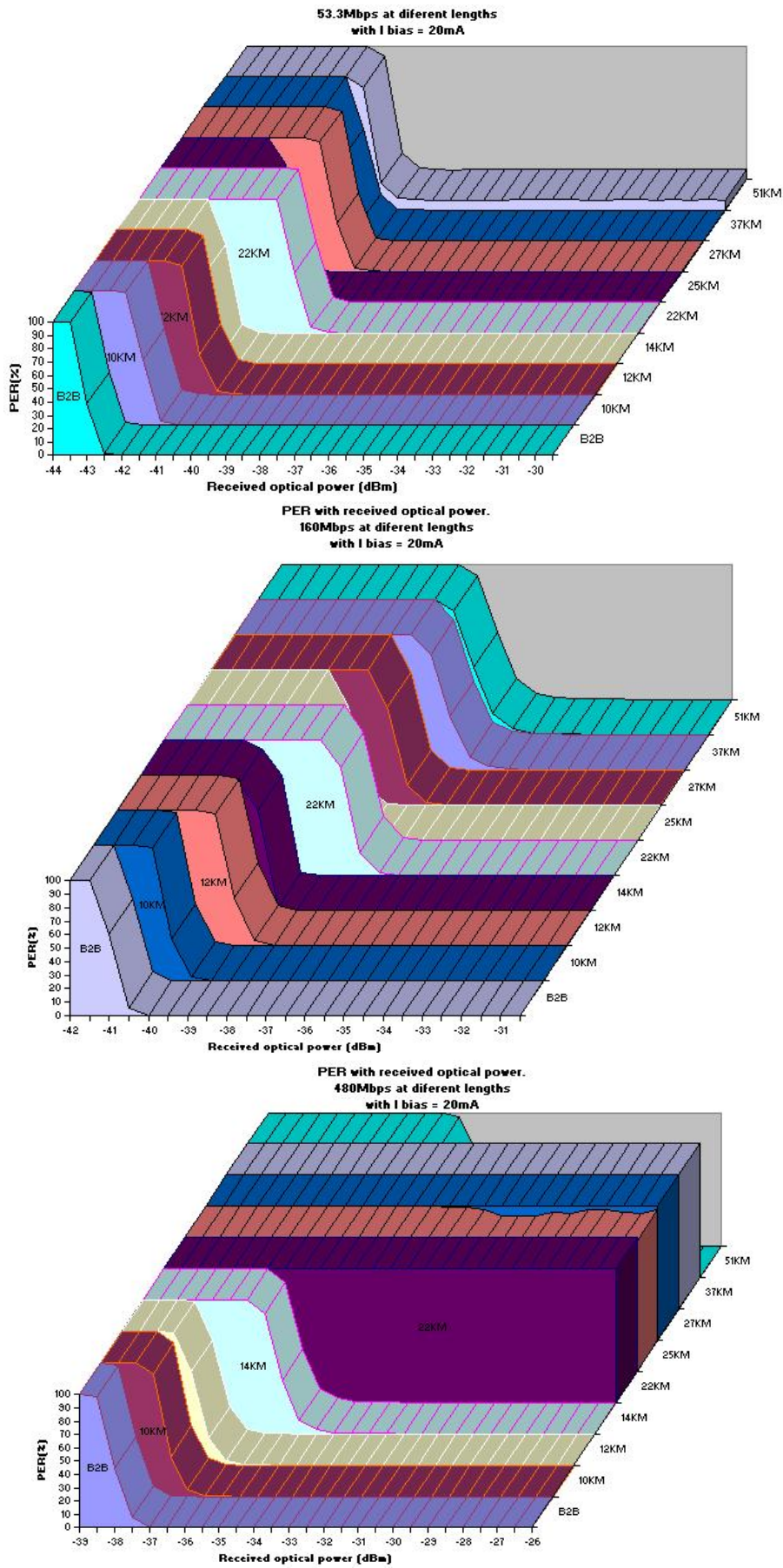
Figure 8.20: PER graphs for different bit-rates and 20mA bias current.
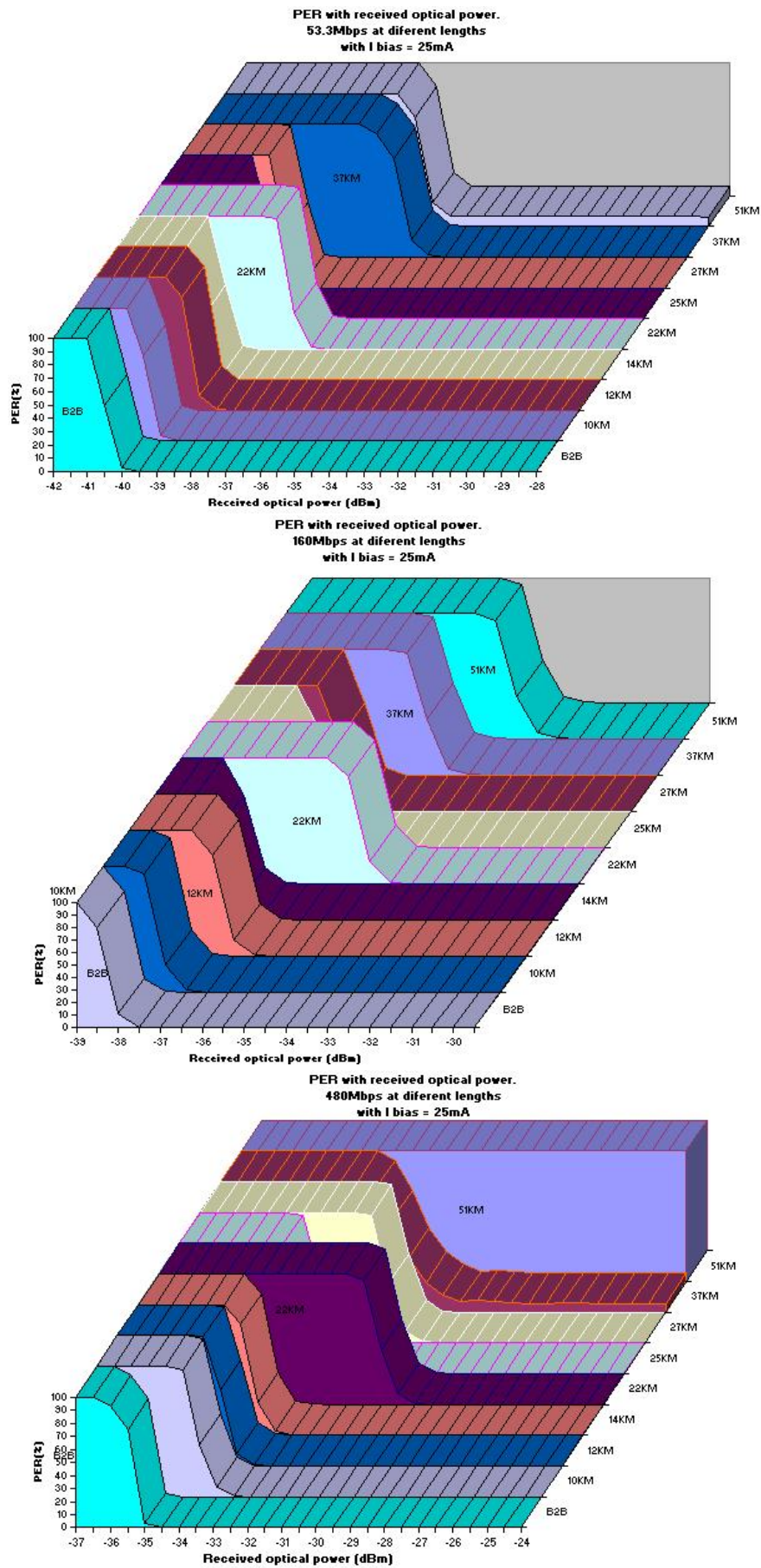
Figure 8.21: PER graphs for different bit-rates and 25mA bias current.

8.5.3 Wireless link and filter

Once the optical transmission system was characterized in detail, **the wireless link was introduced** in our system. This was done after the tests already explained were finished. New tests were then conducted to measure the **changes introduced by the wireless link in the system's performance**.

When the wireless link was introduced, the quality of the link was affected and the PER obtained was reduced by a 20% approximately, although this slightly depended on the fiber length and bias current of the laser. With additional amplification for the wireless link included, on average we would need 3 to 5 dBm more power to keep the same PER figures as the ones without the optical link. This occurred for a wireless link of 35cm and was slightly variable depending on the length of fiber used, up to about 15kms, that was the limit to be able to obtain a proper wireless transmission combining optical and wireless transmission altogether.

The **filter** was useful when transmitting point to point without the wireless link, where it isolated the signal arriving to the Wisair board, **discarding frequencies above and below our band of interest**, given that these boards don't have onboard filtering, as showed by the response of the antennas and measurements done.

As previously mentioned, **once the antennas were included** in the setup, the **filter was not useful**, and that was demonstrated in the tests, where if it was introduced together with the antennas (that also work as band-pass filters as seen in its characterization in this chapter) the performance of the system was affected. This was caused by a not necessary double filtering done both by the antennas and filter, causing an approximately 15% lower performance on the error rate.

8.6 Conclusions

The results obtained from the system give a clear idea of the good quality and real usability this kind of system has. In our tests a maximum optical link of 51Km has been achieved and a wireless connection of some meters could be established for a shorter length of fiber.

These facts clearly show that, with enough optimization and more research, this transmission system could be deployed and used in many different real life scenarios.

9

Conclusions and future work.

9.1 Conclusions

The design cycle of some **UWB filters** and an **UWB ROF transmission system** with room for improvement have been demonstrated in this project. Starting from the design of a single component, the UWB filters, to the tests of the whole developed system, checking its performance and transmission limits. The whole project had the idea in mind of designing and implementing a complete optical distribution system of radio signals. Analyzing and selecting the different components needed and also designing some of them, the filters. Both objectives have been completed with good results, and a final practical system has been demonstrated.

The first part of the work consisted in learning and applying the necessary theoretical techniques to design some **UWB band-pass filters**, based in parallel coupled transmission lines using microstrip technology. During the process, the most important techniques to develop microwave filters were studied and then applied. The design of the filters was done with a computer software, starting from the calculated values, and tuning the performance up to the final version that was finally built.

The whole design process was accomplished, and filters were optimized for its construction using microstrip technology. There were two main limitations: the material behavior at the working frequency and the minimum measurements that could be obtained in the construction process. Both had to be taken into account as key factors, because they would limit and worsen the filter responses.

Once the filters were built, good results have been obtained in the tests, with similar responses as the ones in the simulations. Insertion losses of around 3dB and about 5dB as worst were achieved for the pass-band. Return losses of about 20dB for the whole working band, with a good rejection rate in the stop-band, were also good results obtained.

So it can be said that the filters built comply with the requirements for our system and

have good responses. This is true for the low frequency filter (3.1 to 4.7Ghz), but the higher frequency one (6.3 to 7.9 Ghz) shows a response a bit worse. This is because the FR-4 substrate's characteristics worsen with frequency, causing a different behavior and adverse effects, that modify and round the frequency response, making it not to show flat as we would expect. But in the end, problems have been solved and good enough responses that meet the requirements of our system have been accomplished.

The results of the **system finally developed**, with all the components selected and the filters introduced, are also quite good. It is able to transmit UWB radio signals using optical links for as long as 50Kms, making it possible to use it as an optical distribution system of radio signals, that can then be radiated with a simple transceiver. It would be able to establish a wireless link in the ends of this system, using small antennas, with the possibility to reach some meters. With the necessary adjustments and tuning, this system could accomplish the distribution of RF signals through an optical distribution network of some kilometers. It would also be able to establish wireless links with wireless receivers using different technologies, up to an estimated length (at the speed of 480Mbps) of around 10 meters.

Although the available bandwidth should be improved if more channels want to be used, the main figures are good enough to proof its practical use. This system clearly demonstrates that this kind of distribution of RF signals is feasible and useful, given the high number of optical networks already installed in many different places, where it could be applied to give wireless connections with only minor modifications. This is also demonstrated given the **interest for this kind of systems in the research field** and the **acceptance of a paper to be published** in an international conference (**CIICT 09**) related with the work done here and **presented in the Appendix** of this report.

9.2   Future work

Both topics treated in this project have a big room for improvement and many interesting paths can be followed to continue the work done here.

As for the **UWB filters**, more work could be done to improve these designs. In the first place, to enhance the actual built filters characteristics, the one from 3.1Ghz to 4.7Ghz and mostly the one from 6.3 to 7.9 Ghz. The flatness of the response, the reflection coefficient and maybe the out of band rejection rate could be improved and the filters simplified. In second place it would be very interesting to continue the tuning and finally build the third filter going from 3.1Ghz to 10.6Ghz. Given that, as observed for the other two filters, when the working frequency is increased, a shift in the pass-band is observed for the final filters and more negative effects appear because of the limitations of the substrate material used.

It would be interesting to develop a project centered on trying to push the filters made of **microstrip material** with FR-4 substrate to **higher frequencies**. It is a cheap material, and it is interesting to try to build higher frequency and wider bandwidth filters out of it, overcoming the problems that will arise. An interesting work would be to study in detail the different effects

appearing and how to counteract them, tuning different parts of the design by means of the CAD software tools available.

In the **ROF systems field**, many more tests could be done to characterize the system. The lack of flatness of the frequency response for our working band could be improved, and better noise and attenuation figures could be obtained by changing different components, or using different transmission techniques. It would be interesting to study in detail the signal degradation, both in the optical and wireless link. These would allow for improvements in the wireless link length, that at the present time is the most limiting factor.

So the two most interesting paths to follow for the improvement of the UWB ROF transmission system would be, first the **study of the wireless link figures** like: attenuation, signal quality and signal versus noise levels reaching the opto-electrical transceiver. These would help to improve wireless link length and quality. Second would be to **improve the optical transmission method** to obtain more bandwidth. That way different wireless signals could be sent at a time and allow for the optical distribution system to be shared between different user technologies.

To finish, many more topics could be mentioned, given that this field is in constant expansion, and much research is being done by different groups to push these technologies further. With an increasing interest and many projects searching for different approaches to find the most efficient way to implement these transmission systems. But for the present time, this project has showed the basic ideas behind optical transmission of wireless signals and its feasible application in final commercial systems.

9.3   Conclusiones

El ciclo de diseño de un par de **filtros UWB y un sistema de transmisión UWB ROF** con margen de mejora han sido demostrados en este proyecto. Comenzando desde el diseño de un sólo componente, los filtros UWB, hasta las pruebas del sistema completo desarrollado, comprobando su rendimiento y límites de operación. El proyecto completo tenía la idea en mente de diseñar e implementar un sistema óptico completo de distribución de señales de radio. Analizando y seleccionando los diferentes componentes necesarios y también diseñando algunos de ellos, los filtros. Ambos objetivos han sido completados con buenos resultados, y un sistema completo ha sido demostrado en la práctica.

La primera parte del trabajo consistió en recopilar y aplicar los procedimientos teóricos necesarios para diseñar unos **filtros paso banda UWB**, basados en lineas acopladas paralelas usando tecnología microstrip. Durante el proceso, las técnicas más importantes para desarrollar filtros de microondas fueron estudiadas y después aplicadas. El diseño de los filtros fue llevado a cabo con un software dedicado, comenzando con un prototipo con los valores calculados y ajustándolos para obtener las características necesarias hasta llegar a la versión final construida.

El proceso de diseño completo fue completado, y los filtros fueron optimizados para su construcción usando tecnología microstrip. Para ello había dos limitaciones básicas: el comportamiento del material a la frecuencia de trabajo y las medidas mínimas que podían ser obtenidas con el proceso de construcción utilizado. Ambas tenían que ser tenidas en cuenta como factores clave, dado que limitaían y empeorarían la respuesta de los filtros.

Una vez que los filtros fueron construidos, buenos resultados han sido obtenidos en las pruebas, con respuestas similares a las obtenidas en las simulaciones. Pérdidas de inserción de entre 3dB y alrededor de 5dB como peor valor fueron obtenidas en las bandas de paso. Pérdidas de retorno de alrededor de 20dB para la banda completa de trabajo, con un buen factor de rechazo en la banda eliminada, fueron también buenos resultados obtenidos.

Así que puede decirse que los filtros construidos cumplen los requisitos para nuestro sistema y tienen buenas respuestas. Ésto es cierto para el primer filtro a baja frecuencia (de 3.1 a 4.7Ghz), pero para el de alta frecuencia (de 6.3 a 7.9Ghz) la respuesta es un poco peor. Ésto es debido a que las características del sustrato FR-4 empeoran con la frecuencia, causando un comportamiento diferente y efectos adversos, que modifican y redondean la respuesta en frecuencia, haciendo que no sea tan plana como en principio se esperaría. Pero al final, estos problemas han sido superados y han sido obtenidas respuestas suficientemente buenas que cumplen los requerimientos para nuestro sistema.

Los resultados del **sistema final desarrollado**, con todos los componentes seleccionados y los filtros introducidos, son también bastante buenos. Éste es capaz de transmitir señales de radio UWB usando enlaces ópticos de 50Km de longitud máxima, haciendo posible su uso como sistema óptico de distribución de señales de radio, que pueden luego ser radiadas con un transceptor simple. Así sería capaz de establecer un enlace inalámbrico en los finales de este sistema, usando antenas pequeñas, con la posibilidad de alcanzar varios metros. Con los ajustes

necesarios, este sistema sería capaz de distribuir señales de RF a través de una red óptica de varios kilómetros. También sería capaz de establecer enlaces inalámbricos con receptores usando diferentes tecnologías, hasta una longitud estimada (para una velocidad de 480Mbps) de alrededor de 10 metros.

Aunque el ancho de banda disponible debería ser mejorado si se requiere usar más canales, las figuras principales del sistema son suficientemente buenas como para probar su uso práctico. Este sistema demuestra claramente que este tipo de distribución de señales de RF es viable y útil, dado el alto número de redes ópticas ya instaladas en muchos lugares diferentes, donde podría ser aplicado para dar conexión inalámbrica con tan sólo pequeñas modificaciones. Ésto además queda demostrado dado el **interés creciente en este tipo de sistemas** por parte de diferentes grupos de investigación y la **aceptación para su publicación de un papel** que será incluido en una conferencia internacional (**CIICT 09**) relacionado con el trabajo llevado a cabo en este proyecto y presentado en el **Apendice** de este trabajo.

9.4   Trabajo futuro

Ambos temas tratados en este poryecto tienen un gran margen de mejora y varios caminos interesantes pueden ser seguidos para continuar el trabajo hecho aqui.

En lo que respecta a los **filtros UWB**, más trabajo puede ser desarrollado para mejorar estos diseños. En primer lugar, para mejorar las características de los filtros construidos, el que va de 3.1 a 4.7Ghz, pero sobre todo el de alta frecuencia, de 6.3 a 7.9Ghz. La planicidad de la respuesta, el coeficiente de reflexión y quizá el factor de rechazo, podrían ser mejorados y los filtros simplificados. En segundo lugar sería muy interesante continuar la optimización y finalmente construir el tercer filtro que va de 3.1 a 10.6Ghz. Dado que, por lo observado en los otros dos filtros, cuando la frecuencia de trabajo es incrementada, se observa un desplazamiento en la banda de paso para el filtro final y aparecen efectos negativos debido a las limitaciones del material utilizado como sustrato.

Sería interesante desarrollar un proyecto centrado en intentar diseár filtros llegando al **límite de frecuencia del sustrato FR-4**. Es un material barato, y sería interesante intentar construir filtros a más alta frecuencia y con anchos de banda más grandes, solucionando los problemas que aparezcan. Un trabajo interesante sería estudiar en detalle los diferentes efectos que aparezcan y como contrarestarlos, ajustando diferentes partes del diseño usando las herramientas de software disponibles.

En cuanto al **campo de radio sobre fibra**, muchas más pruebas podrían ser realizadas para caracterizar el sistema. La falta de planicidad en la respuesta en frecuencia podría ser mejorada, y mejores factores de ruido y atenuación podrían ser conseguidos cambiando diferentes componentes, o usando diferentes técnicas de transmisión. Sería interesante estudiar en detalle la degradación sufrida por la señal, tanto en el enlace óptico como en el inalámbrico. Ésto permitiría mejorar la longitud del enlace final inalámbrico, que en el momento actual es el factor que más limita el sistema.

Así que los caminos más interesantes a seguir para mejorar el sistema de transmisión de señales UWB sobre fibra serían, primero el **estudio de las principales figuras del enlace inalámbrico** como: atenuación, calidad de la señal, niveles de señal/ruido que llegan al transceptor opto-eléctrico. Ésto ayudaría a mejorar la longitud del enlace inalámbrico. Lo segundo sería **mejorar el método de transmisión óptico** para obtener más ancho de banda. Así podríamos transmitir diferentes señales inalámbricas al mismo tiempo y permitir que el sistema de distribución fuera compartido entre usuarios de diferentes tecnologías.

Para terminar, bastantes más temas podrían ser mencionados, dado que este campo está en constante expansión, y bastante investigación está siendo llevada a cabo por parte de diferentes grupos para impulsar estas tecnologías. Con un interés creciente y muchos proyectos que buscan diferentes enfoques para encontrar la manera más eficiente de implementar estos sistemas de transmisión. Pero en el momento actual, este proyecto ha mostrado las ideas básicas detrás de la transmisión óptica de señales inalámbricas y su posible aplicación en sistemas comerciales.

Definitions

ADC Analog Digital Converter

ADSL Asymmetric Digital Subscriber Line: it is a form of DSL, a data communications technology that enables fast data transmission over copper telephone lines. It does this by utilizing frequencies that are not used by a voice telephone call, up to 1Mhz, allowing a single telephone connection to be used for both ADSL service and voice calls at the same time. ADSL can generally only be distributed over short distances from the central office, typically less than 4 kilometers, and allows for bit-rates up to 30Mbps down-link, and 4Mbps up-link.

BG Band Group: the UWB frequency spectrum allocated by FCC and ranging from 3168Mhz to 10560Mhz is divided into 5 band groups using each one three sub-bands (except for BG5 which uses two instead) of 528Mhz. It is a method to divide and allocate frequency bands for different uses and configurations inside the UWB spectrum.

Bias current : current fed to an electronic device that is independent of the output. It is fed to a semiconductor or other electronic device to ensure that the device functions at a desired working point and with the required operation characteristics.

BPSK Binary Phase Shift Keying: is a digital modulation scheme that conveys data by changing, or modulating, the phase of a reference signal (the carrier wave). It uses two phases which are separated by 180° and so can also be termed 2-PSK. This modulation is the most robust of all the PSKs since it takes serious distortion to make the demodulator reach an incorrect decision. It is, however, only able to modulate at 1 bit/symbol and so is unsuitable for high data-rate applications when bandwidth is limited.

In the presence of an arbitrary phase-shift introduced by the communications channel, the demodulator is unable to tell which constellation point is which. As a result, the data is often differentially encoded prior to modulation.

CATV Cable Television: is a system of providing television to consumers via radio frequency signals transmitted to televisions through fixed optical fibers or coaxial cables as opposed to the over-the-air method used in traditional television broadcasting (via radio waves) in which a television antenna is required. Other services such as FM radio programming, high-speed Internet, and telephony may also be provided.

CAD Computer-aided Design: refers to programs used on computers to help design and simulate real life systems. They are valuable help and a very useful way of obtaining preliminary

results and speeding the design and construction process. With these programs we are able to know the approximate final behavior of the real life system through its model simulation.

Electrical conductivity : or specific conductance is a measure of a material's ability to conduct an electric current. When an electrical potential difference is placed across a conductor, its movable charges flow, giving rise to an electric current. The conductivity σ is defined as the ratio of the current density J to the electric field strength E:

$J = \sigma E$

Conductivity is the reciprocal (inverse) of electrical resistivity, ρ, and has the SI units of siemens per metre $S \cdot m^{-1}$:

$\sigma = \frac{1}{\rho}$

CW Continuous Wave: is an electromagnetic wave of constant amplitude and frequency; and in mathematical analysis, of infinite duration.

DAC Digital Analog Converter

DSP Digital Signal Processing: stands for the application of digital processing techniques to information signals. These methods are much more powerful than analog processing and allow for the compensation of different effects occurring in transmission environments. It improves signal quality and achieves a high error correction, allowing for data link connections even in complex and changing environments where the response is variable and different adverse effects occur at the same time in the transmission.

DVB-T Digital video broadcasting - Terrestrial:it is the DVB European-based consortium standard for the broadcast transmission of digital terrestrial television. This system transmits compressed digital audio, video and other data in an MPEG transport stream, using COFDM modulation.

ECMA European association for standardizing information and communication systems: is an international, private (membership-based) non-profit standards organization for information and communication systems. It aims to develop standards and technical reports to facilitate and standardize the use of information communication technology and consumer electronics. ECMA publications, including standards, can be freely copied by all interested parties without copyright restrictions. The development of standards and technical reports is done in co-operation with the appropriate national, European and international organizations.

EDFA Erbium Doped Fiber Amplifier: consists of a piece of fiber of length L, whose core is uniformly doped with Erbium ions. It is a device that amplifies an optical signal directly, without the need to first convert it to an electrical signal. It may be thought of as a laser without an optical cavity, or one in which feedback from the cavity is suppressed. It is the most deployed fibre amplifier as its amplification window coincides with the third transmission window of silica-based optical fibre.

EM Electromagnetic

FCC Federal Communications Commission: it is an independent agency of the United States government. It works towards six strategic goals in the areas of broadband, competition, the spectrum, the media, public safety and homeland security. It is charged with regulating all non-federal government use of the radio spectrum (including radio and television broadcasting), and all interstate telecommunications (wire, satellite and cable) as well as all international communications that originate or terminate in the United States.

FR-4 Flame Retardant 4: it is a type of material used for making printed circuit boards (PCBs). It describes the board substrate, with no copper layer. The FR-4 used in PCBs is typically UV stabilized with a tetra-functional epoxy resin system and it is typically of a transparent yellowish color.

HFC Hybrid Fiber coax: is a telecommunications industry term for a broadband network which combines optical fibre and coaxial cable. It has been commonly employed globally by cable TV operators since the early 1990s. A typical fibre optic network extends from the cable operators' master head-end, sometimes to regional head-ends, and out to a neighborhood's hub site where will finally reach a fibre optic node which typically serves around 25 to 2000 homes.

IEEE 802.11 Institute of Electrical and Electronics Engineers standard carrying out wireless local area network (WLAN): IEEE 802.11 is a set of standards carrying out wireless local area network (WLAN) computer communication in the 2.4, 3.6 and 5 Ghz frequency bands. They are implemented by the IEEE LAN/MAN Standards Committee (IEEE 802).

Loss tangent : it is a parameter of a dielectric material that quantifies its inherent dissipation of electromagnetic energy. The term refers to the angle in a complex plane between the resistive (lossy) component of an electromagnetic field and its reactive (lossless) component. Its expression is given by:

$\tan \delta = \frac{\omega \epsilon'' + \sigma}{\omega \epsilon'}$, where:

ε'' is the imaginary amplitude of permittivity attributed to bound charge and dipole relaxation phenomena.

ε' represents the familiar lossless permittivity given by the product of the free space permittivity and the relative permittivity, or $\varepsilon' = \varepsilon_0 \varepsilon_r$

σ represents the free charge conduction, conductivity of the material.

MAC Medium Access Control: it is a data communication protocol, sublayer of the Data Link Layer (layer 2) specified in the seven-layer OSI model. It provides addressing and channel access control mechanisms that make it possible for several terminals or network nodes to communicate within a multipoint network, typically a local area network (LAN) or metropolitan area network (MAN). The hardware that implements the MAC is referred to as a Medium Access Controller.

OSI Model
7 Application Layer
6 Presentation Layer
5 Session Layer
4 Transport Layer
3 Network Layer
2 Data Link Layer $\begin{cases} LLC\ sublayer \\ MAC\ sublayer \end{cases}$
1 Physical Layer

The MAC sub-layer acts as an interface between the Logical Link Control (LLC) sublayer and the network's physical layer. The MAC layer emulates a full-duplex logical communication channel in a multipoint network.

MAN Metropolitan Area Network: are large computer networks usually spanning a city. They typically use wireless infrastructure or Optical fiber connections to link their sites. It spans a metropolitan area or campus and its geographic scope falls between a WAN and LAN. MANs provide Internet connectivity for LANs in a metropolitan region, and connect them to wider area networks like the Internet.

MB-OFDM Multiband Orthogonal Frequency-Division Multiplexing: (see OFDM) it is an OFDM transmission technology modification to transmit using different and independent bands which can be dynamically arranged for different bit-rates and frequency occupation. It is able to transmit at high bit rates without interfering other systems.

NF Noise Figure: is a measure of degradation of the signal to noise ratio (SNR), caused by components in the RF signal chain. The noise figure is the ratio of actual output noise to that which would remain if the device itself did not introduce any noise. It is a number by which the performance of a radio receiver can be specified.

OFDM Orthogonal Frequency-Division Multiplexing: essentially identical to Coded OFDM (COFDM) and Discrete multi-tone modulation (DMT). It is a frequency-division multiplexing (FDM) scheme utilized as a digital multi-carrier modulation method. A large number of closely-spaced orthogonal sub-carriers are used to carry data which is divided into several parallel data streams or channels, one for each sub-carrier. Each of them is modulated with a conventional modulation scheme (such as quadrature amplitude modulation or phase shift keying) at a low symbol rate, maintaining total data rates similar to conventional single-carrier modulation schemes in the same bandwidth.

OOK On-Off Keying: is a type of modulation that represents digital data as the presence or absence of a carrier wave. In its simplest form, the presence of a carrier for a specific duration represents a binary one, while its absence for the same duration represents a binary zero. Some more sophisticated schemes vary these durations to convey additional information.

PAM Pulse Amplitude Modulation: is a form of signal modulation where the message information is encoded in the amplitude of a series of signal pulses. Demodulation is performed by detecting the amplitude level of the carrier at every symbol period. It is widely used in base-band transmission of digital data, with non-base-band applications having been largely superseded by other methods.

Permittivity : is a physical quantity that describes how an electric field affects, and is affected by, a dielectric medium. It is determined by the ability of a material to polarize in response to the field, and thereby reduce the total electric field inside the material. Thus, permittivity relates to a material's ability to transmit (or "permit") an electric field. The permittivity can have real and imaginary components such that:

$\varepsilon = \varepsilon^{'} - j\varepsilon^{''}$

The linear permittivity of a homogeneous material is usually given relative to that of free space ε_0, as a relative permittivity ε_r (also called dielectric constant), where χ_e is the electric susceptibility of the material.

$\varepsilon' = \varepsilon_r \varepsilon_0 = (1 + \chi_e)\varepsilon_0$

PCB Printed Circuit Board: is used to mechanically support and electrically connect electronic components using conductive pathways, or traces, etched from copper sheets laminated onto a non-conductive substrate. Much of the electronics industry's PCB design, assembly, and quality control needs are set by standards that are published by the IPC organization.

PER Packet Error Rate: is used to test the performance of network connection links. PER is the ratio, in percent, of the number of Test Packets (TP) not successfully received in the receiver end to the number of total TP sent by the transmitter end. It is a very important Quality of Service parameter for wireless networks.

PLC Power line communication: is a system for carrying data on a conductor also used for electric power transmission. Broadband over Power Lines (BPL) uses PLC by sending and receiving information bearing signals over power lines to provide access to the Internet. But this technology can be used in any environment involving high speed data transmission over power lines.

PPM Pulse Position Modulation: is a form of signal modulation in which M message bits are encoded by transmitting a single pulse in one of 2M possible time-shifts. This is repeated every T seconds, such that the transmitted bit rate is M/T bits per second. It is primarily useful for optical communications systems, where there tends to be little or no multipath interference.

PSD Power Spectral Density: is a positive real function of a frequency variable associated with a stationary stochastic process, or a deterministic function of time, which has dimensions of power per Hz, or energy per Hz. It is often called simply the spectrum of the signal. Intuitively, the spectral density captures the frequency content of a stochastic process and helps identify periodicities.

Rayleigh distance : is the axial distance from a radiating aperture to a point at which the path difference between the axial ray and an edge ray is $\frac{\lambda}{4}$. Is is normally defined as: $R_r = \frac{D^2}{2\lambda}$ or $\frac{2D^2}{\lambda}$ or even $\frac{D^2}{\lambda}$.

All of them still give a reasonably on-axis power density estimates.

Reactance : it is a circuit element's opposition to an alternating current, caused by the build up of electric or magnetic fields in the element due to the current. Both reactance X and resistance R are required to calculate the impedance Z. Although in some circuits one of these may dominate, an approximate knowledge of the minor component is useful to determine if it may be neglected.

$Z = R + jX$

RF Radio Frequency

RMS Root Mean Square: also known as the quadratic mean, is a statistical measure of the magnitude of a varying quantity. It is especially useful when variates are positive and negative, e.g., sinusoids.

The RMS of a collection of n values $\{x_1, x_2, ..., x_n\}$ is:

$x_{rms} = \sqrt{\frac{x_1^2 + x_2^2 + ... + x_n^2}{n}}$.

And for a continuous function $f(t)$ defined over the interval $T_1 \leq t \leq T_2$:

$f_{rms} = \sqrt{\frac{1}{T_1 - T_2} \int_{T_1}^{T_2} [f(t)]^2 \, dt}$.

If $\bar{x}$ is the arithmetic mean and σ_x is the standard deviation of a population then the following relation applies:

$x_{rms}^2 = \bar{x}^2 + \sigma_x^2$.

From this it is clear that the RMS value is always greater than or equal to the average, in that the RMS includes the "error" (square deviation) as well.

ROF Radio Over Fiber: refers to a technology in which light is modulated by a radio signal and transmitted over an optical fiber link to an optical receptor that will facilitate wireless access by doing an opto-electrical conversion an radiation of the signal to the air. Although radio transmission over fiber is used for multiple purposes, such as in cable television (CATV) networks and in satellite base stations, the term ROF is usually applied when this is done for wireless access.

Susceptance : it is the imaginary part of the admittance (Y). Which is the inverse of the impedance (Z) $Y = \frac{1}{Z}$. In SI units, the susceptance is measured in Siemens.

$Y = G + jB$

Y is the admittance.

G is the conductance.

B is the susceptance.

All measured in Siemens S, the inverse of ohm Ω.

SFDR Spurious Free Dynamic Range: is defined as the ratio of the RMS value of the carrier frequency (maximum signal component) at the input of the ADC or DAC to the RMS value of the next largest noise or harmonic distortion component (which is referred to as a "spurious") at its output. SFDR is usually measured in dBc (i.e. with respect to the carrier frequency amplitude) or in dBFS (i.e. with respect to the ADC's full-scale range). Depending on the test condition, SFDR is observed within a pre-defined frequency window or from DC up to Nyquist frequency of the converter (ADC or DAC).

TE Transverse Electric: transverse mode of an electromagnetic radiation where there is no electric field in the direction of propagation.

TEM Transverse Electro-Magnetic: the transverse mode of a beam of electromagnetic radiation is a particular electromagnetic field pattern of radiation measured in a plane perpendicular (i.e. transverse) to the propagating direction of the beam. Transverse modes occur in radio waves and microwaves confined in waveguides, in light waves in an optical fibre and in a laser's optical resonator. In this mode there is no electric or magnetic field in the direction of propagation.

TM Transverse Magnetic: transverse mode of an electromagnetic radiation where there is no magnetic field in the direction of propagation.

UWB Ultra Wideband: is a radio technology that emits very low energy levels for short-range high-bandwidth communications spread using a large portion of the radio spectrum. FCC and ITU-R define UWB in terms of a transmission from an antenna for which the emitted signal bandwidth exceeds the lesser of 500 MHz or 20% of the center frequency. Thus, pulse-based systems—wherein each transmitted pulse instantaneously occupies the UWB bandwidth, or an aggregation of at least 500 MHz worth of narrow band carriers, for example in orthogonal frequency-division multiplexing (OFDM) fashion—can gain access to the UWB spectrum under the rules.

VNA Vector Network Analyzer: is an instrument used to analyze the properties of electrical networks, especially those properties associated with the reflection and transmission of electrical signals known as scattering parameters (S-parameters). A VNA measures both amplitude and phase properties of the signal transmitted through the network. They are used mostly at high frequencies but the working band can range from 9 kHz to 110 Ghz.

VSWR Voltage Standing Wave Ratio: is the ratio of the maximum to minimum values of the "standing wave" pattern that is created when signals are reflected on a transmission line. This measurement can be taken using a "slotted line" apparatus that allows the user to measure the field strength in a transmission line at different distances along the line.

WAN Wide Area Network: is a computer network that covers a broad area (i.e. any network whose communications links cross metropolitan, regional, or national boundaries). In contrast with personal area networks (PANs), local area networks (LANs), campus area networks (CANs), or metropolitan area networks (MANs) which are usually limited to a

room, building, campus or specific metropolitan area (e.g., a city) respectively. The largest and most well-known example of a WAN is the Internet.

WiMAX Worldwide Interoperability for Microwave Access: it is a telecommunications technology that provides wireless transmission of data using a variety of transmission modes, from point-to-multipoint links to portable and fully mobile Internet access. The technology provides up to 3 Mbps broadband speed without the need for cables. It is based on the IEEE 802.16 standard (also called Broadband Wireless Access). The name "WiMAX" was created by the WiMAX Forum, which was formed in June 2001 to promote conformity and interoperability of the standard. The forum describes WiMAX as "a standards-based technology enabling the delivery of last mile wireless broadband access as an alternative to cable and DSL".

WUSB Wireless Universal Serial Bus: is a short-range, high-bandwidth wireless radio communication protocol created by the Wireless USB Promoter Group. It is based on the WiMedia Alliance's Ultra-WideBand (UWB) common radio platform, which is capable of sending 480 Mbps at distances up to 3 meters and 110 Mbps at up to 10 meters. It was designed to operate in the 3.1 to 4.7 Ghz frequency range. An upcoming 1.1 specification will increase speed to 1 Gbps and working frequencies up to 6 Ghz.

Bibliography

[1] International Standard. Ecma-368. *ECMA International*, 2008.

[2] D. M. Pozar. Microwave engineering. 3rd ed. *John Wiley & Sons*, 2005.

[3] T. C. Edwards. Foundations for microstrip circuit design. *John Wiley and Sons*, 1981.

[4] P. Bretchko R. Ludwig. Rf circuit design: Theory and applications. *Prentice Hall*, 2000.

[5] P. Bhartia R. Mongia, I. Bahl. Rf and microwave coupled-line circuits. *Artech house*, 1999.

[6] Anuj Batra Roberto Aiello. Ultra-wideband systems. *Newnes*, 2006.

[7] Wisair. Wisair dv9110m dvk manual. 2008.

[8] William S. C. Chang. Rf photonic technology in optical fiber links. *Cambridge University Press*, 2002.

[9] G. Matthaei. Microwave filters, impedance-matching networks, and coupling structures. *Artech House*, 1980.

[10] S. B. Cohn R. Levy. A history of microwave filter research, design, and development. *IEEE Transactions on microwave theory and techniques*, 1984.

[11] R. Collin. Foundations for microwave engineering. *McGraw-Hill*, 1966.

[12] B. J. Minnis. Designing microwave circuits by exact synthesis. *Artech House*, 1996.

[13] M. W. Medley. Microwave and rf circuits: analysis, synthesis and design. *Artech House*, 1993.

[14] S. B. Cohn. Parallel-coupled transmission-line-resonator filters. *IRE Transactions on microwave theory and techniques*, 1957.

[15] B. J. Minnis. Printed circuit coupled-line filters for bandwidths up to and greater than an octave. *IEEE Transactions on microwave theory and techniques*, 1981.

[16] R. A. Zackarevicius E. H. Fooks. Microwave engineering using microstrip circuits. *Prentice Hall*, 1990.

[17] M.J. Lancaster J.S. Hong. Microstrip filters for rf/microwave applications. *John Wiley & Sons.*, 2001.

[18] R. H. Jansen M. Kirschning. Accurate wide-range design equations for the frequency-dependent characteristic of parallel coupled microstrip lines. *IEEE Trans. Microwave Theory Tech., Jan issue*, 1984.

[19] K. C. Gupta. Microstrip lines and slotlines. *Artech House*, 1966.

[20] D. Brady. The design, fabrication and measurement of microstrip filter and coupler circuits. *High Frequency Electronics, July issue*, 2002.

[21] R. Hartley. Base materials for high speed, high frequency pc boards.

[22] Protomat. Lpkf protomat h100 reference manual. 2008.

[23] M. Shaw D. Zelinka. A comparative study of tosl, trl, and trl* network analyzer calibration techniques using microstrip test fixtures. *46th ARFTG Conference Digest-Fall.*, 1995.

[24] Lei Zhu Sheng Sun. Multimode-resonator-based bandpass filters. *IEEE microwave magazine*, pages vol 10, n2, 88–98, 2009.

[25] J. Yu Z. Jia. Wireless high-definition services over optical fiber networks. *Journal of Optical Networking.*, 2009.

[26] B. Molinete J. Hernandez, A. Sierra. Integrated project pulsers phase ii. *Pulsers*, 2008.

[27] T. Kaiser A. Anttonen F. Berens, E. Dimitrov. The pulser ii view towards very high data rate ofdm based uwb systems. *Pulsers*, 2008.

[28] A. Kaszubowska. Broadband access networks using hybrid radio/fiber systems. *Thesis (Ph.D.) Dissertation, Dublin City University*, 2004.

[29] F. Smith. Investigation of performance issues affecting optical circuit and packet switched wdm networks. *Thesis (Ph.D.) Dissertation, Dublin City University*, 2008.

[30] G. P. Agrawal. Fiber-optic communication systems. *Wiley-Interscience*, 2002.

[31] A. Djupsjobacka. A linearization concept for integrated-optic modulators. *IEEE Photonic Technology letters*, 1992.

[32] N. Takachio K. Yonenaga. A fiber chromatic dispersion compensation technique with an optical ssb transmission in optical homodyne detection systems. *IEEE Photonic Technology letters*, 1993.

[33] J.E. Mitchell T. Ismail, C.P. Liu. High-dynamic-range wireless-over-fiber link using feed-forward linearization. *J Lightwave technology*, 2007.

[34] M. Ran Y. Ben-Ezra. Wimedia-defined, ultra-wideband radio transmission over optical fibre. *OFC/NFOEC 2008*, 2008.

[35] S. Norskov U. Gliese. Chromatic dispersion in fiber-0ptic microwave and millimeter-wave links. *IEEE Transactions on Microwave Theory and Techniques*, 1996.

[36] J. Yu J Ma. Fiber dispersion influence on transmission of the optical millimeter-waves generated using ln-mzm intensity modulation. *Journal of Lightwave Technology*, 2007.

[37] A. Nirmalathas C. Lim. Mitigation strategy for transmission impairments in millimeter-wave radio-over-fiber networks. *Journal of Optical Networking*, 2009.

[38] J. F. Ramsay. Rayleigh distance as a normalizing range for beam power transmission. *G-MTT Symposium Digest*, 1965.

[39] W. A. Davis S. Licul. Ultra-wideband (uwb) antenna measurements using vector network analyzer. *IEEE Antennas and Propagation Society International Symposium*, 2004.

[40] A. Kerkhoff. S parameter extraction approach to the reduction of dipole antenna measurements. *Thesis (Ph.D.) Dissertation, University of Texas*, 2008.

[41] V.H.Pham M.L. Yee. Performance evaluation of mb-ofdm ultra-wideband signals over single mode fiber. *IEEE Photonics Journal*, pages 74–77, 2007.

[42] M.L.Yee Y.X. Guo. Performance study of mb-ofdm ultra-wideband signals over multimode fiber. *IEEE Photonics Journal*, pages 29–31, 2007.

[43] Christoph Rauscher. Fundamentals of spectrum analysis. *Rohde Schwarz*, 2001.

Appendix

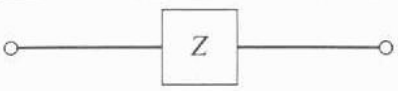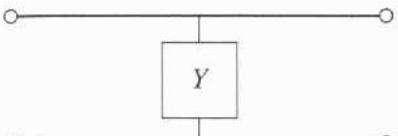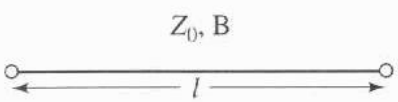## A.- ABCD parameters of some useful two-port networks.
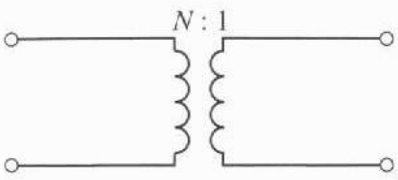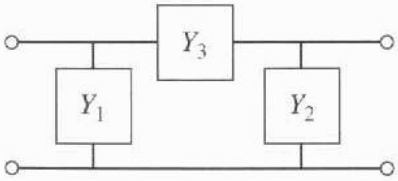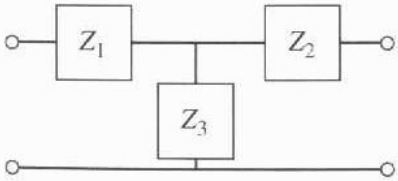
Circuit	*ABCD* Parameters	
Z (series impedance)	$A = 1$ $C = 0$	$B = Z$ $D = 1$
Y (shunt admittance)	$A = 1$ $C = Y$	$B = 0$ $D = 1$
Z_0, B, l (transmission line)	$A = \cos\beta\ell$ $C = jY_0\sin\beta\ell$	$B = jZ_0\sin\beta\ell$ $D = \cos\beta\ell$
$N:1$ (transformer)	$A = N$ $C = 0$	$B = 0$ $D = \dfrac{1}{N}$
Y_3, Y_1, Y_2 (Pi network)	$A = 1 + \dfrac{Y_2}{Y_3}$ $C = Y_1 + Y_2 + \dfrac{Y_1 Y_2}{Y_3}$	$B = \dfrac{1}{Y_3}$ $D = 1 + \dfrac{Y_1}{Y_3}$
Z_1, Z_2, Z_3 (T network)	$A = 1 + \dfrac{Z_1}{Z_3}$ $C = \dfrac{1}{Z_3}$	$B = Z_1 + Z_2 + \dfrac{Z_1 Z_2}{Z_3}$ $D = 1 + \dfrac{Z_2}{Z_3}$

Table 9.1: ABCD parameters of some useful two-port circuits, from [2], Chapter 4.

B.- Two-port networks parameters conversion.

	S	Z	Y	$ABCD$
S_{11}		$\dfrac{(Z_{11}-Z_0)(Z_{22}+Z_0)-Z_{12}Z_{21}}{\Delta Z}$	$\dfrac{(Y_0-Y_{11})(Y_0+Y_{22})+Y_{12}Y_{21}}{\Delta Y}$	$\dfrac{A+B/Z_0-CZ_0-D}{A+B/Z_0+CZ_0+D}$
S_{12}		$\dfrac{2Z_{12}Z_0}{\Delta Z}$	$\dfrac{-2Y_{12}Y_0}{\Delta Y}$	$\dfrac{2(AD-BC)}{A+B/Z_0+CZ_0+D}$
S_{21}		$\dfrac{2Z_{21}Z_0}{\Delta Z}$	$\dfrac{-2Y_{21}Y_0}{\Delta Y}$	$\dfrac{2}{A+B/Z_0+CZ_0+D}$
S_{22}		$\dfrac{(Z_{11}+Z_0)(Z_{22}-Z_0)-Z_{12}Z_{21}}{\Delta Z}$	$\dfrac{(Y_0+Y_{11})(Y_0-Y_{22})+Y_{12}Y_{21}}{\Delta Y}$	$\dfrac{-A+B/Z_0-CZ_0+D}{A+B/Z_0+CZ_0+D}$
Z_{11}	$Z_0\dfrac{(1+S_{11})(1-S_{22})+S_{12}S_{21}}{(1-S_{11})(1-S_{22})-S_{12}S_{21}}$		$\dfrac{Y_{22}}{\|Y\|}$	$\dfrac{A}{C}$
Z_{12}	$Z_0\dfrac{2S_{12}}{(1-S_{11})(1-S_{22})-S_{12}S_{21}}$		$\dfrac{-Y_{12}}{\|Y\|}$	$\dfrac{AD-BC}{C}$
Z_{21}	$Z_0\dfrac{2S_{21}}{(1-S_{11})(1-S_{22})-S_{12}S_{21}}$		$\dfrac{-Y_{21}}{\|Y\|}$	$\dfrac{1}{C}$
Z_{22}	$Z_0\dfrac{(1-S_{11})(1+S_{22})+S_{12}S_{21}}{(1-S_{11})(1-S_{22})-S_{12}S_{21}}$		$\dfrac{Y_{11}}{\|Y\|}$	$\dfrac{D}{C}$
Y_{11}	$Y_0\dfrac{(1-S_{11})(1+S_{22})+S_{12}S_{21}}{(1+S_{11})(1+S_{22})-S_{12}S_{21}}$	$\dfrac{Z_{22}}{\|Z\|}$		$\dfrac{D}{B}$
Y_{12}	$Y_0\dfrac{-2S_{12}}{(1+S_{11})(1+S_{22})-S_{12}S_{21}}$	$\dfrac{-Z_{12}}{\|Z\|}$		$\dfrac{BC-AD}{B}$
Y_{21}	$Y_0\dfrac{-2S_{21}}{(1+S_{11})(1+S_{22})-S_{12}S_{21}}$	$\dfrac{-Z_{21}}{\|Z\|}$		$\dfrac{-1}{B}$
Y_{22}	$Y_0\dfrac{(1+S_{11})(1-S_{22})+S_{12}S_{21}}{(1+S_{11})(1+S_{22})-S_{12}S_{21}}$	$\dfrac{Z_{11}}{\|Z\|}$		$\dfrac{A}{B}$
A	$\dfrac{(1+S_{11})(1-S_{22})+S_{12}S_{21}}{2S_{21}}$	$\dfrac{Z_{11}}{Z_{21}}$	$\dfrac{-Y_{22}}{Y_{21}}$	
B	$Z_0\dfrac{(1+S_{11})(1+S_{22})-S_{12}S_{21}}{2S_{21}}$	$\dfrac{\|Z\|}{Z_{21}}$	$\dfrac{-1}{Y_{21}}$	
C	$\dfrac{1}{Z_0}\dfrac{(1-S_{11})(1-S_{22})-S_{12}S_{21}}{2S_{21}}$	$\dfrac{1}{Z_{21}}$	$\dfrac{-\|Y\|}{Y_{21}}$	
D	$\dfrac{(1-S_{11})(1+S_{22})+S_{12}S_{21}}{2S_{21}}$	$\dfrac{Z_{22}}{Z_{21}}$	$\dfrac{-Y_{11}}{Y_{21}}$	

$|Z| = Z_{11}Z_{22} - Z_{12}Z_{21};$ $\quad |Y| = Y_{11}Y_{22} - Y_{12}Y_{21};$ $\quad \Delta Y = (Y_{11} + Y_0)(Y_{22} + Y_0) - Y_{12}Y_{21};$ $\quad \Delta Z = (Z_{11} + Z_0)(Z_{22} + Z_0) - Z_{12}Z_{21};$ $\quad Y_0 = 1/Z_0.$

Table 9.2: Conversions between two-port network parameters, from [2], Chapter 4.

C.- Element values for different types of filter prototypes.

| Value of n	g_1	g_2	g_3	g_4	g_5	g_6	g_7	g_8	g_9	g_{10}	g_{11}
					0.01-db ripple						
1	0.0960	1.0000									
2	0.4488	0.4077	1.1007								
3	0.6291	0.9702	0.6291	1.0000							
4	0.7128	1.2003	1.3212	0.6476	1.1007						
5	0.7563	1.3049	1.5773	1.3049	0.7563	1.0000					
6	0.7813	1.3600	1.6896	1.5350	1.4970	0.7098	1.1007				
7	0.7969	1.3924	1.7481	1.6331	1.7481	1.3924	0.7969	1.0000			
8	0.8072	1.4130	1.7824	1.6833	1.8529	1.6193	1.5554	0.7333	1.1007		
9	0.8144	1.4270	1.8043	1.7125	1.9057	1.7125	1.8043	1.4270	0.8144	1.0000	
10	0.8196	1.4369	1.8192	1.7311	1.9362	1.7590	1.9055	1.6527	1.5817	0.7446	1.1007
					0.1-dB ripple						
1	0.3052	1.0000									
2	0.8430	0.6220	1.3554								
3	1.0315	1.1474	1.0315	1.0000							
4	1.1088	1.3061	1.7703	0.8180	1.3554						
5	1.1468	1.3712	1.9750	1.3712	1.1468	1.0000					
6	1.1681	1.4039	2.0562	1.5170	1.9029	0.8618	1.3554				
7	1.1811	1.4228	2.0966	1.5733	2.0966	1.4228	1.1811	1.0000			
8	1.1897	1.4346	2.1199	1.6010	2.1699	1.5640	1.9444	0.8778	1.3554		
9	1.1956	1.4425	2.1345	1.6167	2.2053	1.6167	2.1345	1.4425	1.1956	1.0000	
10	1.1999	1.4481	2.1444	1.6265	2.2253	1.6418	2.2046	1.5821	1.9628	0.8853	1.3554
					0.2-dB ripple						
1	0.4342	1.0000									
2	1.0378	0.6745	1.5386								
3	1.2275	1.1525	1.2275	1.0000							
4	1.3028	1.2844	1.9761	0.8468	1.5386						
5	1.3394	1.3370	2.1660	1.3370	1.3394	1.0000					
6	1.3598	1.3632	2.2394	1.4555	2.0974	0.8838	1.5386				
7	1.3722	1.3781	2.2756	1.5001	2.2756	1.3781	1.3722	1.0000			
8	1.3804	1.3875	2.2963	1.5217	2.3413	1.4925	2.1349	0.8972	1.5386		
9	1.3860	1.3938	2.3093	1.5340	2.3728	1.5340	2.3093	1.3938	1.3860	1.0000	
0	1.3901	1.3983	2.3181	1.5417	2.3904	1.5536	2.3720	1.5066	2.1514	0.9034	1.5386
					0.5-dB ripple						
1	0.6986	1.0000									
2	1.4029	0.7071	1.9841								
3	1.5963	1.0967	1.5963	1.0000							
4	1.6703	1.1926	2.3661	0.8419	1.9841						
5	1.7058	1.2296	2.5408	1.2296	1.7058	1.0000					
6	1.7254	1.2479	2.6064	1.3137	2.4758	0.8696	1.9841				
7	1.7372	1.2583	2.6381	1.3444	2.6381	1.2583	1.7372	1.0000			
8	1.7451	1.2647	2.6564	1.3590	2.6964	1.3389	2.5093	0.8796	1.9841		
9	1.7504	1.2690	2.6678	1.3673	2.7239	1.3673	2.6678	1.2690	1.7504	1.0000	
10	1.7543	1.2721	2.6754	1.3725	2.7392	1.3806	2.7231	1.3485	2.5239	0.8842	1.9841

Table 9.3: Elements values for a Chebyshev filter with $g_0 = 1, w_1 = 1$ and n=1 to 10, from [5], Chapter 9.

Value of n	g_1	g_2	g_3	g_4	g_5	g_6	g_7	g_8	g_9	g_{10}	g_{11}
1	2.000	1.000									
2	1.414	1.414	1.000								
3	1.000	2.000	1.000	1.000							
4	0.7654	1.848	1.848	0.7654	1.000						
5	0.6180	1.618	2.000	1.618	0.618	1.000					
6	0.5176	1.414	1.932	1.932	1.414	0.5176	1.000				
7	0.4450	1.247	1.802	2.000	1.802	1.247	0.445	1.000			
8	0.3902	1.111	1.663	1.962	1.962	1.663	1.111	0.3902	1.000		
9	0.3473	1.000	1.532	1.879	2.000	1.879	1.532	1.000	0.3473	1.000	
10	0.3129	0.908	1.414	1.782	1.975	1.975	1.782	1.414	0.908	0.3129	1.000

Table 9.4: Elements values for a Butterworth filter with $g_0 = 1, w_1 = 1$ and n=1 to 10, from [5], Chapter 9.

CHAPTER 9. APPENDIX

D.- Attenuation versus normalized frequency for different types of filter prototypes.
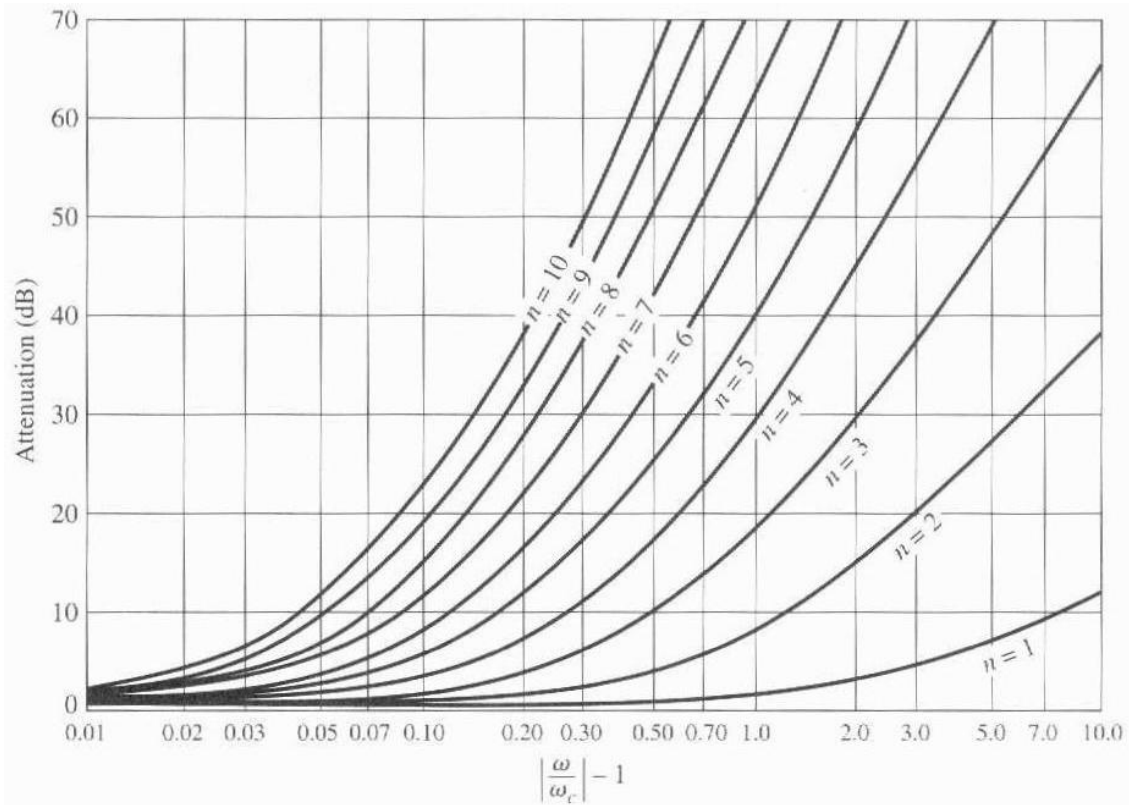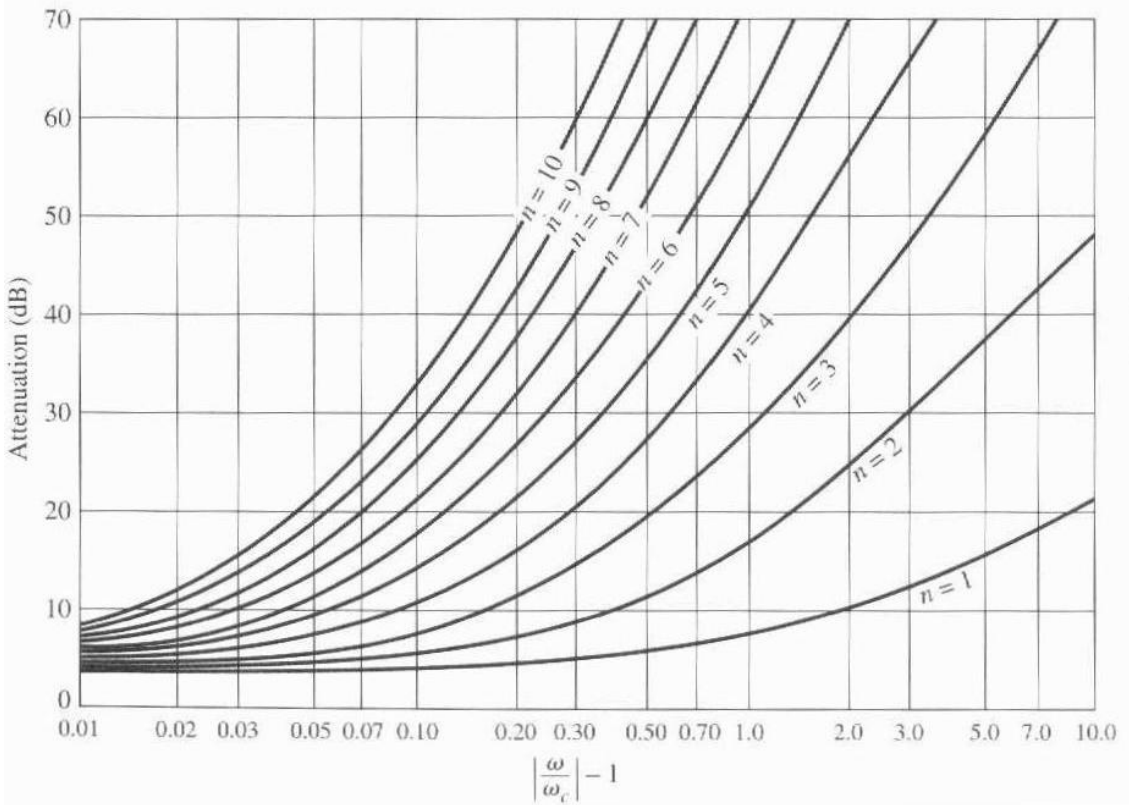

Table 9.5: Attenuation versus normalized frequency for equal-ripple filter prototypes for a) 0.5dB ripple level and b) 3.0dB ripple level, from [9], Chapter 6.
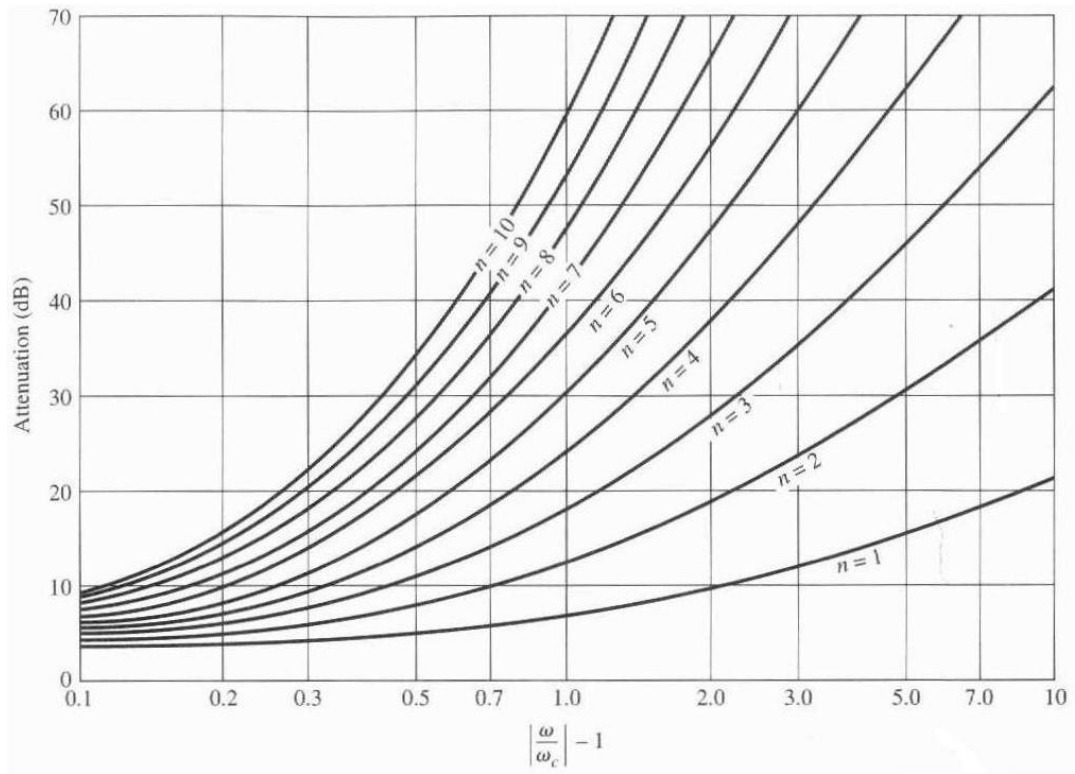
Table 9.6: Attenuation versus normalized frequency for maximally flat filter prototypes, from [9], Chapter 6.

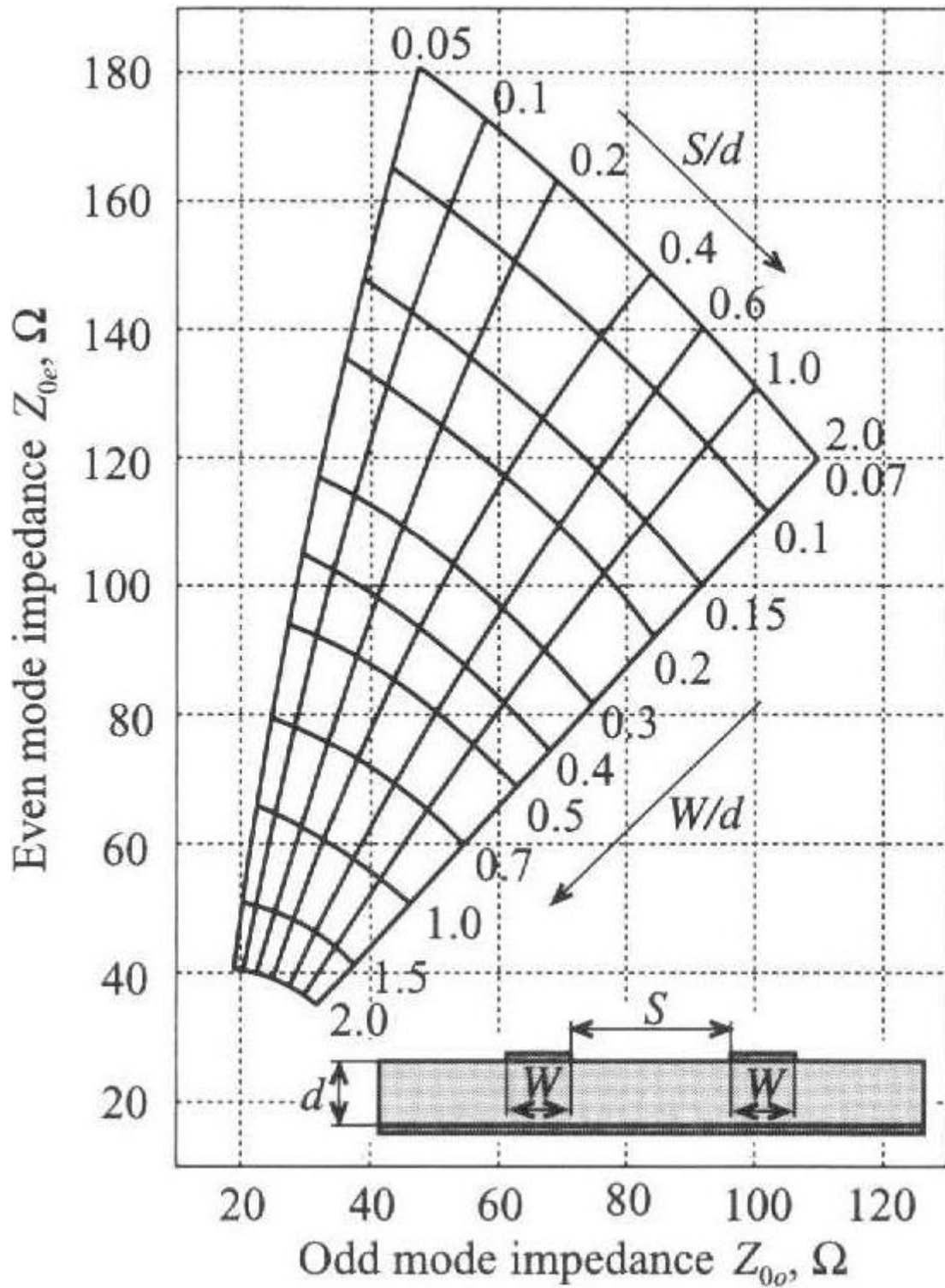## E.- Even and odd mode characteristic impedance design data for coupled microstrip lines.

Table 9.7: Even and odd mode characteristic impedances, from [4], Chapter 6.
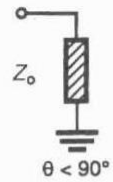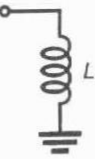
F.- Equivalent RLC networks.
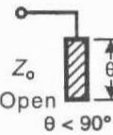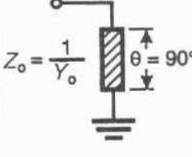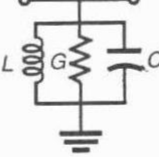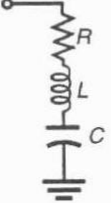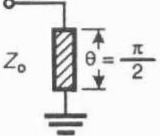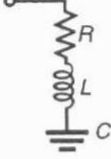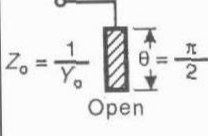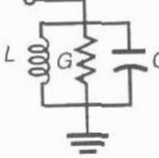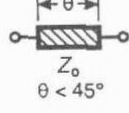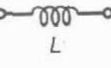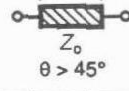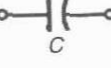
Tx Line Configuration	Equivalent Circuit	Element Values
Z_0, $\theta < 90°$	L	$\omega L = Z_0 \tan\theta$
Z_0 Open, $\theta < 90°$	C	$\omega C = \dfrac{1}{Z_0 \cot\theta}$
$Z_0 = \dfrac{1}{Y_0}$, $\theta = 90°$	L G C	$\omega C = \dfrac{\pi}{4}Y_0$ $\omega L = \dfrac{4Z_0}{\pi}$ $G = Y_0\alpha\theta$ $Q = \dfrac{\omega C}{G} = \dfrac{\pi}{4\alpha\theta}$
$Z_0 = \dfrac{1}{Y_0}$, $\theta = 90°$ Open	R L C	$R = Z_0\alpha\theta$ $\omega L = \dfrac{\pi}{4}Z_0$ $\omega C = \dfrac{4}{\pi Z_0}$ $Q = \dfrac{\omega L}{R} = \dfrac{\pi}{4\alpha\theta}$
Z_0, $\theta = \dfrac{\pi}{2}$	R L C	$\omega L = \dfrac{\pi Z_0}{2}$ $\omega C = \dfrac{2}{\pi Z_0}$ $R = Z_0\alpha\theta$ $Q = \dfrac{\pi}{2\alpha\theta}$
$Z_0 = \dfrac{1}{Y_0}$, $\theta = \dfrac{\pi}{2}$ Open	L G C	$\omega_0 C = \dfrac{\pi}{2}Y_0$ $\omega_0 L = \dfrac{2}{\pi Y_0}$ $R = Y_0\alpha\theta$ $Q = \dfrac{\pi}{2\alpha\theta}$
Z_0, $\theta < 45°$	L	$\omega L = Z_0 \sin\theta$
Z_0, $\theta > 45°$	C	$\omega C = \dfrac{\sin\theta}{Z_0}$

Table 9.8: Equivalent RLC networks for different transmission line lengths, from [5], Chapter 9.

G.- Matlab code to generate Z_{0e} and Z_{0o} for each coupled line section.

Algorithm 9.1 Script to generate intermediate results for the design of the coupled-line filter sections from the 3dB frequencies and coefficients of the filter.

```
%—-Script to obtain ZoJi, Z0o and Z0e—-

ZoJi=[];
Z0o=[];
Z0e=[];

Wu =10.6 %Ghz passband upper freq
Wl =3.1 %Ghz passband lower freq

%N is needed, order of the filter
N=5

%G=[G0,G1,G2... Gn] needed, coefficients filter
%G=[1 1.5963 1.0967 1.5963 1] %Chebyshev 0.5db ripples N=3
%G=[1 3.3487 0.7117 3.3487 1] %Chebyshev 3db ripples N=3
G=[1 3.4817 0.7618 4.5381 0.7618 3.4817 1] %Chebyshev 3db ripples N=5

%Impedances at beginning and end of filter structure
Zout = 50 %Ohm
Zin = 50 %Ohm

%Central frequeency and fractional bandwidth
Wo = (Wu + Wl)/2
BW = (Wu-Wl)/Wo

%J(i)=J(i-1)(i)
for i=1:N+1
    if i==1
    ZoJi(i)=( pi*BW / (2*G(i)*G(i+1)) )^(1/2);
    elseif ((i>1)&(i<N+1))
    ZoJi(i)= pi*BW /(2*(G(i)*G(i+1))^(1/2));
    else
    ZoJi(i)=( pi*BW / (2*G(i)*G(i+1)) )^(1/2);
    end
end
ZoJi

%Z0o(i)=Z0o(i-1)(i)
for i=1:N+1
    Z0o(i)=Zout*(1-ZoJi(i)+(ZoJi(i))^2);
end
Z0o

%Z0e(i)=Z0e(i-1)(i)
for i=1:N+1
    Z0e(i)=Zin*(1+ZoJi(i)+(ZoJi(i))^2);
end
Z0e
```

H.- Published paper in CIICT 09 conference.

Investigation of Dispersive Fading in UWB Over Fiber Systems.

A. Castillo, P. Perry, P. Anandarajah and L.P. Barry

RINCE, Dublin City University, Dublin, Ireland. Antonio.Castillo@eeng.dcu.ie

Abstract

We present an analysis of the response and performance of an optical system for high bit-rate and long-distance RF signal transmission combining the technologies UWB (Ultra-WideBand) and ROF (Radio Over Fibre). We analyse the frequency response of the system and measure the PER obtained at the receiver. This way, we examine the relationship between the main system parameters such as bias current of the laser, frequency response and length of fiber used. We compare the results for two different lasers, obtaining a consistent relationship for a low bandwidth laser, but a more complicated, and inconsistent behaviour in the case that a higher bandwidth laser is used.
.

I. Introduction

Radio Over Fibre (ROF) is a technology that offers the possibility of transmitting RF signals, in a transparent way, over an optical fibre distribution system. It works for long distances with low latency and attenuation, but with a frequency response that is affected by dispersive fading and nonlinear effects in the laser and fiber.

Ultra Wide Band (UWB) technology, since its regulation by FCC in February 2002, has been developed as a commercially attractive method to implement high speed wireless transmission in different end-user technologies with low power consumption. To achieve this, it uses Multi-Band Orthogonal Frequency Division Multiplexing (MB-OFDM) in 528Mhz sub-bands, with 128 sub-carriers each. It achieves maximum speeds between 320Mbps and 480Mbps, and it is expected that it reaches 1Gbps in the near future with new draft specifications.

In this investigation we use the WiSair 9110 Developers Kit which generates an UWB signal in band group 1, from 3.1 to 4.7Ghz, using three sub-bands. The board directly modulates a laser connected through single mode fibre to a photodetector, which in turn feeds the receiver on the peer WiSair board. This system therefore offers a low cost way to extend the reach of UWB systems, only needing an opto-electrical conversion in the receiver ends to be able to radiate the converted signal through UWB antennas using simple transceivers.
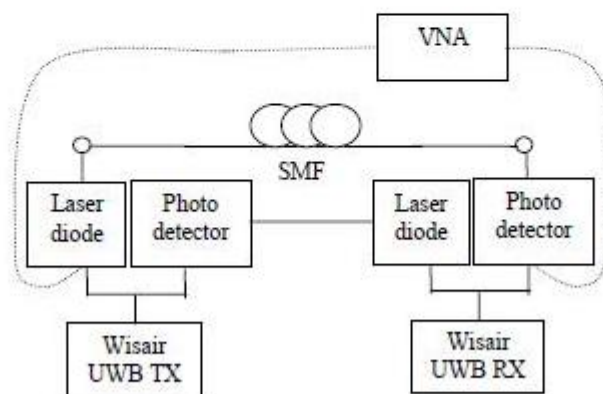

Fig. 1: System setup for dispersive fading test.

CHAPTER 9. APPENDIX

In the system, the RF signal is directly modulated onto the optical carrier as a double sideband (where both sidebands are separated by twice the RF carrier frequency), although different methods could be used to improve these results.

Due to fibre dispersion, these sidebands propagate at different speeds, so that the received RF signal experiences fading behaviour [1]. This causes signal strength reduction and inter-symbol interference resulting in errored bits that can often be corrected by Forward Error Correction (FEC). Although, if the level of FEC is not sufficient to overcome the channel degradation, then packet errors will result.

In this paper, we evaluate the frequency dispersion behaviour of the ROF system and compare this with the application layer level performance. Measuring the Packet Error Rate (PER) obtained in the receiver for two different lasers.

We show the relationship between parameters and the importance of adjusting them depending on the optical power, RF power and the length of fiber used in the transmission, given that the frequency response we will obtain from the system depends on them.

II. Dispersive fading

To analyze dispersive fading and the impact it causes on the overall frequency response, a Vector Network Analyzer (VNA) was connected to both the laser and photo-detector at the ends of the optical transmission system, as shown by the dotted lines in figure 1. The frequency response obtained typically shows a transmission notch [3] that at first appears at a higher frequency than the operating band. The measurements done show that increasing transmission length will make it shift down in frequency and interfere with the RF signal. This is a dispersive fading effect which will cause degradation and should be addressed [6].

Thus, the frequency response was measured for different lengths of fiber and laser bias currents using two different lasers. Figure 2 illustrates the frequency response of a commercially available single mode laser used in the RoF system with 37km of Single Mode Fibre (SMF). The laser was a temperature controlled hermetically sealed high-speed butterfly package, with a bandwidth of about 16GHz at a bias current of 30mA. It has a room temperature emission wavelength of 1545nm and a threshold current of 10mA. Tests show that the non linearities in the laser become more pronounced for lower
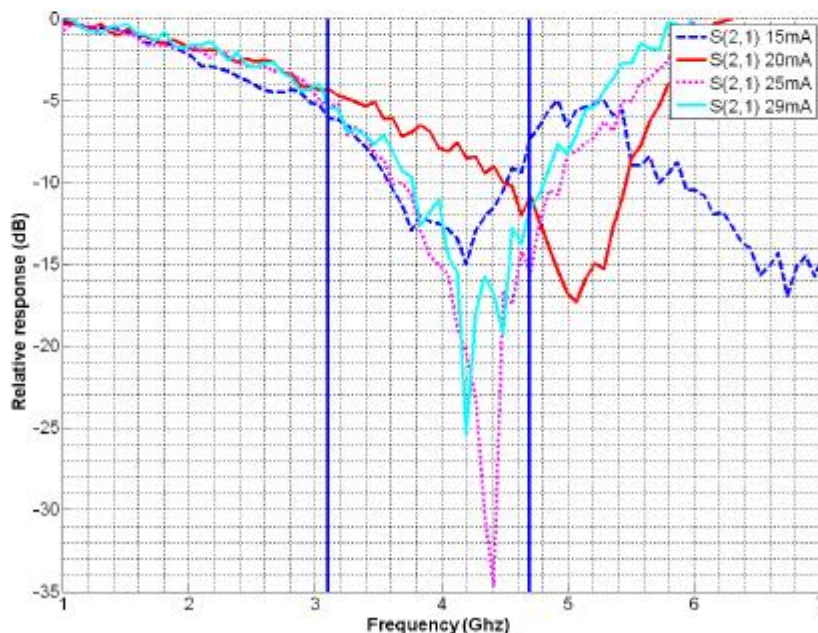

Fig. 2: High bandwidth laser frequency response of the system for a 37km fiber transmission length and different bias currents applied.

bias points and cause the dispersive fading notch to appear at unpredictable frequencies and vary in depth. This is due to the presence of harmonics of the modulating RF signal as multiple sidebands on the optical carrier. It makes the behaviour very complex and system performance difficult to predict, as can be noticed in the graph, where a difference of some milliamps in bias current can make the notch change from a 5dB to a 30dB depth and shift in frequency position. These results show that further investigation would be needed to understand these effects and obtain an adequate response and integrate this type of laser in an UWB ROF system.

The solution chosen to overcome this unpredictable behaviour was the use of a lower bandwidth laser so that higher order harmonics could not be generated. This way, the negative effects affecting our system response would be avoided. As expected in this case, the dispersive fading notches appeared at the expected frequencies and did not shift with changing laser diode bias current, making the system behaviour much more stable and easy to study.

Figure 3, shows the frequency response of this commercially available single mode laser in a hermetically sealed TO-can. It has an emission wavelength of 1540nm and a threshold current of 14mA. Results indicate that the laser has an inherent resonance around 2GHz in its back to back performance due to packaging parasitics, but has reasonably flat response at the Band Group 3 frequencies that we will use. The dispersive fading behaviour is also clearly shown here as the notch appears at 7GHz for 14km, 4.5GHz at 37km and 3.8GHz at 51km. These curves are not bias dependent, which indicates a high degree of linearity in the system. Using this laser, it will be easier to predict system performance and tune parameters to obtain the better possible PER, as opposed to the system behaviour for the high bandwidth laser.

Both results shown in figure 2 and 3 have the working band of our system, between 3.1 and 4.7 GHz, highlighted.

III. Packet error rate (PER)

To characterize the achievable PER, a bidirectional system was set up, because of the requirement of the Wisair boards to see each other to establish transmission, as indicated by the solid lines in figure 1. As shown there, the uplink optical connection was done back to back, instead of over the fiber reel, to avoid using multiple optical amplifiers and to isolate the performance of a single transmitting path. The transmission parameters changed for the tests were the bias current of the laser, the fiber length and the bitrate of the transmission, using most
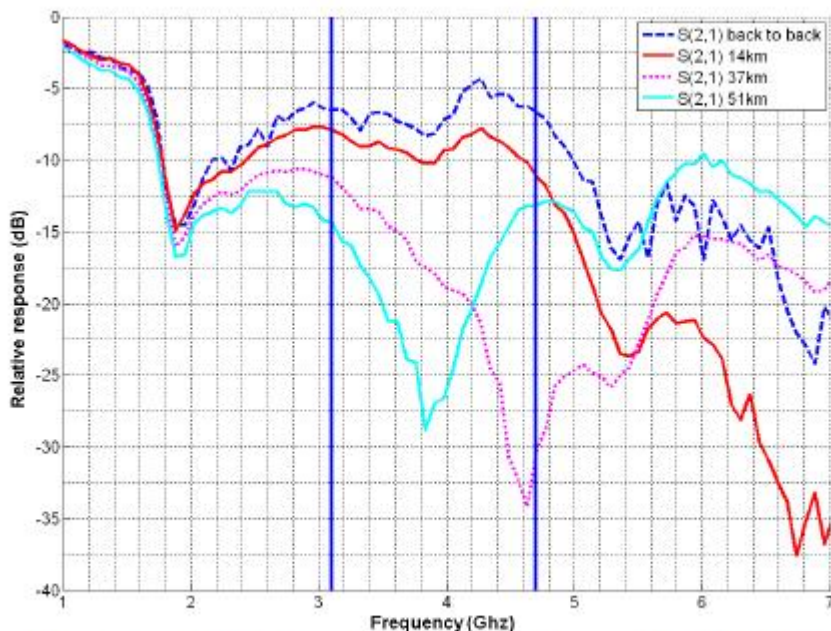
Fig. 3: Low bandwidth laser frequency response of the system for different fiber transmission lengths and a 25mA bias current applied.

of the different speeds UWB standard supports: 53.3Mbps, 80Mbps, 160Mbps, 320Mbps and 480Mbps. PER was measured from the receiver Wisair board application software for the different scenarios [2], [5].

The PER graphs for the high bandwidth laser are shown in figure 4 and indicate rather peculiar behaviour which seems to be a result of the complex interaction of the laser nonlinearities and the fibre dispersion, so that the effective channel the Wisair Radio is experiencing is unpredictable. However, the results in figure 5 showing the performance for the low bandwidth laser correlate well

Fig. 4: High bandwidth laser 10% PER points for different transmission bitrates and fiber lengths with: a) 15mA, b) 20mA and c) 25mA bias currents applied to the laser.

with the frequency response graphs seen before in figure 3. It can be seen from these graphs that transmission cannot be established for distances greater than 14km for the 480Mbps case as this scheme uses no FEC. By contrast, reduced bit rates use higher levels of FEC and are capable of overcoming the channel degradations caused by dispersive fading.

Moreover, for the low bandwidth laser, Dispersion Compensating Fiber (DCF) could be used to improve PER

and obtain at 37km a similar performance to the one at 12km. By contrast using DCF did not improve system performance when using the higher bandwidth laser. This is explained by the fact that the main phenomenon affecting performance for the low bandwidth laser is dispersion. But additional effects occur in the system for the higher bandwidth laser, keeping the performance low.

It is also interesting to note that the received optical power to achieve 10% PER needs to be approximately
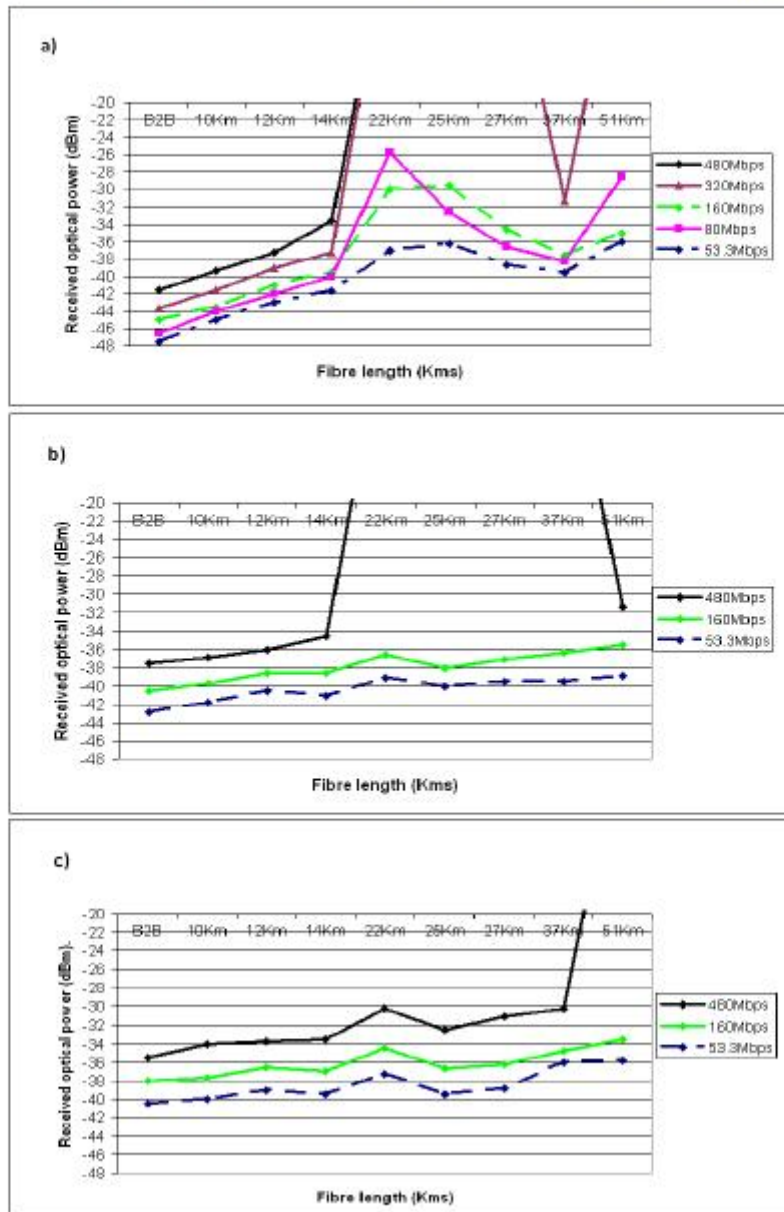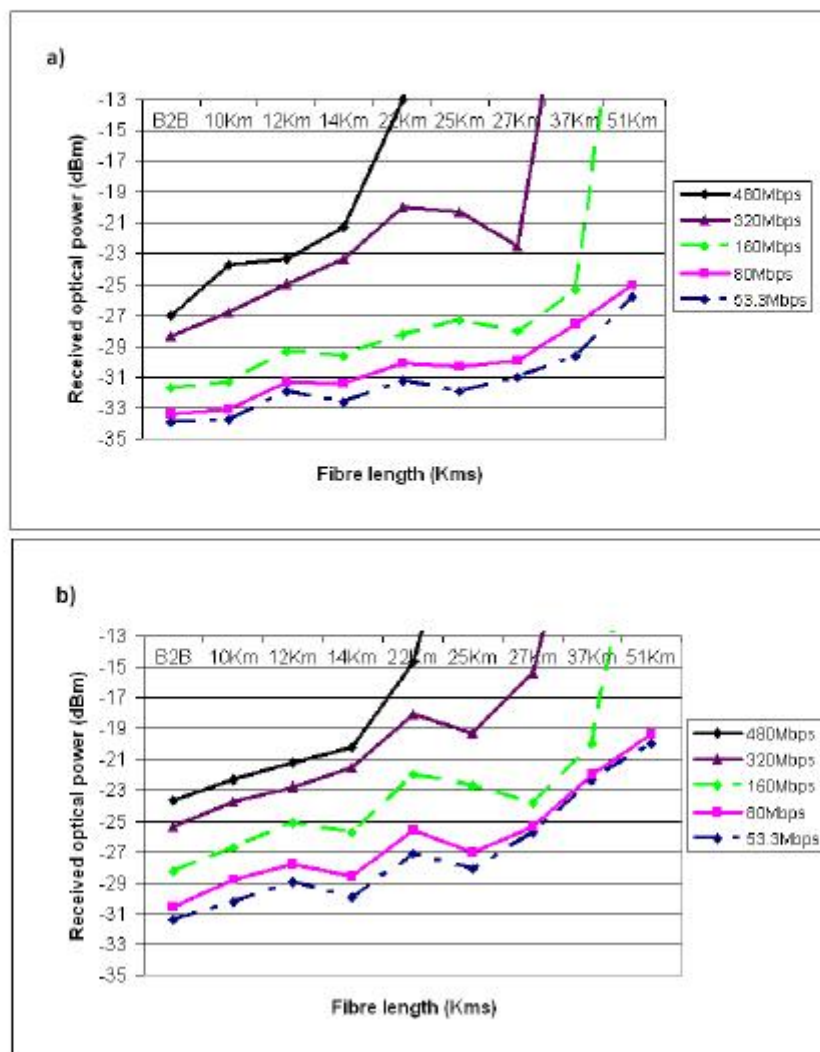

Fig. 5: Low bandwidth laser 10% PER points for different transmission bitrates and fiber lengths with: a) 20mA and b) 25mA bias currents applied to the laser.

3dB higher for the laser biased at 25mA than that at 20mA for a given distance. This is due to the reduction in modulation depth and the associated increase in carrier power when bias current is increased.

IV. Conclusions

In this paper we have shown that the simple dispersive fading model is insufficient for explaining the behaviour of UWBoF systems when the directly modulated lasers have a high bandwidth. By contrast, a low cost laser with restricted bandwidth offers improved system performance that is predictable and could be integrated in commercial systems.

Furthermore, the increased receiver sensitivity that can be gained by using a low bias current will give benefits for short lengths of fibre, needing less power to obtain similar error rates.

To summarize, it is shown that these systems have a clear practical application and could be used to distribute UWB signals with many advantages over other approaches. It could be done using optical fiber for a long distance with low attenuation and with a good frequency behaviour, taking into account the relationship between the different parameters involved and studied in this paper.

Acknowledgements

References

1. S. Yaakobl, W. R. Wan Abdullahl, *Effect of Laser Bias Current to the Third Order Intermodulation in the Radio over Fibre System*, International RF and Microwave Conference Proceedings (2006)

2. M.L. Yee, V.H. Pham, *Performance Evaluation of MB-OFDM Ultra-Wideband Signals over Single mode Fiber*, IEEE International Conference on Ultra-Wideband ICUWB (2007)

3. F. Ramos, J. Marti, *Frequency Transfer Function of Dispersive and Nonlinear Single-Mode Optical Fibers in Microwave Optical Systems*, IEEE Photonics Technology Letters (2000)

4. T. Alves, A. Cartaxo, *Performance Degradation Due to OFDM-UWB Radio Signal Transmission Along Dispersive Single-Mode Fiber*, IEEE Photonics Technology Letters (2009)

5. A. Pizzinat, P. Urvoas, *1.92Gbit/s MB-OFDM Ultra Wide Band Radio Transmission over Low Bandwidth Multimode Fiber*, OFC/NFOEC (2007)

6. Y. Ben-Ezra, M. Ran, *Wimedia-Defined, Ultra-Wideband Radio Transmission over Optical Fibre*, OFC/NFOEC (2008)

7. A.J.Lowery, *Fiber nonlinearity pre- and post-compensation for long-haul optical links using OFDM, vol 15, no 20*, Optics Express (2007)

CIICT 2009

China-Ireland International Conference on Information and Communications Technologies
19th - 21st August 2009
Maynooth, Ireland

NUI MAYNOOTH
Ollscoil na hÉireann Má Nuad

Overview · ← Submissions   English · Chinese   **User:** castiyo

Contribution Details

Conference Track / Type of Submission: **Full Paper**
Investigation of Dispersive Fading in UWB Over Fiber Systems.   **144**

Castillo Leon, Antonio; Perry, Philip; Anandarajah, Prince; Barry, Liam
Organization(s): DCU, Ireland (Republic of)
Submitted by: Antonio Castillo Leon (DCU)
Presenting Author: Castillo Leon, Antonio (antonio.castilloleon2@mail.dcu.ie)
Short CV of presenting author:
Student in the last year of his Telecommunication Engineering degree at Autonoma de Madrid University in Spain. At present time researching on UWB ROF systems in Dublin City University, at RINCE optics laboratory.
Topics: Communications and Networks 8, Optics and Optoelectronics 12
Keywords: Ultra-Wideband, UWB, ROF, fading

Review Result of the Program Committee

Congratulations! This contribution has been accepted.

Overview of Reviews

Questions		**Review 1**	**Review 2**
Familiarity of the reviewer with the topic		6	4
Content	10%	8	8
Significance	10%	8	6
Originality	10%	8	6
Relevance	10%	8	10
Presentation	10%	10	6
Recommendation	50%	10	8
Total points (out of 100)		92	76

Review 1

Evaluation of the contribution

Content	Significance	Originality	Relevance	Presentation	Recommendation	Total points (out of 100)
8 (10%)	8 (10%)	8 (10%)	8 (10%)	10 (10%)	10 (50%)	92

Reviewer's comments on the contribution

Contribution of the submission:
This paper presents an analysis of the response and performance of an optical system for high bit-rate and long-distance RF signaltransmission combining the technologies UWB(Ultra-WideBand) and ROF (Radio Over Fibre).

Comments for the authors:
This paper makes a good analysis the frequency dispersion behaviour of the ROF system andcompares this with the application layer level performance. I think the work is solid and significant.

Review 2

Evaluation of the contribution

Content	Significance	Originality	Relevance	Presentation	Recommendation	Total points (out of 100)
8 (10%)	6 (10%)	6 (10%)	10 (10%)	6 (10%)	8 (50%)	76

Reviewer's comments on the contribution

Contribution of the submission:
This paper describes experimental results for optical coupling and transmission of UWB over fibre.

Comments for the authors:
This paper gives a good presentation of the topic and experimental data but more significantly demonstrates an ability to draw broader conclusions from the experimental work undertaken.

> **index** > reviewResults   Print View

Presupuesto

1) **Ejecución Material**

- Compra de ordenador personal (Software incluido)

  8.000 €

- Compra de impresora láser

  400 €

- Material de oficina

  200 €

- Material de fabricación

  500 €

- Alquiler maquinaria para la fabricación

  1.000 €

- Herramientas para el montaje

  100 €

- Analizador vectorial de redes

  30.000€

- Kit de calibración

  3.400 €

- **Total de ejecución material**

  43.600 €

2) **Gastos generales**

- **16 % sobre ejecución material**

  6.976 €

3) **Beneficio Industrial**

- **6 % sobre ejecución material**

  2.616 €

4) **Honorarios Proyecto**

- **1200 horas a 15 €/ hora**

  18.000 €

5) **Material fungible**

- Gastos de impresión

    280 €

- Encuadernación

    200 €

- **Total de material fungible**

    480 €

6) **Subtotal del presupuesto**

- **Subtotal Presupuesto**

    71.672 €

7) **I.V.A. aplicable**

- **16 % Subtotal Presupuesto**

    11.467,52 €

8) **Total presupuesto**

- **Total Presupuesto**

    82.139,52 €

Madrid, Noviembre 2009

El Ingeniero Jefe de Proyecto

Fdo.: Antonio Castillo León

Ingeniero Superior de Telecomunicación

Pliego de condiciones

Pliego de condiciones

Este documento contiene las condiciones legales que guiarán la realización, en este proyecto, titulado *"Design of ultra-wideband filters for a wireless broadband communications system."*. En lo que sigue, se supondrá que el proyecto ha sido encargado por una empresa cliente a una empresa consultora con la finalidad de realizar dicho sistema. Dicha empresa ha debido desarrollar una línea de investigación con objeto de elaborar el proyecto. Esta línea de investigación, junto con el posterior desarrollo de los programas está amparada por las condiciones particulares del siguiente pliego.

Supuesto que la utilización industrial de los métodos recogidos en el presente proyecto ha sido decidida por parte de la empresa cliente o de otras, la obra a realizar se regulará por las siguientes:

Condiciones generales.

1. La modalidad de contratación será el concurso. La adjudicación se hará, por tanto, a la proposición más favorable sin atender exclusivamente al valor económico, dependiendo de las mayores garantías ofrecidas. La empresa que somete el proyecto a concurso se reserva el derecho a declararlo desierto.

2. El montaje y mecanización completa de los equipos que intervengan será realizado totalmente por la empresa licitadora.

3. En la oferta, se hará constar el precio total por el que se compromete a realizar la obra y el tanto por ciento de baja que supone este precio en relación con un importe límite si este se hubiera fijado.

4. La obra se realizará bajo la dirección técnica de un Ingeniero Superior de Telecomunicación, auxiliado por el número de Ingenieros Técnicos y Programadores que se estime preciso para el desarrollo de la misma.

5. Aparte del Ingeniero Director, el contratista tendrá derecho a contratar al resto del personal, pudiendo ceder esta prerrogativa a favor del Ingeniero Director, quien no estará obligado a aceptarla.

6. El contratista tiene derecho a sacar copias a su costa de los planos, pliego de condiciones y presupuestos. El Ingeniero autor del proyecto autorizará con su firma las copias solicitadas

por el contratista después de confrontarlas.

7. Se abonará al contratista la obra que realmente ejecute con sujeción al proyecto que sirvió de base para la contratación, a las modificaciones autorizadas por la superioridad o a las órdenes que con arreglo a sus facultades le hayan comunicado por escrito al Ingeniero Director de obras siempre que dicha obra se haya ajustado a los preceptos de los pliegos de condiciones, con arreglo a los cuales, se harán las modificaciones y la valoración de las diversas unidades sin que el importe total pueda exceder de los presupuestos aprobados. Por consiguiente, el número de unidades que se consignan en el proyecto o en el presupuesto, no podrá servirle de fundamento para entablar reclamaciones de ninguna clase, salvo en los casos de rescisión.

8. Tanto en las certificaciones de obras como en la liquidación final, se abonarán los trabajos realizados por el contratista a los precios de ejecución material que figuran en el presupuesto para cada unidad de la obra.

9. Si excepcionalmente se hubiera ejecutado algún trabajo que no se ajustase a las condiciones de la contrata pero que sin embargo es admisible a juicio del Ingeniero Director de obras, se dará conocimiento a la Dirección, proponiendo a la vez la rebaja de precios que el Ingeniero estime justa y si la Dirección resolviera aceptar la obra, quedará el contratista obligado a conformarse con la rebaja acordada.

10. Cuando se juzgue necesario emplear materiales o ejecutar obras que no figuren en el presupuesto de la contrata, se evaluará su importe a los precios asignados a otras obras o materiales análogos si los hubiere y cuando no, se discutirán entre el Ingeniero Director y el contratista, sometiéndolos a la aprobación de la Dirección. Los nuevos precios convenidos por uno u otro procedimiento, se sujetarán siempre al establecido en el punto anterior.

11. Cuando el contratista, con autorización del Ingeniero Director de obras, emplee materiales de calidad más elevada o de mayores dimensiones de lo estipulado en el proyecto, o sustituya una clase de fabricación por otra que tenga asignado mayor precio o ejecute con mayores dimensiones cualquier otra parte de las obras, o en general, introduzca en ellas cualquier modificación que sea beneficiosa a juicio del Ingeniero Director de obras, no tendrá derecho sin embargo, sino a lo que le correspondería si hubiera realizado la obra con estricta sujeción a lo proyectado y contratado.

12. Las cantidades calculadas para obras accesorias, aunque figuren por partida alzada en el presupuesto final (general), no serán abonadas sino a los precios de la contrata, según las condiciones de la misma y los proyectos particulares que para ellas se formen, o en su defecto, por lo que resulte de su medición final.

13. El contratista queda obligado a abonar al Ingeniero autor del proyecto y director de obras así como a los Ingenieros Técnicos, el importe de sus respectivos honorarios facultativos por formación del proyecto, dirección técnica y administración en su caso, con arreglo a las tarifas y honorarios vigentes.

14. Concluida la ejecución de la obra, será reconocida por el Ingeniero Director que a tal efecto designe la empresa.

15. La garantía definitiva será del 4 % del presupuesto y la provisional del 2 %.

16. La forma de pago será por certificaciones mensuales de la obra ejecutada, de acuerdo con los precios del presupuesto, deducida la baja si la hubiera.

17. La fecha de comienzo de las obras será a partir de los 15 días naturales del replanteo oficial de las mismas y la definitiva, al año de haber ejecutado la provisional, procediéndose si no existe reclamación alguna, a la reclamación de la fianza.

18. Si el contratista al efectuar el replanteo, observase algún error en el proyecto, deberá comunicarlo en el plazo de quince días al Ingeniero Director de obras, pues transcurrido ese plazo será responsable de la exactitud del proyecto.

19. El contratista está obligado a designar una persona responsable que se entenderá con el Ingeniero Director de obras, o con el delegado que éste designe, para todo relacionado con ella. Al ser el Ingeniero Director de obras el que interpreta el proyecto, el contratista deberá consultarle cualquier duda que surja en su realización.

20. Durante la realización de la obra, se girarán visitas de inspección por personal facultativo de la empresa cliente, para hacer las comprobaciones que se crean oportunas. Es obligación del contratista, la conservación de la obra ya ejecutada hasta la recepción de la misma, por lo que el deterioro parcial o total de ella, aunque sea por agentes atmosféricos u otras causas, deberá ser reparado o reconstruido por su cuenta.

21. El contratista, deberá realizar la obra en el plazo mencionado a partir de la fecha del contrato, incurriendo en multa, por retraso de la ejecución siempre que éste no sea debido a causas de fuerza mayor. A la terminación de la obra, se hará una recepción provisional previo reconocimiento y examen por la dirección técnica, el depositario de efectos, el interventor y el jefe de servicio o un representante, estampando su conformidad el contratista.

22. Hecha la recepción provisional, se certificará al contratista el resto de la obra, reservándose la administración el importe de los gastos de conservación de la misma hasta su recepción definitiva y la fianza durante el tiempo señalado como plazo de garantía. La recepción definitiva se hará en las mismas condiciones que la provisional, extendiéndose el acta correspondiente. El Director Técnico propondrá a la Junta Económica la devolución de la fianza al contratista de acuerdo con las condiciones económicas legales establecidas.

23. Las tarifas para la determinación de honorarios, reguladas por orden de la Presidencia del Gobierno el 19 de Octubre de 1961, se aplicarán sobre el denominado en la actualidad "Presupuesto de Ejecución de Contrata" y anteriormente llamado "Presupuesto de Ejecución Material" que hoy designa otro concepto.

Condiciones particulares.

La empresa consultora, que ha desarrollado el presente proyecto, lo entregará a la empresa cliente bajo las condiciones generales ya formuladas, debiendo añadirse las siguientes condiciones particulares:

1. La propiedad intelectual de los procesos descritos y analizados en el presente trabajo, pertenece por entero a la empresa consultora representada por el Ingeniero Director del Proyecto.

2. La empresa consultora se reserva el derecho a la utilización total o parcial de los resultados de la investigación realizada para desarrollar el siguiente proyecto, bien para su publicación o bien para su uso en trabajos o proyectos posteriores, para la misma empresa cliente o para otra.

3. Cualquier tipo de reproducción aparte de las reseñadas en las condiciones generales, bien sea para uso particular de la empresa cliente, o para cualquier otra aplicación, contará con autorización expresa y por escrito del Ingeniero Director del Proyecto, que actuará en representación de la empresa consultora.

4. En la autorización se ha de hacer constar la aplicación a que se destinan sus reproducciones así como su cantidad.

5. En todas las reproducciones se indicará su procedencia, explicitando el nombre del proyecto, nombre del Ingeniero Director y de la empresa consultora.

6. Si el proyecto pasa la etapa de desarrollo, cualquier modificación que se realice sobre él, deberá ser notificada al Ingeniero Director del Proyecto y a criterio de éste, la empresa consultora decidirá aceptar o no la modificación propuesta.

7. Si la modificación se acepta, la empresa consultora se hará responsable al mismo nivel que el proyecto inicial del que resulta el añadirla.

8. Si la modificación no es aceptada, por el contrario, la empresa consultora declinará toda responsabilidad que se derive de la aplicación o influencia de la misma.

9. Si la empresa cliente decide desarrollar industrialmente uno o varios productos en los que resulte parcial o totalmente aplicable el estudio de este proyecto, deberá comunicarlo a la empresa consultora.

10. La empresa consultora no se responsabiliza de los efectos laterales que se puedan producir en el momento en que se utilice la herramienta objeto del presente proyecto para la realización de otras aplicaciones.

11. La empresa consultora tendrá prioridad respecto a otras en la elaboración de los proyectos auxiliares que fuese necesario desarrollar para dicha aplicación industrial, siempre que no haga explícita renuncia a este hecho. En este caso, deberá autorizar expresamente los proyectos presentados por otros.

12. El Ingeniero Director del presente proyecto, será el responsable de la dirección de la aplicación industrial siempre que la empresa consultora lo estime oportuno. En caso contrario, la persona designada deberá contar con la autorización del mismo, quien delegará en él las responsabilidades que ostente.